UC Berkeley
UC Berkeley Electronic Theses and Dissertations

Title
The Importance of Phylogeny in Regional and Temporal Diversity and Disparity Dynamics

Permalink
https://escholarship.org/uc/item/1cp9v9rh

Author
Ferrer, Elizabeth Anne

Publication Date
2015

Peer reviewed|Thesis/dissertation

eScholarship.org Powered by the California Digital Library
University of California

The Importance of Phylogeny in Regional and Temporal Diversity and Disparity Dynamics

By

Elizabeth Anne Ferrer

A dissertation submitted in partial satisfaction of the

requirements for the degree of

Doctor of Philosophy

in

Integrative Biology

in the

Graduate Division

of the

University of California, Berkeley

Committee in charge:

Professor Kevin Padian, Chair
Professor Charles Marshall
Professor Jun Sunseri

Summer 2015

Abstract

The Importance of Phylogeny in Regional and Temporal Diversity and Disparity Dynamics

By

Elizabeth Anne Ferrer

Doctor of Philosophy in Integrative Biology

University of California, Berkeley

Professor Kevin Padian, Chair

To understand how various patterns of biodiversity evolve, we must understand not only how various factors influence these patterns, but also the effects of evolutionary history on these patterns. A continuing discussion in biology is the relationship among various levels and forms of diversity. Most studies that focus on past, current, or predicted future changes in diversity use a phylogenetic context, yet lack a phylogenetic framework. Closing that conceptual gap can help to produce a more coherent understanding of diversity patterns and can be more useful when integrated with new dimensions (i.e., time). Here I focus on how extinction and origination rates affect measures of taxonomic (taxic), phylogenetic (sensu Faith's diversity), and morphological diversity.

In chapter 1, I analyze the relationship between taxonomic and phylogenetic diversity in canids and varanids using time calibrated phylogenies. To understand how phylogenetic diversity and taxonomic diversity compare temporally, analyses were run on whole trees as well as trees modified to represent designated time bins. All statistical analyses showed that although taxonomic and phylogenetic diversity can be strongly correlated in certain instances, they also often diverge. This divergence indicates a significant shift in tree geometry (overall assembly of branches across the tree within and across time bins), especially during the extinction of evolutionarily deep, and thus vital, lineages.

In chapter 2, I use 2D geometric morphometric analysis of the skulls of extant monitors and some fossil relatives to quantify and compare morphological diversity. I then test the robustness of these patterns using a phylogenetic framework alongside taxonomic and phylogenetic diversity on a molecular tree both temporally and spatially. Monitor lizards are a good model for these shape analyses because they are morphologically conservative, but regionally variable in diversity. Fossil varanoids fall well within the range of extant morphological variation, but the region of lowest taxonomic but relatively

high phylogenetic diversity relates to a large amount of shape disparity. Phylomorphospace and phylogenetic signal analyses also showed that evolutionary history is a strong influence on size and shape patterns, but the influence of allometry on shape patterns decreases when accounting for evolutionary history.

In chapter 3, I analyze disparity through time (sensu Slater) on a time calibrated molecular varanid tree using size and cranial geometric morphometric data (from chapter 2) to compare with taxonomic diversity. Disparity starts high and falls through time because the nestedness of originations increases across the phylogeny. Size disparity often falls below the expected measures of disparity whereas shape disparity rises above expected. Although considered morphologically conservative, ecological variation within *Varanus* is portrayed in aspects of size and cranial shape disparity, and the originations of certain groups (e.g., largest and smallest taxa) are correlated with certain patterns of disparity through time. These results also corroborate inferences made in studies of *Varanus* fossil material that size variation in *Varanus* (which influences shape variation) may have been higher in the past.

These results suggest that in order to understand the evolutionary consequences and causes of diversity shifts, we cannot just look at diversity today or one metric alone. Origination and extinction rates can have disparate effects on morphological and phylogenetic diversity, and integrating evolutionary history into these studies can result in different inferences about underlying processes. As a consequence, trying to understand extant and past diversity using the power of a phylogenetic framework may provide a wealth of information on the effects of origination and extinctions on evolutionary depth.

For my family, finally.

TABLE OF CONTENTS

ABSTRACT 1
DEDICATION i
TABLE OF CONTENTS ii
ACKNOWLEDGEMENTS iv

CHAPTER 1: Introduction 1
REFERENCES 4

CHAPTER 2: The relationship between taxonomic and phylogenetic diversity through time: a case study using canids. 6

INTRODUCTION 6
Phylogenetic diversity metrics through time 7
METHODS 7
Trees used 8
Community identification 9
Diversity metrics 9
Phylogenetic “chainsawing” 11
RESULTS 11
Lineages through time 11
Diversity metrics 12
DISCUSSION 16
Why the disconnect? 16
The influence of chainsawing 17
Factors influencing patterns 18
CONCLUSIONS 20
ACKNOWLEDGEMENTS 22
REFERENCES 22
TABLES 27
FIGURES 29
APPENDIX 50

CHAPTER 3: Testing the influences on disparity patterns among regions, habitat, and size in monitor lizard skulls
INTRODUCTION 63
Geometric morphometrics 64
METHODS 64
Specimens 65
Phylogeny 65
Taxonomic and Phylogenetic Diversity 66
Geometric Morphometrics 66
Evaluating subgroups 67
Disparity 68
Phylogeny and shape 68

Size and shape 68
RESULTS 70
Taxonomic and Phylogenetic Diversity 70
Principal axes of *Varanus* cranial variation 70
Group shape variation and disparity 71
Size and shape 73
Phylogeny and shape 74
DISCUSSION 75
Taxonomic diversity and morphological disparity 75
Ecology and shape 76
Phylogeny and shape 76
Size and shape 78
What the fossils tell us 79
Implication for morphometrics analysis 80
CONCLUSIONS 80
REFERENCES 82
TABLES 88
FIGURES 98
APPENDICES 126

CHAPTER 4: Taxonomic Diversity, Morphospace occupation and Subclade Disparity Through Time in Monitor Lizards 156
INTRODUCTION 156
Monitor lizards 157
METHODS 158
Tree choice 158
Lineages through time 158
Diversification tests 159
Morphospace through time 159
Disparity through time 161
RESULTS 161
Lineages through time 161
Diversification tests 162
Morphospace through time 162
Disparity through time 163
DISCUSSION 164
Diversification 164
Taxonomic and morphological diversity 165
Morphospace occupation vs subclade disparity through time 165
The evolution of disparity in *Varanus* 166
CONCLUSIONS 168
ACKNOWLEDGEMENTS 169
REFERENCES 169
TABLES 175
FIGURES 177
APPENDICES 187

Acknowledgements

I would never have been able to complete my dissertation without the help and support from many individuals.

To my adviser, Dr. Kevin Padian, your guidance, advice, and patience helped me to learn how to pave my own research path, and for that I am immensely grateful. You were always there to help whenever I needed it, and you hosted some of the best dinner parties around, so again, I thank you immensely. I would like to thank my dissertation committee. Dr. Charles Marshall, you were always very helpful and patient when short 5 minute meetings turned into hour(s) long endeavors, and Dr. Jun Sunseri, your life and career advice helped make the daunting last year of grad school seem more like an exciting transition into a new world. I would also like to thank my qualifying exam committee members, Drs. Marvalee Wake, Tony Barnosky, and Walter Alvarez. You helped broaden my scientific horizons and showed me that taking the research road less traveled is not such a bad idea. To Dr. Patricia Holroyd, although you were never an official member of any of my committees, you played an integral role in both the development of my dissertation and the maintenance of my sanity throughout my graduate career. I would like to express a very special thanks to the UC Museum of Paleontology, because I have never been part of such a supportive and helpful community. My graduate career would have been very difficult without the UCMP family.

To my old and new labmates, thank you for your help, suggestions, and making time in lab just the right amount of crazy. To my fellow graduate and undergraduate student comrades in arms (there are too many of you to name!), without you this grad school adventure would have been harder and much lonelier. To my family, thank you for always believing in me. To my parents, thank you for always pushing me to better myself. To my friends new and old, thank you for helping me survive these past 6 years. Finally, to my grandfather, thank you for never letting me stop chasing my dreams.

Chapter 1: Introduction

In biology, the term diversity has many meanings, including the variety found among species and ecosystems, to variation in shape, ecology, and higher level taxonomy(Faith and Baker, 2006; Gotelli and Colwell, 2011; Vellend et al., 2011). The study of how to measure diversity is a constantly adapting area of research. Taxa differ from each other in more than just taxonomic diversity, and the amount of differences among taxa can differ depending on the set of taxa being measured. The influence of evolutionary history on measures of diversity is not well understood, and many metrics have been developed to account for the effects of phylogeny (Gotelli and Colwell, 2001; Mishler et al., 2014). Nevertheless, combining several levels of diversity measures and integrating phylogeny may be helpful in understanding processes that affect diversity patterns in taxa (Faith, 1992; Faith and Baker, 2006; Velland et al. 2011; Mishler et al., 2014; Oliver et al., 2014)

Taxonomic diversity and other forms of variation such as morphological or phylogenetic diversity are often linked (Faith and Baker, 2006; Mishler et al., 2014), but many studies have shown that measures of taxonomic and morphological disparity may not be correlated (Foote, 1993; Adams et al., 2009; Ricklefs, 2012). The influences of evolutionary history can be measured separately by various diversity measures, and it is imperative to include phylogeny in these studies to parse out influences of evolutionary history, ecology, allometry, taxonomic interaction, and other factors that influence diversity dynamics.

In this dissertation I pose three questions to address the influence of evolutionary history on and the relationships among several patterns of diversity: how phylogeny affects taxonomic diversity, what affects morphological diversity, and what these patterns look like through time. I investigate the relationships among various diversity patterns by using phylogenetic comparative methods, morphometrics, and temporal diversity analyses of canids (Mammalia: Carnivora) and varanids (Squamata: Varanidae) in chapter 2 and aspects of morphological diversity of varanids in chapters 3 and 4.

Case studies

Canids. The family Canidae comprises three subfamilies: Hesperocyoninae, Borophaginae, and Caninae. The borophagines and canines (sister groups) evolved from the hesperocyonines approximately 34 Mya. The borophagines dominated for a long time before their decline, which began approximately 15 Mya. As the borophagine numbers dwindled, the canines took over, and today only the canine subfamily survives (Tedford, Taylor, and Wang, 1995; Wang, Tedford, and Taylor, 1999). A great deal of work has been done on the phylogeny of this group, and the timing of the rise of fall of the subfamilies is well understood (Tedford, Taylor, and Wang, 1995; Wang, Tedford, and Taylor, 1999). What has not been studied is the effect of taxonomic loss through

time on the geometry of the canid tree at any given time and how this shifted through time.

Varanids. Varanids were chosen as a main model system in this dissertation because they show varying levels of diversity across their geographic range, are ecologically diverse, and have a recent time calibrated phylogeny. The family Varanidae has a fossil record spanning almost 90 million years (Molnar, 2004; Conrad, Balcarcel, and Mehling, 2012). They are represented by the single genus Varanus and many subgenera. Their geographic range is exclusively southern, spanning Africa, southern Asia, south Asian islands and Australia (Molnar, 2004). Although larger monophyletic groups are fairly well established, the increase in discovery of new Varanus species has made research on their taxonomy and relationships a constant area of research. Vidal et al. (2012) produced a taxonomically comprehensive phylogeny that I have used for various analyses. Monitor lizards have also been used as a model system for various ecological and evolutionary studies (Losos and Greene, 1988; Pianka, 1995; Collar et al., 2011), so a great deal of information on the types of variation in this group is fairly accessible. Because varanids show such remarkably varying ecologies and sizes, but have a fairly generalized and conservative body plan, they are a good system for a study aimed at analyzing factors that influence variation at various levels in a phylogenetic context.

Chapter 2

In chapter 2, I chose canids as a main case study because previous work has established a baseline understanding of the relationships and timing of diversity shifts in the history of the group (Tedford, Taylor, and Wang, 1994; Wang, Tedford, and Taylor, 1999). Taxonomic loss and gain across a phylogeny are not equal, because the loss of taxa with deep lineages should hold more weight in extinctions, and to an extent originations, than short lived taxa because deeper lineages represent a greater amount of evolutionary history (Faith, 1992; Faith and Baker, 2006). In chapter 1, I focused on measures of phylogenetic versus taxonomic diversity across time bins and geographic regions. Phylogenetic Diversity (PD) is essentially a measure of the ‘evolutionary distinctness’ of a taxon (Vellend et al. 2011; Faith 1992; Faith and Baker, 2006; Mishler et al., 2014). The idea of PD has been of major interest to biodiversity researchers for several reasons, such as incorporating species differences as opposed to simply species numbers in studies, and understanding the influence of history of ecological systems for conservation status (Mishler et al., 2014). PD metrics are influenced by factors such as ecological processes and even the distribution of taxa among sites. Canids and varanids were interesting case studies to test the relationships of taxonomic numbers and relatedness because the interesting species diversity patterns either through time or across regions, and the various magnitudes of influences that ecological processes may have had on diversity. Chapter 2 focuses on Faith’s specific measure of

PD, a metric focused on measuring the branch lengths connecting all of the taxa of interest on a phylogeny, relative to taxic diversity, and other metrics that require a phylogeny in their analyses.

Chapter 3

In 1942, Mertens published a monograph on the Varanidae, proposing around 24 species (Mertens, 1942). Today, over 70 species are recognized, with the highest taxonomic diversity, or species richness, in Indo-Australia (Koch et al., 2013). Africa is the region with lowest diversity, with only around 6 recognized species, and Southeast Asia and the Indo-Australian archipelago hold an estimated 60% of the varanid global diversity, which is composed of a number of island endemics (Koch et al., 2013). Including taxa from all main regions allows us to test how levels of morphological diversity vary across ranges made up of different numbers of taxa using a phylogenetic framework.

In chapter 3, I use 30 extant and 2 extinct *Varanus* species as a test-case for the quantitative study of factors that influence shape in a morphologically conservative group. I briefly review the concept of disparity and various ways of measuring morphological variation and the use of geometric morphometrics in these studies and benefits and challenges of the technique. I expand on why Varanus is a good test case based on their ecological, size, and regional variation. The main goals of this chapter are: (1) to expand on previous morphometric studies of Varanus skull variation by including a broader taxonomic sample with different landmark locations, (2) to show the contributions of various factors to morphological variation in a morphologically conservative group, and (3) to discuss the implications of morphological variation in Varanus and what kind of information, samples, and techniques are recommended for similar studies in the future.

Chapter 4

The term disparity refers to the difference among taxa, and is not necessarily correlated with taxonomic diversity. A high diversity, or many species, could have low disparity, or very few specializations or differences among taxa, or vice versa. Studying the evolution of morphological disparity through time is a challenging task, and even more so when using a phylogenetic framework or comparing with taxic diversity (Harmon et al., 2003; Slater et al., 2010). In Chapter 4, I tackle this problem by comparing patterns of size, GMM data, and taxonomic diversity through time in Varanus using the Vidal et al. (2012) time calibrated phylogeny. In this chapter, diversity relates to the number of taxa living at one time determined by a time calibrated phylogeny, and disparity denotes the relative differences among taxa based on average squared distance of the data across the tree through time. Expanding on the GMM results from chapter 3, I measure size and shape disparity through time across the Vidal et al.

(2012) tree. I discuss the results in terms of changes in taxonomic diversity through time, diversification style (e.g. Yule, 2-rate, etc), ecological aspects of size and shape variation, and abiotic factors.

References

Adams, D. C., C. M. Berns, K. H. Kozak and J. J. Wiens. 2009. Are rates of species diversification correlated with rates of morphological evolution? Proceedings of the Royal Society of London B: Biological Sciences, rspb-2009.

Collar, D. C., I. I. Schulte, A. James, and J. B. Losos. 2011. Evolution of extreme body size disparity in monitor lizards (Varanus). Evolution, 65(9): 2664-2680.

Conrad, J. L., A.M. Balcarcel, and C.M. Mehling. 2012. Earliest Example of a Giant Monitor Lizard (Varanus, Varanidae, Squamata) Plos One, *7*(8), e41767-e41767.

Faith, D. P. 1992. Conservation evaluation and phylogenetic diversity. Biological conservation, 61(1): 1-10.

Faith, D. P., and A. M. Baker. 2006. Phylogenetic diversity (PD) and biodiversity conservation: some bioinformatics challenges. Evolutionary bioinformatics online, 2, 121.

Foote, M. 1993. Discordance and concordance between morphological and taxonomic diversity. Paleobiology, 185-204.

Gotelli, N. J., and R. K. Colwell. 2001. Quantifying biodiversity: procedures and pitfalls in the measurement and comparison of species richness. Ecology letters 4(4): 379-391.

Harmon, L. J., J. A. Schulte, A. Larson, and J. B. Losos. 2003. Tempo and mode of evolutionary radiation in iguanian lizards. Science, 301(5635), 961-964.

Koch, A., T. Ziegler, W. Boehme, E. Arida, and M. Auliya. 2013. Pressing Problems: Distribution, threats, and conservation status of the monitor lizards (Varanidae*:* Varanus spp.) of Southeast Asia and the Indo-Australian Archipelago. Herpetological Conservation and Biology, 8: 1-62.

Losos, J. B., and H. W. Greene. 1988. Ecological and evolutionary implications of diet in monitor lizards. Biological Journal of the Linnean Society, 35(4): 379-407.

Molnar, R. E. 2004. Dragons in the Dust: The Paleobiology of the Giant Monitor Lizard Megalania. Indiana University Press (Bloomington/Indianapolis)

Mertens, R. 1942. Die Familie der Warane. Abhandlungen der Senckenbergischen Naturforschenden Gesellschaft 462:1–116; 465:117– 234; 466:235–391.

Mishler, B. D., N. Knerr, C. E. González-Orozco, A. H. Thornhill, S. W. Laffan, and J. T. Miller. 2014. Phylogenetic measures of biodiversity and neo-and paleo-endemism in Australian Acacia. Nature communications, 5.

Oliver, I., D. J. Eldridge, C. Nadolny, W. K. Martin. 2014. What do site condition multi-metrics tell us about species biodiversity? Ecological Indicators, 38: 262–271

Pianka, E. R. 1995. Evolution of body size: varanid lizards as a model system. American Naturalist, 398-414.

Ricklefs, R. E. 2012. Species richness and morphological diversity of passerine birds. Proceedings of the National Academy of Sciences, 109(36): 14482-14487.

Slater, G. J., S. A. Price, F. Santini, and M. E. Alfaro. 2010. Diversity versus disparity and the radiation of modern cetaceans. Proceedings of the Royal Society of London B: Biological Sciences, 277(1697): 3097-3104.

Tedford, R. H., B. E. Taylor, and X. Wang. 1995. Phylogeny of the Caninae (Carnivora, Canidae): the living taxa. American Museum Novitates 3146.

Tedford, R. H., X. Wang, and B. E. Taylor. 2009. Phylogenetic systematics of the North American fossil caninae (Carnivora: Canidae). Bulletin of the American Museum of Natural History: 1-218.

Vellend, M., W. K. Cornwell, K. Magnuson-Ford, and A. Ø. Mooers. 2011. Measuring phylogenetic biodiversity. Biological diversity: frontiers in measurement and assessment. Oxford University Press, Oxford, UK: 194-207.

Vidal, N., J. Marin, J. Sassi, F. U. Battistuzzi, S. Donnellan, A. J. Fitch, B. G. Fry, et al. 2012. Molecular evidence for an Asian origin of monitor lizards followed by Tertiary dispersals to Africa and Australasia. Biology letters: rsbl20120460

Wang, X., R. H. Tedford, and B. E. Taylor. 1999. Phylogenetic systematics of the Borophaginae (Carnivora, Canidae). Bulletin of the AMNH, 243.

Chapter 2: The relationship between taxonomic and phylogenetic diversity through time: a case study using canids.

INTRODUCTION

Reconstructing evolutionary histories and measuring diversity (Phillips, 1860; Wilson, 1988), have been fundamental lines of research in biology and paleontology. Phylogenies provide insight into a number of evolutionary dynamics - group representation, timing of evolutionary events, character evolution, evolutionary tempo, biogeographic patterns, ecological shifts, developmental patterns, and even quantifying diversity (Felsensetein, 1985; Maddison and Maddison, 1989; Pagel, 1999; Bowers et al., 2003; Harzsch and Hafner, 2006; Cavender-Bares et al., 2009; Jablonski and Finarelli, 2009; Davies and Buckley, 2011; Ronquist and Sanmart, 2011; Roncal et al., 2012). Recurring issues tend to be the gaps relating to the perception of diversity. For example, neontologists tend to place strong emphasis on ecology and conservation, whereas paleontologists integrate a stronger temporal component. Depending on the question of interest, this might not be a problem, but it becomes difficult when research spans several biological realms.

Diversity is a product of evolution, so it is no surprise that one measurement alone cannot provide all insight into patterns and underlying processes (Whittaker, 1972; Quental and Marshall, 2010). If a study is interested in clade or evolutionary dynamics, then taxic counts alone, which are one of the most common modes of measuring diversity, will not provide a great deal of insight (Whittaker, 1972; Robeck, Maley, and Donoghue, 2000; Colwell, 2009). Taxa are often considered equally distinct, but certain groups can provide more weight to overall diversity (Clarke and Warwick, 1999). Although many innovative studies using evolutionary history in diversity measures exist, it still remains underrated in certain areas of biology that can gain from integrating a phylogenetic approach (Felsenstein, 1985; Faith, 1992; Miles and Dunham, 1993; Webb et al. 2002; Davies and Buckley, 2011; Mishler et al. 2014). Many studies have developed ways to use evolutionary history in diversity research, and one of the most widely used metrics is Daniel Faith's Phylogenetic Diversity (PD; Faith, 1992). Researchers have extensively explored this metric, for example to see how it can inform on endemism (Mishler et al. 2014), or how incorporating abundances affects results (Cadotte et al. 2010). Focus has been on spatial scales, but temporal patterns are less explored because time is often thought to be incorporated into phylogenetic studies as taxonomic durations (Graham and Fine, 2008).

I was interested in how incorporating phylogeny, not only in context but as a framework, could provide a more informative picture of temporal diversity. In this study, my goal was to compare a modified measure of PD alongside other diversity metrics through time. Not all phylogenies are created equal, so I tested simulated trees, a fossil

phylogeny (canids), and a molecular phylogeny (varanids) to determine how the underlining data and tree shape might affect temporal patterns of PD. Analyses were run on taxonomic communities from designated time bins, and all results were measured across whole trees and on trees indicative of each time bin using a new "chainsawing" method described later in this paper.

Phylogenetic diversity metrics through time

Phylogenetic Diversity relies on the premise that where taxa fall on the tree of life can provide information on clade dynamics at different hierarchical levels (Faith, 1992). The loss or gain of certain taxa should reflect the loss or gain of underlying features, or evolutionary history. This perception of PD is important, for example, when prioritizing the conservation of certain taxa with deep lineages, or those considered to hold a great deal of evolutionary information (Faith, 1992; Faith and Baker, 2006). The same taxon count would be obtained when comparing five species of rabbit with one species of lizard, bird, snail, fish, and insect. Instinctively, one knows that these numbers are not equivalent representations of diversity. Normal diversity metrics, such as species richness, are insensitive to phylogeny (Colwell, 2009). PD uses the phylogenetic relationships of the members of a sample, no matter what hierarchical level.

PD measures how much of a phylogeny is traveled among a set of taxa by summing the total branch lengths connecting them (Faith, 1992; Faith and Baker, 2006; Schweiger et al. 2008). The traditional measure uses the presence or absence of taxa, and can be done without branch lengths by simply adding the number of nodes separating taxa. The basic formula when using branch lengths is:

$$PD(S) = \sum_{e} \lambda\, w(e)$$

Where S=a subset of taxa, λ= records the branch length, and e= indicates which branches of the tree belong to taxa. In traditional uses of PD, taxonomic communities are compared to a larger taxon pool or within a larger phylogeny (Faith, 1992; Faith and Baker, 2006; Cadotte et al. 2010; Mischler et al. 2014). That same traditional measure will be used in this study along with a modified version. PD of communities (in this case, a group of taxa existing in a defined time bin) will be measured across a larger phylogeny and also on a phylogeny exclusively of taxa from time bin communities without regard to any larger tree (Cadotte et al. 2010).

MATERIALS AND METHODS

The research goals were to (1) see how taxic counts compare with phylogenetic diversity metrics in simulated birth-death trees, (2) measure patterns of taxonomic richness and phylogenetic diversity metrics between subfamilies in a morphological

canid tree with fossils through time, and (3) measure patterns of richness and phylogenetic diversity metrics among regional clades in a fully molecular *Varanus* tree through time. Discussion will cover factors that could influence differences in patterns of diversity. All coding and analyses were computed in the statistical program, R v3.0.0 (R Development Core, 2014).

Trees used

All phylogenies were either simulated, digitized, or modified using the *ape* (Paradis, Claude and Strimmer, 2004), *geiger* (Harmon et al. 2008), and *phylobase* (R Hackathon, 2014) packages in R.

Simulated birth-death trees – Three simulated trees growing under a uniform birth-death process were generated using the *sim.bdtree* function from the *geiger* (Harmon et al. 2008) package in R (Fig. 1). At any unit of time, each lineage was given a constant probability of originating or going extinct. If the birth rate (b) given is greater than the death rate (d), then the number of lineages is expected to grow exponentially, and vice versa. Together, b and d equal 1. The three simulated trees were:

1. High birth/origination and low death/extinction rates (b=.7, d=.3) (Fig 1.A)
2. Low birth/origination and high death/extinction rates (b=.3, d=.7) (Fig 1. B)
3. Equal birth/origination and death/extinction rates (b=.5, d=.5) (Fig 1. C)

Analyses on the simulated trees were used to demonstrate how patterns of phylogenetic diversity measures through time can differ based on the tree shape. Hereafter, the terms birth and origination as well as death and extinction will be used synonymously.

Canids- A combined phylogeny (Fig. 2) assembled from Tedford, Taylor and Wang (1995) and Wang, Tedford, and Taylor (1999) was digitized. The canid tree is morphological with fossil taxa, and is time calibrated based on the first and last appearances of taxa.

Approximately 50 Mya in the Eocene, the carnivorans split into the feliformes and the caniformes. Around 10 My later, the first recognizable canids appeared. The family Canidae consists of 3 subfamilies: Hesperocyoninae, Borophaginae, and the Caninae. The hesperocyonines existed between around 39 Mya to 15 Mya. They gave rise to both the borophagines and canines around 34 Mya. The borophagines went extinct approximately 3-2 Mya and the canines are the only currently living members of the Canidae (Tedford, Taylor, and Wang, 1995; Wang, Tedford, and Taylor, 1999). All of these subfamilies had shown a trend of increased body size, and some members even evolved hypercarnivory. It has been postulated that these factors might have made them prone to extinction (Van Valkenberg, Wang and Damuth, 2004). An interesting

question in canid evolution is how patterns of canine and borophagine diversity compare through time.

Varanids – For an example of a molecular tree with no extinction, I used Vidal et al. (2012)'s fairly comprehensive extant *Varanus* phylogeny (Fig. 3). The tree is time calibrated and contains no extinction. Changes in diversity within regional groups was of main interest in this analyses. I have used the same regional identifications as Vidal et al. (2012) (color coded in Fig. 3).

The extant family Varanidae contains a single genus, *Varanus*, including subgenera such as *Odatria* (pygmy varanids). They fall within the Varanoidea, which contains the extinct mosasaurs, dolichosaurs, and necrosaurs, and the extant helodermatids (Gila monsters and beaded lizards) and *Lanthanotus* (earless monitor lizards) (Molnar, 2004). The family Varanidae includes the largest-known extinct (*Megalania* or *Varanus priscus*, ~6 m) and extant (*Varanus komodoensis*, ~3 m) terrestrial lizards (Conrad, Balcarcel, and Mehling, 2012). There are over 70 recognized living species of *Varanus,* and their present distribution is limited to three continents: Africa, Asia, and Australia. Fossil varanids lived beyond their present range: pre-Miocene (> 23 Mya) fossils are found in Asia and North America, and by the middle Miocene (~15 Mya) they are also found in Europe, Africa, and Australia. *Varanus marathonensis* may have lived in Europe up to the Pliocene (~5.3 Mya). Some fossil varanids are well-preserved and fairly complete, but most specimens are fragmentary and may be recognized as varanid but contentiously identified as *Varanus*. (Holmes et al. 2010; Conrad, Balcarcel, and Mehling, 2012). A better understanding of extant regional diversity patterns may help shed light on the origin and past distributions of this group.

Community identification

In ecology, the term "community" normally refers to "an association of interacting species inhabiting some defined area" (Molles, 2000). The area can be designated at various regional scales or based on factors such as habitat type. In this study, community will mostly refer to taxa existing at defined time bins, subclades, or regions. This is possible because with analyses used here, the community datasets may consist of any taxonomic sample set with an associated phylogeny. As long as relationships of the taxa of interest are established, there are no specific limitations. In all analyses, time bin communities will be measured as well as subfamilies in canids and regional groups in varanids.

Diversity metrics

Phylogenetic diversity metrics were conducted with functions from the *picante* (Kembel et al. 2010) and *vegan* (Oksanen et al., 2015) packages in R, and are

described in detail in Helmus et al. (2007) and Webb, Ackerly, and Kimbel, (2008). These metrics are considered phylogenetic diversity metrics because they use trees in their formulas, so to not conflate them with Faith's PD herein they will generally be referred to as phylogenetically weighted diversity (PWD) measures.

Lineages through time: Lineages through time (LTT) plots were calculated using a modified version of the _R_tree_functions_v1.R code developed by Nicholas Matzke (Matzke, 2011). This code computes the numbers of lineages crossing specified time slices.

Phylogenetic diversity (PD): PD calculates the sum of the branch lengths across a phylogeny for one or more samples. PD is not statistically independent of species richness (higher richness, or number of taxa, tends to correlate with higher PD), but what it provides is the degree of relatedness across a sample. Because there is unequal richness of samples across regions and time bins, observed PD was compared to expected values under several randomizations based on taxonomic diversity in time bins. These comparisons help indicate if certain taxa are more informative in explaining measures of PD than others.

Expected and variance phylogenetic diversity: Both are calculated by resampling the tree at differing numbers of tips based on time bin taxonomic diversity with a single probability of all tips being sampled. The variance measure provides a confidence interval for expected PD by obtaining measures of variance within a set of bounds.

Phylogenetic species variability (PSV): PSV is statistically independent of species richness, but directly related to mean phylogenetic distance. PSV works by modeling a hypothetical neutral trait across a tree When looking at a sample of taxa, it is one when all taxa are unrelated and nears zero the more related the taxa in the sample. Proportions of deviations from the mean by different taxa were obtained by rerunning analyses after removing individual taxa from the dataset in different iterations. This provides information of individual species contribution to PSV.

Phylogenetic species richness (PSR) - PSR is directed related to PSV because it is measured by multiplying species variability with species richness. It can be considered taxic diversity of a sample after omitting relatedness. It can have a maximum value of the total species richness in the sample, but, like PSV, approaches zero the more related the taxa in a sample.

Mean nearest taxon distance (MNTD): MNTD calculates the average distance separating each taxon in a community from its closest relative. The standardized effect sizes of communities were also measured. This compares the observed relatedness of a community to a null model of expected relatedness. The null model is generated by randomizing the community and dividing by standard deviations of phylogenetic

distances of the model data. This is another measure of relatedness in a community, but by conducting pairwise comparisons as opposed to measures across a whole tree.

Inter-community pairwise distance: This is a type of beta diversity. Pairwise distance was used to calculate the mean pairwise distance separating taxa *between* time bin communities.

Phylogenetic chainsawing

Code in R was developed to remove particular tree tips at different time intervals, creating a phylogeny representative of those time bins. The *prune.tree* function in R is often used to create trees representative of a discrete subset of taxa from a given phylogeny. The issue with using this technique is that branch lengths would not necessarily reflect the length of time taxa have existed to a particular time bin. The function retains the whole branch length of the taxa, whereas the tip-dropping method used here will adapt taxon branch lengths to reflect the length of time they had existed to time bins. This method will be referred to a “chainsawing” trees.

After a tree has been digitized, time bins across the phylogeny are identified. Tree tips that do not exist in the designated bin are dropped from the phylogeny. Any branch lengths of taxa in that bin that extend past that time interval are also removed. In some cases, the list of tree tips existing at these time bins was returned and used to create the temporal community list. This modification meant that phylogenetically weighted diversity could be measured on trees representative of time bins as well as across the total unmodified tree for comparison.

RESULTS

Lineages through time

Simulated trees – In all simulated trees, 0 Mya will represent the present. All original rates were kept constant. The simulated high-birth tree, which generated 102 total tips, maintained a fairly low diversity (10 – 5 Mya) followed by a sharp increase in diversification to the present. This pattern exists because as more lineages appear, albeit slowly, even more lineages can arise. Peak diversity is at the present, with about 60 lineages. In the case of the high-death rate tree (Fig 4. B), 2 lineages originate, but only one survives to the present. The high death rate prevented any sufficient origination of new taxa. With the equal birth and death rate tree (Fig 4. C), there is an increase in the number of lineages from 10 – 8 Mya before counts seem to stabilize (although with a great deal of wobble around a mean). At 6 Mya, there is another burst of diversification followed by, at about 2 Mya, a steady extinction of taxa. It should be stated that equal birth and death rates do not mean that lineage numbers remain stable around some mean; it simply reflects the equal probability of lineages either going extinct or originating.

Canidae - There is a distinct difference between the inclusion and exclusion of fossils when looking at canid lineages through time. Figure 5 is a modified spindle diagram from Tedford, Wang, and Taylor (2009) showing species diversity of the Borophaginae and Caninae from their origin to the present. There is waxing and waning of borophagines through time before a steady decrease beginning approximately 15 Mya, followed by their extinction 2-3 Mya. The canines originate around the same time as the borophagines, in the early Oligocene, but remain at a low diversity until the start of the borophagine downfall. At that time, their numbers steadily increase to the present where they reach the highest diversity.

The LTT (Fig. 6) plot was generated using the species level phylogeny seen in Figure 2. The line containing fossil taxa is variable through time, with repeated periods of increases and decreases in taxonomic diversity. After 30 Mya, the overall trend (or net change, because there is a great deal of wobble) is a decrease in diversity to the present. The LTT line excluding fossil taxa was generated by only including lineages that extend to the present. The non-fossil LTT line simply represents the history of caninae that exist today. The non-fossil line is nonexistent until the sharp increase from 13-10Mya. Excluding fossils can create a very different story of canid diversity.

Varanus – Using the Vidal et al. (2012) tree, the highest diversity of *Varanus* is found in Indo-Australia (Fig. 7), which is true when considering current regional variation. It should also be repeated that Vidal et al.'s (2012) phylogeny does not represent the whole true regional diversity of extant *Varanus*. Diversity in Asia is higher than represented in the tree, and a main reason is because of island endemics. Africa contains the lowest level of diversity, with 5-6 species. The tree contains no extinction, so it shows a trend of increasing diversity through time (Fig. 8). The pattern is very similar to the LTT pattern of the simulated high-birth tree. The slope is linear and steady, indicating a fairly constant increase in diversity across the tree. A slight flattening of the LTT line indicates origination slowing down and stabilizing approximately 5 Mya.

Diversity metrics

Simulated high origination –On the high-birth rate tree, patterns of PD and taxonomic diversity are very similar (Fig. 9). Because there is a negligible amount of extinction on this tree, changes in PD are mostly influenced by the origination of new taxa. This is because taxa tend to survive long periods of time, thus maintaining long branch-lengths. They continue to be part of measures of PD in subsequent time bins, then, along with any new originating taxa. The slight jump in taxonomic diversity 5 Mya is not matched by an equivalent increase in PD. This might be because several taxa that originated within that time bin were short lived. Changes in taxonomic diversity do not reveal whether taxa are short lived, long lived, or how they relate to each other, whereas PD is strongly influenced by those elements. Measures of PD tend to be lower when

measured on chainsawed trees (Fig. 10). PD measures the total tree traveled when connecting a defined set of tips, or a community. If a tree is large because it contains many taxa, a great deal of a tree may need to be traveled to connect all taxa of a community, causing measures of PD to come out larger. On the chainsawed trees, however, tree tips not existing at each time bin was removed, reducing tree size, so measures of PD were lower.

Simulated high extinction – Measuring phylogenetic diversity on the simulated high extinction tree was not possible because only two taxa originated and any measurements would be uninformative.

Simulated equal birth and death – From the base of the tree to 6 Mya, measures of taxonomic richness and PD follow similar trends (Fig. 11). There is a general increase in PD from 6 Mya to 4 Mya, whereas taxonomic diversity jumps at 5 Mya. The jump is correlated with the origination of short lived taxa, which is why this increase may not be reflected in PD. Both taxonomic diversity and PD plateau, followed by a gradual decline to 1 Mya. There is a final, small burst of origination near the present. Both whole tree and chainsawed PD values follow a similar trend (Fig. 12).

Canid tree – Taxonomic diversity increases steadily from 35 Mya to approximately 15 Mya, which is then followed by a fairly steady level of high diversity to the present fluctuating between 41 and 46 species (Fig 13 A). After the mid-Miocene (~15 Mya), there is a shift in the proportion of taxa that make up the majority of the diversity. Borophagines are still the most common 15-10 Mya, but as canine numbers increase, they begin to make up a larger portion of the time bin communities. Borophagine diversity begins to drastically decline before their extinction approximately 2-3 Mya. PD follows a similar pattern from the base of the tree to 20-15 Mya, but then there is a drastic increase in total PD (Fig. 13 B). The increase in canine diversity towards the present does not appear to play a large role in measures of PD on the total tree. When time bin community PD is measured on chainsawed time bin trees (Fig. 14), PD begins much lower. Interestingly, the drastic increase to 20-15 Mya followed by a general drop to the present is fairly similar to measurements on the total tree. Most interesting is that chainsawed PD rises above the total tree results in the recent. As borophagines become extinct and their tree tips are removed from the chainsawed trees toward the recent, chainsawed PD is more reflective of analysis of a predominantly canine phylogeny.

Almost all time bin communities fall into the range of expected PD when measured on the total tree (Fig .15). The sole outlier is the recent (5-0 Mya), which falls below expected range. Although it lies in the high end of species richness (toward the right of the plot), PD is not at expected levels because of the overwhelming number of

canines in the community. This simply means that the recent time bin community does differ significantly from the expected range of results obtained from resampling the canid tree 1000 times using observed taxonomic diversity.

Other phylogenetically weighted diversity measures were very informative. PSV, which is related to mean phylogenetic distance, approaches 0 toward the present. Reduced mean phylogenetic distance means that taxa in more recent communities are more closely related to one another (Fig 16 A). When analyzing the contribution of certain taxa to PSV through time by subsampling, it appears that there is not a significant difference between borophagine and canine members (Fig. 16 B). The few larger deviations from the general mean are found in two borophagine taxa, *Phlaocyon latidens* and *Rhizocyon oregonensis*. This is not surprising because they are two very deep lineages. Although PSR falls slightly below SR, they both generally increase to 15 Mya (Fig 17). While SR remains fairly stable, PSR decreases from 15 Mya to the recent. Essentially this indicates (similarly to PSV), that although taxa are originating, they tend to originate in one area of the tree.

Chainsawing the tree at each time bin and running the phylogenetically weighted diversity metrics tends to have an effect on the degree and direction of change (Fig. 18). Total tree PSV and chainsawed PSV both begin relatively high, but there is a dramatic drop in chainsawed PSV followed by an increase toward the present (Fig. 18 A). While total PSR and chainsawed PSR both increase to 20-15 Mya, there is more of a drastic decrease in the chainsawed PSR relate to the whole tree measure (Fig. 18 B). Both chainsawed PSV and PSR increase above the total tree measures toward the recent. Because PSR is related to PSV in how it is quantified, their similar patterns are to be expected. It appears that by pruning the tree to be representative of time bins when measuring temporal communities, these metrics were able to capture how extinction resulted in surviving taxa being relatively closely related to each other. Later diversifications of taxa in certain portions of the chainsawed trees increased variability measures approaching the recent. This is because chainsawed trees do not hold any information on extinct taxa (tree span consisting of extinct branches is not measured, unlike total tree analyses).

Community structure analyses were helpful in understanding how time bin taxonomic relationships relate to diversity. Canid time bin MNTD gave results with similar evolutionary implications to previous analyses (Table 1). In general, observed MNTD decreased through time toward the recent. When analyses were standardized to effective size by resampling, three time bins came out as clustered (with negative Z values), or with smaller phylogenetic distances among species in the time bin than expected. These time bins occurred during or directly after the massive decrease in borophagine diversity (Fig. 2; Table 1). Community comparisons, using taxon distances within and between time bins, gave even more weight to the effect of borophagine extinction. Normally, distance measures, or community difference, are small when

comparing successive time bins and large when comparing bins that are far in time from one another (Figure. 19). The largest distance in successive time bins is found between the 20-15 Mya and 15-10 Mya. Tree structure changed drastically at that time during the switch from borophagine dominated to canine dominated time bin communities.

Varanids – Future work will focus on more refined measures of regional contribution to phylogenetically weighted diversity measures, but here I will include a general description of patterns for comparison with the canid results. Also, it should be noted that the Vidal et al. 2012 tree contains only a portion of all *Varanus* species, so results are only reflective of the representative taxa used in their reconstruction.

Overall, PD and species richness both increase through time, because taxa are only originating in the *Varanus* phylogeny (Fig. 20. A). Also, with the taxa included on this tree, new lineages seem to appear at a steady rate. It is interesting that PD and species richness are so tightly correlated that, at least within all the taxa included on this tree, each region appears to contribute the same level of taxic and phylogenetic diversity (Fig. 20. B). Although PD steadily increases though time, there were a disproportionate number of originations within major geographic regions (Fig. 21). Indo-Australia is extremely diverse, and originations in that region began to increase almost in parallel with the increase in PD. Interestingly, early in the tree additions to the African community also had a relatively strong effect in PD. A more in-depth analysis of varanids in that region will be covered in future studies. Time bin communities also all fall tightly into expected ranges of PD through time (Fig. 22), which is not surprising because SR and PD are tightly correlated. The spread of taxa spans all regions near the origin of the tree and continues similarly through time. Because of the equal origination across the tree, PSV starts high and remains so (Fig. 23). The slight decreasing PSV toward the recent is most likely because much of the origination tending to occur more or less in the Indo-Australian portion of the tree.

Varanus MNTD was more enlightening that other diversity analyses (Table. 2). Although all Z scores were positive and p values were close to 1, indicating evenness among time bin communities (which was expected because LTT analyses showed a fairly steady increase in diversity through time and there is no extinction), scores 15-10 Mya reflect the highest amount of evenness ($Z = 2.9$, $p = 1$). Origination was occurring in all areas of the tree and within smaller subclades in the Indo-Australian region (Fig. 3). Total tree origination slightly increased around this time, and evenness numbers are generally highest near the recent (Table 2). MNTD pairwise comparisons of time bin communities (Fig. 24) show that those bins succeeding 20 Mya tend to be very similar to each other more so than those earlier in the tree (this can be seen as the clumping of all time bin communities beginning 20 Mya). This means that taxonomic distinctiveness and structure within time bins seem to have stabilized.

DISCUSSION

Why the disconnect?

Although tightly linked conceptually, measures of PD and taxonomic diversity often depart from one another. Phylogenetic diversity measures the shared history of taxa in a sample, and thus greatly relies on the relationships of taxa. This is also the case for other phylogenetically weighted diversity measures. Focusing on taxic counts, no matter how phylogenetically contextual, may not provide enough insight into the evolutionary history of those counts.

Insights from simulations - In a tree with no extinction, or a high birth rate, PD appears to be solely influenced by the addition of new taxa. In this case, taxic counts alone can be informative on a deeper phylogenetic level. With the inclusion of extinction, taxic counts alone might not provide information on underlying evolutionary dynamics. The simulated birth-death tree showed that equal origination and extinction rates through time do not mean a steady level of taxonomic diversity (Fig. 4 C). Although taxic counts wax and wane, there is no inherent information on whether lineages are young, old, and how they relate to one another. PD generally increased, showing that origination occurred across the tree, but not all sharp increases in taxonomic richness resulted in sharp increases in PD (Fig. 11). Deeper lineages are more influential in measures of PD, so looking at both PD and taxonomic richness together can paint a more refined picture of patterns of diversity.

Insights from canids and varanids – Both the canid and varanid trees were useful in looking at how these metrics can be used to study the relationships of subgroups within a larger phylogeny, whether taxonomically or regionally defined, in a temporal context.

The canid tree, by taxon counts alone, shows a pattern of increasing diversity through time and maintaining the highest diversity (net diversity) near the recent (Fig. 6; Fig. 13 A). Interestingly, through time high diversity is maintained by different groups (Fig.13 A). The extinction of borophagines coincides with a drastic increase in diversity within the canines. Although canines are helping maintain taxonomic diversity, the PD existing within the canid phylogeny takes a very hard hit in all versions of analyses (Fig 13 B; Fig. 14). A large fraction of the canid evolutionary history, and thus PD, is lost with the extinction of the borophagines. One of the most interesting finds was the pattern of PSV (Fig. 16; Fig. 18). PSV is influenced more by how the taxa in the sample *relate to one another* rather than how those taxa *relate to the tree*. PSV, then, decreased through time when looking at canid temporal communities because the taxa making up the samples were more closely related to one another. PSR deviates greatly from species richness after the borophagines begin declining in numbers (Fig. 17). There is less phylogenetic variability in the tree, a measure which species richness

alone is insensitive to. Tree resampling and whole community analyses persistently show a significant difference in time bin community structure toward the recent (Fig. 15; Fig. 19; Table 1). Any disconnect is readily caused by the difference in sensitivity of analyses to evolutionary history.

The varanid tree, which had no extinction, was very similar in general pattern of PD and species richness to the simulated high-birth tree. Taxonomic counts and PD are tightly linked in the *Varanus* tree (Fig. 20 A). Although PD reflects total taxonomic diversity, there is differential impact from regional taxa (Fig. 20 B; Fig. 21). Similarly to results from the canids, PSV was more reflective of the relationships among taxa in the time bins (Fig 23). As the tree approached the recent, more origination in Indo-Australia caused temporal community measured to appear more related. Because taxa through time still span the whole tree, the subtle whole community comparison analyses were able to show how increased origination seemed to make temporal communities increasingly similar to one another (Fig.24; Table 2). Although the tree contained only origination and taxic counts were very informative, subtle origination dynamics might have been overlooked without use of phylogenetically weighted comparisons. Specific diversity patterns were not discussed here because future work will focus on their relationships within these regions, and how they correlate with morphological disparity.

The influence of chainsawing

Depending on tree shape through time, in some instances chainsawing affected the magnitude of diversity metrics measured. For example, the slight divergence between PD on the whole and chainsawed simulated high-birth tree reflected taxa maintaining long branches on the total tree, whereas chainsawing the tree by time bin reduced the amount of tree traveled when measuring those same time bin communities (Fig. 10). The taxic diversity peak at 5my on the simulated equal birth-death tree was not matched by an equivalent peak in PD, and was indicative of an origination of short branched taxa (Fig. 11). These tend to not greatly affect PD because they do not continue to contribute evolutionary depth to the tree through time. Generally, measures of chainsawed PD are lower than total tree PD, although the overall temporal trends do not seem to differ (Fig. 12; Fig. 14).

More detailed analysis of the canid tree helped shed light on the dynamics which might be affecting each of these metrics. For example, the slight discrepancy in the amount of increase in PD at the beginning of the canid tree exists because borophagines as a group represent a great deal of evolutionary depth of the whole canid tree. When this tree is chainsawed to reflect specific time bins, as stated before, measures of PD decrease because the trees measures are smaller. This is true especially early on in the canid tree because all taxa have short branches (and were made up primarily of borophagine taxa). The chainsawed tree gives no indication to

future shifts in taxonomic diversity, unlike the total tree which may be affected by future branches although communities are identified as time bin taxonomic samples. They may extend the length of the tree needing to be traveled even if the metric is not measuring the branch of that specific taxon.

Total and chainsawed measures of PSR and PSV significantly diverge beginning at the borophagine diversity drop approximately 20-15 Mya (Fig.18). Because PSR is directly related to PSV and the patterns are the same, discussion will only focus on PSV. PSV measured on the total tree began to sharply decrease 10 Mya. Time bin communities toward the recent began to be made up of mostly canine groups, meaning a decrease in PSV when measured on the total tree. Chainsawed PSV truly captures how the *phylogeny itself* was affected by the loss of deep borophagine taxa. Because the chainsawed trees do not contain any branches that exist after the designated time bins, PSV measured is more reflective of specific time bins and the history leading to them. Chainsawed PSV sharply decreased 20 – 15 Mya because of the deep loss of borophagine taxa, but the increase toward the recent represents both the maintenance of older canine groups as well as the diversification of new canine taxa. PSV is only measured based on time bin taxonomic communities and a provided tree, it contains no specifics to when, or how, on a tree diversification is occurring. It will simply provide information on variance of the subset of tips on a designated tree.

Community distance analysis showed that recent time bin samples are “less related” to older community time bins. This essentially means that the types of originations within time bins, when measures on a chainsawed or the total tree, are reflecting different clustering community patterns. Recent canid communities have more taxa in common with each other than they do with previous time bins because of extinction of more phylogenetically disparate lineages (Fig. 19). Varanids, on the other hand, show less and less differences among recent communities because origination occurs across the phylogeny (not in isolated areas) in the same subclades, and no taxa were lost (Fig. 24).

Factors influencing patterns

Canids – Evolution of large size and specialization may have played a role in patterns of taxonomic diversity and PD. Wang et al. (1999), Van Valkenburgh et al. (2004), and Finarelli (2007) discussed size patterns within canid evolution. In borophagines (whether looking at species or monophyletic subsets), small taxa, from their first to last appearances, tend to have longer overall durations. Interestingly, when looking at only groups with short durations in all subfamilies, there did not seem to be any significant difference between the numbers of large or small taxa. The findings differ for long branches of the tree: there are no long lived large taxa (of course, for canines, this pattern is cut off by the present so we do not know if given more time this might not be the case) (Wang et al., 1999). Through time, in both borophagines and

hesperocyonines, there is a general trend of increased body size. This seeming selection for large size (or Cope's rule) is associated with shorter species durations and increased hypercarnivory. After the appearance of the Caninae about 34 Mya, they stayed limited to a group of small taxa throughout the Oligocene, showing very little diversification until the end of the mid-Miocene. Borophagines, though, had a very different history. There was an origination of all their major sub-clades from the Oligocene to mid-Miocene, yet by 12 Ma only a few fox-sized borophagines remained, most of which would be considered hypocarnivores. At this point, certain versatile Canine subclades (such as the Vulpini) appeared including both mesocarnivore and hypocarnivore members. On a smaller scale, they displayed a range of adaptations comparable to the original radiation of the Borophaginae (Tedford, Wang, and Taylor, 2009). This truly seems to be a replacement, both in numbers and ecology, of the borophagines by the canines.

This trend of species duration decrease seems to correlate with the general pattern of decreasing PD through time in the canid tree. When separating the proportion of PD defined by borophagines and canids, borophagine diversity decline and eventual extinction greatly influenced PD decrease. This may be because the lineage tended to large size (or possibly specialization) and short branched taxa through time. However, a slight jump in PD 10 - 5 Mya correlates with a burst of young canine lineages in addition to their remaining long-branched members. Canines, as the only remaining canids, may return PD to previous levels seen in the canid tree if older members are maintained. Conversely, if they follow the trend to increased body size and specialization as seen by their relatives, PD might never reach previous proportions. Of course, this is assuming that there is no extinction of current canines or appearance of new canid lineages in the future.

Varanids - The Vidal et al. (2012) tree, because it contains no extinction, shows a proportionate amount of PD increase correlating with the appearances of new lineages through time. It should be stated that this pattern is only reflective of the tree used and not all monitors, because quite a number of Indo-Asian and Indo-Australian taxa were not included. Many factors may be influencing current regional diversity patterns. Recent threats to monitors include habitat destruction, consumption by humans, and commercialism (both national and international) (Koch et al. 2013). Human population densities are higher in Asia and Africa than Australia, and the most exploited monitor species for their skin are two African species, *V. niloticus* and *V. exanthematicus*, and the Asian *V. salvator* (Pianka, 2012). There are other endangered Asian species because of decimated populations, and there has also been massive habitat destruction in semiarid regions of Asia and Africa. In contrast, most Australian monitors are not considered threatened. Although they are hunted by locals, much of the Australian habitat is comparatively unscathed and the country has never allowed

faunal exports (zoos being the exception), although of course illegal trade is known to occur (Pianka, 2012). The fossil record has so far shown that the oldest varanid material comes from central Asia (Molnar, 2004; Conrad et al. 2012). These threats may have reduced populations historically, or kept diversity levels low in areas where radiations may have otherwise occurred.

Size and ecology might also play a role in diversity patterns within *Varanus*. Over 60% of extant varanid diversity is established in the Southeast Asia and Indo-Australian archipelago region. Approximately half of known varanid species occur in the Indo-Australian Archipelago (43 species, 8 subspecies) (Koch et al., 2013), and species richness is lower in Africa and mainland Asia (Pianka, 2012). When you include South Asian island endemics, though, the diversity counts in Asia are considerably higher (Pianka, 2012). The history of these regions may play a large role into variation of *Varanus* diversity. For example, in Indo-Australia, geologic and tectonic events resulted in the Earth's biggest archipelago made up of thousands of islands comprising a diversity of climates and ecosystems (Koch et al., 2013). These conditions have led to radiations of and within many groups (Mittermeier et al. 2004). Also, African and mainland Asian monitors tend to be large and are aquatic or terrestrial. Small size in *Varanus* evolved twice independently, once southeast Asia and again in Australia, the Australian radiation having given rise to the diverse pygmy monitor subgenus, *Odatria* (Pianka, 2004; Pianka, 2012). Half of the Australian varanid members are made up of the pygmy *Odatria* group, and many species in the country overlap in geographic and size range (Pianka, 2004). Variation in size might reduce competition among *Varanus* and increase diversity in some regions.

The fossil record, as well as the Vidal et al. 2012 paper, both suggest an Asian origin for monitors, and lineages may have entered both African and Australian regions around the same time (based on divergence dates). Many of the factors mentioned above, such as size differentiation across regions, habitat variability, taxonomic co-occurrences, and human impact are possible influences of the regional diversity and PD differences among monitors today and through time. Other work in this dissertation will focus on varanid diversity patterns by means of morphology, comparing patterns of shape and ecology, size and shape, fossil and extant varanids, range size and shape, and temporal shape patterns.

Conclusions

In this study I have compared different phylogenetically weighted diversity measures through time. These metrics represent a phylogenetically dedicated way of measuring biodiversity. PWD metrics have been embraced in community ecology, but ecological patterns are subject to evolutionary processes. Placing them in a temporal context lends an evolutionary perspective to these ecological metrics. Second, by comparing several diversity metrics, we can begin to parse out the processes underlining patterns by

observing how they change synchronously or independently at any given time. Finally, it is important to note that different processes can produce the same patterns, and understanding the history of a group is essential for determining which processes may have impacted results.

I applied this PWD framework with simulated, a fossil canid and molecular varanid trees. I found that tree shape is a significant influencer of PD through time. Extinction may not only reduce overall taxic diversity, but depending on where it occurs across a tree, it can cause differential effects on phylogenetic diversity metrics. Also, if origination through time produces many taxa, but with short durations, diversity counts may be stable but phylogenetically weighted diversity will reflect the underlying tree dynamics. In my study, disconnect of taxic counts and phylogenetic diversity metrics occurred both across the whole tree through time, and among clades and regions. Depending on the objectives of the study, traditional diversity counts alone may not answer specific questions of interest. Phylogenetic diversity metrics can be used complimentarily to traditional diversity counts to gain a better understanding of the impact of evolutionary history in patterns today and through time.

My results act as a springboard for a more rigorous investigation aligning evolutionary history with diversity. I imagine many possible directions for future research. Phylogenetic reconstructions are a major aspect of paleontological and neontological research. Because of this increase in cladistic work, studies can more readily integrate a phylogenetic approach to diversity studies. The framework of my study has provided a manageable means of quantifying evolutionary history in regard to diversity. Community ecology phylogenetic diversity metrics rely heavily on the definitions of community. It is important to be clear on the diagnosis of community used to understand what the results are showing in regard to the subset of taxa being studied. Second, I have used these phylogenetic diversity metrics in a temporal context, but this is only the first step toward developing a way to compare hypotheses or predict temporal patterns. For example, testing simulations can act as a starting point for generating testable hypotheses.

A focus of the second half of this project was on comparing total and chainsawed PWD of two major canid clades and regions in varanids. Previous studies have focused on the taxonomic diversity of these groups to distinguish between regional or clade diversity (Tedford, Taylor, and Wang, 1995; Wang, Tedford, and Taylor, 1999; Vidal et al. 2012). Although taxic diversity has allowed for quantitative comparisons of these patterns, by including phylogenetic diversity patterns we can extend measures to other scales or more easily infer mechanistic processes. This study has not used or determined any overarching theory to distinguish between underlying processes, but using a phylogenetic framework for temporal diversity has the potential to test causal hypotheses more efficiently, and compare various scales of clade dynamics.

Acknowledgements

First, I thank my adviser, Dr. Kevin Padian, for his advice and guidance in the development and throughout the duration of this project. This research began as a phylogenetics class project led by Drs. Brent Mishler and David Lindberg, who I wish to thank for introducing me to these methods and lines of questioning. Drs. Patricia Holroyd and Charles Marshall were instrumental in discussing methods and results. Last, but not least, I thank Dr. Nicholas Matzke who helped with the generation of much of the code in this study as well as discussion.

References

"What is biodiversity?". United Nations Environment Programme, World Conservation Monitoring Centre.

Bowers, J. E., B.A. Chapman, J. Rong and A.H. Paterson. 2003. Unravelling angiosperm genome evolution by phylogenetic analysis of chromosomal duplication events. Nature, 422: 433-438.

Cadotte, M.W., T.J. Davies, J. Regetz, S.W. Kembel, E. Cleland, and T.D. Oakley. 2010. Phylogenetic diversity metrics for ecological communities: integrating species richness, abundance and evolutionary history. Ecology Letters, 13: 96-105.

Cavender-Bares, J., K. H. Kozak, P. V. A. Fine, and S. W. Kembel. 2009. The merging of community ecology and phylogenetic biology. Ecology Letters, 12: 693–715.

Clarke, K.R., and R. M. Warwick. 1999. The taxonomic distinctness measure of biodiversity: weighting of step lengths between hierarchical levels. Mar Ecol Prog Ser, 184: 21-29.

Colwell, R. K. 2009. Biodiversity: Concepts, Patterns and Measurement. In: Simon A. Levin. The Princeton Guide to Ecology. Princeton: Princeton University Press. pp. 257–263.

Conrad, J. L., A.M. Balcarcel, and C.M. Mehling. 2012. Earliest Example of a Giant Monitor Lizard (Varanus, Varanidae, Squamata). Plos One, *7*(8), e41767-e41767.

Convention on Biological Diversity. 1992. Secretariat of the Convention on Biological Diversity, Montreal, Canada

Davies, T. J., and L. B. Buckley. 2011. Phylogenetic diversity as a window into the evolutionary and biogeographic histories of present-day richness gradients for mammals. Philosophical Transactions of the Royal Society B: Biological Sciences, 366 (1576): 2414-2425.

Faith D.P. 1992. Conservation evaluation and phylogenetic diversity. Biological Conservation, 61: 1-10.

Faith, D. P., and A. M. Baker. 2006. Phylogenetic diversity (PD) and biodiversity conservation: some bioinformatics challenges. Evolutionary bioinformatics online, 2: 121-128.

Felsenstein J. 1985. Phylogenies and the comparative method. Am Nat, 125:1-15.

Finarelli, J. A. 2007. Mechanism behind active trends in body size evolution of the Canidae (Carnivora: Mammalia). The American Naturalist, 170(6): 876-885.

Foote, M. 1997. The evolution of morphological diversity. Annual Review of Ecology and Systematics, 28: 129-152.

Graham, C. H., and P. V. Fine. 2008. Phylogenetic beta diversity: linking ecological and evolutionary processes across space in time. Ecology letters,11(12):1265-1277.

Harmon, L. J, J. T. Weir, C. D. Brock, R. E Glor, and W. Challenger. 2008. GEIGER: investigating evolutionary radiations. Bioinformatics, 24:129-131.

Harzsch, S. and G. Hafner. 2006. Evolution of eye development in arthropods: phylogenetic aspects. Arthropod Struct. Dev., 35: 319–40.

Helmus, M. R.,T. J. Bland, C. K. Williams, and A. R. Ives. 2007. Phylogenetic measures of biodiversity. Am. Nat., 169(3), E68-E83.

Holmes, R. B., A. M. Murray, Y. S. Attia, E. L. Simons, and P. Chatrath. 2010. Oldest known Varanus (Squamata: Varanidae) from the Upper Eocene and Lower Oligocene of Egypt: support for an African origin of the genus. Palaeontology, 53:1099-1110.

Jablonski, D. and J. A. Finarelli. 2009. Congruence of morphologically-defined genera with molecular phylogenies. PNAS, 106 (20): 8262-8266.

Kembel, S. W., P. D. Cowan, M. R. Helmus, W. K. Cornwell, H. Morlon, D. D. Ackerly, S. P. Blomberg, and C. O. Webb. 2010. Picante: R tools for integrating phylogenies and ecology. Bioinformatics, 26:1463-1464.

Koch, A., T. Ziegler, W. Böhme, E. Arida, and M. Auliya. 2013. Pressing problems: distribution, threats, and conservation status of the monitor lizards (Varanidae: Varanus ssp.) of Southeast Asia and the Indo-Australian Archipelago. Herpetological Conservation and Biology, 8: 1-62.

Lane, A., C.M. Janis, and J. Sepkoski Jr. 2005. Estimating paleodiversities: a test of the taxic and phylogenetic methods. Paleobiology, 31: 21-34.

Lee, A.C. and B. Mishler. 2014. Phylogenetic Diversity and Endemism: Metrics for Identifying Critical Regions of Conifer Conservation in Australia. Berkeley Scientific Journal, 18(2). our_bsj_22486.

Maddison, W. P., and D.R. Maddison. 1989. Interactive analysis of phylogeny and character evolution using the computer program MacClade. Folia Primatol (Basel),. 53(1-4):190-202.

Marshall, C.R. 1991. Estimation of taxonomic ranges from the fossil record. In: Analytical Paleobiology, ed. NL Gilinsky, PW Signor, pp. 19–38. Knoxville, TN: Paleontol. Soc.216 pp.

Matzke, N. 2011. " _R_tree_functions_v1.R: many useful utility functions for dealing with phylogenetic trees in R." (http://ib.berkeley.edu/courses/ib200b/scripts/_R_tree_functions_v1.R)

Miles, D. B. and Dunham, A. E. 1993. Historical perspectives in ecology and evolutionary biology: the use of phylogenetic comparative analyses. Annu. Rev. Ecol. Syst., 24: 587–619.

Mishler, B. D., N. Knerr, C. E. González-Orozco, A. H. Thornhill, S. W. Laffan, and J. T. Miller. 2014. Phylogenetic measures of biodiversity and neo-and paleo-endemism in Australian Acacia. Nature communications, 5.

Mittermeier, R.A., P.R. Gil, M. Hoffman, J. Pilgrim, T. Brooks, C.G. Mittermeier, J. Lamoreux, and G.A.B. da Fonseca. 2004. Hotspots Revisited: Earth's Biologically Richest and Most Threatened Terrestrial Ecoregions. Cemex, Conservation International, Mexico City, Mexico

Molles, M. C., Jr. 2000. Ecology: Concepts and Applications. Boston: McGraw-Hill.

Molnar, R. E. 2004. Dragons in the Dust: The Paleobiology of the Giant Monitor Lizard Megalania. Indiana University Press (Bloomington/Indianapolis)

Norell, M. A. 1992. Taxic origin and temporal diversity: the effect of phylogeny. In: Extinction and Phylogeny, pp. 89-118. Colombia University Press, New York.

Norell, M. A. 1993. Tree-based approaches to understanding history; comments on ranks, rules and the quality of the fossil record. American Journal of Science, 293(A): 407-417.

Norell, M. A. 1996. Ghost Taxa, Ancestors, and Assumptions: A Comment on Wagner. Paleobiology, 22(3):453-455.

Oksanen, J., F. G. Blanchet, R. Kindt, P. Legendre, P. R. Minchin, R. B. O'Hara, G. L. Simpson, P. Solymos, M.H. Stevens and H. Wagner. 2015. Vegan: Community Ecology Package. R package version 2.2-1. http://CRAN.R-project.org/package=vegan

Pagel, M. 1999. Inferring the historical patterns of biological evolution. Nature,401(6756): 877-884.

Pianka E. R. 2004. Evolution of body size and reproductive tactics. In: Varanoid Lizards of the World. Pp. 549-555. Editors, Pianka ER, King DR. Indiana University Press, Bloomington, Indiana, USA.

Pianka, E. R. 2012. Can humans share spaceship earth. Amphibian and Reptile Conservation, 6(1): 1-24.

Paradis, E., J. Claude and K. Strimmer. 2004. APE: analyses of phylogenetics and evolution in R language. Bioinformatics, 20: 289-290.

Phillips, J. 1860. Life on the Earth: Its Origin and Succession, MacMillan

Quental, T. B., and C. R. Marshall. 2010. Diversity dynamics: molecular phylogenies need the fossil record. Trends in Ecology and Evolution, 25(8): 434-441.

R Hackathon et al. 2014. Phylobase: Base package for phylogenetic structures and comparative data. R package version 0.6.8. http://CRAN.R-project.org/package=phylobase

Robeck, H.E., C. C. Maley and M. J. Donoghue. 2000. Taxonomy and temporal diversity patterns. Paleobiology 26(2): 171-187.

Roncal, J., A. Henderson, F. Borchsenius, S. R. Sodre-Cardoso, and H. Balslev. 2012. Can phylogenetic signal, character displacement, or random phenotypic drift explain the morphological variation in the genus Geonoma (Arecaceae)? Biological Journal of the Linnean Society 106: 528–539.

Ronquist, F. and I. Sanmart. 2011. Phylogenetic Methods in Biogeography. Annu. Rev. Ecol. Evol. Syst. 42:441-464.

Schweiger, O., S. Klotz, W, Durka, and I. Kühn. 2008. A comparative test of phylogenetic diversity indices. Oecologia, 157(3), 485-495.

Sepkoski Jr, J. J. 1982. Mass extinctions in the Phanerozoic oceans: a review. Geological Society of America Special Papers 190: 283-290.

Sepkoski Jr, J. J. 1992. A compendium of fossil marine animal families. Contributions in biology and geology/Milwaukee Public Museum 83: 1-156.

Sepkoski Jr, J. J. 1993. Ten Years in the Library: New Data Confirm Paleontological Patterns. Paleobiology 19: 43-51.

Tedford, R. H., X. Wang, and B. E. Taylor. 2009. Phylogenetic systematics of the North American fossil caninae (Carnivora: Canidae). Bulletin of the American Museum of Natural History: 1-218.

Tedford, R. H., B. E. Taylor, and X. Wang. 1995. Phylogeny of the Caninae (Carnivora, Canidae): the living taxa. American Museum Novitates 3146.

Van Valkenburgh, B., X. Wang, and J. Damuth. 2004. Cope's Rule, Hypercarnivory, and Extinction in North American Canids. Science 306 (5693): 101–104.

Vidal, N., J. Marin, J. Sassi, F. U. Battistuzzi, S. Donnellan, A. J. Fitch, B. G. Fry, et al. 2012. Molecular evidence for an Asian origin of monitor lizards followed by Tertiary dispersals to Africa and Australasia. Biology letters: rsbl20120460

Wagner, P.J. 1995. Stratigraphic tests of cladistic hypotheses. Paleobiology 21:153-178.

Wagner, P. J. 1996. Contrasting the underlying patterns of active trends in morphologic evolution. Evolution 50(3): 990-1007.

Wagner, P. J. 2000. The quality of the fossil record and the accuracy of phylogenetic inferences about sampling and diversity. Systematic Biology 49(1): 65-86.

Wang, X., R. H. Tedford, and B. E. Taylor. 1999. Phylogenetic systematics of the Borophaginae (Carnivora, Canidae). Bulletin of the AMNH 243.

Webb, C. O., D. D. Ackerly and S. W. Kembel. 2008. Phylocom: software for the analysis of phylogenetic community structure and trait evolution. Bioinformatics, 24: 2098-2100.

Webb, C. O., D. D. Ackerly, M. A. McPeek and M.J. Donoghue. 2002. Phylogenies and community ecology. Annu. Rev. Ecol. Syst. 33: 475–505.

Whittaker, R.H. 1972. Evolution and measurement of species diversity. Taxon 21: 213–251.

Wilson, E. O., (ed.) 1988. BioDiversity. Washington: National Academy Press.

Table 1. Canid mean nearest taxon distance (MNTD) measures with effect size standardized results (Gray shaded boxes) from 1000 runs. Negative Z values and low quantiles ($p < 0.05$) indicate clustering (bolded results).

Time bin	SR	Observed MNTD	Randomized mean	Randomized Stand. Dev.	Observed rank	Observed Z	Observed p
35-30	20	12.26238	8.156776	1.3385228	998	3.067268	0.998
30-25	23	11.65649	7.634785	1.1455625	998	3.510679	0.998
25-20	31	9.0337	6.617001	0.8805016	997	2.744684	0.997
20-15	44	7.687752	5.577191	0.6266936	998	3.367771	0.998
15-10	41	4.035637	5.775414	0.6679313	1	**-2.604725**	**0.001**
10-5'	39	5.189438	5.90922	0.6963145	156	**-1.033702**	0.156
5-0'	41	2.417035	5.785841	0.6884261	1	**-4.89349**	**0.001**

Table 2. Varanid mean nearest taxon distance (MNTD) measures with effect size standardized results (Gray shaded boxes) from 1000 runs. More positive Z values, and quantiles (p) closer to one indicate more evenness among taxa. Results for the recent time bin (5-0 Mya) are not significant in resampling since all taxa on the tree exist in the community.

Time bin (Mya)	SR	Observed MNTD	Randomized mean	Randomized Stand. Dev.	Observed rank	Observed Z	Observed p
40-35	3	71.08741	51.09173	11.2932839	952	1.770581	0.952
35-30	5	60.89514	45.48661	8.7372855	978	1.763538	0.978
30-25	6	56.33985	43.24898	8.2178717	965	1.592976	0.965
25-20	10	48.69745	37.28124	5.6744542	986	2.01186	0.986
20-15	18	38.13624	30.37761	3.1650316	997	**2.451359**	**0.997**
15-10	24	33.5305	27.27592	2.1440949	1000	**2.91712**	**1**
10-5'	36	24.9472	23.16453	0.7583346	996	**2.350766**	**0.996**
5-0'	39	22.51459	22.51459	0	500.5	NA	0.5005

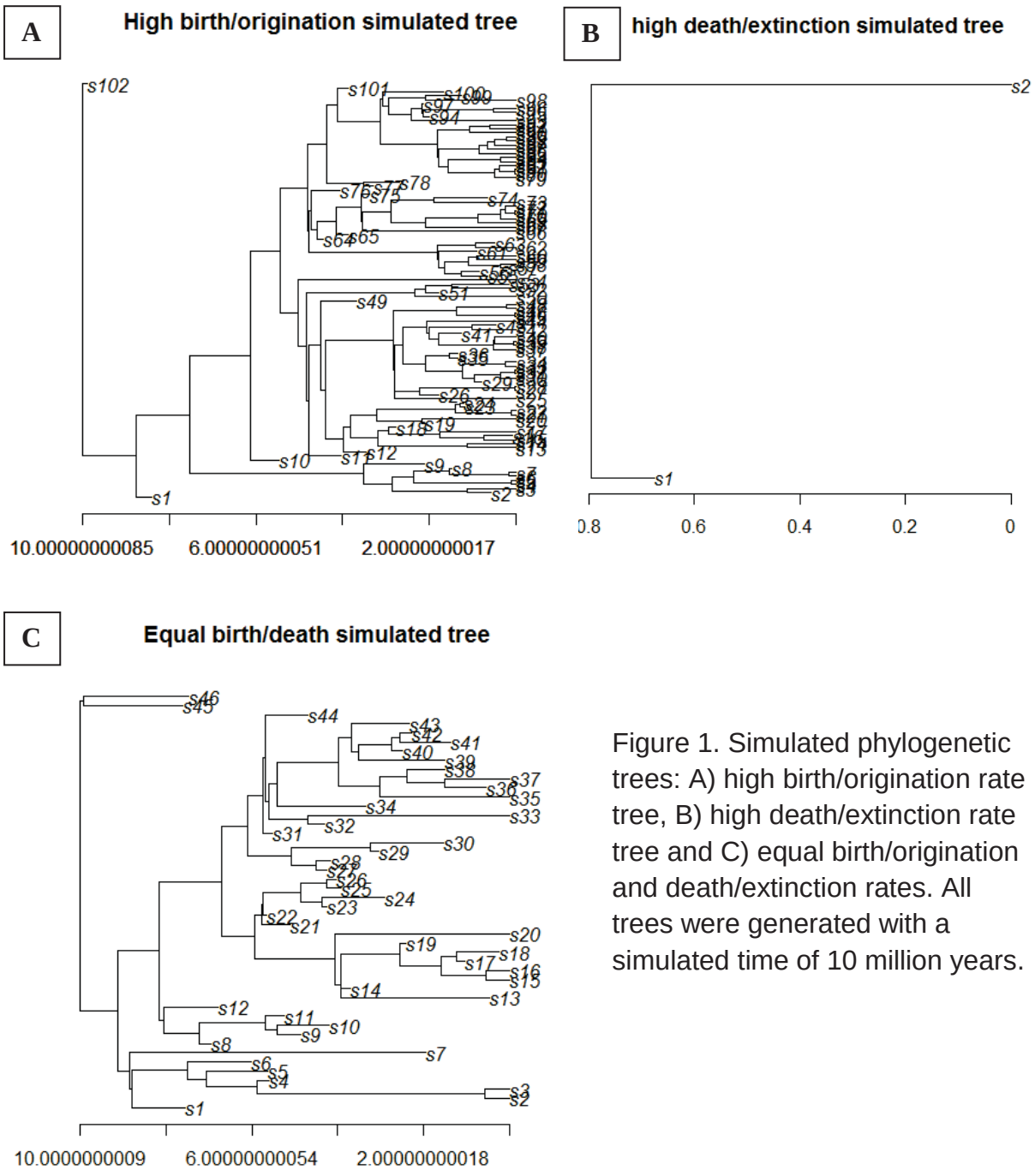


Figure 1. Simulated phylogenetic trees: A) high birth/origination rate tree, B) high death/extinction rate tree and C) equal birth/origination and death/extinction rates. All trees were generated with a simulated time of 10 million years.

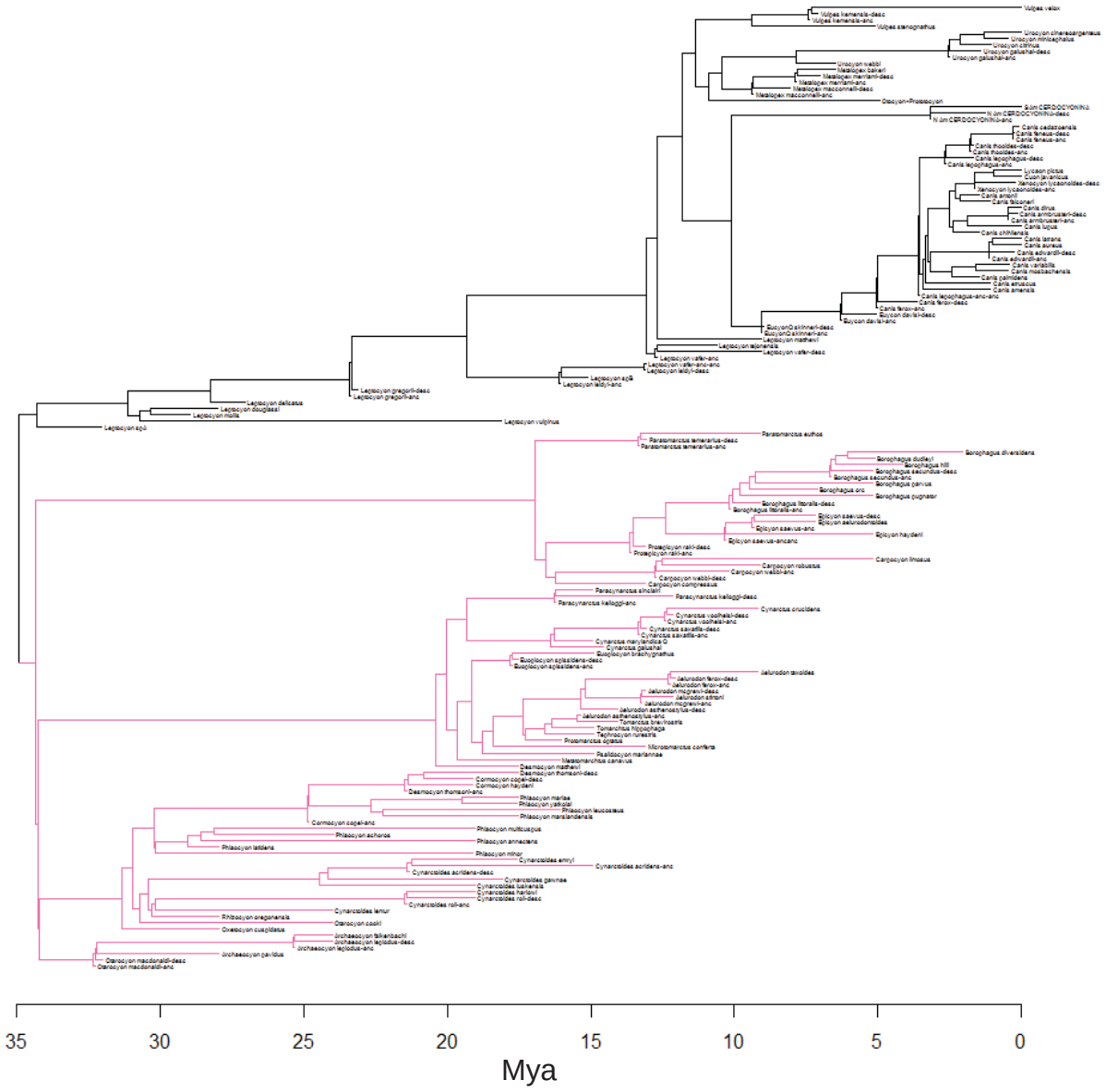


Figure 2. Modified canid tree from Tedford, Taylor and Wang (1995) and Wang, Tedford, and Taylor (1999). Subfamilies are color coded: Pink= Borophaginae, and Black = Caninae. A table of the 154 taxa on the tree can be found in Appendix 1.

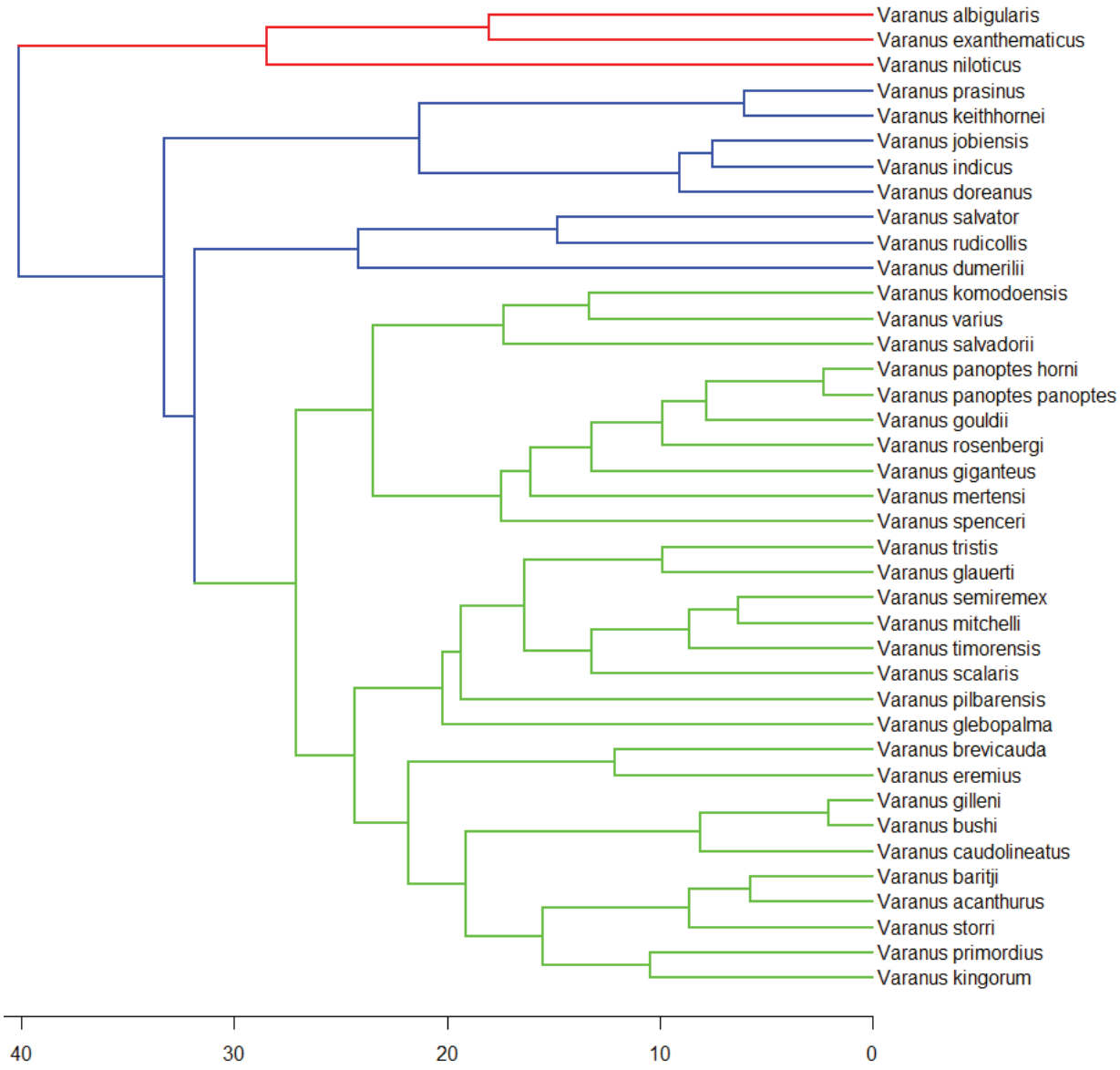


Figure 3. *Varanus* tree modified from Vidal et al. 2012. Branches are color coded to regions: Red=Africa, Blue=Indo-Asia, and Green=Indo-Australia. Regions are based on groupings used in Vidal et al. 2012. Notice that regional groups tend to be monophyletic.

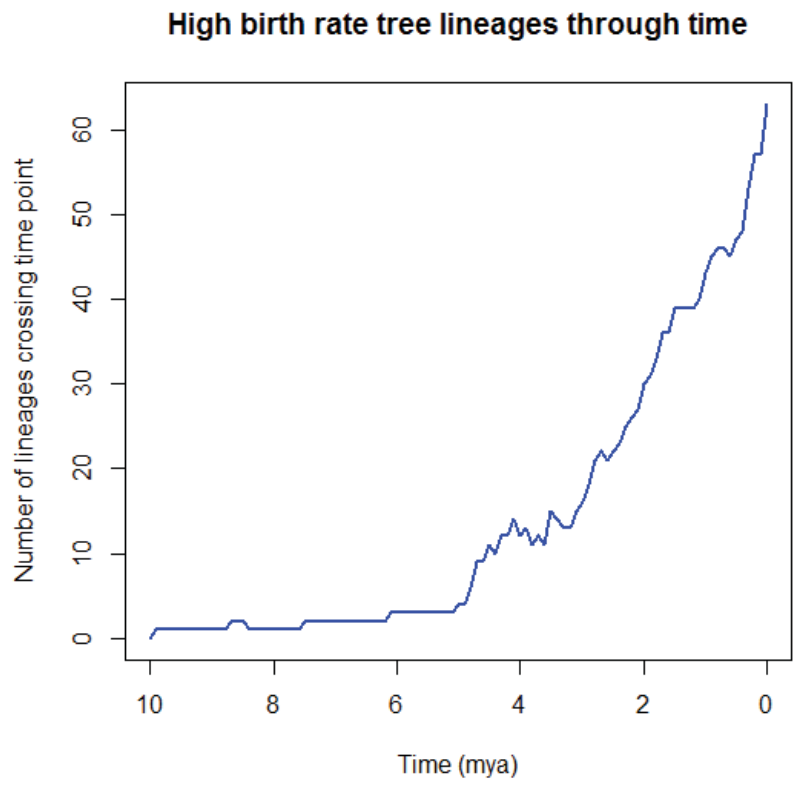


Figure 4 (A). Lineage through time plots for simulated trees: A) High-birth tree

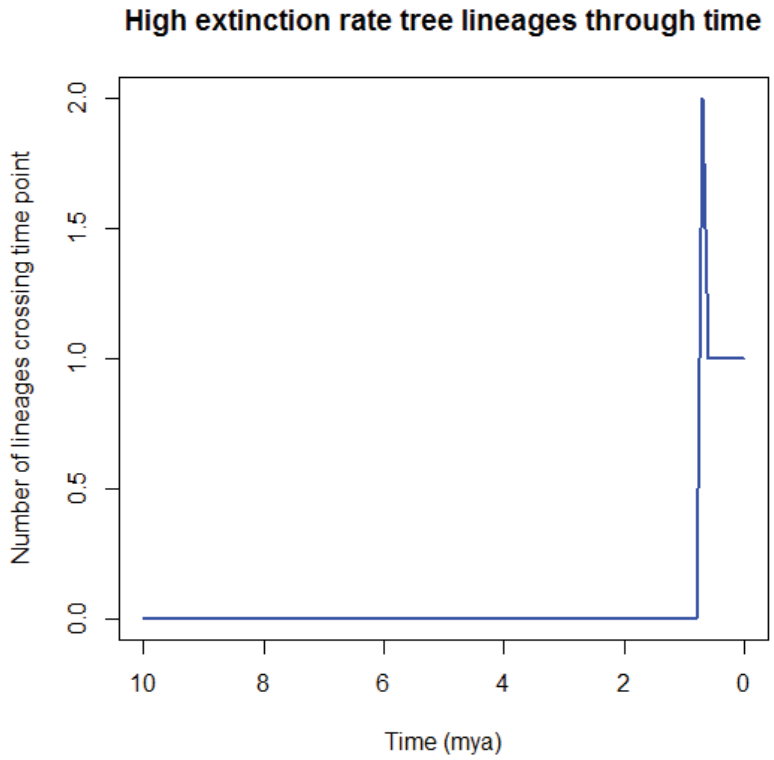


Figure 4 (B). Lineage through time plots for simulated trees: B) high-death tree

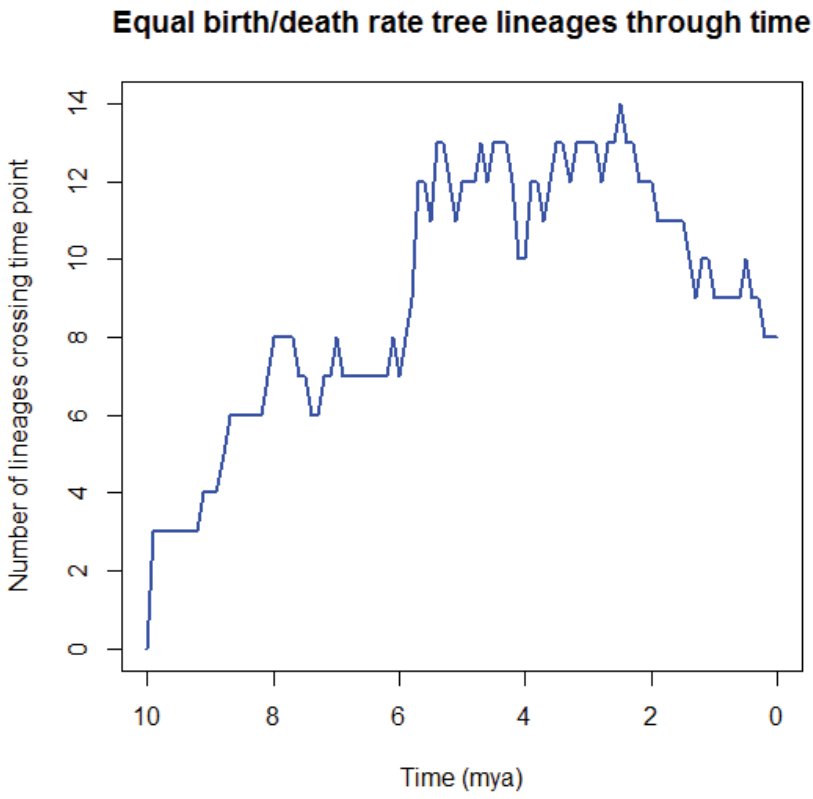


Figure 4 (C). Lineage through time plots for simulated trees: C) equal birth-death tree.

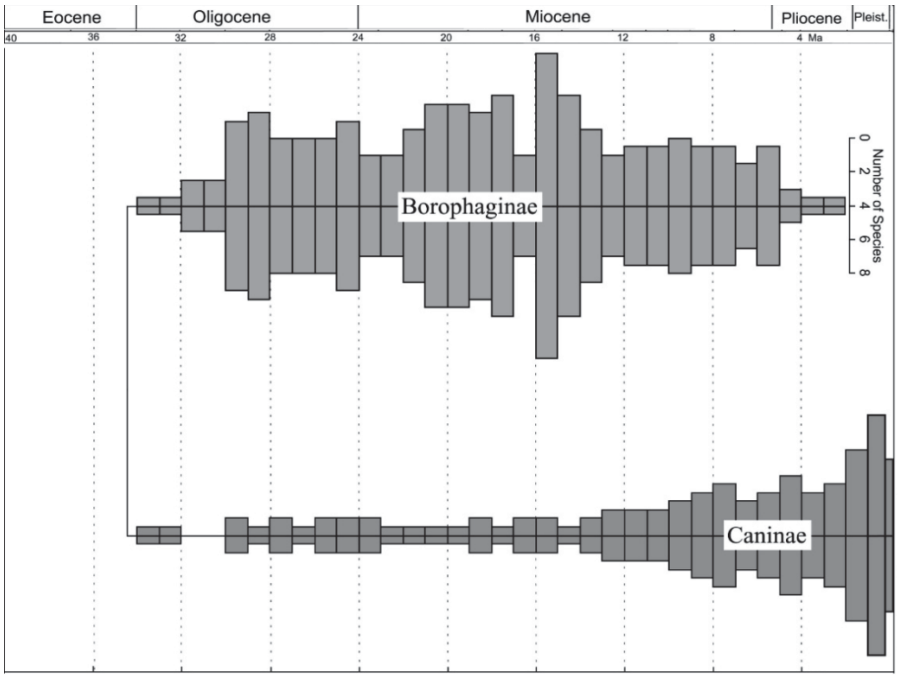


Figure 5. Modified spindle diagram of species diversity of the Borophaginae and Caninae through time from Tedford, Wang, and Taylor 2009).

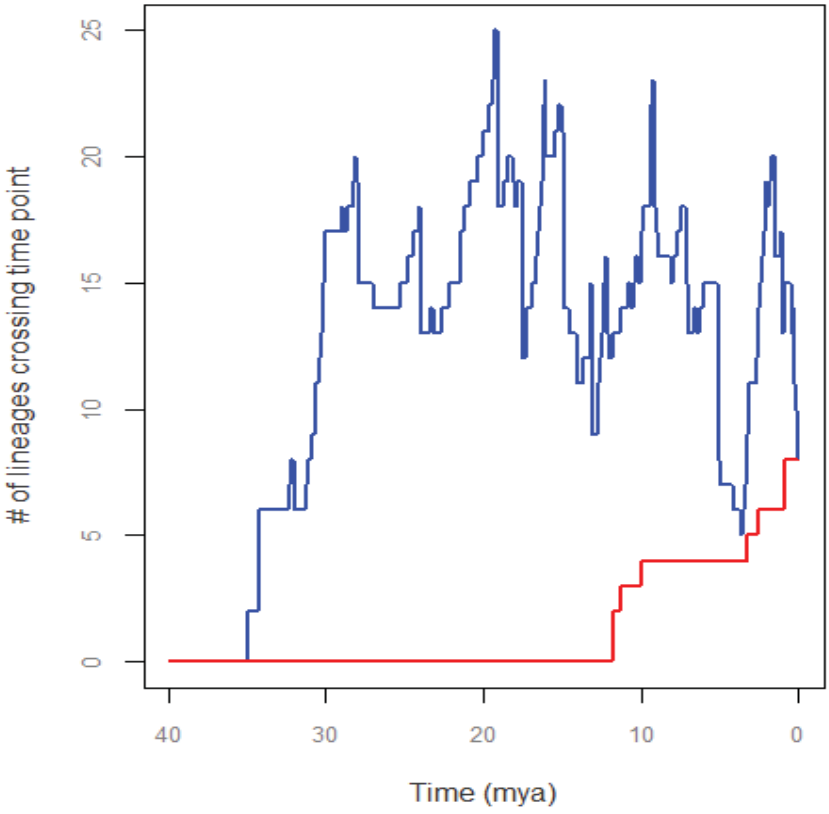


Figure 6. Canid lineage through time plot based on the phylogeny from Figure 2. The blue line represents all taxa in the tree, and the red line is without fossil taxa (only including lineages that extend to the present).

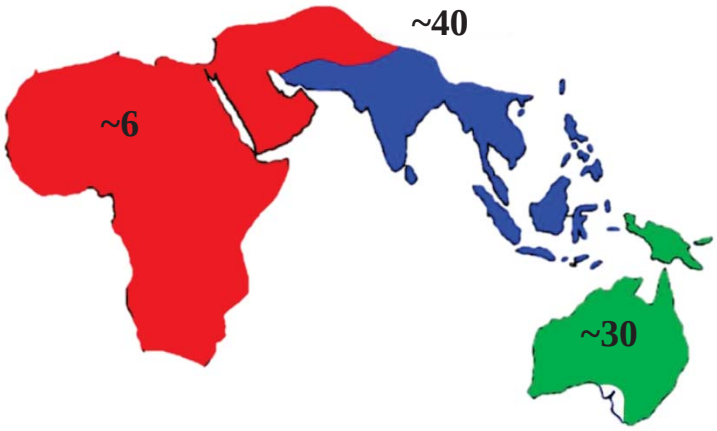


Figure 7. Extant varanid geographic range. Colors are representative of regional groups: red- Africa, blue – Indo-Asia, and green – Indo-Australia. Numbers are estimated species diversity in these regions

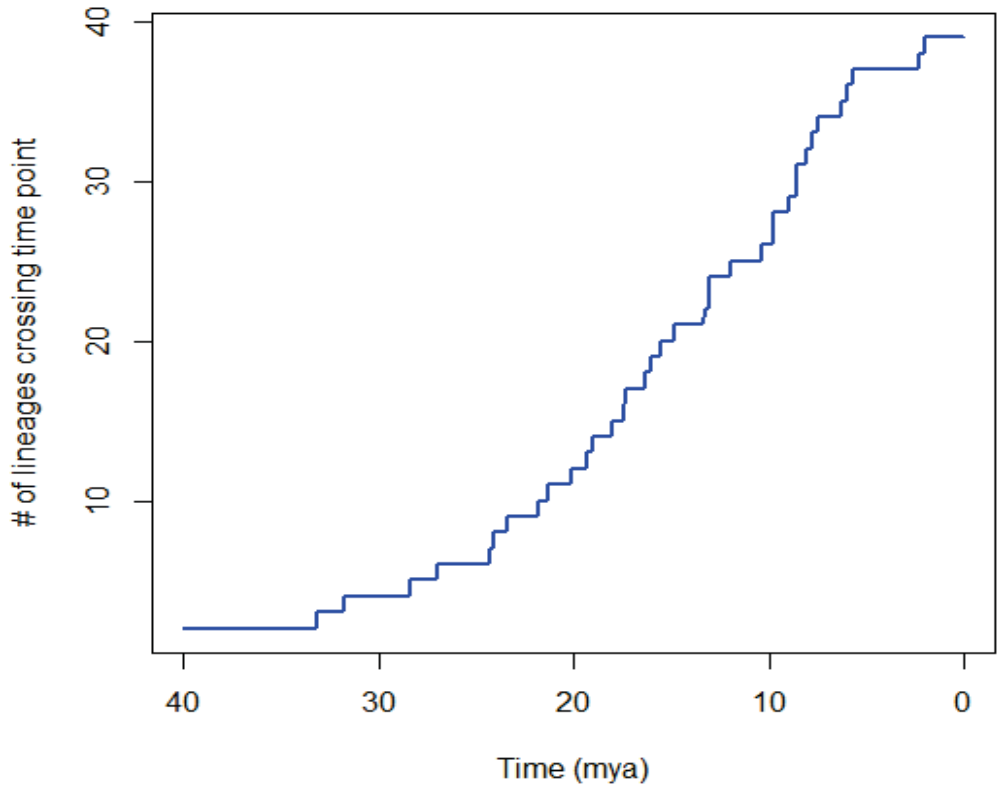


Figure 8. Varanus lineage through time plot of Vidal et al. 2012 phylogeny.

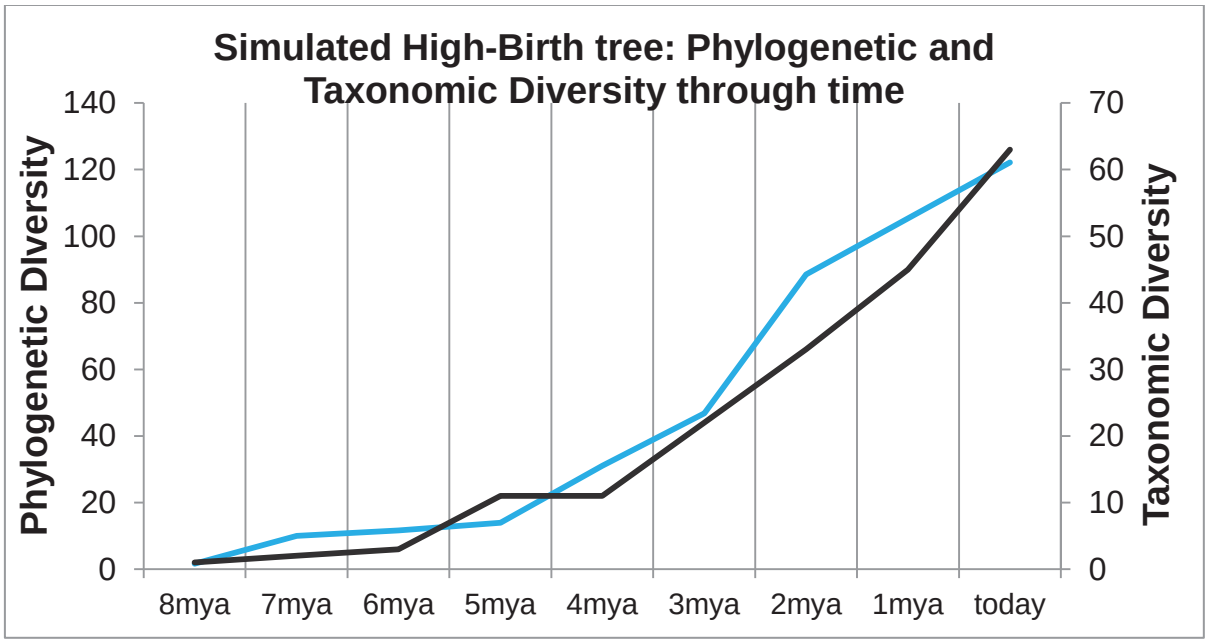


Figure 9. Simulated high-birth tree Phylogenetic Diversity (PD; blue) and total taxic richness (black) through time. PD was analyzed on communities defined by taxa existing in designated time bins.

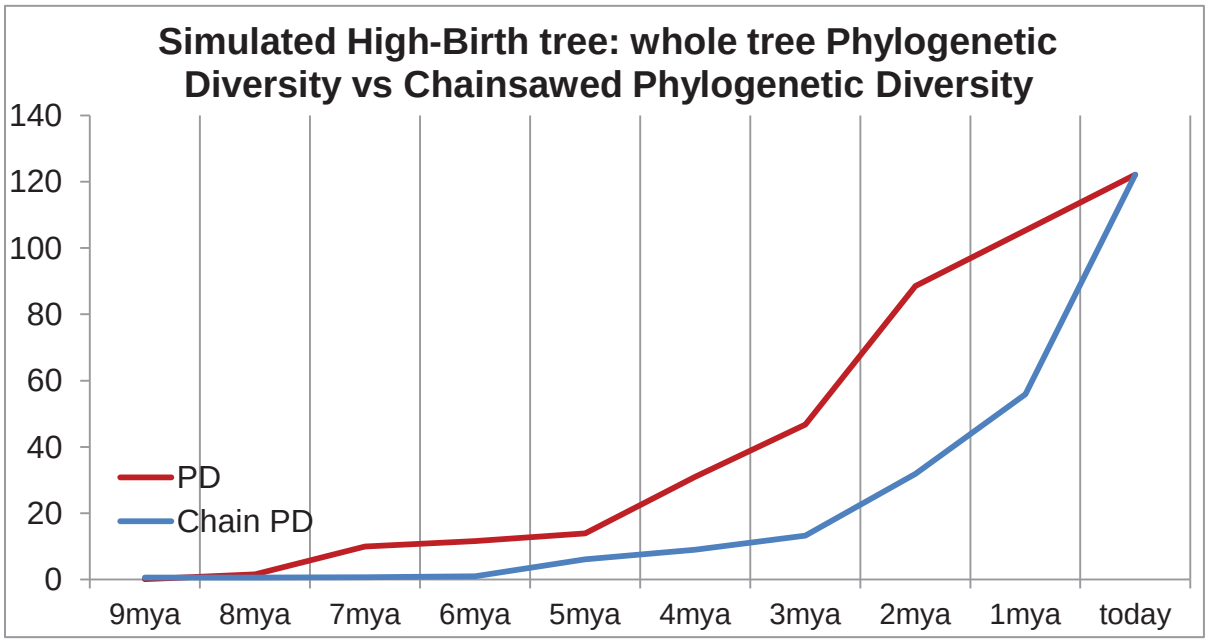


Figure 10. High-birth rate tree Phylogenetic Diversity (PD; red) versus chainsawed PD (blue) through time. PD was analyzed on communities defined by taxa existing in designated time bins.

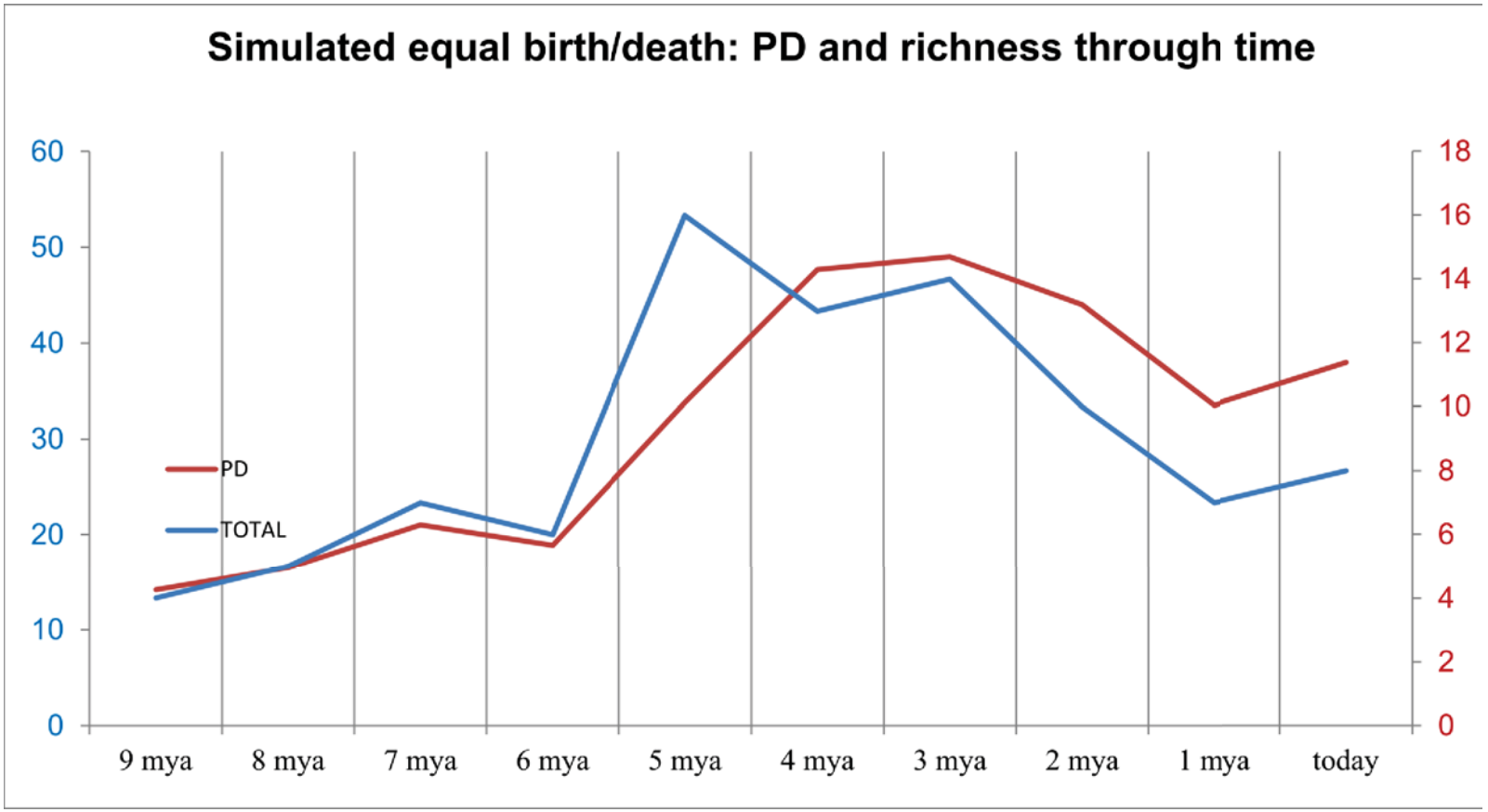


Figure 11. Simulated equal birth-death tree Phylogenetic Diversity (PD; red) versus taxic richness (blue) through time. Communities analyzed are defined as taxa existing in designated time bins.

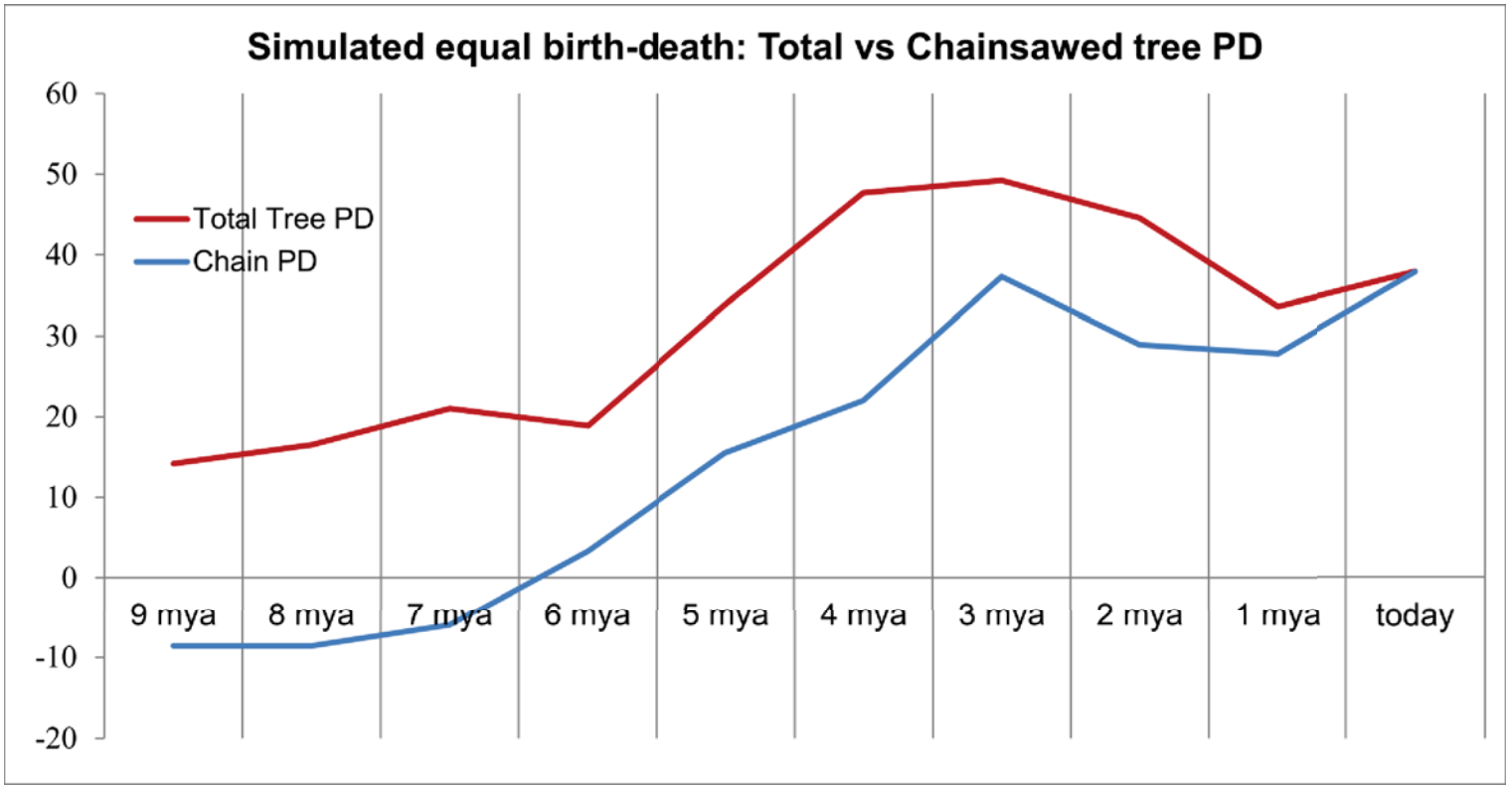


Figure 12. Simulated equal birth-death whole tree Phylogenetic Diversity (PD; red) versus chainsawed PD (blue). Communities analyzed are defined as taxa existing in designated time bins.

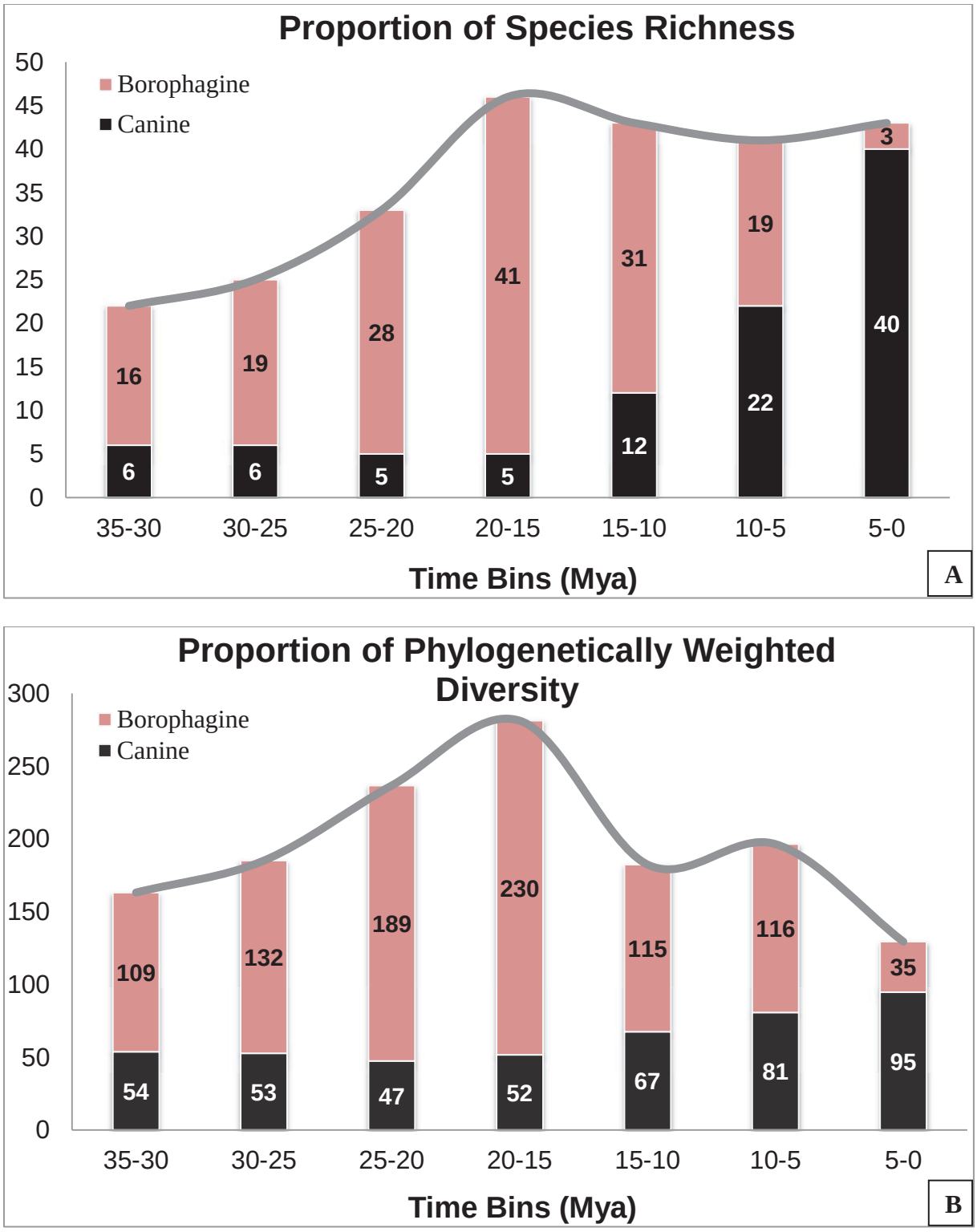


Figure 13. A) Proportion of species richness and B) phylogenetic diversity occupied by canine or borophagines through time on the phylogeny from Figure 2.

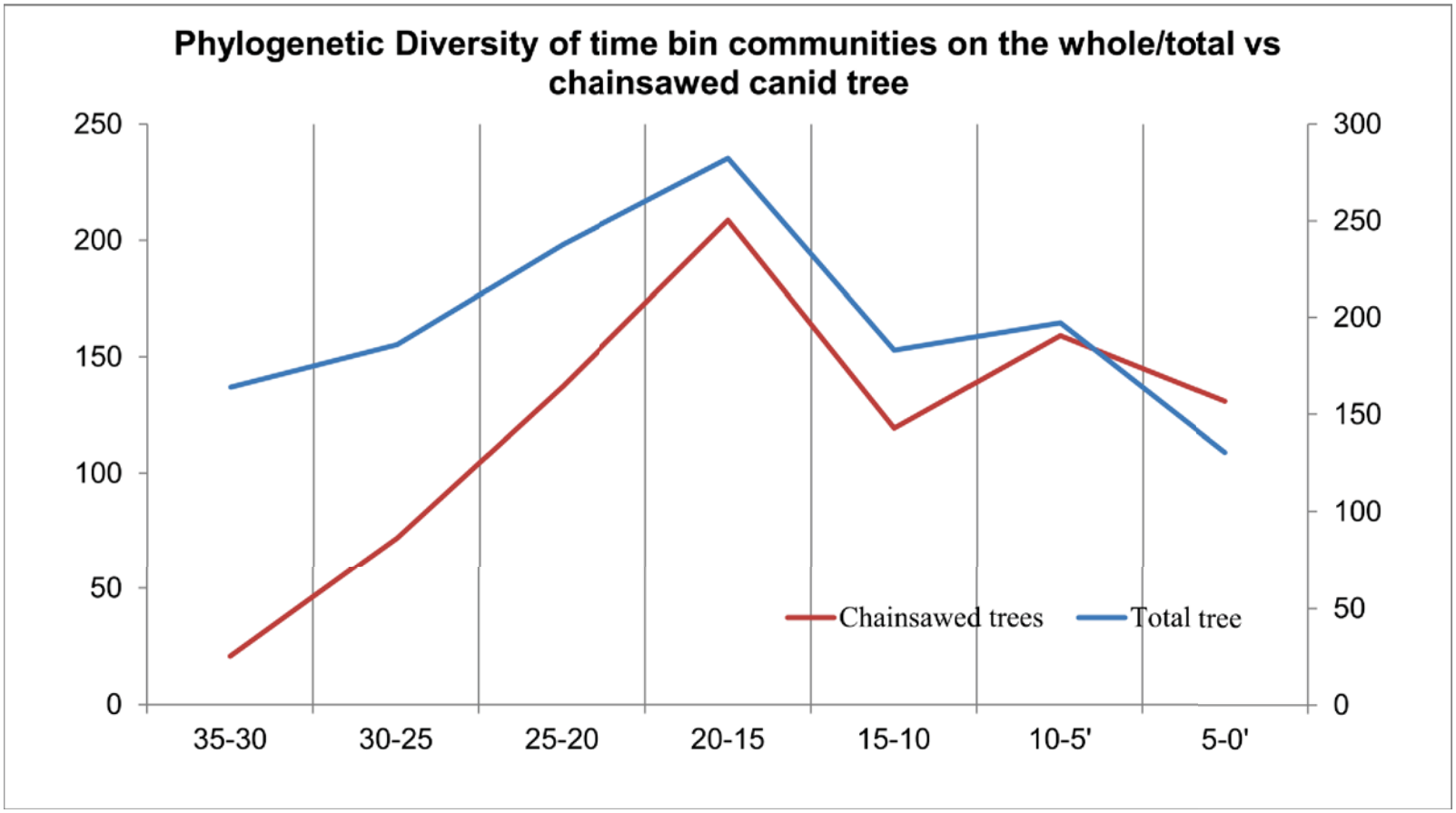


Figure 14. The canid (Fig. 2) total tree versus chainsawed tree Phylogenetic Diversity through time.

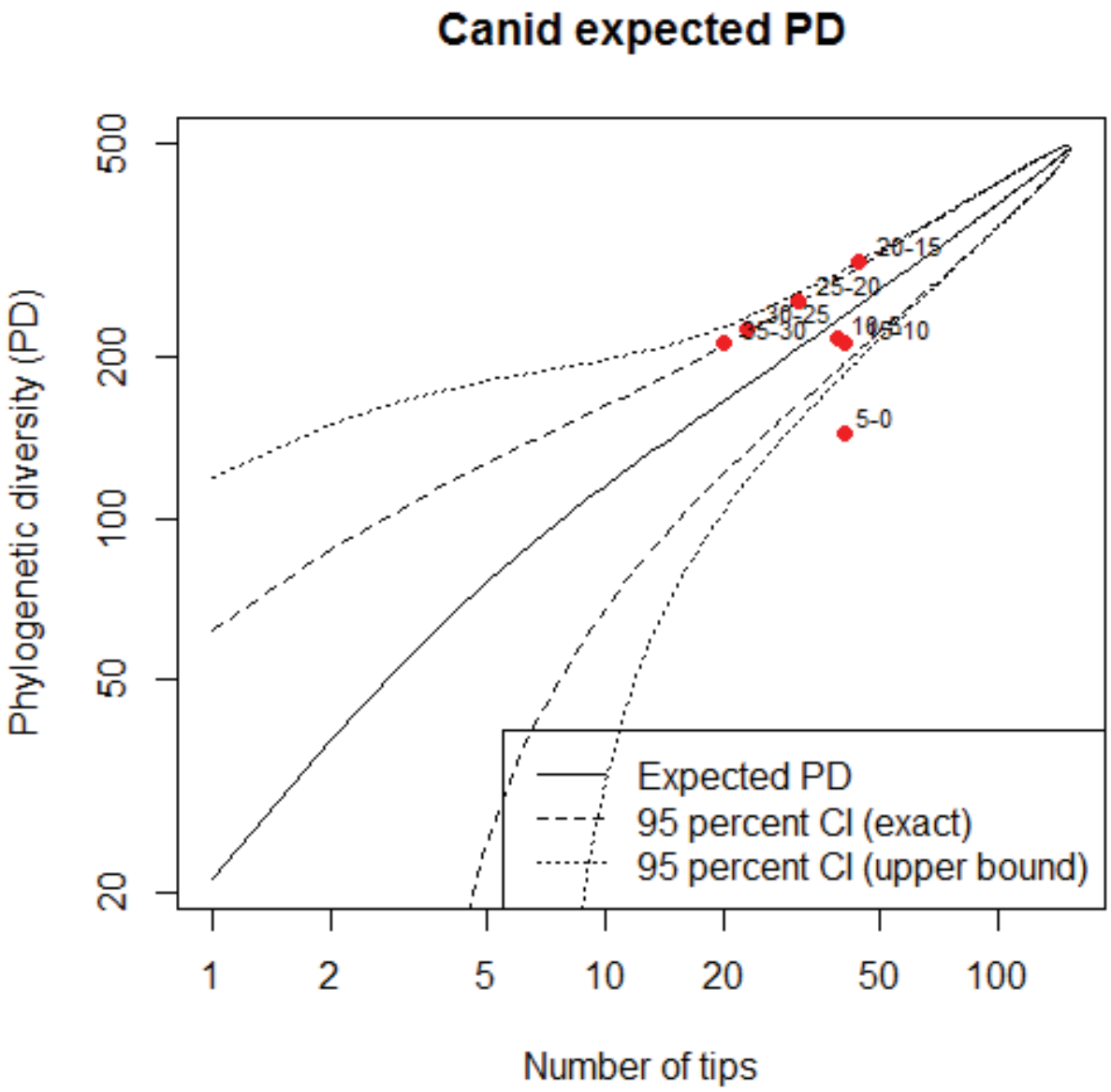


Figure 15. Canid tree expected Phylogenetic Diversity(PD) when resampled at different numbers of tree tips. Observed measures of total PD at specified time bins are plotted as red points. The most recent time bin (5-0 Mya) falls outside of expected range.

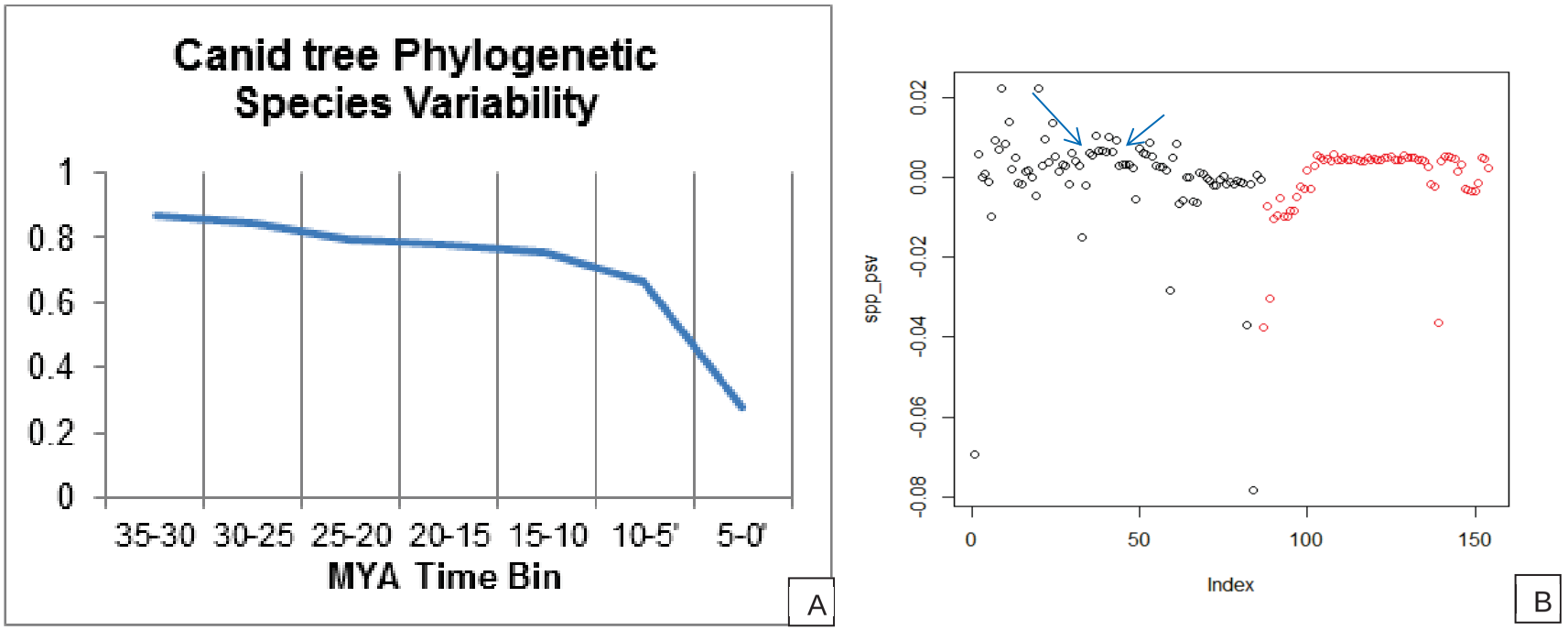


Figure 16. A) Canid Phylogenetic Species Variability (PSV) through time. B) Standardized PSV, or proportions of the total deviation from the mean PSV that occurs when all species are removed from the data set one at a time. The X axis spans all taxa on the tree: black = borophagines, and red = canines. Most taxa do not greatly deviate from the mean, and there is not much difference in distributions of mean deviations between canine and borophagines. Uppermost two taxa in borophagines (marked by arrows) are: *Phlaocyon latidens* and *Rhizocyon oregonensis*.

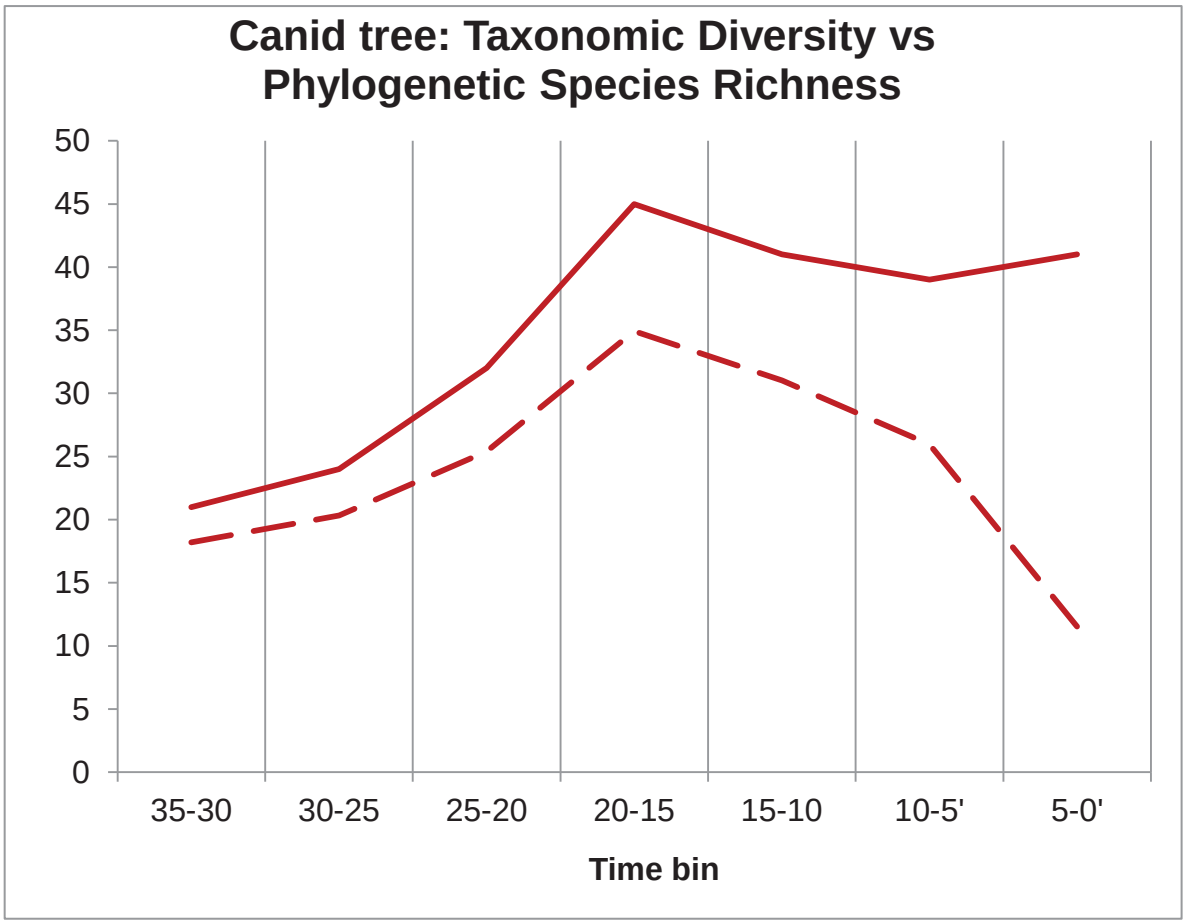
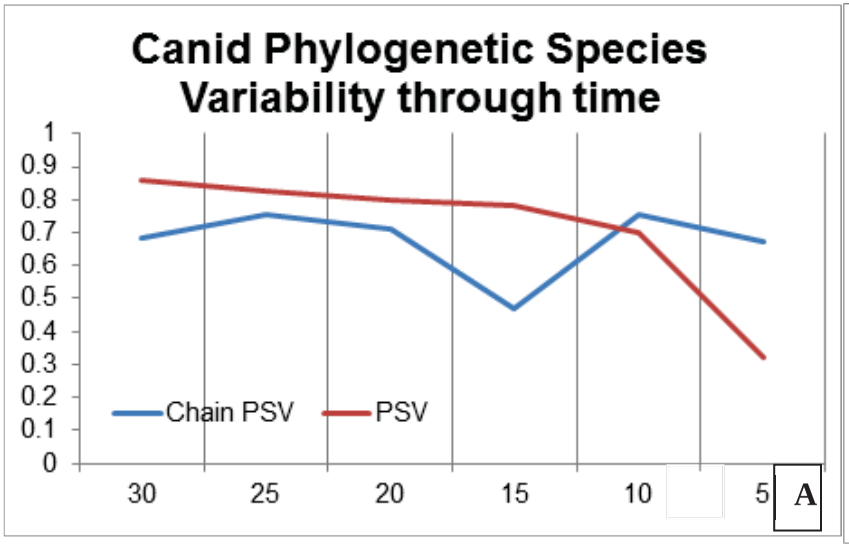


Figure 17. Canid tree taxonomic diversity (solid line) versus Phylogenetic Species Richness (dotted line) through time. Notice the different trends beginning 20-15 Mya.



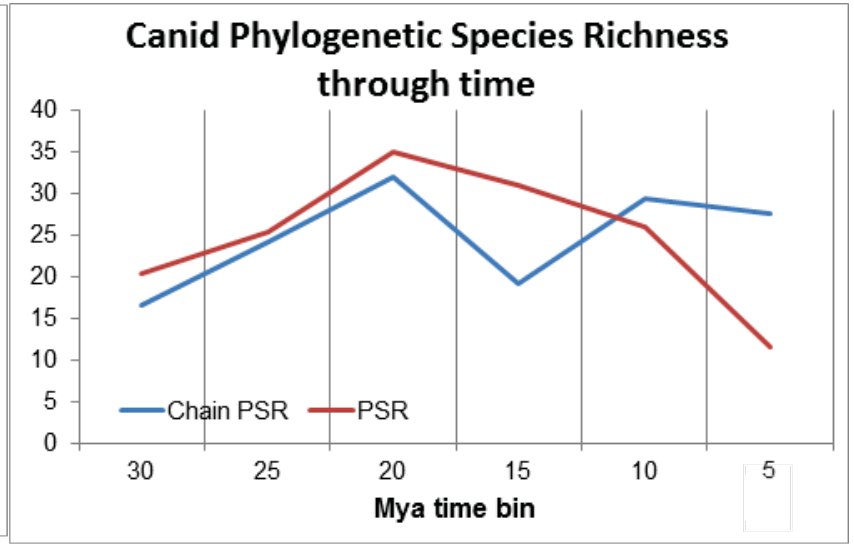
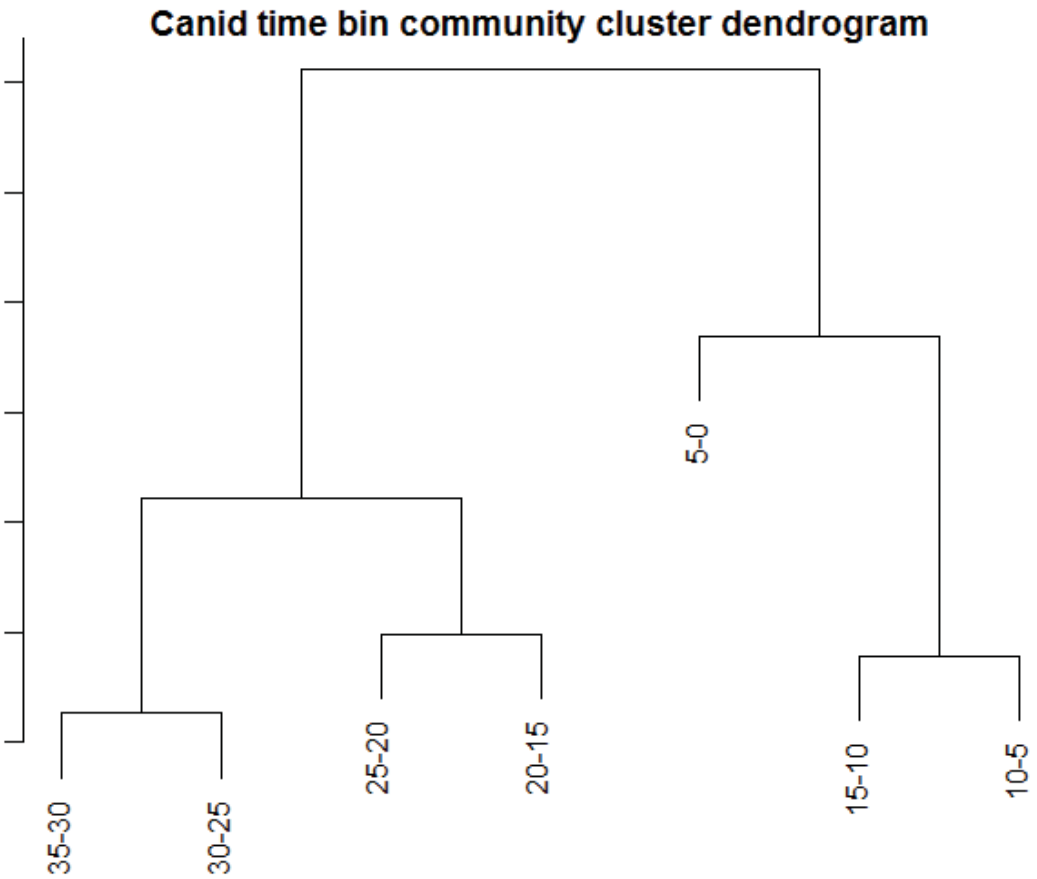


Figure 18. Total tree and chainsawed tree measures of A) canid Phylogenetic Species Variability through time and B) canid Phylogenetic Species Richness through time.



Distance measure between pairs of canid time bin communities.

	35-30	30-25	25-20	20-15	15-10	10-5
30-25	1.347381					
25-20	5.17417	3.931875				
20-15	11.1088	10.78364	4.913702			
15-10	18.15052	18.72733	19.30421	**11.0214**		
10-5	19.08448	20.01475	22.29138	16.75915	3.947396	
5-0	23.61086	24.54292	27.40229	30.55948	18.48037	6.460762

Figure 19. Time bin community dendrogram generated from the canid time bin distance matrix (below dendrogram). Time bins directly next to one another tend to clump, but notice the distinct separation of communities after 20 – 15 Mya.

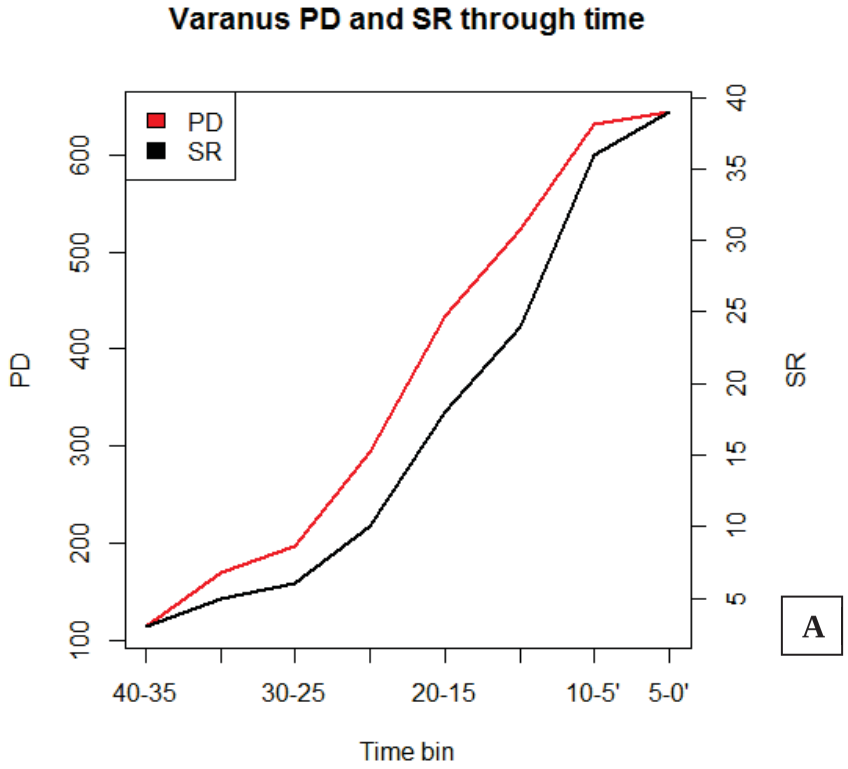




Figure 20. *Varanus* total tree analysis. A) *Varanus* Phylogenetic Diversity (PD) and Species Richness (SR) through time on the Vidal et al. 2012 phylogeny. B) Proportion of PD and SR made up of regional varanid groups.

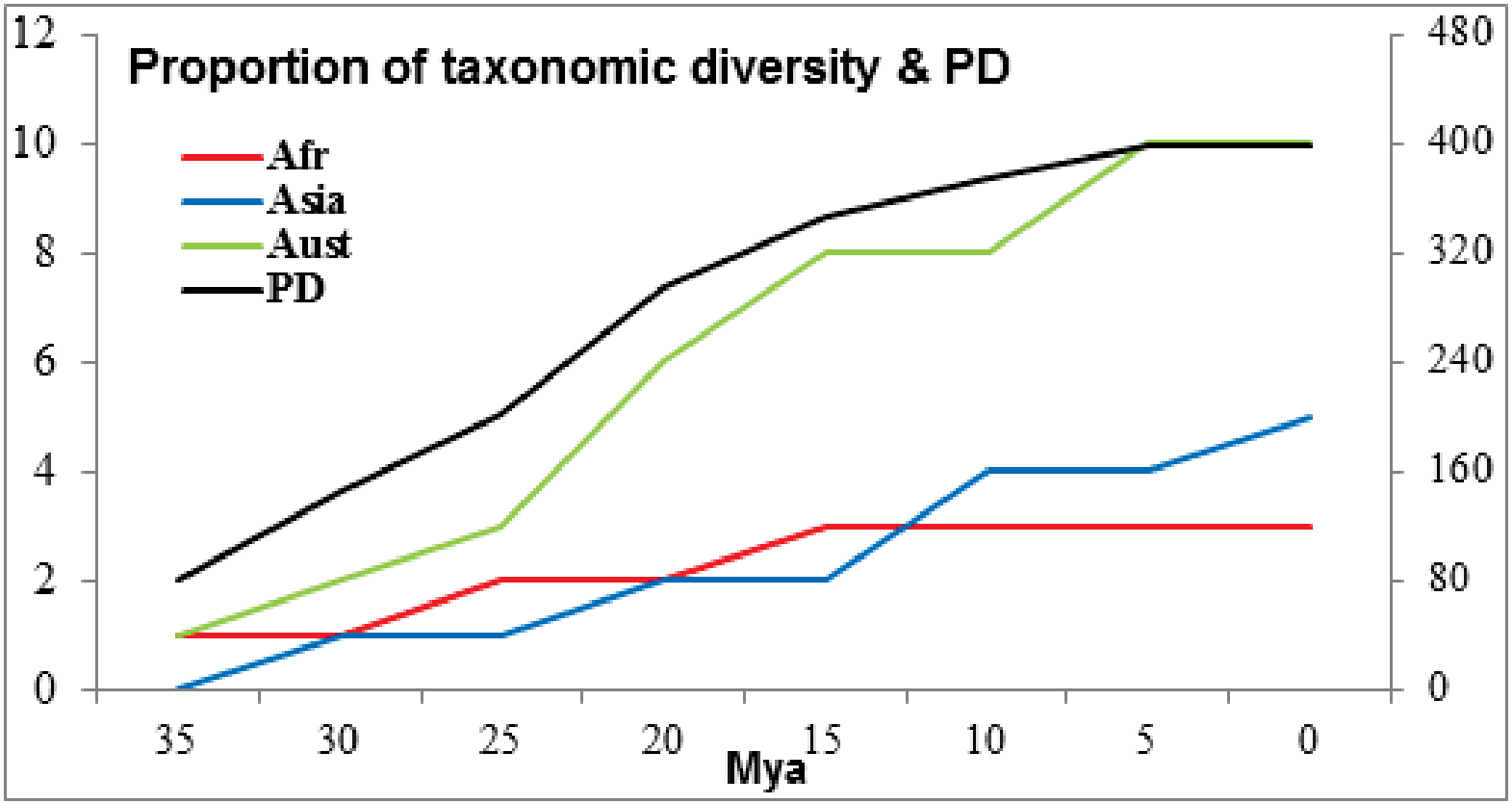


Figure 21. *Varanus* tree proportion of regional taxa that makeup Phylogenetic Diversity (PD) through time.

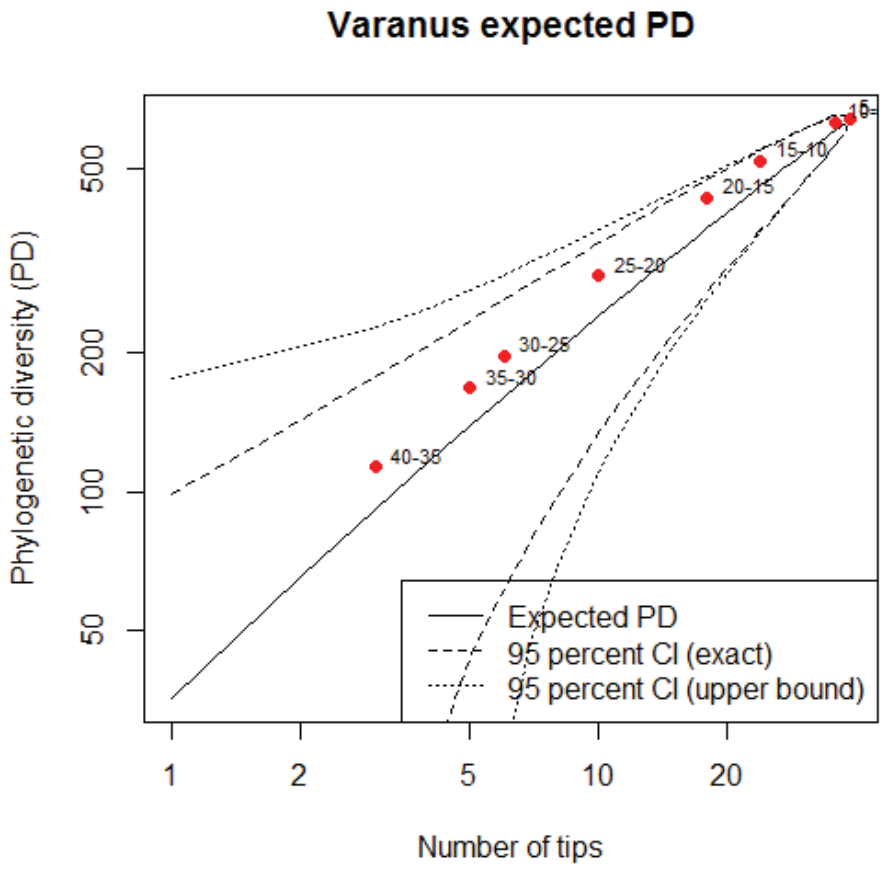


Figure 22. *Varanus* expected Phylogenetic Diversity (PD) through time. All time bin communities (red dots) fall well within expected measures.

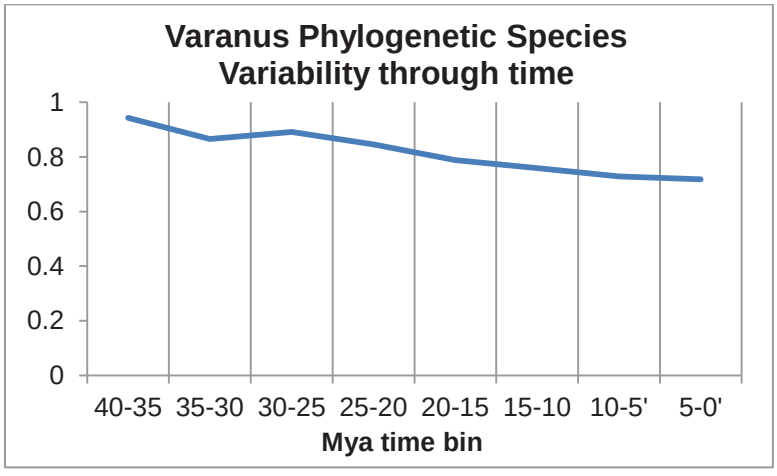
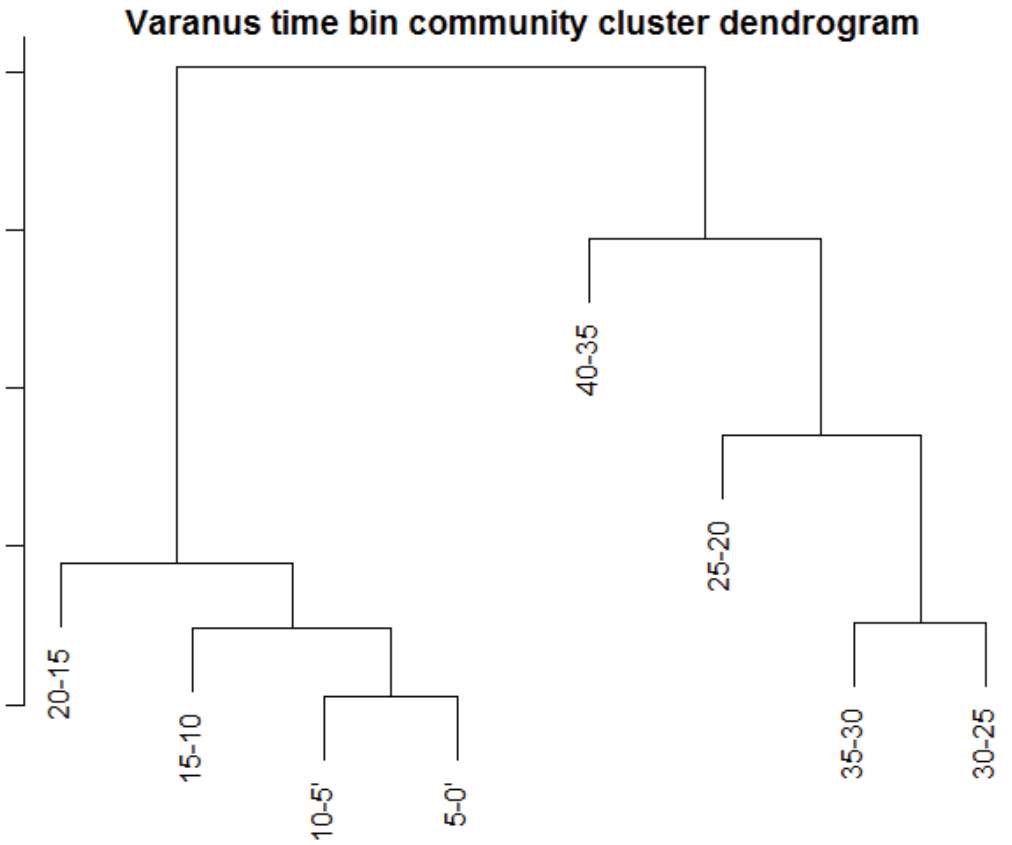


Figure 23. *Varanus* PSV through time. The spread of taxa spans all regions near the beginning of the tree and continues to originate, so PSV begins high and remains fairly so. It begins to decrease slightly near the recent as most of the origination begins to occur more or less on one portion of the tree (Indo-Australia).



	40-35	35-30	30-25	25-20	20-15	15-10	10-5'
35-30	13.84266						
30-25	18.62639	5.172386					
25-20	29.40491	17.07486	12.45166				
20-15	35.06935	25.99857	22.54462	10.02928			
15-10	40.29337	30.86372	27.93839	15.38067	**5.15032**		
10-5'	40.10672	33.44608	31.29507	16.33846	**7.929179**	**3.718299**	
5-0'	40.29061	34.07575	32.05415	17.30074	**8.933867**	**4.82782**	**0.494896**

Figure 24. Time bin community dendrogram generated from *Varanus* time bin distance matrix (above). As expected, time bins directly next to one another tend to clump, but after 20 Mya, communities tend to stabilize and there is very little difference between time bins (bolded). Those time bins separate out from the rest in the dendrogram.

Appendix 1. List of canid taxa included in analyses

Taxon	Subfamily	Subgroup
Otarocyon macdonaldi-anc	Borophaginae	Basal Boro
Otarocyon macdonaldi-desc	Borophaginae	Basal Boro
Archaeocyon pavidus	Borophaginae	Basal Boro
Archaeocyon lepiodus-anc	Borophaginae	Basal Boro
Archaeocyon lepiodus-desc	Borophaginae	Basal Boro
Archaeocyon falkenbachi	Borophaginae	Basal Boro
Oxetocyon cuspidatus	Borophaginae	Basal Boro
Otarocyon cooki	Borophaginae	Basal Boro
Rhizocyon oregonensis	Borophaginae	Basal Boro
Cynarctoides lemur	Borophaginae	Phlaocyonini
Cynarctoides roii-anc	Borophaginae	Phlaocyonini
Cynarctoides roii-desc	Borophaginae	Phlaocyonini
Cynarctoides harlowi	Borophaginae	Phlaocyonini
Cynarctoides luskensis	Borophaginae	Phlaocyonini
Cynarctoides gawnae	Borophaginae	Phlaocyonini
Cynarctoides acridens-desc	Borophaginae	Phlaocyonini
Cynarctoides acridens-anc	Borophaginae	Phlaocyonini
Cynarctoides emryi	Borophaginae	Phlaocyonini
Phlaocyon minor	Borophaginae	Phlaocyonini
Phlaocyon latidens	Borophaginae	Phlaocyonini
Phlaocyon annectens	Borophaginae	Phlaocyonini
Phlaocyon achoros	Borophaginae	Phlaocyonini
Phlaocyon multicuspus	Borophaginae	Phlaocyonini
Cormocyon copei-anc	Borophaginae	Borophagini
Phlaocyon marslandensis	Borophaginae	Phlaocyonini
Phlaocyon leucosteus	Borophaginae	Phlaocyonini
Phlaocyon yatkolai	Borophaginae	Phlaocyonini
Phlaocyon mariae	Borophaginae	Phlaocyonini
Desmocyon thomsoni-anc	Borophaginae	Phlaocyonini
Cormocyon haydeni	Borophaginae	Phlaocyonini
Cormocyon copei-desc	Borophaginae	Phlaocyonini
Desmocyon thomsoni-desc	Borophaginae	Phlaocyonini
Desmocyon matthewi	Borophaginae	Phlaocyonini
Metatomarchtus canavus	Borophaginae	Phlaocyonini
Psalidocyon mariannae	Borophaginae	Phlaocyonini
Microtomarctus conferta	Borophaginae	Phlaocyonini
Protomarctus optatus	Borophaginae	Phlaocyonini

Appendix 1. (cont.)

Tephrocyon rurestris	Borophaginae	Phlaocyonini
Tomarctus hippophaga	Borophaginae	Aelurodontina
Tomarctus brevirostris	Borophaginae	Aelurodontina
Aelurodon asthenostylus-anc	Borophaginae	Aelurodontina
Aelurodon asthenostylus-desc	Borophaginae	Aelurodontina
Aelurodon mcgrewi-anc	Borophaginae	Aelurodontina
Aelurodon stirtoni	Borophaginae	Aelurodontina
Aelurodon mcgrewi-desc	Borophaginae	Aelurodontina
Aelurodon ferox-anc	Borophaginae	Aelurodontina
Aelurodon ferox-desc	Borophaginae	Aelurodontina
Aelurodon taxoides	Borophaginae	Aelurodontina
Euoplocyon spissidens-anc	Borophaginae	Borophagini
Euoplocyon spissidens-desc	Borophaginae	Borophagini
Euoplocyon brachygnathus	Borophaginae	Borophagini
Cynarctus galushai	Borophaginae	Cynarctina
Cynarctus marylandica Q	Borophaginae	Cynarctina
Cynarctus saxatilis-anc	Borophaginae	Cynarctina
Cynarctus saxatilis-desc	Borophaginae	Cynarctina
Cynarctus vooiheisi-anc	Borophaginae	Cynarctina
Cynarctus vooiheisi-desc	Borophaginae	Cynarctina
Cynarctus crucidens	Borophaginae	Cynarctina
Paracynarctus kelloggi-anc	Borophaginae	Cynarctina
Paracynarctus kelloggi-desc	Borophaginae	Cynarctina
Paracynarctus sinclairi	Borophaginae	Cynarctina
Carpocyon compressus	Borophaginae	Borophagina
Carpocyon webbi-desc	Borophaginae	Borophagina
Carpocyon webbi-anc	Borophaginae	Borophagina
Carpocyon robustus	Borophaginae	Borophagina
Carpocyon limosus	Borophaginae	Borophagina
Protepicyon raki-anc	Borophaginae	Borophagina
Protepicyon raki-desc	Borophaginae	Borophagina
Epicyon saevus-ancanc	Borophaginae	Borophagina
Epicyon haydeni	Borophaginae	Borophagina
Epicyon saevus-anc	Borophaginae	Borophagina
Epicyon aelurodontoides	Borophaginae	Borophagina
Epicyon saevus-desc	Borophaginae	Borophagina
Borophagus littoralis-anc	Borophaginae	Borophagina
Borophagus littoralis-desc	Borophaginae	Borophagina

Appendix 1 (cont.)

Borophagus pugnator	Borophaginae	Borophagina
Borophagus orc	Borophaginae	Borophagina
Borophagus parvus	Borophaginae	Borophagina
Borophagus secundus-anc	Borophaginae	Borophagina
Borophagus secundus-desc	Borophaginae	Borophagina
Borophagus hilli	Borophaginae	Borophagina
Borophagus dudleyi	Borophaginae	Borophagina
Borophagus diversidens	Borophaginae	Borophagina
Paratomarctus temerarius-anc	Borophaginae	Borophagina
Paratomarctus temerarius-desc	Borophaginae	Borophagina
Paratomarctus euthos	Borophaginae	Borophagina
Leptocyon spA	Caninae	First Caninae
Leptocyon vulpinus	Caninae	First Caninae
Leptocyon mollis	Caninae	First Caninae
Leptocyon douglassi	Caninae	First Caninae
Leptocyon delicatus	Caninae	First Caninae
Leptocyon gregorii-anc	Caninae	First Caninae
Leptocyon gregorii-desc	Caninae	First Caninae
Leptocyon leidyi-anc	Caninae	First Caninae
Leptocyon spB	Caninae	First Caninae
Leptocyon leidyi-desc	Caninae	First Caninae
Leptocyon vafer-anc-anc	Caninae	First Caninae
Leptocyon vafer-anc	Caninae	First Caninae
Leptocyon vafer-desc	Caninae	First Caninae
Leptocyon tejonensis	Caninae	First Caninae
Leptocyon matthewi	Caninae	First Caninae
EucyonQ skinneri-anc	Caninae	First Caninae
EucyonQ skinneri-desc	Caninae	First Caninae
Euycon davisi-anc	Caninae	First Caninae
Euycon davisi-desc	Caninae	First Caninae
Canis ferox-anc	Caninae	Canini
Canis ferox-desc	Caninae	Canini
Canis lepophagus-anc-anc	Caninae	Canini
Canis amensis	Caninae	Canini
Canis etruscus	Caninae	Canini
Canis palmidens	Caninae	Canini
Canis mosbachensis	Caninae	Canini
Canis variabilis	Caninae	Canini

Appendix 1 (cont.)

Canis edwardii-anc	Caninae	Canini
Canis edwardii-desc	Caninae	Canini
Canis aureus	Caninae	Canini
Canis latrans	Caninae	Canini
Canis chihliensis	Caninae	Canini
Canis lupus	Caninae	Canini
Canis armbrusteri-anc	Caninae	Canini
Canis armbrusteri-desc	Caninae	Canini
Canis dirus	Caninae	Canini
Canis falconeri	Caninae	Canini
Canis antonii	Caninae	Canini
Xenocyon lycaonoides-anc	Caninae	Canini
Xenocyon lycaonoides-desc	Caninae	Canini
Cuon javanicus	Caninae	Canini
Lycaon pictus	Caninae	Canini
Canis lepophagus-anc	Caninae	Canini
Canis lepophagus-desc	Caninae	Canini
Canis thooides-anc	Caninae	Canini
Canis thooides-desc	Caninae	Canini
Canis feneus-anc	Caninae	Canini
Canis feneus-desc	Caninae	Canini
Canis cedazoensis	Caninae	Canini
N Am CERDOCYONINA-anc	Caninae	Canini
N Am CERDOCYONINA-desc	Caninae	Canini
S Am CERDOCYONINA	Caninae	Canini
Otocyon+Prototocyon	Caninae	Canini
Metalopex macconnelli-anc	Caninae	Vulpini
Metalopex macconnelli-desc	Caninae	Vulpini
Metalopex merriami-anc	Caninae	Vulpini
Metalopex merriami-desc	Caninae	Vulpini
Metalopex bakeri	Caninae	Vulpini
Urocyon webbi	Caninae	Vulpini
Urocyon galushai-anc	Caninae	Vulpini
Urocyon galushai-desc	Caninae	Vulpini
Urocyon citrinus	Caninae	Vulpini
Urocyon minicephalus	Caninae	Vulpini
Urocyon cinereoargenteus	Caninae	Vulpini
Vulpes stenognathus	Caninae	Vulpini

Appendix 1 (cont.)

Vulpes kemensis-anc	Caninae	Vulpini
Vulpes kemensis-desc	Caninae	Vulpini
Vulpes velox	Caninae	Vulpini

Appendix 2. Vidal et al. 2012 phylogeny taxon list.

Species	Region	Habitat
Varanus_kingorum	Australia	Rock/Terrestrial
Varanus_primordius	Australia	Terrestrial
Varanus_storri	Australia	Terrestrial
Varanus_acanthurus	Australia	Terrestrial
Varanus_baritji	Australia	Terrestrial
Varanus_caudolineatus	Australia	Arboreal
Varanus_bushi	Australia	Arboreal
Varanus_gilleni	Australia	Arboreal
Varanus_eremius	Australia	Terrestrial
Varanus_brevicauda	Australia	Fossorial
Varanus_glebopalma	Australia	Arboreal
Varanus_pilbarensis	Australia	Rock/Terrestrial
Varanus_scalaris	Australia	Arboreal
Varanus_timorensis	Australia	Arboreal
Varanus_mitchelli	Australia	Aqua/Arboreal
Varanus_semiremex	Australia	Aqua/Arboreal
Varanus_glauerti	Australia	Arboreal
Varanus_tristis	Australia	Arboreal
Varanus_spenceri	Australia	Terrestrial
Varanus_mertensi	Australia	Aquatic
Varanus_giganteus	Australia	Terrestrial
Varanus_rosenbergi	Australia	Terrestrial
Varanus_gouldii	Australia	Terrestrial
Varanus_panoptes_panoptes	Australia	Terrestrial
Varanus_panoptes_horni	Australia	Terrestrial
Varanus_salvadorii	Australia	Arboreal
Varanus_varius	Australia	Arb/Terrestrial
Varanus_komodoensis	Australia	Terrestrial
Varanus_dumerilii	Asia	Terrestrial
Varanus_rudicollis	Asia	Arboreal
Varanus_salvator	Asia	Aquatic
Varanus_doreanus	Asia	Terrestrial
Varanus_indicus	Asia	Aqua/Arboreal
Varanus_jobiensis	Asia	Arboreal
Varanus_keithhornei	Asia	Arboreal
Varanus_prasinus	Asia	Arboreal
Varanus_niloticus	Africa	Aquatic
Varanus_exanthematicus	Africa	Terrestrial
Varanus_albigularis	Africa	Terrestrial

Appendix 3. Time bin community assignment

Vidal et al. 2012 *Varanus*	35 Mya	30 Mya	25 Mya	20 Mya	15 Mya	10 Mya	5 My	0 Mya
Varanus_kingorum	0	0	0	0	0	0	1	1
Varanus_primordius	0	0	0	0	0	1	1	1
Varanus_storri	0	0	0	0	0	0	1	1
Varanus_acanthurus	0	0	0	1	1	1	1	1
Varanus_baritji	0	0	0	0	0	0	1	1
Varanus_caudolineatus	0	0	0	0	0	0	1	1
Varanus_bushi	0	0	0	0	0	0	0	1
Varanus_gilleni	0	0	0	0	0	0	0	1
Varanus_eremius	0	0	0	0	1	1	1	1
Varanus_brevicauda	0	0	0	0	0	1	1	1
Varanus_glebopalma	0	0	0	0	1	1	1	1
Varanus_pilbarensis	0	0	0	0	1	1	1	1
Varanus_scalaris	0	0	0	0	1	1	1	1
Varanus_timorensis	0	0	0	0	0	1	1	1
Varanus_mitchelli	0	0	0	0	0	0	1	1
Varanus_semiremex	0	0	0	0	0	0	1	1
Varanus_glauerti	0	0	0	0	0	0	1	1
Varanus_tristis	0	0	0	1	1	1	1	1
Varanus_spenceri	0	0	0	0	1	1	1	1
Varanus_mertensi	0	0	0	0	0	1	1	1
Varanus_giganteus	0	0	0	0	0	1	1	1
Varanus_rosenbergi	1	1	1	1	1	0	1	1
Varanus_gouldii	0	0	0	0	0	0	1	1
Varanus_panoptes	0	0	0	0	1	1	1	1
Varanus_panoptes_horni	0	0	0	0	0	0	0	1
Varanus_salvadorii	0	0	0	0	1	1	1	1
Varanus_varius	0	0	0	0	0	1	1	1
Varanus_komodoensis	0	1	1	1	1	1	1	1
Varanus_dumerilii	0	0	0	1	1	1	1	1
Varanus_rudicollis	0	0	0	0	0	1	1	1
Varanus_salvator	0	1	1	1	1	1	1	1
Varanus_doreanus	0	0	0	0	0	0	1	1
Varanus_indicus	0	0	0	0	0	0	1	1
Varanus_jobiensis	0	0	0	1	1	1	1	1
Varanus_keithhornei	0	0	0	0	0	0	1	1
Varanus_prasinus	1	1	1	1	1	1	1	1

Varanus_niloticus	0	0	1	1	1	1	1	1
Varanus_exanthematicus	0	0	0	0	1	1	1	1
Varanus_albigularis	1	1	1	1	1	1	1	1

Appendix 3. (cont.)

Canid tree	Mya Time Bin						
	35 Mya	30 Mya	25 Mya	20 Mya	15 Mya	10 Mya	5 Mya
Otarocyon_macdonaldi-anc	1	0	0	0	0	0	0
Otarocyon_macdonaldi-desc	1	0	0	0	0	0	0
Archaeocyon_pavidus	1	1	0	0	0	0	0
Archaeocyon_lepiodus-anc	0	1	0	0	0	0	0
Archaeocyon_lepiodus-desc	1	1	1	0	0	0	0
Archaeocyon_falkenbachi	0	1	1	0	0	0	0
Oxetocyon_cuspidatus	1	1	0	0	0	0	0
Otarocyon_cooki	1	1	1	0	0	0	0
Rhizocyon_oregonensis	1	1	0	0	0	0	0
Cynarctoides_lemur	1	1	1	0	0	0	0
Cynarctoides_roii-anc	0	0	1	0	0	0	0
Cynarctoides_roii-desc	1	1	1	1	0	0	0
Cynarctoides_harlowi	0	0	1	1	0	0	0
Cynarctoides_luskensis	0	0	1	1	0	0	0
Cynarctoides_gawnae	0	0	1	1	0	0	0
Cynarctoides_acridens-desc	0	0	1	0	0	0	0
Cynarctoides_acridens-anc	1	1	1	1	0	0	0
Cynarctoides_emryi	0	0	1	1	0	0	0
Phlaocyon_minor	1	1	1	1	0	0	0
Phlaocyon_latidens	0	1	0	0	0	0	0
Phlaocyon_annectens	1	1	1	1	0	0	0
Phlaocyon_achoros	0	1	1	0	0	0	0
Phlaocyon_multicuspus	0	1	1	1	0	0	0
Cormocyon_copei-anc	0	0	1	0	0	0	0
Phlaocyon_marslandensis	0	0	1	1	0	0	0
Phlaocyon_leucosteus	0	0	1	1	0	0	0
Phlaocyon_yatkolai	0	0	1	1	0	0	0
Phlaocyon_mariae	0	0	0	1	0	0	0
Desmocyon_thomsoni-anc	0	0	1	0	0	0	0
Cormocyon_haydeni	0	0	1	1	0	0	0
Cormocyon_copei-desc	0	0	1	1	0	0	0
Desmocyon_thomsoni-desc	1	1	1	1	0	0	0
Desmocyon_matthewi	0	0	1	1	0	0	0
Metatomarchtus_canavus	0	0	0	1	0	0	0
Psalidocyon_mariannae	0	0	0	1	0	0	0
Microtomarctus_conferta	0	0	0	1	1	0	0
Protomarctus_optatus	0	0	0	1	0	0	0

Appendix 3 (cont.)	**Mya Time Bin**						
Tephrocyon_rurestris	0	0	0	1	0	0	0
Tomarchtus_hippophaga	0	0	0	1	0	0	0
Tomarctus_brevirostris	0	0	0	1	1	0	0
Aelurodon_asthenostylus-anc	0	0	0	1	0	0	0
Aelurodon_asthenostylus-desc	0	0	0	1	1	0	0
Aelurodon_mcgrewi-anc	0	0	0	0	1	0	0
Aelurodon_stirtoni	0	0	0	0	1	0	0
Aelurodon_mcgrewi-desc	0	0	0	0	1	0	0
Aelurodon_ferox-anc	0	0	0	0	1	0	0
Aelurodon_ferox-desc	0	0	0	0	1	0	0
Aelurodon_taxoides	0	0	0	1	1	1	0
Euoplocyon_spissidens-anc	0	0	0	1	0	0	0
Euoplocyon_spissidens-desc	0	0	0	1	0	0	0
Euoplocyon_brachygnathus	0	0	0	1	0	0	0
Cynarctus_galushai	0	0	0	1	1	0	0
Cynarctus_marylandica_Q	0	0	0	1	0	0	0
Cynarctus_saxatilis-anc	0	0	0	0	1	0	0
Cynarctus_saxatilis-desc	0	0	0	0	1	0	0
Cynarctus_vooiheisi-anc	0	0	0	0	1	0	0
Cynarctus_vooiheisi-desc	0	0	0	0	1	0	0
Cynarctus_crucidens	1	1	1	1	1	1	0
Paracynarctus_kelloggi-anc	0	0	0	1	0	0	0
Paracynarctus_kelloggi-desc	0	0	0	1	1	0	0
Paracynarctus_sinclairi	0	0	0	1	0	0	0
Carpocyon_compressus	0	0	0	1	1	0	0
Carpocyon_webbi-desc	0	0	0	0	1	0	0
Carpocyon_webbi-anc	0	0	0	0	1	0	0
Carpocyon_robustus	0	0	0	0	1	1	0
Carpocyon_limosus	0	0	0	1	1	1	0
Protepicyon_raki-anc	0	0	0	0	1	0	0
Protepicyon_raki-desc	0	0	0	0	1	0	0
Epicyon_saevus-ancanc	0	0	0	0	1	0	0
Epicyon_haydeni	0	0	0	0	1	1	0
Epicyon_saevus-anc	0	0	0	0	0	1	0
Epicyon_aelurodontoides	0	0	0	0	0	1	0
Epicyon_saevus-desc	0	0	0	0	0	1	0
Borophagus_littoralis-anc	0	0	0	0	1	0	0
Borophagus_littoralis-desc	0	0	0	0	0	1	0
Borophagus_pugnator	0	0	0	0	0	1	0
Borophagus_orc	0	0	0	0	0	1	0

Appendix 3 (cont.)		**Mya Time Bin**					
Borophagus_parvus	0	0	0	0	0	1	0
Borophagus_secundus-anc	0	0	0	0	0	1	0
Borophagus_secundus-desc	0	0	0	0	0	1	0
Borophagus_hilli	0	0	0	0	0	1	1
Borophagus_dudleyi	0	0	0	0	0	1	0
Borophagus_diversidens	1	1	1	1	1	1	1
Paratomarctus_temerarius-anc	0	0	0	0	1	0	0
Paratomarctus_temerarius-desc	0	0	0	0	1	0	0
Paratomarctus_euthos	0	0	0	1	1	1	0
Leptocyon_spA	1	0	0	0	0	0	0
Leptocyon_vulpinus	1	1	1	1	0	0	0
Leptocyon_mollis	1	1	0	0	0	0	0
Leptocyon_douglassi	1	1	0	0	0	0	0
Leptocyon_delicatus	0	1	0	0	0	0	0
Leptocyon_gregorii-anc	0	0	1	0	0	0	0
Leptocyon_gregorii-desc	0	0	1	0	0	0	0
Leptocyon_leidyi-anc	0	0	0	1	0	0	0
Leptocyon_spB	0	0	0	1	0	0	0
Leptocyon_leidyi-desc	0	0	0	0	1	0	0
Leptocyon_vafer-anc-anc	0	0	0	0	1	0	0
Leptocyon_vafer-anc	0	0	0	0	1	0	0
Leptocyon_vafer-desc	0	0	0	0	1	1	0
Leptocyon_tejonensis	0	0	0	0	1	0	0
Leptocyon_matthewi	0	0	0	0	1	1	0
EucyonQ_skinneri-anc	0	0	0	0	0	1	0
EucyonQ_skinneri-desc	0	0	0	0	0	1	0
Eucyon_davisi-anc	0	0	0	0	0	1	0
Eucyon_davisi-desc	0	0	0	0	0	1	0
Canis_ferox-anc	0	0	0	0	0	1	0
Canis_ferox-desc	0	0	0	0	0	0	1
Canis_lepophagus-anc-anc	0	0	0	0	0	0	1
Canis_amensis	0	0	0	0	0	0	1
Canis_etruscus	0	0	0	0	0	0	1
Canis_palmidens	0	0	0	0	0	0	1
Canis_mosbachensis	0	0	0	0	0	0	1
Canis_variabilis	0	0	0	0	0	0	1
Canis_edwardii-anc	0	0	0	0	0	0	1
Canis_edwardii-desc	0	0	0	0	0	0	1
Canis_aureus	0	0	0	0	0	0	1

Appendix 3 (cont.)	**Mya Time Bin**						
Canis_latrans	0	0	0	0	0	0	1
Canis_chihliensis	0	0	0	0	0	0	1
Canis_lupus	0	0	0	0	0	0	1
Canis_armbrusteri-anc	0	0	0	0	0	0	1
Canis_armbrusteri-desc	0	0	0	0	0	0	1
Canis_dirus	0	0	0	0	0	0	1
Canis_falconeri	0	0	0	0	0	0	1
Canis_antonii	0	0	0	0	0	0	1
Xenocyon_lycaonoides-anc	0	0	0	0	0	0	1
Xenocyon_lycaonoides-desc	0	0	0	0	0	0	1
Cuon_javanicus	0	0	0	0	0	0	1
Lycaon_pictus	0	0	0	0	0	0	1
Canis_lepophagus-anc	0	0	0	0	0	0	1
Canis_lepophagus-desc	0	0	0	0	0	0	1
Canis_thooides-anc	0	0	0	0	0	0	1
Canis_thooides-desc	0	0	0	0	0	0	1
Canis_feneus-anc	0	0	0	0	0	0	1
Canis_feneus-desc	0	0	0	0	0	0	1
Canis_cedazoensis	0	0	0	0	0	1	1
N_Am_CERDOCYONINA-anc	0	0	0	0	0	0	1
N_Am_CERDOCYONINA-desc	0	0	0	0	0	0	1
S_Am_CERDOCYONINA	1	1	1	1	1	1	1
Otocyon+Prototocyon	0	0	0	0	1	1	1
Metalopex_macconnelli-anc	0	0	0	0	0	1	0
Metalopex_macconnelli-desc	0	0	0	0	0	1	0
Metalopex_merriami-anc	0	0	0	0	0	1	0
Metalopex_merriami-desc	0	0	0	0	0	1	0
Metalopex_bakeri	0	0	0	0	1	1	0
Urocyon_webbi	0	0	0	0	0	1	0
Urocyon_galushai-anc	0	0	0	0	0	0	1
Urocyon_galushai-desc	0	0	0	0	0	0	1
Urocyon_citrinus	0	0	0	0	0	0	1
Urocyon_minicephalus	0	0	0	0	0	0	1
Urocyon_cinereoargenteus	0	0	0	0	1	1	1
Vulpes_stenognathus	0	0	0	0	0	1	0
Vulpes_kemensis-anc	0	0	0	0	0	1	0
Vulpes_kemensis-desc	0	0	0	0	0	1	0
Vulpes_velox	0	0	0	0	1	1	1

Chapter 3: Testing the influences on disparity patterns among regions, habitat, and size in monitor lizard skulls

INTRODUCTION

Measuring morphological variation, and the factors that affect it, is a key area of research in evolutionary biology. These studies often deconstruct the influences of organismal shape, such as environment, ontogenetic stage, and phylogeny, and their effect on morphology. Although shape variation can be extremely informative at various scales, be it within a lineage, temporally, across geographic ranges, or among individuals of different sizes, even more interesting is the extent to which shape might be maintained at any given scale. Certain lineages are considered morphologically conservative, in that they have either maintained a general morphology for a long period of time or they show a small range of shape variation across some taxonomic or regional level. In this study I use geometric morphometrics to describe general patterns of morphological diversity across the phylogeny and geographic range of varanids, a morphologically conservative group. I compare morphological variation to patterns of taxonomic and phylogenetic diversity, and consider possible factors influencing differences in measures of diversity. I quantified shape in their skulls to tests for the influences of taxonomic diversity, phylogeny, size, region, and ecology on shape variation to better understand if it is possible to determine what factors influence shape in this morphologically conservative group, and if so, how influential these factors are.

Monitor lizards (Varanidae:*Varanus*) have been used as a model system in ecological and morphological studies (Pianka, 1995; Collar et al., 2011). The approximately 73 species of extant monitor lizards are found in a number of habitats, from terrestrial, arboreal, and aquatic, to some combination thereof (Pianka, 1994; Pianka, 1995; Pepin, 2001; Pianka, King and King, 2004). *Varanus* are solely found in southern continents, ranging from Africa to the Middle East, throughout Southeast Asia, Malaysia, Indonesia, Philippines, and New Guinea to Australia (Bennett and Lim, 1995). Extant members span a wide range of body sizes, from the pygmy monitor, *V. brevicauda* (20 cm total length and ~10g), to *V. komodoensis* (>100 kg and 3 m total length), representing four orders of magnitude in body mass and an order of magnitude in length (Pianka, 1995; Pianka, King, and King, 2004; Collar et al., 2011). Extinct varanids extend both the size and geographical range of the group. The extinct Australian species, *Varanus priscus* (*Megalania,* ~40 kya), reached an estimated 6-9 meters in length and 600 to 650 kilograms (Hecht, 1975). Some fossil varanid relatives lived beyond their present geographic range: pre-Miocene (> 23 mya) fossils are found in Asia and North America, and by the middle Miocene (~15 mya) in Europe, Africa, and Australia (Conrad et al., 2009). Monitor lizards have been used as a model organism for investigating size evolution, but variation and patterns in shape have seldom been assessed (Pianka, 1995; Collar et al., 2011; Openshaw and Keogh, 2014).

Although size has, and still does, vary dramatically in varanids, they have been considered conservative in body shape. In monitor lizards, body size is strongly linked to habitat and ecology, and the amount of body size variation differs across their geographic range (Pepin, 1995; Collar et al., 2011; Fig. 1). Openshaw and Keogh (2014) conducted an Australian-focused geometric morphometric study of external

Varanus skull anatomy, finding that shape variation evolved through the interaction of habitat use, phylogeny, and size evolution. In this study, phylogenetic, size, morphological, geographic range, and habitat data were collected for extant *Varanus* species spanning all of their geographic regions to test: (i) the effect of phylogeny on skull size or shape variation in monitors; (ii) the spread of size and shape variation among geographic regions; (iii) the relationship of ecology and shape, and (iv) how two fossil taxa can be placed in extant morphospace.

Geometric Morphometrics

Describing and comparing organismal anatomy has been central to biology because it is important in the classification and understanding of diversity (Zelditch, Swiderski, and Sheets, 2012). The early 20th century saw what Bookstein (1998) called a "quantification revolution" in biology, referring mostly to morphological analyses. Morphometrics is the quantitative study of shape and its relationship with other variables (Bookstein, 1991; Dryden and Mardia, 1998). The advent of methods such as Geometric Morphometrics transformed how researchers measure and perceive morphology. Even in traditional, or linear, morphometrics, the phenotype could be understood and analyzed in multivariate space, and specific hypotheses of shape may be tested (Zelditch, Swiderski, and Sheets, 2012). Understanding the importance of or removing the influence of size on shape became important, as well as determining a true mathematical definition of shape. Geometric morphometrics was born of this (Bookstein, 1998), and because its versatility in use and the many statistical analyses that can be conducted, this was the main technique I used to quantify and test the influences on morphology.

Landmark based morphometrics

Traditional morphometrics, which is based on linear measurements of specimens, does not retain the spatial information of shape (Zelditch, Swiderski, and Sheets, 2012). Landmark-based morphometrics, on the other hand, retains the geometry of a specimen. Landmark data are coordinates placed across a specimen that represent discrete anatomical loci. The data for each specimen consists of a configuration of landmarks. These landmarks, or loci, are geometrically (not evolutionarily) homologous among all specimens (i.e., they are regarded as the same point in each specimen). There are several types of landmarks: those that are defined locally (Type 1: i.e., suture intersections), minima/maxima of structures (Type 2), or points far from another landmark (Type 3). Semilandmarks are points with arbitrary positions along a curve that provide information about curvature. This study will use a mix of landmarks and semilandmarks (Bookstein, 1994; Bookstein, 1997; Zelditch, Swiderski, and Sheets, 2012.)

MATERIALS AND METHODS

To assess the breadth of inter- and intraspecific morphological variation in the skulls of varanids, my methods involved (a) data collection, (b) two-dimensional geometric morphometric analyses of 30 extant and two illustrative fossil taxa, (c) estimating morphological disparity among defined groups compared to taxonomic and

phylogenetic diversity, and (d) assessing phylogenetic signal in shape. Figure 2 summarizes the specific steps, which I describe in more detail below.

Specimens

Varanus taxonomy is an active field, and the number of species described continues to grow rapidly. For example, in 1942, Mertens proposed approximately 24 species, and now there are over 70 recognized species (Mertens, 1942; Koch et al. 2013). This study will not focus on the description of any new taxa or inclusions of any undescribed materials.

In total, I sampled 313 skulls representing 30 *Varanus* species, and a reduced set of 295 were used in this study (Table 1). Photographs of the skulls were taken in dorsal and lateral views. All photographs included a scale bar. Some specimens are only included in either the dorsal or lateral data sets, depending on the condition of the skull (Table 1). Most specimens were from skeletal collections, and some data were obtained from prepared wet specimens or X-rays. A main interest of this study was the comparison of regional morphological disparity, so the final data set contained a comparable mix of taxa from Africa, southern Asia, and Indo-Australia (Table 1). Taxonomic classification and collection data were obtained from associated specimen data and specimen tags when available. Two fossil taxa were included in the analyses for comparison with extant shape space (Table 2).

In this study the skull was measured because, in squamates, the cranium is important in prey capture, foraging, defense, and other behaviors (Herrel et al., 2007; Openshaw and Keogh, 2014). Cranial size influences the range of prey sizes, and although many studies have focused on the relationships of cranial size to important biological factors (Pianka, 1995; Collar et al. 2001), less work has been done in measuring shape (Openshaw and Keogh, 2014). Not only is the skull very informative in understanding lizard ecology, it also contains many diagnostic characters for identifying *Varanus* species (Pepin, 2001).

Phylogeny

Because new extant and fossil taxa of *Varanus* are constantly being discovered, and molecular analyses are becoming more refined, hypothesized relationships are often ambiguous or even contentious. Cladistic analyses of *Varanus* have used both molecular and morphological data. Ast (2001) generated a molecular tree that was relatively inclusive of extant *Varanus.* The results of that analysis differed significantly from Conrad, Rieppel, and Grande's (2008) morphology-based tree, which had included a number of non-varanid and fossil taxa, and several extant *Varanus*. Many studies tend to differ in taxonomic breadth and sampling. In my study, I decided to use the tree produced by Vidal et al. (2012) because it is time-calibrated and contains a broad taxonomic sample of extant *Varanus* (Fig. 1). The time-calibrated molecular phylogeny was digitized and used as a framework to determine how patterns of lineage diversification and disparity compare in historical patterns of this extant clade

Taxonomic and Phylogenetic diversity

Using the phylogeny of Vidal et al. (2012), regional taxonomic diversity was computed by counting the number of tree tips attributed to regions. Phylogenetic diversity measures how much of a phylogeny is traveled among a set of taxa by summing the total branch lengths connecting them (Faith, 1992; Faith and Baker, 2006; Schweiger et al., 2008). Because Africa contains the lowest taxonomic diversity in the Vidal et al. (2012) tree (3 taxa), to make comparable comparisons across regions, other regional subgroups were subsampled to the same taxonomic diversity as for Africa. Taxonomic and phylogenetic diversity was compared to cranial shape variation in these regions.

Geometric Morphometrics

Photography. I photographed *Varanus* skulls from 8 museums: University of California Museum of Paleontology, CA (UCMP); University of California Museum of Vertebrate Zoology, CA (MVZ); California Academy of Sciences, CA (Cal Acad); American Museum of Natural History, NY (AMNH), Yale Peabody Museum, CT (YPM); National Museum of Natural History, Washington, D.C. (NMNH), Australian Museum, Sydney, AU (AM); and the Western Australian Museum, Perth, AU (WAM). Dorsal and right lateral view photos were taken using a Canon D60 on a table tripod with leveler. All images were taken with the same tripod and camera in all locations. Black felt material was used for photo backgrounds, lighting was adjusted as needed to reduce shadows, and centimeter scale bars were placed below specimens to measure scale factors when digitizing. To reduce the effects of vibration, the camera was tethered to a laptop for photographing and all adjustments on photos were done using the EOS Utilities software.

*Landmarks***.** Landmarks and semilandmarks were placed on skulls in dorsal and lateral views. Figure 3 show landmarks placement on example skulls, and Table 3 holds descriptions of landmark placements. The dorsal landmark set focused on distance from the snout to the back of the skull, and was made up of 40 semilandmarks and 3 landmarks. The lateral view data set contained 25 semilandmarks and 6 landmarks, focused on curvatures of the skull and snout as well as distances in the nasal, orbit, and posterior of the skull. Definitions of landmark locations can be found in Table 3. Semilandmarks were placed on specimens as curves and resampled to 40 points in dorsal view and 25 in lateral. Landmarks were collected in TPSDig V. 1.31 (Rohlf, 2001). All landmarks were collected by the same individual. Repetitions of specimen landmarking were conducted to factor in possible measurement error, which was found to be negligible.

Quantifying shape. I used Procrustes superimposition, a widely implemented method to rotate, scale, and translate objects to remove that information (considered nuisance parameters) and keep solely shape differences (Zelditch, Swiderski, and Sheets, 2012). Other optimization techniques might use a pair of landmarks as a framework for supermposition whereas Procrustes optimization used the centroid of all the landmarks in a specimen as basis for superimposition. This provides an advantage over linear methods because it controls for possible dimensional redundancy (Zelditch,

Lundrigan, and Garland, 2004). Principal component analyses were run on all data sets to visualize the general spread of variation in the skulls. Procrustes superimposition was done by overlaying geometrically homologous landmarks based on centroids and then minimizing Procrustes distances among them (Rohlf and Slice, 1990; Goodall, 1991). With geometric morphometrics, shape variation of the cranium was quantified independent of size factors (Zelditch, Lundrigan, and Garland, 2004). Generalized Procrustes superimposition was run on landmark point coordinates using the *geomorph* (Adams and Otarola-Castillo, 2013) package in R (R Core Team, 2014). Semilandmarks were placed along curves and resampled based on distance, so each point is not geometrically homologous among specimens. To deal with this, during superimposition, the locations of semilandmarks were optimized by minimizing the bending energy between the reference and target specimens (Bookstein, 1997).

Evaluating subgroups

Although morphological variation may be attributed to age or sexual dimorphism, the lack of reliable information for these characteristics with these specimens makes it impossible to test. Analyses were run on only the largest specimens of each taxon and results produced similar patterns. All data sets were analyzed for phylogenetic or size generated patterns. Additionally, the data sets for each view were divided into regional and habitat subgroups. Regional sets were defined based on groupings identified in Vidal et al. 2012. Habitat groups were defined based on work by Pepin (2001) as well as a literature search (Pianka, 1995; Collar et al., 2011, Koch et al., 2013). See Table 1.

Using the shape coordinates derived from the Procrustes superimposition, I assessed the relative amounts of variation among subgroups with Procrustes ANOVA. The analysis quantifies the relative amount of shape variation attributable to defined factors in a model and assesses this variation via permutation. This ANOVA was used to test the attribution of taxonomy, geographic region, size, and habitat in cranial shape. Phylogenetic generalized least squares analyses were also run to determine whether results were influences by evolutionary history. Canonical variates analysis (CVA), which maximizes the differences between groups relative to the variation within groups (Klingenberg et al*.,* 2012), was also used to quantitatively compare groups. CVA finds the set of axes that discriminate between two or more groups using the means of the groups as a basis. It essentially simplifies the description of the differences among groups of interest to be able to form quantitative functions to classify specimens to certain categories. Group membership is assumed to be known *a priori*. CVA plots were generated to visually compare shape differences. I then calculated probabilities of specimens belonging to their specified groups after resampling using the chi-squared distribution of the Mahalanobis distance (explained in the disparity section) based on the principal components describing at least 95% of the shape variance. Because this simply provides the probability of an observation belonging to a given multivariate normal distribution, it was used to determine how often specimens were correctly assigned to their group based on the shape data. If groups are located in distinct regions of morphospace, it is expected that specimens belonging in that group will more often be classified in those groups than in other groups. Conversely, if groups overlap in morphospace, specimens are expected to be identified as belonging to several groups

equally. Resampling was done separately for each group. All analyses were done using functions from the *geomorph* (Adams and Otarola-Castillo, 2013) and *Morpho* (Stefan, 2014) packages in R (R Core Team, 2014). All these methods provide visualizations of the shape difference between groups, tests of statistical significance of shape differences among groups, tests determining influence of groups or other factors on shape variation, and tests of classifications of group membership.

Disparity analyses

I measured morphological disparity between and within subgroups. From CVA analyses, I obtained Mahalanobis Distances (MD) among group means. Along each axis, Mahalanobis measures the number of standard deviations away from the mean or centroid of one group is to another. MD is 0 if the means of the two groups overlap, and increases the farther the means are from each other. I measured morphological disparity of subgroups using the Procrustes superimposed coordinates with pairwise comparisons to identify differences between groups. Within-group disparity relative to shape space was estimated using the Procrustes variance (PV) for each group. In practice, PV is measured as the sum of the diagonal elements of the given group's covariance matrix (e.g., Zelditch, Swiderski, and Sheets, 2012). Essentially, PV estimates the shape space occupied by a group by quantifying the average scatter of data points of specimens in groups around the mean shape of that group (Drake and Klingenberg, 2010).The PVs are then treated as test values, permuted 1000 times where residual vectors are randomized across the groups. Of course, any estimate of disparity greatly depends on variables from which it is derived (Macleod, 1999) as well as the method of analysis. Resampling was done because it increased the robustness of measures by determining if similar patterns appear repeatedly.

Phylogeny and shape.

PCA finds the orthogonal axes representing the maximum shape variance, so it is appropriate for exploring the phenotypic variation in the various orientations of *Varanus* skulls (Zelditch, Swiderski, and Sheets, 2012). Previously, a separate PCA was computed for each orientation of the skull, allowing analysis of the distribution of species, regional, and habitat groups in phenotypic or shape space based on independent specimens. To test how phylogeny influenced these factors, I generated phylomorphospaces based on the PCAs of the means of taxa. Using the first two dimensions of tangent space (principal components 1 and 2), the *Varanus* phylogenetic tree was superimposed on the plots. Because the geometric morphometric analysis did not include all of the taxa from the Vidal et al. (2012) tree, a modified version of the tree only included taxa from which the geometric morphometric dataset was created (Fig. 4). It should also be stated that there were specimens included in the basic morphometric analyses that were not part of the Vidal et al. (2012) tree, and thus were not included in the phylomorphospace. Analyzing patterns on the tree helps reveal aspects of how shape evolved (Rohlf, 2002; Klingenberg and Gidaszewski, 2010). The phylomorphospaces generated included the ancestral states for each node of the phylogenetic tree. Ancestral states were obtained by estimating maximum likelihoods of

node states after re-rooting the phylogeny at all internal nodes and computing character state contrasts at that root. Finally, phylogenetic signal was measured using a multivariate version of the K-statistic called Kmult (Adams, 2014). The degree of phylogenetic signal is measured from the Procrustes-aligned specimens. Kmult measures the degree of phylogenetic signal in a dataset compared to an expected signal under Brownian motion. All analyses were done using functions from the *phytools* (Revell, 2012) and *geomorph* (Adams and Otarola-Castillo, 2013) packages in R.

Size and shape.

Significance of size differences

Centroid sizes (CS) calculated during Procrustes superimposition were used as a proxy for size for all specimens. This method relies on integrating shape into an x,y plane using landmarks, and moves the centroids of specimen (or more specifically their shapes) to (0,0). The average of the landmark's x coordinates is the centroid's *x* coordinate, and similarly the *y* coordinate of the centroid is the average of the *y*-coordinates. This is done for geometric morphometric analysis, where all specimen shapes become scaled to what is called unit centroid size, or the square root of the summed squared distances of each landmark to the centroid (Zelditch, Swiderski, and Sheets, 2012). CS variations within groups were visualized using box plots. Average snout-vent lengths (SVL) of all taxa from the Vidal et al. (2012) tree were collected for all species in this study through a literature search (Pianka, 1995; Pepin, 2001; Collar et al. 2011). Two graphical representations of shape across monitors were generated. First, to visualize cranial size across varanid shape space, specimen points were scaled to log centroid size in PCA space of the first two principal components. This helps to view patterns of size within shape space. Second, color coded phylogenies mapped by SVL or CS across the Vidal et al. (2012) tree were generated. Size states at internal nodes were estimated using Maximum Likelihood (ML) and interpolations of the states along each edge were done using methods from Felsenstein (1985). These continuous character map trees were generated using the *contMap* function from the *phytools* (Revell, 2012) package in R.

An Analysis of Variance (ANOVA) test was used to calculate the significance of different sizes among all specimens, subgroups, and across the phylogeny. ANOVA is a commonly used statistical technique for investigating data by comparing the means of subsets of the data. Phylogenetic signal of size in monitors was measured using the same Kmult statistic used to test the signal of shape mentioned previously (Adams, 2014). Analyses were run using base functions and functions from the *geomorph* (Adams and Otarola-Castillo, 2013) package in R.

Measuring the relationship of size and shape

Several tests were also run to measure the influence of size on shape across the data set. A Procrustes ANOVA was run to test the influence of size on shape, similar to the evaluation of subgroup designation on shape. The Common Allometric Component (CAC) of each specimen was measured using methods from Mitteroecker et al. (2004). The CAC is a vector in shape space computed by regressing shape variables on log size. It is a standardized measure of specimen shape relative to the mean specimen

shape of designated groups. CACs of the whole data set (which is the same as computing a shape regression score) and also accounting for subgroup variation (by first measuring allometric components within groups) were measured and regressed against log (CS). Warp grids of the smallest and largest specimens were included in the figures.

RESULTS

Taxonomic and phylogenetic diversity

Regionally, taxonomic (species) diversity varies. Approximately 6 species are found in Africa (3 on the Vidal et al. tree), and the rest of the approximately 73 total species of *Varanus* are found in Indo-Asia and Indo-Australia (Pepin, 2001; Koch et al., 2013). Mainland Asia is low in diversity, and the numbers increase when counting Indo-Asian island endemics. Indo-Australia, on the other hand, is dominated in numbers from mainland Australia (Koch et al., 2013). A recent phylogeny of Vidal et al. 2012 was analyzed for measures of Phylogenetic Diversity among these 3 regions (Fig. 5). It should be said that the analysis is biased only on the taxa included in the tree. Phylogenetic diversity is highest in Indo-Australia, followed by Indo-Asia, and finally by Africa. This is to be expected because often phylogenetic diversity and taxonomic diversity can strongly correlate on a molecular tree with no extinction (Faith and Baker, 2006). Analysis was also run on regions subsampled to 3 taxa to match the least diverse region, Africa. I chose the 3 deepest lineages from Indo-Asia and Indo-Australia. I found that in this case, phylogenetic diversity of the 3 African taxa becomes more similar to measures of the 3 taxa from other regions (Table 4). This is not surprising because Africa, although low in diversity, contains some of the deepest lineages of the *Varanus* tree.

Principal axes of *Varanus* cranial variation

Dorsal snout

The first five PCs accounted for approximately 95% of the total variance in shape out of 86 total components (Appendix 1). The first 3 PCs, accounting for over 89% of the variation, are discussed below. Shape changes along the first 3 PCs can be seen in Figure 6. The first PC explained 63.1% of the variance, and represented changes in snout shape and length. PC1 showed a shift from elongate, relatively thinner snouts in the negative end of PC1 to more blunt snouts in the positive direction. The positive direction of shape variation on PC1 was mostly populated by African taxa, and this is to be expected because species such as *V. exanthematicus* and *V. albigularis* have distinct, relatively blunt skulls (Fig. 6; Fig. 7). Variation along PC2 reflects a widening of the posterior portion of the snout and a shortening of the distance between the posterior of the skull to the snout. The most positive end of this axis was populated by Indo-Asian taxa, but mostly there were no large gaps among any groups of specimens in morphospace. When looking at PC1 versus PC3, *V. komodoensis* pulls away from the rest of the specimens (Fig. 7).

Lateral

The first eleven PCs accounted for approximately 95% of the total variation in shape out of 62 total components (Appendix 1). Because the first 3 PCs account for over half of the shape variation (62%), they will be the focus of the discussion of shape variation. Shape changes along the 3 PCs can be seen in Figure 9. The first 2 PCs explained approximately the same amount of shape variation: 29% and 21% respectively. PC1 represents a shift from more posterior-anterior curved skulls on the negative end, to flatter, more posterior-anterior elongate skulls on the negative end along with the distances of nostril and orbit landmarks to the posterior portion of the snout. Whereas PC2 describes similar shape change, although with more elongate skulls in the negative end and curved in the positive, the focus is more on the rostral-caudal elongation or shortening of the anterior portion of the snout. PC3 describes mostly changes in curvature, or changes in semilandmarks without as much regard to landmarks (Fig. 9). There is a great deal more regional overlap with Indo-Asia and arboreal habitat group specimens in lateral view than dorsal snout (Fig 10; Fig. 11).

Group shape variation and disparity

Dorsal snout

The Procrustes ANOVA tests for differences among species and regions were significant (Table 5). In principal component space, Indo-Asian specimens were primarily found near the negative direction along PC1, whereas Indo-Australian and Africa specimens spanned almost the entire morphospace (Fig. 7). This is reflected in measures of Procrustes variance (Table 6). There was extensive overlap of most Indo-Australian and African taxa, and partial overlap of Indo-Asian and Indo-Australian specimens. There is very low overlap of African and Indo-Asian shape space. With habitat groups, terrestrial taxa encompass the largest amount of morphospace, spanning across all of PC1. This means that terrestrial taxa tend to display more shape variation than other groups. Arboreal, aquatic, and taxa showing a combination of those ecologies tend to clump in the negative portion of PC1 space, and thus have low Procrustes variances overall (Table 6). The fossil taxon *Saniwa* falls in the direct center of morphospace, indicating it is close to the average shape of all varanid specimens included in this analysis (Fig. 7).

The CVA results were some of the most interesting. Figure 10 shows CVA plots (CV1 and CV2) for analysis based on species (Fig. 12), region (Fig. 13), and habitat (Fig. 14) groups. Visual representations of shape change along the first major axis are included in Appendix 2. When based on species, there was a strong overlap of most taxa whereas *V. komodoensis* was separated from all other species (Fig. 12). It appears that the dorsal snout shape of *V. komodoensis* makes all other taxa look more similar to each other. CVA produced a very distinct separation of all regions (Fig. 13). Regional separation in CVA space may be conflated by phylogeny, because regions tend to form monophyletic groups, so taxa in each region are more related to one another than across regions. Finally, the CVA of habitat showed a separation of terrestrial and arboreal/terrestrial taxa from all other groups (Fig. 14). All other habitat groups overlap fully in CVA space. It appears that any fully or moderately terrestrial group has a distinct enough shape to make other specimens look more similar to one another. The Mahalanobis distances for all CVA results can be found in Appendix 2.

A final test of group differences was a group classification test, which determined the probability of an observation belonging to a chi-squared distribution of a given classification. Numbers were based on resampling of a defined group and quantifying instances of specimens falling within other groups based on shape. In general, specimens fell within their regional groups (Fig. 15), except the large number of African specimens that were classified as Indo-Australian. This is not unexpected, because there was a great deal of overlap between African and Indo-Australian shape space (Fig. 9). When grouped by habitat (Fig 16), terrestrial taxa are very distinct in shape and tend to be classified as terrestrial. Another strong classification is arboreal/terrestrial. Aquatic taxa fall within aquatic, aquatic/arboreal, and arboreal/terrestrial classifications, and other groups also seem to be classified in several classes. This matches the CVA analyses, showing strong overlap of aquatic, arboreal, and aquatic/arboreal taxa, which tend to have longer, thinner snouts.

Lateral

The Procrustes ANOVAs of species, region, and habitat were significant (Table 5). This means that the average shape within these subgroups differs significantly from each other. In PCA space, African specimens are found near the center and negative ends of morphospace, Indo-Australian forms are near the center and upper regions, and Indo-Asian forms, surprisingly, take up a great deal of the center and positive portions of morphospace (Fig. 11). All unknown specimens fell in the central portion of morphospace. Measures of Procrustes variance also reflect these differences in morphospace occupancy (Table 6). The pairwise comparisons of regional groups were high for the comparison of Indo-Asia and Africa, and in PCA space, a great deal of their specimens do overlap. It should be restated that the Procrustes variance is based on the superimposed coordinates as a whole, and not the PC1 and PC2 space visualized. In PC1 and PC3 shape space, Indo-Asian taxa take up a large amount of shape space, which differs greatly from dorsal snout results. Similar to dorsal snout results, though, terrestrial specimens encompass a large amount of shape space, but are surprisingly followed by arboreal specimens. This pattern is similar in PC1 and PC2 shape space. Measures of PV reflect the large disparity in terrestrial taxa. Pairwise comparisons among habitat groups were high for combinations of aquatic-arboreal/terrestrial and arboreal-terrestrial (Table 6). Aquatic and arboreal/terrestrial taxa overlap greatly in shape space, and arboreal and terrestrial morphospace occupation is large, so their strong pairwise comparison is not surprising.

CVA of species showed more dispersion of taxa across CV1 and CV2 space than the dorsal view results (Fig. 17). CV1 and CV2 explained similar amounts of shape variation among groups (20.1% and 15% respectively). The CVA by species, color coded by region, showed interesting patterns in CVA space. African taxa tend to be found within the positive CV1 axis and negative CV2, Indo-Australian taxa in the negative end of the CV1 axis, and Indo-Asian taxa in the positive end of the CV2 axis. CVA by region showed very little overlap among regions (Fig 18) and similar distances between groups, with very similar Mahalanobis distances among regions, the largest between Africa and Indo-Australia (Appendix 2). CVA for habitat separated groups that were greatly overlapped in dorsal CVA analysis. Shape variations described by CV1 and CV2 focus on differences among groups that tend to be broad-skulled versus groups that have longer and flatter skulls. Unlike dorsal CVA, where only terrestrial and

arboreal/terrestrial specimens were separated from all other groups, lateral CVA analyses showed separation of arboreal, arboreal/terrestrial, aquatic/arboreal, and terrestrial specimens (Fig. 19). Mahalanobis distances were greatest between aquatic/arboreal specimens and all other habitat groups (Appendix 2).

Regional classification test results showed that Indo-Australian specimens were the most probable to fall within their own group, with low values among other regions (Fig. 20). The low values indicate a similar probability of specimens falling within their own as well as other regional groups. This matches the massive overlap of regions in PCA space, and explains why most Indo-Australian specimens only overlap slightly with Indo-Asian and almost not at all with African shape space. Habitat classification results show that terrestrial specimens tend to fall within their own groups, which matches patterns seen from the PCA results (Fig. 21). Terrestrial specimens span a great deal of morphospace, with most specimens not overlapping with other groups. All other classifications fall within low to middle values, which follow from the overlap of all other groups in morphospace.

Size and shape

Dorsal snout

As expected, centroid sizes (CS) differed greatly among species (Fig. 22; ANOVA, F=19.7, p=<0.001). ANOVA of species, region, and habitat on size were all significant (Table 7). From the multivariate regression (log CS versus shape regression scores), I found that there was a strong relationship between shape and size (Fig. 23, R=0.75) after a 1000 iteration randomized residual permutation test (F=20.08, p=0.004). Greater cranium size, with regards to dorsal snout shape, is associated with broader snouts and larger posterior portions of the skull (Fig. 23). Smaller size is associated with thinner anterior portions of the snout and more reduced posterior portions of the skull. There is a small gap between the largest specimens and the rest of the sample. The largest specimens are of *V. komodoensis*, and they seem to be a large influence in measuring the relationship between size and shape. Common allometric components, when measured accounting for groups, still showed a strong correlation with shape (Pearson's Product correlation; Species=0.79, Region=0.71, Habitat=0.7; see Appendix 3 for figures). Figure 24 shows PCA space of PC1 and PC2 with specimen points scaled to centroid size, revealing that size variation across specimens is not attributed to one PC axis, but rather is distributed across morphospace. Phylogenetic signal for size was also strong (Kmult=0.78), but with a significance of p=0.066. This phylogenetic pattern of size is apparent when visualized across a phylogeny, with the smallest and largest species found in the Indo-Australian portion of the tree (Fig. 25).

Lateral

Differences in lateral CS were statistically significant (ANOVA; *F*= 15.488, p<0.001). ANOVA of species, region, and habitat on size was only significant for species (which is to be expected because sizes do not vary much within species, but do vary greatly among species) (Table 7). The multivariate regressions showed a strong relationship between shape and size (Pearson's product correlation, 0.70), after a 1000 iteration randomized residual permutation test (Table 7). In lateral view, it appears that greater skull size is characterized by a slightly more curved posterior skull and elongate

anterior snout region. The smaller specimens tend to have overall dorso-ventrally flatter skulls (Fig. 26). There is no large gap among any of the specimens in the regression, unlike the dorsal snout analysis in which *V. komodoensis* was located away from the rest of the specimens. The common allometric components, when measured accounting for groups, still showed a strong relationship of shape and size (Appendix 3). Figure 27 shows the lateral PCA plot with specimen points scaled to CS, revealing that, similarly to the dorsal snout pattern, size variation across specimens is not attributed to one PC axis. Phylogenetic signal for size was also strong (Kmult=0.8), but with a p-value of 0.08. None of the results regarding size and phylogenetic patterns are unexpected because a strong relationship of phylogeny and size was already shown in the dorsal analyses of the skull.

Phylogeny and shape

Dorsal snout.

Phylogenetic signal is the tendency for closely related species to display similar trait values due to their common ancestry. Analyses indicated that dorsal snout shape in *Varanus* exhibited significant phylogenetic signal (Kmult =0.771, p =0.004). This indicates that closely related species were more similar to one another in dorsal snout head shape than was expected under a Brownian motion model of evolution (Fig. 28). High phylogenetic signal is normally attributed to processes related to ecological or evolutionary conservatism (e.g.,Swenson et al. 2007; Losos 2008). It should be stated that links between these processes and phylogenetic signal is not straightforward because several processes may produce similar patterns (Blomberg et al. 2003; Ackerly, 2009).

Phylogenetic signal in snout shape was evident when viewing the phylomorphospace of the first two PCs based on analysis of mean shape of each species (Fig. 29).The PCA of the average shape for each species showed a fairly broad spread of taxa across the shape space. The first five PCs explained over 96% of variation in snout shape (Appendix 4). My data show that monitor lizards form a fairly tightly packed star burst pattern in phylomorphospace. Different clusters are not very easily recognizable (Fig. 29). African monitors are found near the positive PC1 axis, and Indo-Australian and Indo-Asian monitors overlap, with many branches crossing. The spread of taxa is largest along PC1, indicating that taxa vary greatly in anterior snout shape (Fig. 29). There is less spread of African taxa across PC2. Sister species, or closely related taxa, tend to clump in similar regions of shape space, and more distantly related taxa further in shape space. Interestingly, there were also some taxa that spread to areas of morphospace far from closely related taxa, such as *V. prasinus* and *V. komodoensis*. The overlapping branches in the tree imply some level of convergence in snout shape. These taxa may factor into any overall reduction of phylogenetic signal of snout shape. Phylomorphospace also appears to spread from a central location, and extant taxa tend to occupy regions away from hypothesized ancestors (black nodes). So, although there is phylogenetic signal in dorsal head shape, it can be inferred that diversification in *Varanus* is a matter of interactions among several factors.

Lateral

Analyses indicated that lateral skull shape in *Varanus* exhibited a stronger phylogenetic signal than the dorsal snout analysis (Kmult = 0.83, p =0.001). Figure 30 shows the observed signal value against the Brownian motion models of evolution. The first 7 PCs of the PCA of species means explained over 96% of the variance, and the first 3 PCs over 90% (Appendix 4). The lateral phylomorphospace showed more separation of taxa than the dorsal snout analysis, and more generally showed more separation among regional groups. African taxa are found along the negative end of the PC1 axis, Indo-Asian taxa in the most central and upper part of morphospaces, and Indo-Australian taxa in the central and positive ends of the space (Figure 31). Regional taxa form monophyletic clades, so this is not surprising because the result of phylogenetic signal in shape was high. The phylomorphospace is defined by changes in the overall distance of landmarks across the skull and curvature of the anterior portion of the snout (Fig. 31). Similar to the dorsal snout analysis, closely related taxa tend to clump in space, although some of the exceptions are *V. niloticus, V.salvator*, and *V. dumerilii*. Monitors lizards have been known to behave differently when under varying conditions (Pianka, King, and King, 2004). For example, the ecology of *V. dumerilii* is considered to be a mix of terrestrial, arboreal, and aquatic, and in captivity they appear to prefer terrestrial habitats over elevated ones. It is possible that supposed preferred terrestriality in this group has clumped them near the two primarily terrestrial African *V. exanthematicus* and *V. albigularis*. *V. niloticus* is primarily aquatic and does differ in morphology from the other African taxa. *V. niloticus* clumps with the more aquatic Indo-Asian taxa near the center of shape space. Taxa spread from a central location in shape space, which is populated with many of the hypothesized ancestral nodes, with extant taxa occupying more peripheral areas of morphospace. There is less overall overlap of branches in shape space, so morphological divergences of lateral shape in taxa tend to occur in regions of morphospace occupied by closely related taxa.

Discussion

Using geometric morphometrics, I quantified shape variation across extant varanids in order to determine factors influencing morphological disparity in the skull. I included two fossil specimens to determine the degree of conservation in skull shape. I tested the influence of many factors on shape variation, in both a phylogenetic and non-phylogenetic context. My findings show that many characteristics that have previously been identified as important factors in varanid evolution – phylogeny, region, ecology, and size – all significantly describe skull shape variation, affirming many earlier studies (Pianka, 1995; Losos, 2008; Collar et al. 2011; Openshaw and Keogh, 2014).

Taxonomic diversity and morphological disparity

Taxonomic diversity varied across regions in varanids. Africa contains the lowest taxonomic diversity and Indo-Australia the highest. One main aspect of this study was to test the degree of shape variation in a taxonomically diverse versus a taxonomically depauperate region. By simply treating the specimens as representative of a region, I was able to compare morphological variation without regard to taxonomy or phylogeny. In the dorsal snout analysis, the degree of African disparity was similar to Indo-Australia although it contained fewer taxa. Shape variation was very distinct within each of these

regions. CVA separated each region almost equally in shape space because Mahalanobis distances among groups were similar. There are many explanations for this finding. Habitat was shown to be influential in dorsal head shape variation, and morphological disparity varied among habitats. Terrestrial specimens spanned the whole morphospace whereas all other groups fell well within terrestrial shape space. CVA analyses also found distinct differences between terrestrial and arboreal/terrestrial specimens and all other habitats. Classification analyses, for both dorsal and lateral views, consistently recognized terrestrial taxa over others, followed by aquatic taxa. The African taxa included in the regional analysis were the terrestrial *V. albigularis, V. exanthematicus, V.griseus*, and the aquatic *V. niloticus*. Because the taxa making up the African data set are from some of the most distinct habitat shape categories, this might factor into why morphological variation of those specimens is very high. Most of the terrestrial taxa found in the negative PC1 region of shape space were African monitors, a region of morphospace with no aquatic specimens.

Ecology and shape

In this study, habitat designations were used as a proxy for ecology. Habitats vary in complexity, taxonomic associations, predation, competition, and may other factors (Collar et al., 2011). Because there are different pressures imparted by different habitats, morphological disparity has been suggested to be a function of habitat use (Collar et al., 2011; Openshaw and Keogh, 2014). Previous research has shown that body size and shape variation in monitor lizards across the genus and within subgroups has been contributed to by many factors including foraging type, retreat choice, and even habitat (Pianka, 1995; Pianka, King, and King, 2004; Collar et al., 2011; Openshaw and Keogh, 2014). I also found that habitat use explained a great deal of head shape variation in monitors when analyzed across the whole data set in dorsal view (Table 5). Analysis of the influence of habitat designation on shape in lateral view was not significant. It appears that if habitat use does affect patterns of shape evolution, certain distinguishable effects only appear in dorsal view.

When measured across all specimens in general PCA morphospace in both dorsal and lateral views, terrestrial specimens have the highest Procrustes variance. The terrestrial designation is used very broadly in this dataset, and it includes both primarily terrestrial and even saxicolous taxa. Out of all the habitat designation in this dataset, the largest size variation was also in terrestrial taxa. Some of the smallest taxa such as *V. storri,* part of the dwarf *Odatria* subgenus, are saxicolous, and the largest species such as *V. komodoensis* and *V. giganteus* are terrestrial. Because size and phylogeny have been shown to have strong influences in shape variation, great phylogenetic breadth and size variation are most likely causing the large morphological variation of terrestrial specimens.

Phylogeny and shape

It is often thought that evolutionary rates within a lineage may affect measures of phylogenetic signal. Previous work has shown that signal, measured as Kmult, is not related to rate (Adams, 2014). Discussion of signal will not cover evolutionary rate, then, which will instead be covered in chapter 4. There are also several caveats in measuring signal based on the morphological data and molecular phylogeny used. For example,

any errors in tree topology, estimations of shared histories among taxa, or taxon shape means will bias measures of Kmult (Adams, 2014). Even so, these factors will influence *any* measure of phylogenetic signal. Kmult is still a good measure of signal because it is not necessarily confounded by measured of evolutionary rate. Phylogenetic signal was significant in both dorsal and lateral views, meaning that taxa in this analysis exhibit a significant degree of phylogenetic structure in patterns of dorsal and lateral skull shape variation among species. Some have interpreted high phylogenetic signal with conservatism, suggesting a conservation of niches (however defined) or selective forces on lineages, but previous work has shown little evidence for this because many different evolutionary processes can produce similar phylogenetic signals (Klingenberg and Gidaszewski, 2010).

In phylomorphospace, the separate distribution of taxa in both dorsal and lateral views suggests a strong influence of evolutionary history in skull shape. Most of the reconstructed ancestral states were found near the center of phylomorphomorphospaces. Although there is a general star pattern from a set of central ancestral states, reconstructed ancestral states generally indicate that states were acquired fairly early in the evolution of lineages and, once obtained, stayed fairly constant within subclades. Closely related taxa often tended to clump in similar regions of shape space (with some exceptions), and more distantly related taxa further in shape space. In dorsal phylomorphospace analysis, for example. *V. komodoensis* was found in a region of morphospace far from any close relatives. *V. komodoensis* had shown, in numerous analyses, dorsal shape distinct from other specimens. The CVA results by species showed *V. komodoensis* as a distinct group from all other taxa. Essentially the existence of *V. komodoensis* causes all of the other specimens to look more like each other than to *V. komodoensis*. A great deal of the skull shape differences in *V. komodoensis* may be attributed to their large size and terrestriality. Analyses in both dorsal and lateral views consistently found size to be important in describing shape variation.

Interestingly, although African monitor lizards were very variable in shape when specimens were considered independent of one another, when looking at the average of each taxon in both dorsal and lateral phylomorphospace, they are found near the negative end of PC1 and not spread across shape space. Habitats were spread across lateral phylomorphospace, but produced fairly interesting patterns in dorsal view. *V. giganteus* is found in the positive end of PC1, away from other terrestrial taxa. *V. giganteus* is fairly close to other large monitor taxa such as *V. salvadorii* and *V. salvator*, so its location may be attributed to certain allometric effects. Arboreal taxa span across PC2, and near the positive end are found clumped with a number of terrestrial taxa. The terrestrial taxa in the positive end of PC2 are smaller (some of the smallest taxa), rock dwelling species. The effects of allometry might be influencing the location of these taxa in shape space, because *V. storri* and *V. acanthurus* cross a large amount of morphospace away from their close relatives (this can be seen by their longer branch lengths spanning far from their ancestral nodes).

Size and shape

Many studies have shown a relationship between shape and size in many groups (Klingenberg and Gidaszewski, 2010; Drake and Klingenberg, 2010; Drake, 2011; Sanger et al*.,* 2011, Klingenberg et al*.,* 2012). Monitors show a large (and similar) amount of variation in SVL and CS across the Vidal et al. (2012) phylogeny, so use of CS as a proxy for SVL in these analyses was reasonable. All tests of signal in size among specimens, species, regions and habitats were significant. Many factors related to species, such as physiology, phylogeny, morphology, and ecology are tightly linked to body size (Losos and Greene, 1988; Pianka, 1995; Collar et al., 2011). Different habitats or ecologies impart different types and amounts of selection on organisms. Research has shown that different pressures imposed by habitats have likely led to differential selection on body size in *Varanus* (Pianka, 1995; Collar et al., 2011, Openshaw and Keogh, 2014). For example, arboreal habitats impose constraints on the size and mass of *Varanus* taxa. Rock-dwelling taxa also tend to have small size. The link between size and ecology in monitors is apparent in behaviors seen throughout ontogeny (Pianka, King, and King, 2004). Juveniles of large taxa have been known to climb trees for protection against predators until they are too large. Interestingly, some of the largest monitors have also been known to occasionally climb trees even as adults (Auffenberg, 1981; Pianka, King, and King, 2004).

Analyses of both dorsal snout and lateral views showed a strong relationship between size and shape. This link between size and shape is in agreement with other studies which have shown allometric patterns in monitors (Christian and Garland, 1996; Thompson and Withers, 1997; Collar et al*.,* 2011; Openshaw and Keogh, 2014). In dorsal view, the largest specimens display very distinctive wide, rounded snouts, whereas smaller taxa display thin, pointed snouts. In lateral view, larger specimens tend to show more rounded, long snouts, and smaller taxa overall flatter skulls. Regions in shape space were encompassed by different sized specimens. Both dorsal and lateral shape results showed a positive relationship with centroid size among all specimens and when accounting for regional and habitat groups. Size variation of *Varanus* in Africa is low, and extremely high in Indo-Australia. The high morphological disparity in Indo-Australia may reflect that varanids encompass a variety of habitats and sizes. Although many statistics showed a relationship between shape and habitat patterns, often specimens from different habitats might be found in several regions of shape space. Within habitat size variation is also important to consider. For example, the arboreal *V. salvadorii* is relatively large in terms of size variation in monitors, but has been known to easily maneuver across the tree canopy (Pianka and King, 2004). Work by Openshaw and Keogh (2014) has also suggested that the allometric scaling of dwarf varanids may differ from large monitors. Allometric trends can evolve, and it is important to integrate phylogeny into in-depth studies of allometry, because allometric patterns are not just a function of functional constraints or adaptation, but reflect historical patterns (Klingenberg, 2010; Openshaw and Keogh, 2014). Generally, there are many confounding factors influencing shape in monitors.

What the fossils tell us

The fossil record of varanids spans over 90 million years (Pianka, King, and King, 2004; Molnar, 2004; Conrad et al. 2012). Although fossil specimens attributed to the genus *Varanus* or close relatives are normally based on fragmentary material, the more complete material seems to indicate a great deal of morphological conservatism within this group. *Saniwa* and *V. priscus* fall well within extant *Varanus* cranial shape space. Because there was only one *Saniwa* and *V. priscus* specimen in this study, I did not include it in classification or CVA analyses. Phylogenetic analyses of the Eocene fossil taxon *Saniwa* repeatedly place the genus as sister to *Varanus* (and sometimes within) because there is so much morphological similarity (Conrad et al., 2008). The extinct Australian taxon, *Megalania prisca* (1.8 Mya – 40 kya) was renamed *Varanus priscus* because there are such strong morphological similarities to extant goannas (Molnar, 2004), and continued recent cladistic work places it within extant *Varanus* (Conrad et al., 2008). Based on morphology and size, *Saniwa* has been hypothesized to have a life history much like extant sub-aquatic and/or arboreal monitors (Rieppel and Grande, 2007). This analysis supports those inferences, because *Saniwa* falls within the morphospace range of aquatic and arboreal specimens. *V. priscus* is a large, terrestrial varanid. *V. priscus* falls in extant lateral skull morphospace, and also within Indo-Australian and terrestrial shape space. These fossil specimens falling within extant shape space indicates that the varanid body plan and range of morphologies seems to have appeared early on in varanid history, supporting many previous studies (Molnar, 2004; Rieppel and Grande, 2007; Conrad et al., 2012).

The already large variation in body size of *Varanus* increases when including fossil material. *V. priscus* was a top predator in Australia 4 Mya-30 Kya. The estimated body length of *V. priscus* has ranged between 26 ft to 11 ft in total body length, depending on the method and analyses used (Wroe, 2002; Molnar, 2004; Conrad et al., 2012). Recently, the earliest example of a large *Varanus* comes from the Miocene of Greece, and is estimated to be >600 mm pre-caudal length (Conrad et al. 2012). *V. priscus* falls close to the largest monitors included in this study, *V. komodoensis*, in both PCA and allometry analyses, indicating that it follows the general monitor lizard patterns of allometry. This opens questions about the cause of evolution of large size in this group. Studies had proposed that a lack of mammalian competitors might have allowed evolution of large size, but, for example, the newly discovered large *Varanus* from Greece achieved gigantism in a region populated by a fairly diverse community of mammalian competitors (Conrad et al. 2012). Cladistic analysis also nests the fossil within an East Asian clade, expanding the evolution of large size outside the Indo-Australian portion of the tree (Conrad et al., 2012).

Analyses of morphospace through time (Chapter 4 in this dissertation), and the fossil material falling within extant *Varanus* shape space indicate that monitor lizards may have explored large amounts of shape space early in their evolution. This exploration of shape variation also raises the question whether exploration of size and shape occurred similarly across the phylogeny. The oldest known fossil taxon recognized as part of extant *Varanus* is probably *Varanus rusingensis*. If true, this taxon shows that *Varanus* diversified and reached Africa by the Early Miocene (Clos, 1995; Conrad et al., 2008). A major question regarding *Varanus* has been where the lineage

originated, and discovery of more fossil material, analyses of sister groups, diversification rates, shape variation, and interrelationships will shed more light on this question.

Implication for morphometric analyses

Variation within populations is overlooked in a number of geometric morphometric analyses. When comparing a number of groups, for example, often one specimen is used to represent a taxon. Different taxa may exhibit a different amount of morphological variation, and the specimen selected may be an outlier in terms of shape variation. This analysis showed that when considered as the average shape, African taxa, for example, encompass a small amount of shape space. When a number of specimens are considered, though, they show a great deal of shape variation. Depending on the question of interest, it is important to consider variation within as well as among taxa.

Although generally dorsal and lateral results were similar, there were slight discrepancies in some instances. For example, all factors measured explained variation in skull shape in dorsal view, but only taxonomic designation was significant in lateral view. It may be interpreted, then, that lateral shape has more lability in shape and dorsal view more conservatism. Lateral shape, though, showed strong phylogenetic signal. Based on data here, it cannot be said that one view shows more or less lability in shape variation.

Landmark choice is another important factor to consider in geometric morphometric analyses. In this study, general snout shape and skull curvature was analyzed, but other studies of squamates have focused on distinct landmark placement on sutures and other type 1 landmark locations (Openshaw and Keogh, 2014). All biological inferences made in morphometric analyses should be based on the morphology analyzed, and shape variation of a distinct set of landmarks should not be considered to be representative of total variation in a group.

CONCLUSION

This study showed that several confounding factors can influence shape variation in a group. Variation within one or several factors may help maintain morphological disparity. Although there are many factors which may have played a role in the differences in taxonomic diversity across the geographic range of *Varanus*, this is not reflected in their cranial morphological variation. There is an overarching imprint of phylogenetic history on extant *Varanus* head shapes; however, there is extensive variation within lineages. Phylogeny, region, habitat, and size were significantly influential in explaining shape variation, but these factors are not necessarily independent of one another in *Varanus*. For example, previous studies have shown a strong relationship between size and shape (Pianka, 1995; Christian and Garland, 1996; Thompson and Withers, 1997; Pianka, King, and King, 2004; Collar et al., 2011; Openshaw and Keogh, 2014). Ecological relationships play a strong role in morphological variants within regional species pools, and this study showed that ecology is a reflection of both size and shape. There does not appear to be a strong

signal of evolutionary allometry in this study, but when specimens are considered independent of phylogeny, size and shape do correlate (especially in dorsal snout analyses), meaning it is important to decouple the evolutionary patterns of size on shape.

Cranial morphological variation in varanids, although considered conservative, showed differing patterns of overlap or divergence among habitat types, geographic ranges, and body size ranges. African specimens, represented by 4 taxa in this analysis, showed shape variation in morphospace equivalent to regions made up of numerous taxa, like Indo-Australia which was represented by 26 and 14 taxa in various analyses in this study. Although it's often expected that morphological disparity and taxonomic diversity will correlate, many studies have shown that this is not always the case (Foote, 1993; Faith and Baker, 2006; Adams et al., 2009; Ricklefs, 2012; Mishler et al., 2014). African and Indo-Australian specimens encompass a substantial proportion of overlapping morphospace, indicating similar shape variants found in taxa from different regions. Africa is low in taxonomic diversity, so the high morphological disparity was at first surprising, but because African taxa are made up of two of the most disparate habitats describing skull shape (terrestrial and aquatic), they span a great deal of morphospace. Indo-Australian monitor lizards show the largest amount of size variation, and also a great deal of species geographic range overlap (Pianka, 1994). Variation in size may have led to reduced competition in these regions. The increased size variation, as well variation in ecologies, may have played a role in increased morphological variation. One question of interest has focused on the reason for an absence of small monitors lizards in Asian and African deserts and forests. Results of a study that focused on life history strategies of varying sized monitor lizards showed that neither phylogenetic constraints or limitation in dispersal capabilities can explain the lack of small monitors in these regions (Sweet and Pianka, 2007). Extinct and extant monitor lizards are found alongside ecologically equivalent mammalian carnivores (Conrad, Balcarcel, and Mehling, 2012), so it may be that predatory interactions, more that competitive exclusion, may explain part of this restricted distribution of small monitors.

The effects of phylogenetic history on shape were interesting. Analysis of both dorsal and lateral shape results in a Kmult less than, but fairly close to 1, indicating slightly less phylogenetic signal than expected. However, it's important to emphasize that phylogenetic signal is not only based on the morphological data being tested, but also on the tree used as well as the taxonomic sample. Analyses on the average shape of taxa in phylomorphospace showed that regions, which form monophyletic clades, tend to be found in similar regions of morphospace. There were some exceptions which may have influenced the reduced Kmult. For example when *V. niloticus* (aquatic) is found in separate regions from other African taxa (terrestrial). Terrestrial taxa, and specifically the African species, are very distinct in cranial shape, and *V. niloticus* fall more along with general average elongate and aquatic or arboreal monitor lizard shape space.

In monitors, it appears that a generalized morphology has allowed effective exploitation of a wide variety of resources and habitats or ecologies. Species richness might be influenced by size variation, which in part increases ecological variation, which then both increase morphological disparity. Of course there are many caveats to this

study. The morphological measurements used in this analysis are undoubtedly incomplete indicators of these relationships. In regard to diet and other aspects of ecology like foraging behaviors, additional factors like physiology and locomotory adaptations also play a large role. Many monitor lizards show a large range of behaviors and ecologies, as adults or throughout ontogeny, but in this study morphology was measured relative to the primary habitat of each species. Moreover, each species is represented by a point in phylomorphospace, but a volume in PCA morphospace. Even this these caveats, research on ecologically versatile, but morphologically conservative groups can help provide information on factors influencing morphological diversification within a across species in a group, and what aspects of morphology can be informative in the underlying processes affecting shape variation.

References

Adams, D. C. 2014. A generalized K statistic for estimating phylogenetic signal from shape and other high-dimensional multivariate data. Systematic biology 63(5): 685-697.

Adams, D. C., C. M. Berns, K. H. Kozak and J. J. Wiens. 2009. Are rates of species diversification correlated with rates of morphological evolution? Proceedings of the Royal Society of London B: Biological Sciences, rspb-2009.

Adams, D. C., and E. Otarola-Castillo. 2013. geomorph: an R package for the collection and analysis of geometric morphometric shape data. Methods in Ecology and Evolution. 4:393-399.

Ackerly, D. 2009. Conservatism and diversification of plant functional traits: evolutionary rates versus phylogenetic signal. Proceedings of the National Academy of Sciences 106.Supplement 2: 19699-19706.

Ast, J. C. 2001. Mitochondrial DNA evidence and evolution in Varanoidea (Squamata). Cladistics 17:211–226.

Auffenberg, W. 1981. The behavioral ecology of the Komodo monitor. University Press of Florida.

Bennett, D., and B. L. Lim. 1995. A note on the distribution of Varanus dumerilii and V. rudicollis in Peninsular Malaysia. Malayan Nature Journal 49: 113-116.

Blomberg, S. P., T. Garland Jr, and A. R. Ives. 2003. Testing for phylogenetic signal in comparative data: behavioral traits are more labile. Evolution 57(4): 717-745.

Bookstein, F.L. 1991. Morphometric Tools for Landmark Data: Geometry and Biology. Cambridge University Press, Cambridge.

Bookstein, F. L. 1994. Can biometrical shape be a homologous character? in Homology: the hierarchical basis of comparative biology (B. K. Hall, ed.). Academic Press, New York., 197- 227

Bookstein, F. J. 1997 Landmark Methods for Forms without Landmarks: Morphometrics of Group Differences in Outline Shape. Medical Image Analysis 1(3):225-243.

Bookstein, F. L. 1998. A hundred years of morphometrics. Acta Zoologica Academiae Scientiarum Hungaricae 44 (1-2): 7-59.

Christian, A., and T. Garland Jr. 1996. Scaling of limb proportions in monitor lizards (Squamata: Varanidae). Journal of Herpetology, 219-230.

Clos, L. M. 1995. A new species of Varanus (Reptilia: Sauria) from the Miocene of Kenya. Journal of Vertebrate Paleontology, 15(2), 254-267.

Collar, D. C., I. I. Schulte, A. James and J.B. Losos. 2011. Evolution of extreme body size disparity in monitor lizards (Varanus). Evolution, 65(9), 2664-2680.

Conrad, J. L., A.M. Balcarcel and C. M. Mehling. 2012. Earliest example of a giant monitor lizard (Varanus, Varanidae, Squamata). PloS one, 7(8), e41767-e41767.

Conrad, J. L., O. Rieppel, and L. Grande. 2008. Re-assessment of varanid evolution based on new data from Saniwa ensidens Leidy, 1870 (Squamata, Reptilia). American Museum Novitates, 1-15.

Drake A. G. 2011. Dispelling dog dogma: an investigation of heterochrony in dogs using 3D geometric morphometric analysis of skull shape. Evol. Dev. 13: 204–213

Drake, A. G., and C. P. Klingenberg. 2010. Large-scale diversification of skull shape in domestic dogs: disparity and modularity. The American Naturalist 175(3): 289-301.

Dryden, I. L., and K. V. Mardia. 1998. Statistical shape analysis. Vol. 4. Chichester: Wiley.

Faith, D. P. 1992. Conservation evaluation and phylogenetic diversity.Biological conservation, 61(1), 1-10.

Faith, D. P., and A. M. Baker. 2006. Phylogenetic diversity (PD) and biodiversity conservation: some bioinformatics challenges. Evolutionary bioinformatics online 2, 121.

Felsenstein, J. 1985. Confidence limits on phylogenies: an approach using the bootstrap. Evolution 783-791.

Foote, M. 1993. Discordance and concordance between morphological and taxonomic diversity. Paleobiology, 185-204.

Goodall, C. 1991. Procrustes methods in the statistical analysis of shape. Journal of the Royal Statistical Society. Series B (Methodological): 285-339.

Hecht, M. 1975. The morphology and relationships ofthe largest known terrestrial lizard, Megalania prisca Owen, from the Pleistocene of Australia. Proceedings of the Royal Society of Victoria 87: 239-251.

Herrel, A., V. Schaerlaeken, J.J. Meyers, K.A. Metzger, and C. F. Ross. 2007. The evolution of cranial design and performance in squamates: consequences of skull-bone reduction on feeding behavior. Integrative and Comparative Biology 47(1):107-117.

Klingenberg, C. P. 2010. Evolution and development of shape: integrating quantitative approaches. Nature Reviews Genetics, 11(9), 623-635.

Klingenberg, C. P., and N. A. Gidaszewski. 2010. Testing and quantifying phylogenetic signals and homoplasy in morphometric data. Systematic biology 59(3): 245-261.

Klingenberg, C. P., S. Duttke, S. Whelan, and M. Kim. 2012. Developmental plasticity, morphological variation and evolvability: a multilevel analysis of morphometric integration in the shape of compound leaves. Journal of evolutionary biology 25(1): 115-129.

Koch, A., T. Ziegler, W. Boehme, E. Arida and M. Auliya. 2013. Pressing Problems: Distribution, threats, and conservation status of the monitor lizards (Varanidae: Varanus spp.) of Southeast Asia and the Indo-Australian Archipelago. Herpetological Conservation and Biology 8: 1-62.

Losos, J. B., and H. W. Greene. 1988. Ecological and evolutionary implications of diet in monitor lizards. Biological Journal of the Linnean Society, 35(4), 379-407.

Losos, J. B. 2008. Phylogenetic niche conservatism, phylogenetic signal and the relationship between phylogenetic relatedness and ecological similarity among species. Ecology letters 11(10): 995-1003.

MacLeod, N. 1999. Generalizing and extending the eigenshape method of shape space visualization and analysis. Paleobiology 25,107–138.

Mertens, R. 1942. Die Familie der Warane. Abhandlungen der Senckenbergischen Naturforschenden Gesellschaft 462:1-116; 465:117-234; 466:235-391.

Mishler, B. D., N. Knerr, C. E. González-Orozco, A. H. Thornhill, S. W. Laffan, and J. T. Miller. 2014. Phylogenetic measures of biodiversity and neo-and paleo-endemism in Australian Acacia. Nature communications, 5.

Mitteroecker P., P. Gunz, M. Bernhard, K. Schaefer, F. L. Bookstein. 2004. Comparison of cranial ontogenetic trajectories among great apes and humans. J Human Evol 46: 679-698.

Molnar, R. E. 2004. The long and honorable history of monitors and their kin.Varanoid Lizards of the World, 10-67.

Openshaw, G. H., and J. S. Keogh. 2014. Head shape evolution in monitor lizards (Varanus): interactions between extreme size disparity, phylogeny and ecology. Journal of evolutionary biology 27(2): 363-373.

Pepin, D. J. 2001. Evolution and life history of varanid lizards. Ph.D. thesis. Washington Univ., St. Louis, MO.

Pianka, E. R. 1994. Comparative ecology of Varanus in the Great Victoria desert. Australian Journal of Ecology, 19(4), 395-408.

Pianka, E.R. 1995. Evolution of body size: varanid lizards as a model system. American Naturalist: 398-414.

Pianka, E. R., D. King, and R. A. King. 2004. Varanoid lizards of the world. Indiana University Press.

R Core Team (2014). R: A language and environment for statistical computing. R Foundation for Statistical Computing, Vienna, Austria.URL http://www.R-project.org/.

Revell, L. J. 2012. phytools: An R package for phylogenetic comparative biology (and other things). Methods Ecol. Evol. 3: 217-223. doi:10.1111/j.2041-210X.2011.00169.x

Ricklefs, R. E. 2012. Species richness and morphological diversity of passerine birds. Proceedings of the National Academy of Sciences, 109(36), 14482-14487.

Rieppel, O., and L. Grande, L. 2007. The anatomy of the fossil varanid lizard Saniwa ensidens Leidy, 1870, based on a newly discovered complete skeleton.Journal Information, 81(4).

Rohlf, F. J. 2001. tps Dig–Thin Plate Spline Digitizer, version 1.31. State University of New York at Stony Brook, New York.

Rohlf, F. J. 2002. Geometric morphometrics and phylogeny. In Morphology, shape and phylogeny 175-193.

Rohlf, F. J., and D. Slice. 1990. Extensions of the Procrustes method for the optimal superimposition of landmarks. Systematic Biology, 39(1): 40-59.

Sanger, T. J., D. L. Mahler, A. Abzhanov,and J. B. Losos. 2011. Roles for modularity and constraint in the evolution of cranial diversity among anolis lizards. Evolution 66: 1525–1542

Stefan S. 2014. Morpho: Calculations and visualisations related to Geometric Morphometrics. R package version 2.2.http://CRAN.R-project.org/package=Morpho

Schweiger, O., S. Klotz, W. Durka, and I. Kühn. 2008. A comparative test of phylogenetic diversity indices. Oecologia, 157(3), 485-495.

Sweet, S. S., and E. R. Pianka. 2007. Monitors, mammals and Wallace's Line.Mertensiella, 16, 79-99.

Swenson, N. G., B. J. Enquist, J. Thompson, and J. K. Zimmerman. 2007. The influence of spatial and size scale on phylogenetic relatedness in tropical forest communities. Ecology 88(7): 1770-1780.

Thompson, G. G., and P. C. Withers. 1997. Standard and maximal metabolic rates of goannas (Squamata: Varanidae). Physiological zoology, 307-323.

Vidal, N., J. Marin, J. Sassi, F. U. Battistuzzi, S. Donnellan, A. J. Fitch, B. G. Fry et al. 2012. Molecular evidence for an Asian origin of monitor lizards followed by Tertiary dispersals to Africa and Australasia. Biology letters: rsbl20120460.

Wroe, S. 2002. A review of terrestrial mammalian and reptilian carnivore ecology in Australian fossil faunas, and factors influencing their diversity: the myth of reptilian domination and its broader ramifications. Australian Journal of Zoology, 50(1), 1-24.

Zelditch, M. L., L. B. Lundrigan, and T. Garland. 2004. Developmental regulation of skull morphology. I. Ontogenetic dynamics of variance. Evolution and development 6(3): 194-206.

Zelditch, M. L., D. L. Swiderski, and H. D. Sheets. Geometric morphometrics for biologists: a primer. Academic Press, 2012.

Table 1. *Varanus* Specimen list.				
Species	**Museum**	**Spec. #**	**Region**	**Habitat**
acanthurus	AM	R143882	Australia	Terrestrial
acanthurus	AM	R166371	Australia	Terrestrial
acanthurus	YPM	14951	Australia	Terrestrial
albigularis	NMNH	72027	Africa	Terrestrial
albigularis	NMNH	216472	Africa	Terrestrial
albigularis	NMNH	216260	Africa	Terrestrial
albigularis	AMNH	47725	Africa	Terrestrial
albigularis	AMNH	47726	Africa	Terrestrial
albigularis	AMNH	47727	Africa	Terrestrial
albigularis	AMNH	70154	Africa	Terrestrial
beccarii	MVZ	ACCN 14440	Australia	Arboreal
beccarii	MVZ	ACCN 14441	Australia	Arboreal
beccarii	AMNH	139340	Australia	Arboreal
beccarii	AMNH	141072	Australia	Arboreal
beccarii	YPM	11899	Australia	Arboreal
bengalensis	UCMP	121238	Asia	Arb/Terrestrial
bengalensis	UCMP	121238	Asia	Arb/Terrestrial
bengalensis	UCMP	140490	Asia	Arb/Terrestrial
bengalensis	UCMP	141181	Asia	Arb/Terrestrial
bengalensis	UCMP	141182	Asia	Arb/Terrestrial
bengalensis	UCMP	141183	Asia	Arb/Terrestrial
bengalensis	UCMP	141184	Asia	Arb/Terrestrial
bengalensis	UCMP	141185	Asia	Arb/Terrestrial
bengalensis	UCMP	141186	Asia	Arb/Terrestrial
bengalensis	UCMP	141187	Asia	Arb/Terrestrial
bengalensis	UCMP	141188	Asia	Arb/Terrestrial
bengalensis	UCMP	141189	Asia	Arb/Terrestrial
bengalensis	UCMP	141238	Asia	Arb/Terrestrial
bengalensis	Cal Acad	NA	Asia	Arb/Terrestrial
bengalensis	AMNH	117786	Asia	Arb/Terrestrial
bengalensis	AMNH	118715	Asia	Arb/Terrestrial
bengalensis	AMNH	118716	Asia	Arb/Terrestrial
bengalensis	AMNH	71195	Asia	Arb/Terrestrial
bengalensis bengalensis	NMNH	14753	Asia	Arb/Terrestrial
bengalensis bengalensis	NMNH	149140	Asia	Arb/Terrestrial
bengalensis nebulosis	NMNH	221891	Asia	Arb/Terrestrial
bengalensis nebulosis	NMNH	220280	Asia	Arb/Terrestrial
bengalensis nebulosis	NMNH	220281	Asia	Arb/Terrestrial
bengalensis nebulosis	NMNH	23099	Asia	Arb/Terrestrial

Table 1 (cont.)

doreanus	YPM	11061	Australia	Terrestrial
dumerilii	NMNH	24022	Asia	Terrestrial
dumerilii	NMNH	26205	Asia	Terrestrial
dumerilii	NMNH	94951	Asia	Terrestrial
dumerilli	YPM	11176	Asia	Terrestrial
dumerilli	YPM	11203	Asia	Terrestrial
dumerilli	YPM	12148	Asia	Terrestrial
exanthematicus	MVZ	ACCN 144981	Africa	Terrestrial
exanthematicus	MVZ	NA	Africa	Terrestrial
exanthematicus	MVZ	NA	Africa	Terrestrial
exanthematicus	UCMP	137818	Africa	Terrestrial
exanthematicus	UCMP	140816	Africa	Terrestrial
exanthematicus	UCMP	141024	Africa	Terrestrial
exanthematicus	UCMP	141137	Africa	Terrestrial
exanthematicus	UCMP	141237	Africa	Terrestrial
exanthematicus	AMNH	140804	Africa	Terrestrial
exanthematicus	AMNH	137237	Africa	Terrestrial
exanthematicus	AMNH	137238	Africa	Terrestrial
exanthematicus	AMNH	140801	Africa	Terrestrial
exanthematicus	AMNH	140802	Africa	Terrestrial
exanthematicus	AMNH	140803	Africa	Terrestrial
exanthematicus	AMNH	155251	Africa	Terrestrial
exanthematicus	AMNH	155251	Africa	Terrestrial
exanthematicus	AMNH	29297	Africa	Terrestrial
exanthematicus	YPM	11062	Africa	Terrestrial
exanthematicus	YPM	11187	Africa	Terrestrial
exanthematicus	YPM	11191	Africa	Terrestrial
exanthematicus	YPM	13940	Africa	Terrestrial
giganteus	AM	R59190	Australia	Terrestrial
glauerti	MVZ	NA	Australia	Terrestrial
glauerti	WAM	R80505	Australia	Terrestrial
gouldii	NMNH	67734	Australia	Terrestrial
gouldii	AM	R21418	Australia	Terrestrial
gouldii	AM	R142826	Australia	Terrestrial
gouldii	AM	R143848	Australia	Terrestrial
gouldii/panoptes	AM	R51920	Australia	Terrestrial
griseus	NMNH	292065	Africa	Terrestrial
griseus	NMNH	220282	Africa	Terrestrial
griseus	YPM	10370	Africa	Terrestrial

Table 1 (cont.)

griseus	YPM	10383	Africa	Terrestrial
griseus	NMNH	132275	Africa	Terrestrial
griseus	NMNH	132276	Africa	Terrestrial
griseus	NMNH	228164	Africa	Terrestrial
indicus	NMNH	122469	Australia	Aqua/Arboreal
indicus	NMNH	237693	Australia	Aqua/Arboreal
indicus	NMNH	323717	Australia	Aqua/Arboreal
indicus	AMNH	142623	Australia	Aqua/Arboreal
indicus	YPM	10381	Australia	Aqua/Arboreal
indicus indicus	NMNH	194863	Australia	Aqua/Arboreal
jobiensis	AM	R166376	Australia	Arboreal
jobiensis	YPM	13659	Australia	Arboreal
komodoensis	AM	R175720	Australia	Terrestrial
komodoensis	NMNH	101444	Australia	Terrestrial
komodoensis	AMNH	109498	Australia	Terrestrial
komodoensis	AMNH	37908	Australia	Terrestrial
komodoensis	AMNH	37909	Australia	Terrestrial
komodoensis	AMNH	37910	Australia	Terrestrial
komodoensis	AMNH	37911	Australia	Terrestrial
komodoensis	AMNH	37912	Australia	Terrestrial
komodoensis	YPM	10881	Australia	Terrestrial
komodoensis	YPM	16943	Australia	Terrestrial
melinus	YPM	11202	Australia	Arboreal
mertensi	YPM	11658	Australia	Aquatic
niloticus	UCMP	123073	Africa	Aquatic
niloticus	UCMP	141023	Africa	Aquatic
niloticus	UCMP	141190	Africa	Aquatic
niloticus	NMNH	60554	Africa	Aquatic
niloticus	NMNH	42260	Africa	Aquatic
niloticus	NMNH	72026	Africa	Aquatic
niloticus	NMNH	72028	Africa	Aquatic
niloticus	NMNH	216247	Africa	Aquatic
niloticus	NMNH	220294	Africa	Aquatic
niloticus	AMNH	10499	Africa	Aquatic
niloticus	AMNH	10500	Africa	Aquatic
niloticus	AMNH	10501	Africa	Aquatic
niloticus	AMNH	10502	Africa	Aquatic
niloticus	AMNH	10511	Africa	Aquatic
niloticus	AMNH	10512	Africa	Aquatic
niloticus	AMNH	10519	Africa	Aquatic

Table 1 (cont.)

niloticus	AMNH	10522	Africa	Aquatic
niloticus	AMNH	119222	Africa	Aquatic
niloticus	AMNH	137116	Africa	Aquatic
niloticus	AMNH	140805	Africa	Aquatic
niloticus	AMNH	57969	Africa	Aquatic
niloticus	AMNH	7252	Africa	Aquatic
niloticus	AMNH	74570	Africa	Aquatic
niloticus	AMNH	74603	Africa	Aquatic
niloticus	AMNH	74604	Africa	Aquatic
niloticus	AMNH	88635	Africa	Aquatic
niloticus	YPM	10775	Africa	Aquatic
niloticus	YPM	10877	Africa	Aquatic
olivaceus	NMNH	222400	Asia	Arboreal
olivaceus	NMNH	27776	Asia	Arboreal
ornatus	AMNH	10515	Africa	Aquatic
panoptes	MVZ	ACCN 14498	Australia	Terrestrial
panoptes	MVZ	ACCN 14499	Australia	Terrestrial
panoptes	AM	R143871	Australia	Terrestrial
panoptes	AM	R143874	Australia	Terrestrial
panoptes	AM	R143873	Australia	Terrestrial
panoptes	AM	R172225	Australia	Terrestrial
panoptes	YPM	10394	Australia	Terrestrial
panoptes horni	MVZ	NA	Australia	Terrestrial
panoptes rubidus	AM	R100500	Australia	Terrestrial
prasinus	AM	R166378	Australia	Arboreal
prasinus	UCMP	123076	Australia	Arboreal
prasinus	AMNH	104683	Australia	Arboreal
prasinus	YPM	10328	Australia	Arboreal
prasinus	YPM	11747	Australia	Arboreal
prasinus cordensis	AM	R166379	Australia	Arboreal
prasinus cordensis	AM	R166380	Australia	Arboreal
rudicollis	AM	R166377	Asia	Arboreal
rudicollis	AMNH	141071	Asia	Arboreal
rudicollis	YPM	11082	Asia	Arboreal
rudicollis	YPM	12234	Asia	Arboreal
rudicollis	YPM	12235	Asia	Arboreal
salvadorii	YPM	12095	Asia	Aquatic
salvator	MVZ	ACCN EBV 2012	Asia	Aquatic

Table 1 (cont.)

salvator	MVZ	ACCN EBV 2013	Asia	Aquatic
salvator	MVZ	ACCN EBV 2014	Asia	Aquatic
salvator	Cal Acad	NA	Asia	Aquatic
salvator	NMNH	68098	Asia	Aquatic
salvator	NMNH	35762	Asia	Aquatic
salvator	NMNH	28083	Asia	Aquatic
salvator	NMNH	24021	Asia	Aquatic
salvator	NMNH	287413	Asia	Aquatic
salvator	NMNH	163810	Asia	Aquatic
salvator	NMNH	68125	Asia	Aquatic
salvator	NMNH	220284	Asia	Aquatic
salvator	NMNH	220286	Asia	Aquatic
salvator	NMNH	220285	Asia	Aquatic
salvator	NMNH	287381	Asia	Aquatic
salvator	NMNH	221892	Asia	Aquatic
salvator	NMNH	220283	Asia	Aquatic
salvator	NMNH	220287	Asia	Aquatic
salvator	MVZ	NA	Asia	Aquatic
salvator	UCMP	123078	Asia	aquatic
salvator	UCMP	123080	Asia	Aquatic
salvator	UCMP	123080	Asia	Aquatic
salvator	UCMP	123081	Asia	Aquatic
salvator	UCMP	123082	Asia	Aquatic
salvator	UCMP	123083	Asia	Aquatic
salvator	UCMP	123084	Asia	Aquatic
salvator	UCMP	123085	Asia	Aquatic
salvator	AMNH	139671	Asia	Aquatic
salvator	AMNH	141148	Asia	Aquatic
salvator	AMNH	141155	Asia	Aquatic
salvator	AMNH	147174	Asia	Aquatic
salvator	AMNH	49230	Asia	Aquatic
salvator	AMNH	NA	Asia	Aquatic
salvator	YPM	10756	Asia	Aquatic
salvator	YPM	11022	Asia	Aquatic
salvator	YPM	11064	Asia	Aquatic
salvator	YPM	11147	Asia	Aquatic
salvator	YPM	11177	Asia	Aquatic

Table 1 (cont.)

salvator	YPM	11773	Asia	Aquatic
salvator	UCMP	65531	Asia	Aquatic
salvator	UCMP	123077	Asia	Aquatic
salvator	NMNH	23092	Asia	Aquatic
salvator	NMNH	23094	Asia	Aquatic
salvator	NMNH	23095	Asia	Aquatic
salvator	NMNH	23097	Asia	Aquatic
salvator	NMNH	26509	Asia	Aquatic
salvator	NMNH	30799	Asia	Aquatic
salvator	NMNH	30800	Asia	Aquatic
salvator	NMNH	30801	Asia	Aquatic
salvator	NMNH	30802	Asia	Aquatic
salvator	NMNH	37867	Asia	Aquatic
salvator cumingi	NMNH	305884	Asia	Aquatic
salvator cumingi	NMNH	30751	Asia	Aquatic
salvator cumingi	NMNH	30752	Asia	Aquatic
salvator cumingi	NMNH	36993	Asia	Aquatic
salvator cumingi	NMNH	39889	Asia	Aquatic
salvator marmoratus	NMNH	512318	Asia	Aquatic
salvator marmoratus	NMNH	498916	Asia	Aquatic
spenseri	UCMP	140815	Australia	Terrestrial
storri	AM	R143912	Australia	Terrestrial
storri	YPM	11042	Australia	Terrestrial
timorensis	MVZ	ACCN 144981	Australia	Arboreal
timorensis	AM	R138712	Australia	Arboreal
timorensis	AM	R12371	Australia	Arboreal
timorensis	AM	R61488	Australia	Arboreal
tristis	AM	R143919	Australia	Arboreal
tristis	WAM	R106054	Australia	Arboreal
tristis	YPM	11175	Australia	Arboreal
unknown	NMNH	536545	NA	NA
unknown	NMNH	536546	NA	NA
unknown	AM	R172485	NA	NA
unknown	Cal Acad	NA	NA	NA
unknown	AMNH	123313	NA	NA
unknown	AMNH	Unk	NA	NA
unknown	AMNH	Unk	NA	NA
unknown	YPM	10534	NA	NA
unknown	YPM	10878	Africa	NA
unknown	YPM	10879	Africa	NA

Table 1 (cont.)

unknown	YPM	10880	Africa	NA
unknown	MVZ	NA	NA	NA
unknown	NMNH	94952	Asia	NA
unknown	NMNH	101309	Asia	NA
varius	AM	R86079	Australia	Arb/Terrestrial
varius	AM	R12247	Australia	Arb/Terrestrial
varius	AM	R131283	Australia	Arb/Terrestrial
varius	AM	R158212	Australia	Arb/Terrestrial
varius	AMNH	28698	Australia	Arb/Terrestrial
varius	YPM	16800	Australia	Arb/Terrestrial

Table 2. Extinct *Varanus* used in the study.

Taxon	Time	Region	Habitat	Reference
Varanus priscus (Megalania prisca)	Pleistocene	Australia	Terrestrial	Molnar, 2004; Wroe, 1981
Saniwa ensidens	Eocene	North America	Aquatic/Arboreal	Conrad, Rieppel, and Grande, 2008

Table 3. Landmark placement descriptions

Dorsal view

Semilandmarks	40 surround the snout from posterior end of each orbit
Landmarks	1 and 3: Posterior end of quadrate seen in dorsal view 2: Posterior point of the midline of the parietal

Lateral view

Semilandmarks	25 along the dorsal part of the skull from tip of snout to dorsal point of the foramen magnum
Landmarks	1. Anterior point of the nasal opening 2. Posterior point of the nasal opening 3. Anterior orbit, contact between jugal and lacrimal 4. Posterior point of the maxilla tooth row 5. Posterior point of the lateral view of orbit near anterior of parietal 6. Base of the quadrate

Table 4. Phylogenetic Diversity (PD) of the Vidal et al. (2012) tree.
PD was measured on taxa represented regions across the whole tree
and on a number of taxa subsampled to the region with the lowest diversity, Africa (3 taxa), for more comparability across regions.

	Taxonomic. Diversity	Total PD	Subsampled subgroup PD
Africa	3	66.08	86.5
Indo-Asia	10	172.99	92.6
Indo-Australia	26	464	91.5

Table 5. Procrustes ANOVA results. Randomized Residual Permutation used.

Dorsal snout			
	F	**Z**	**P.value**
Region	78.37	19.55	0.001
Habitat	26.86	11.73	0.001
Species	8.06	5.13	0.001
Region:Habitat	0.5005		
Region:Species	0.5005		
Habitat:Species	0.5005		
Region:Habitat:Species	0.5005		
Lateral			
	F	**Z**	**P.value**
Region			0.50
Habitat			0.50
Species	6.3777	3.098	0.001
Region:Habitat			0.50
Region:Species			0.50
Habitat:Species			0.50
Region:Habitat:Species			0.50
Residuals			0.50
Total			

Table 6. Procrustes variance results for dorsal and lateral views

Dorsal snout			
Region	**PV**	**Habitat**	**PV**
Africa	4.96E-03	Arboreal	4.99E-03
Indo-Asia	2.95E-03	Aquatic	2.87E-03
Indo-Australia	5.21E-03	Terrestrial	6.57E-03
		Arboreal/Aquatic	6.69E-04
		Arboreal/Terrestrial	2.00E-03
Lateral			
Region	**PV**	**Habitat**	**PV**
Africa	4.16E-03	Arboreal	6.11E-03
Indo-Asia	5.00E-03	Aquatic	3.37E-03
Indo-Australia	3.22E-03	Terrestrial	4.65E-03
		Arboreal/Aquatic	1.61E-03
		Arboreal/Terrestrial	3.63E-03

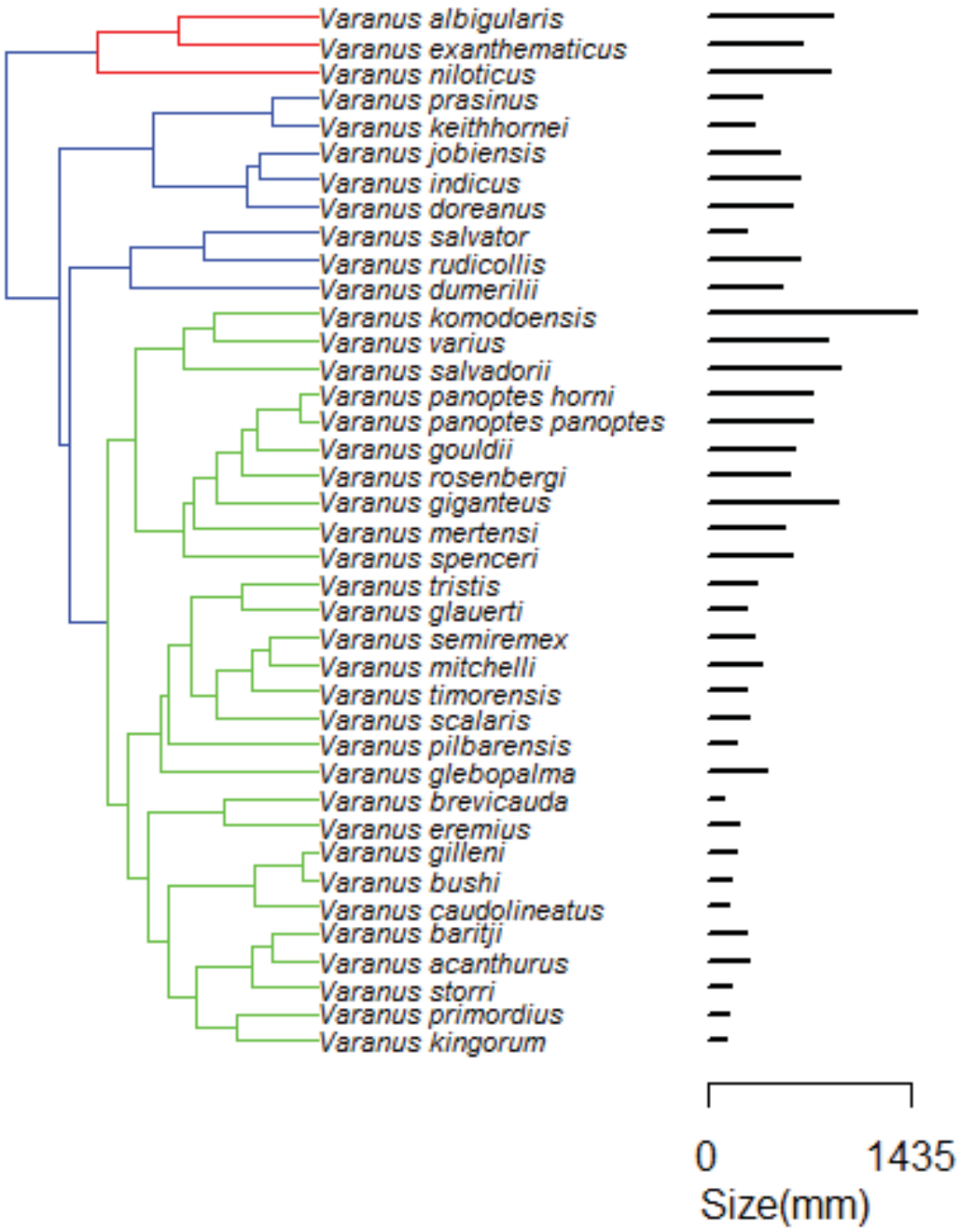


Figure 1. Geographic range of Varanus with regional groups color coded. Africa – red, Indo-Asia-Blue, and Indo-Australia-Green. The phylogeny is from Vidal et al. 2012. Segments are average Snout Vent Length (SVL) of taxa. Notice the great deal of size variation among Indo-Australian taxa.

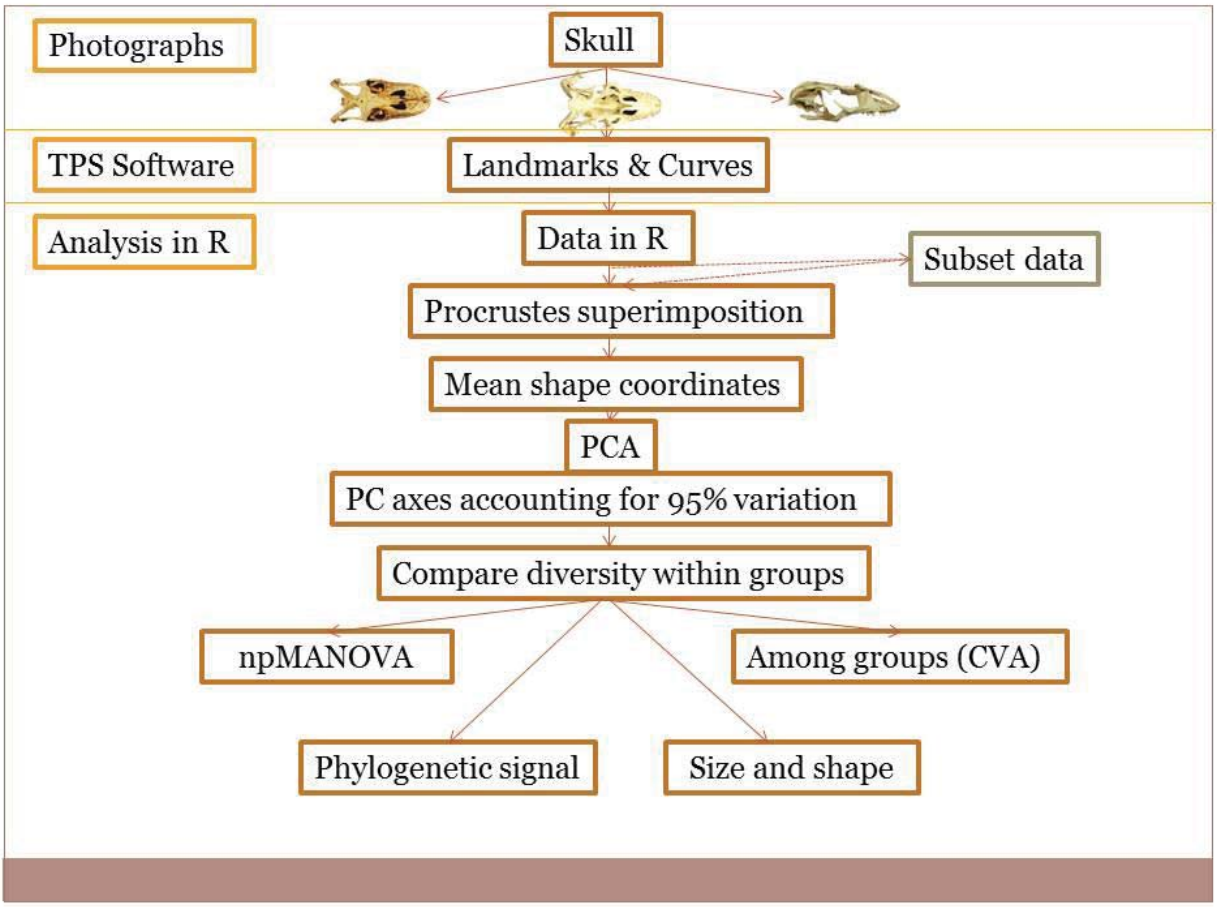


Figure 2. Outline of methods in this study.

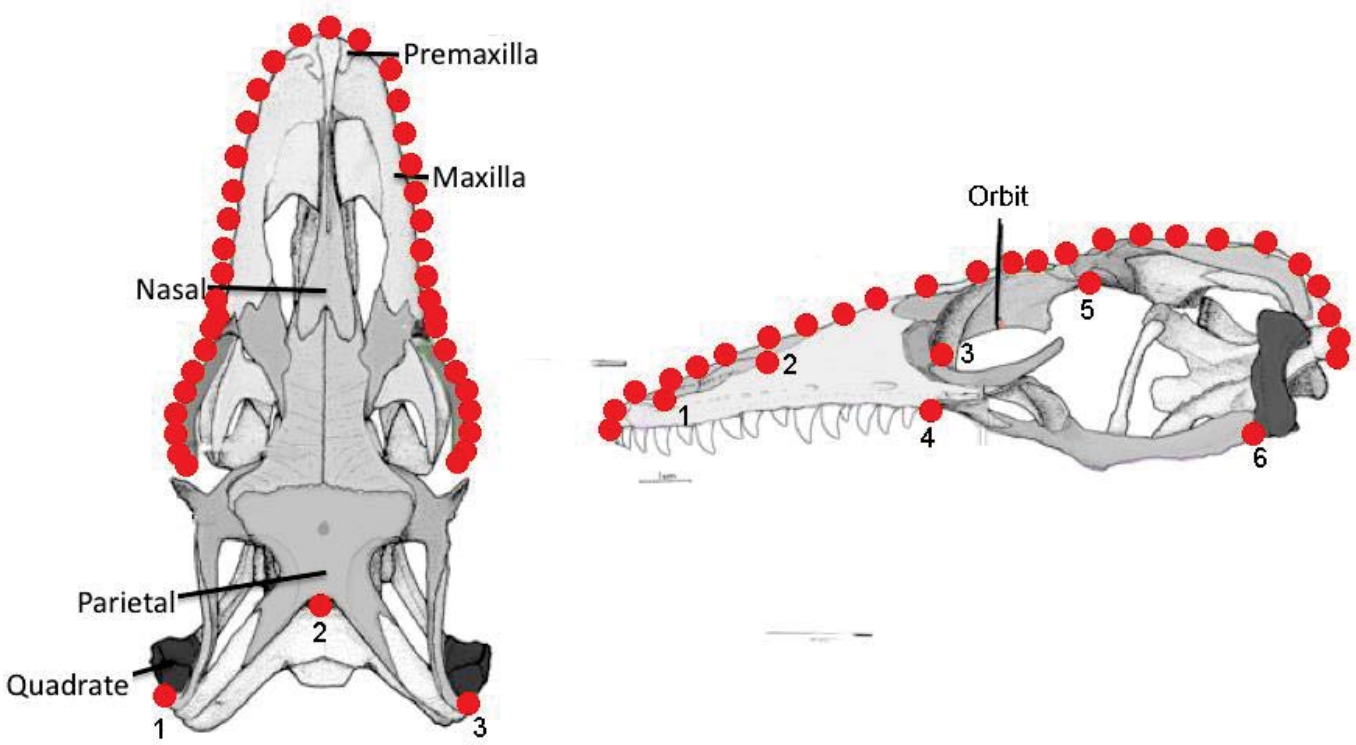


Figure 3. Landmark and semilandmark placement on skulls in dorsal and lateral views. Specific descriptions of landmarks placement can be found in Table 3. Image is modified from G. A. Boulenger, Fauna of British India.

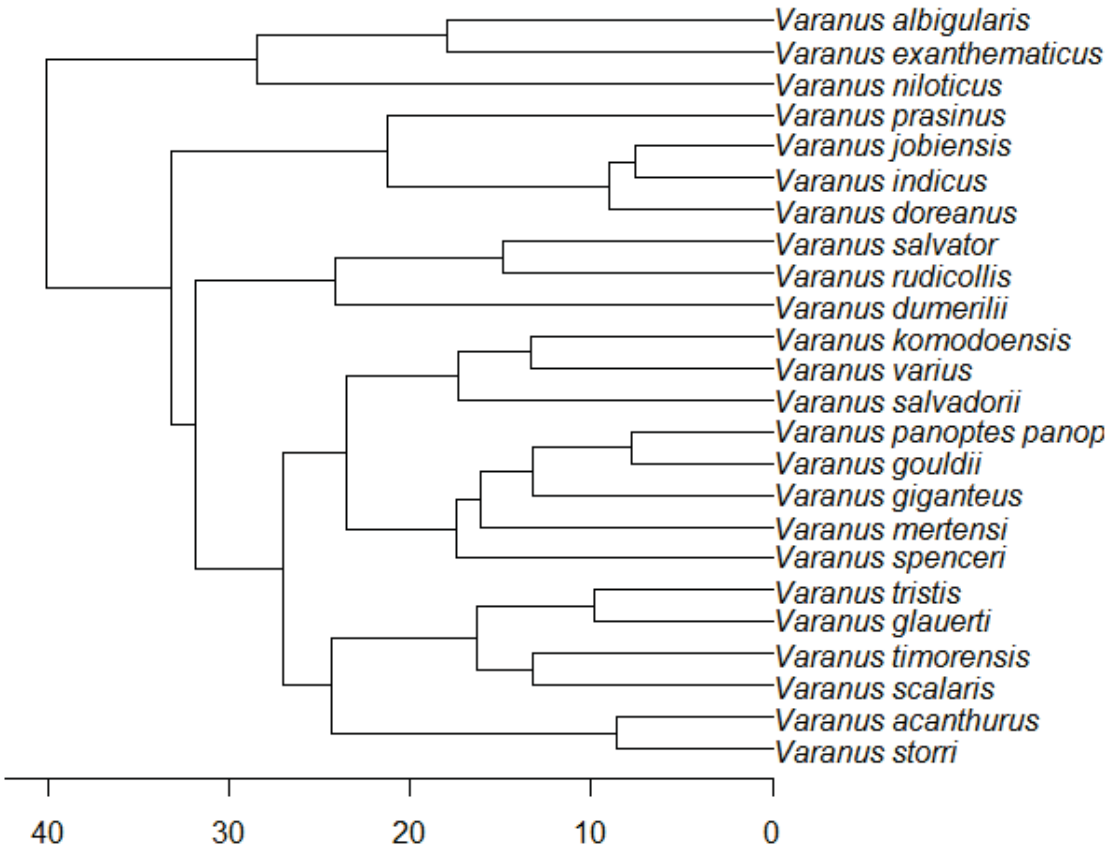


Figure 4. Modified version of the Vidal et al. tree containing only taxa for which geometric morphometric data was available in this study.

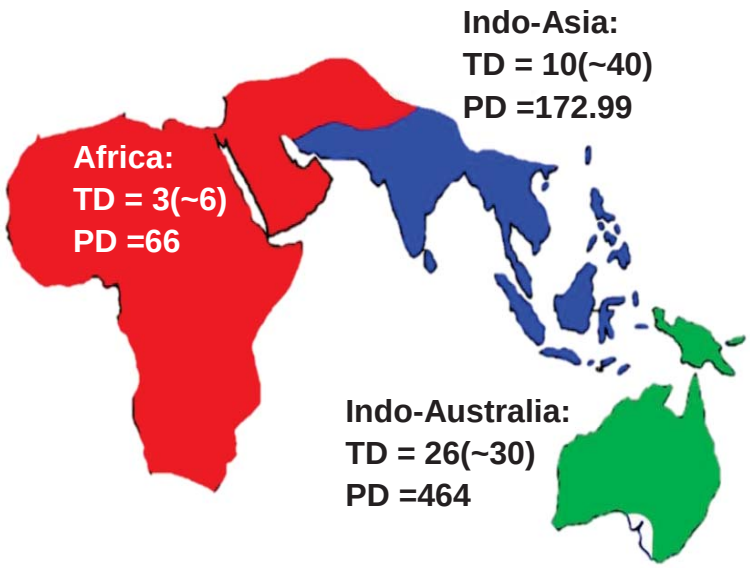


Figure 5. Taxonomic (TD) and Phylogenetic Diversity (PD) of extant Varanus based on the Vidal et al. (2012) phylogeny. Numbers in parentheses are current full taxonomic diversity, which is not represented in the Varanus tree. PD is shown on the whole tree, see Table 4 for subsampled results.

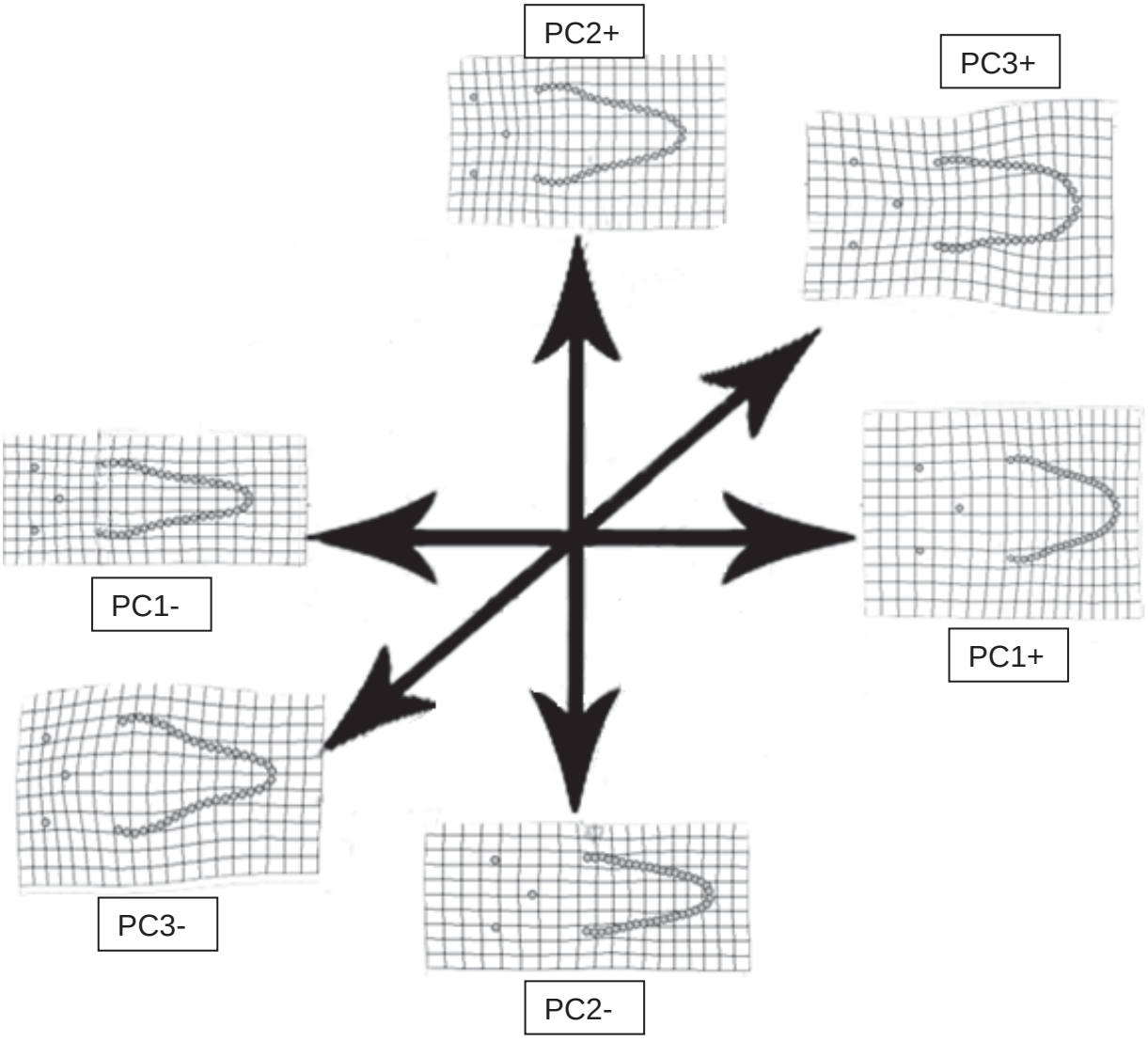


Figure 6. Shape variation along the first 3 dorsal snout principal component axes.

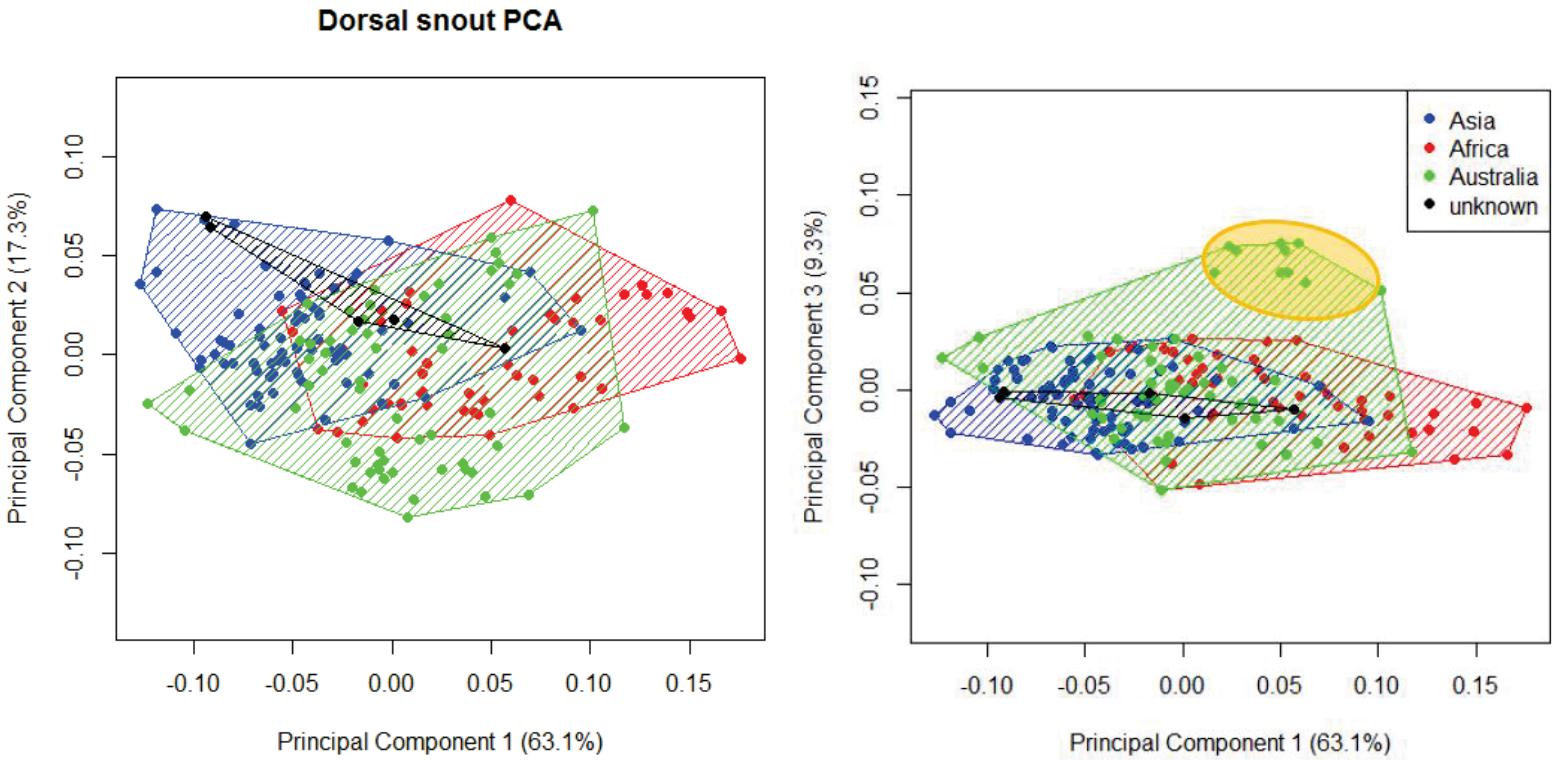


Figure 7. Dorsal snout principal components analyses results with convex hulls colored based on region. Left figure is Principal component 1 vs Principal component 2, and right figures Principal component 1 vs Principal component 3. The orange circle on the right figure shows where *V. komodoensis* is found in shape space.

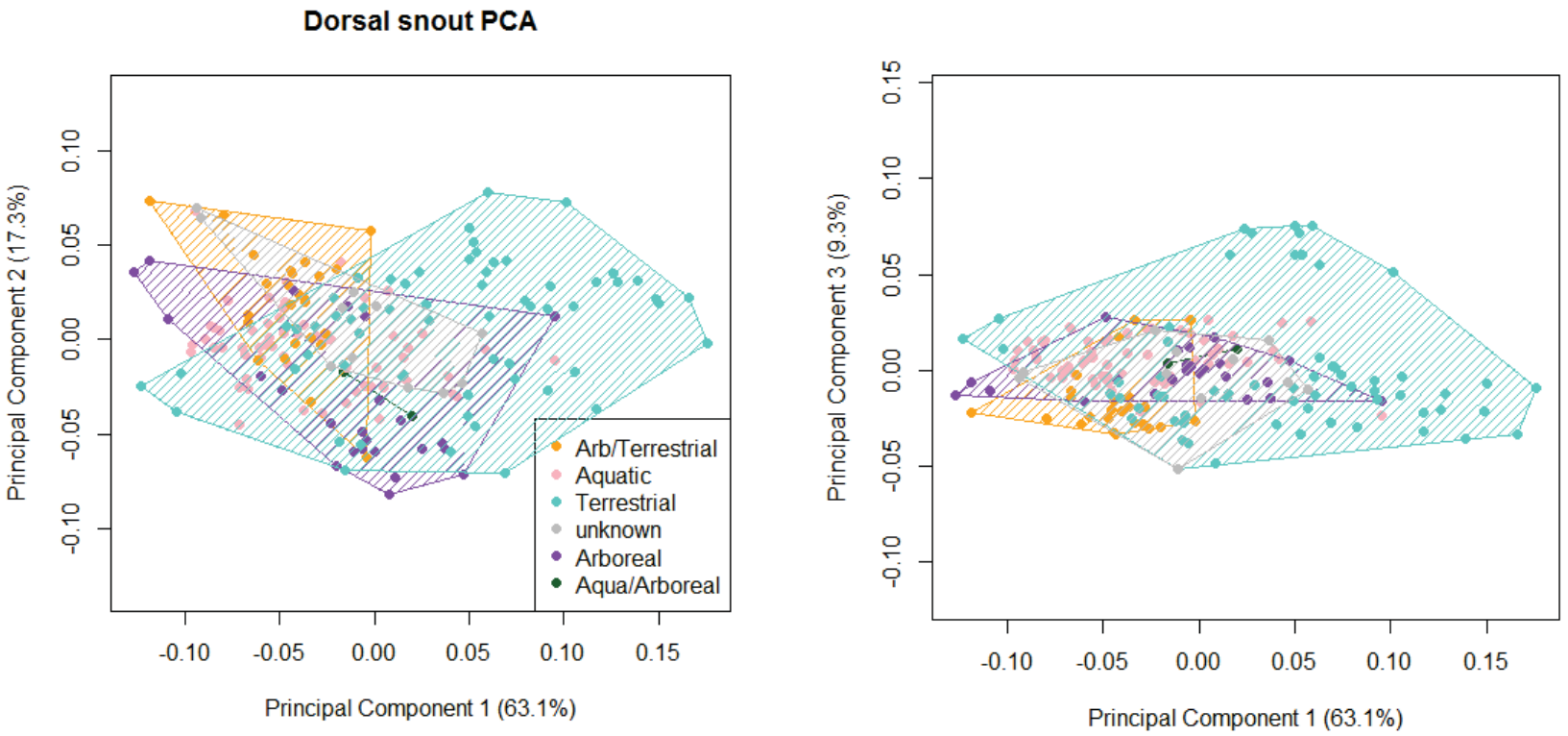


Figure 8. Dorsal snout principal component analysis results with convex hulls colored by habitat. Left figure is Principal component 1 versus principal component 2, and right figure is principal component 1 versus principal component 3.

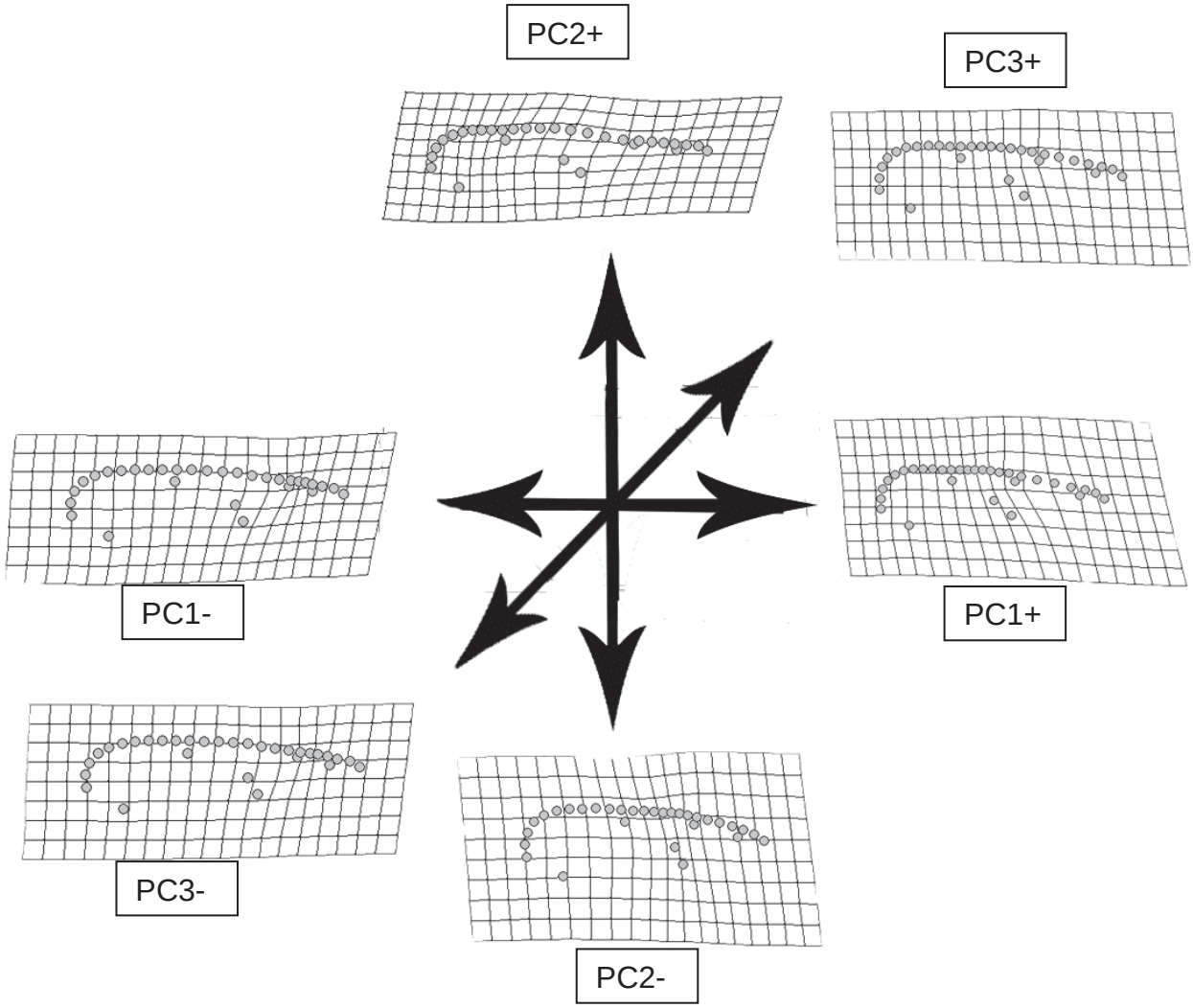


Figure 9. Lateral skull shape change along the first 3 principal axes.

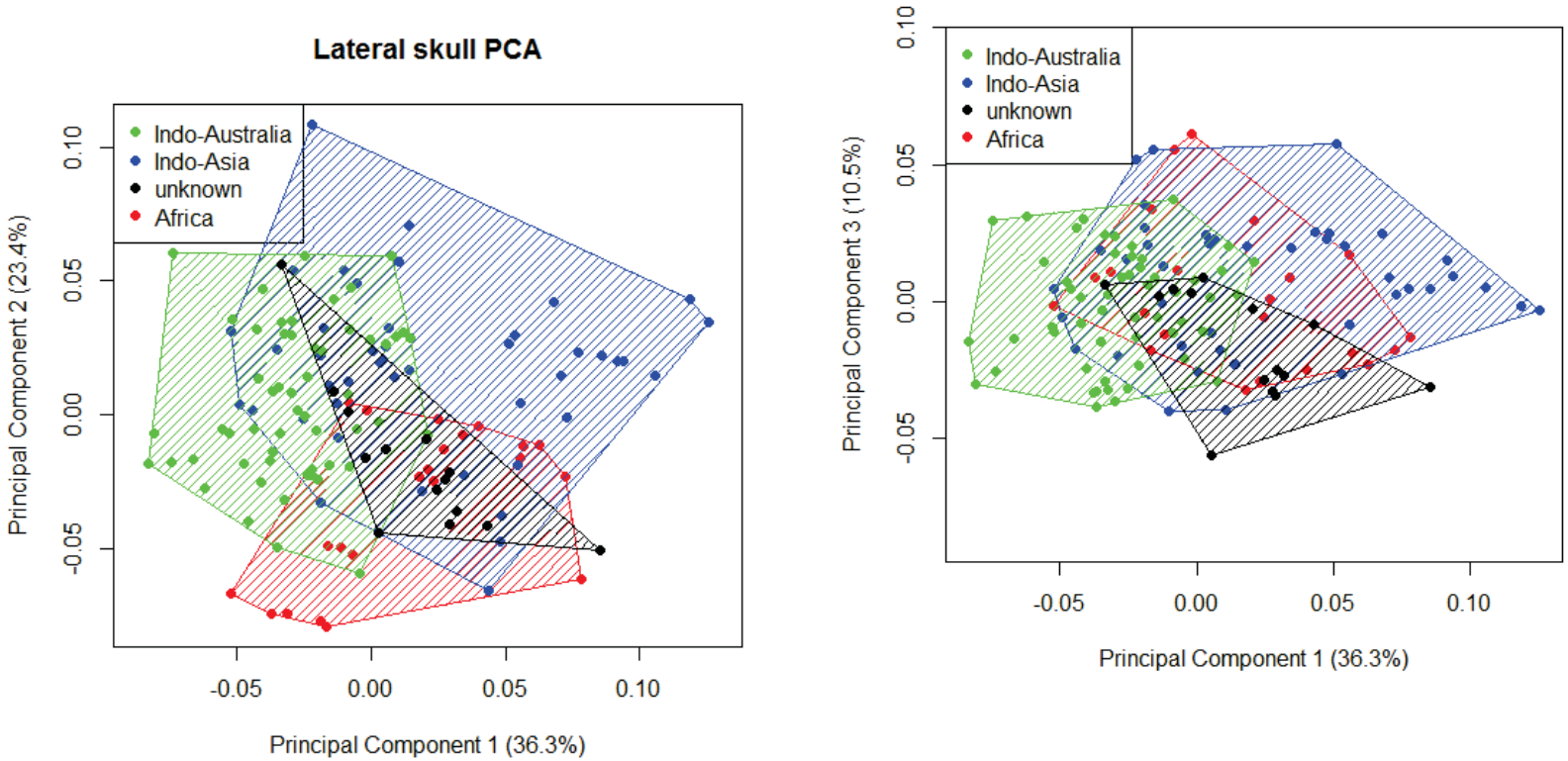


Figure 10. Lateral skull principal component analysis results with convex hulls colored by region. Left figure is Principal component 1 versus principal component 2, and right figure is principal component 1 versus principal component 3.

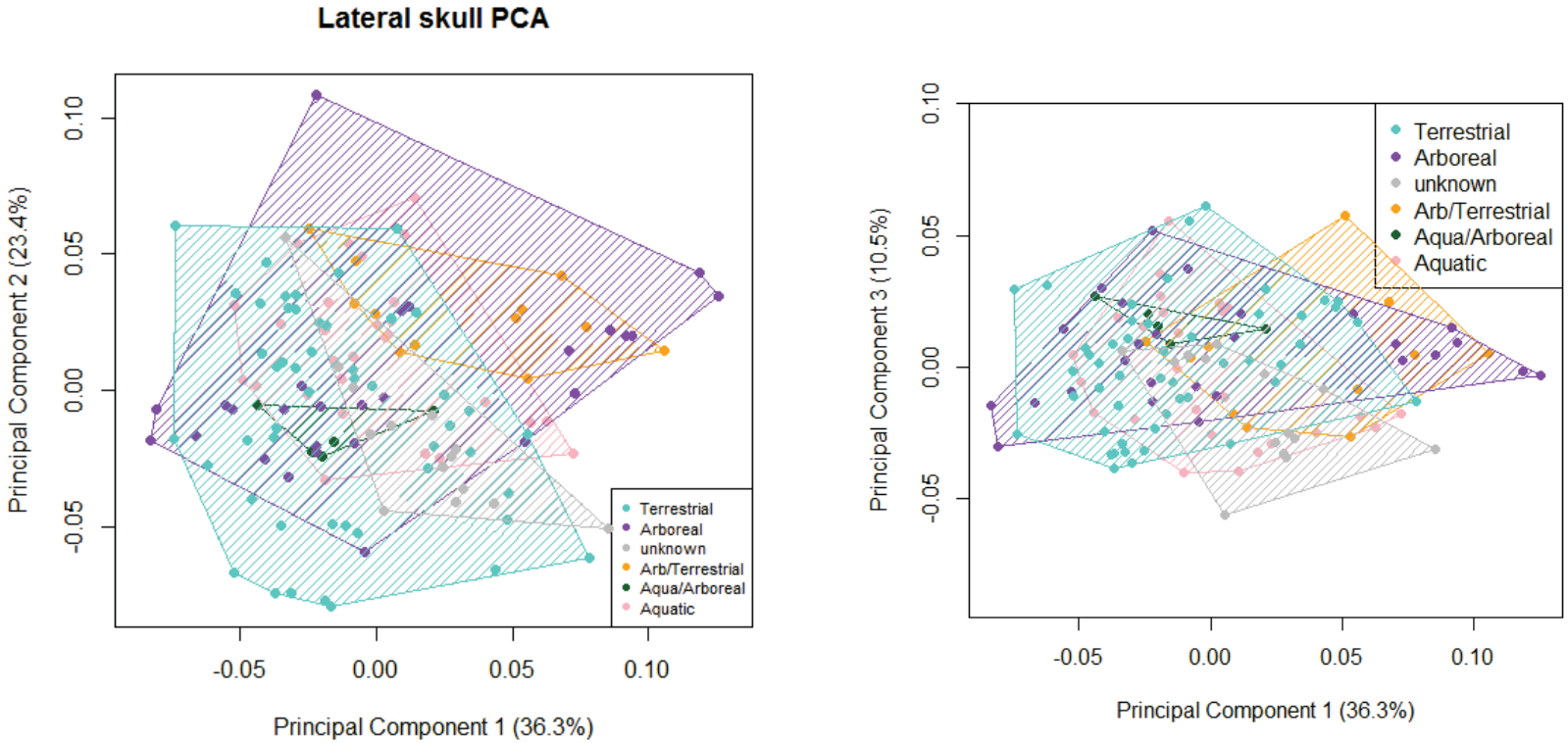


Figure 11. Lateral skull principal component space with convex hulls color coded by habitat. On the left is principal component 1 versus principal component 2, and on the right principal component 1 versus principal component 3.

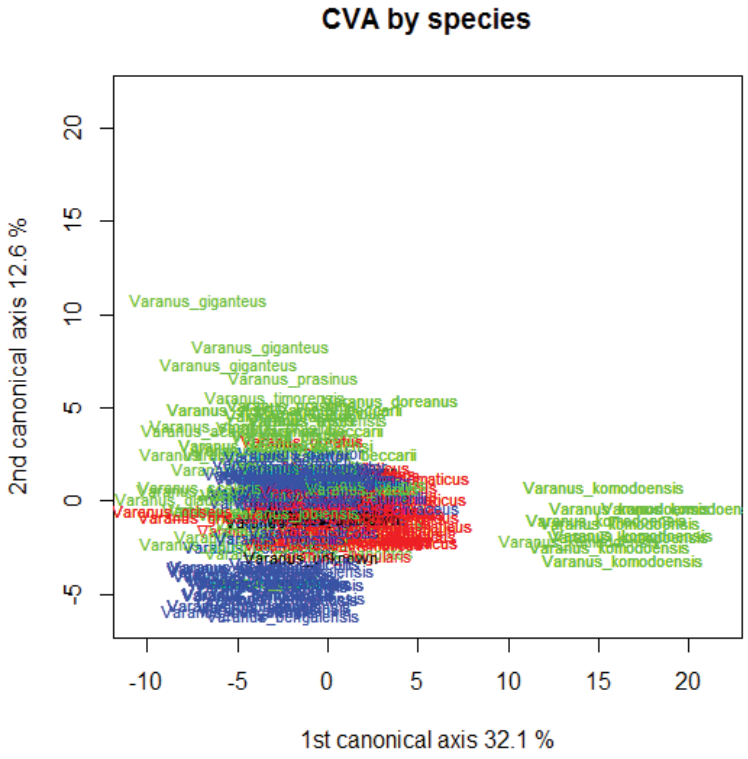


Figure 12. Dorsal snout Canonical Variates Analysis by species. Notice that *V. komodoensis* pulls away from the rest of the taxa. The snout shape of *V. komodoensis* causes all of the other taxa to more similar to each other based on the analysis. Taxa are color coded by region: red=Africa, green=Indo-Australia, and blue=Indo-Asia.

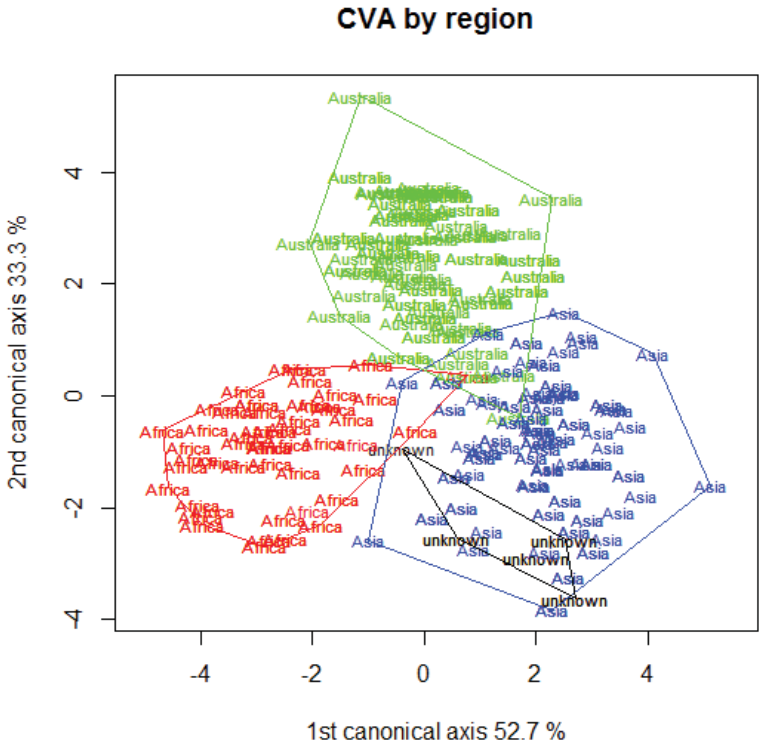


Figure 13. Dorsal snout Canonical Variates Analysis by region: red=Africa, green=Indo-Australia, and blue=Indo-Asia.

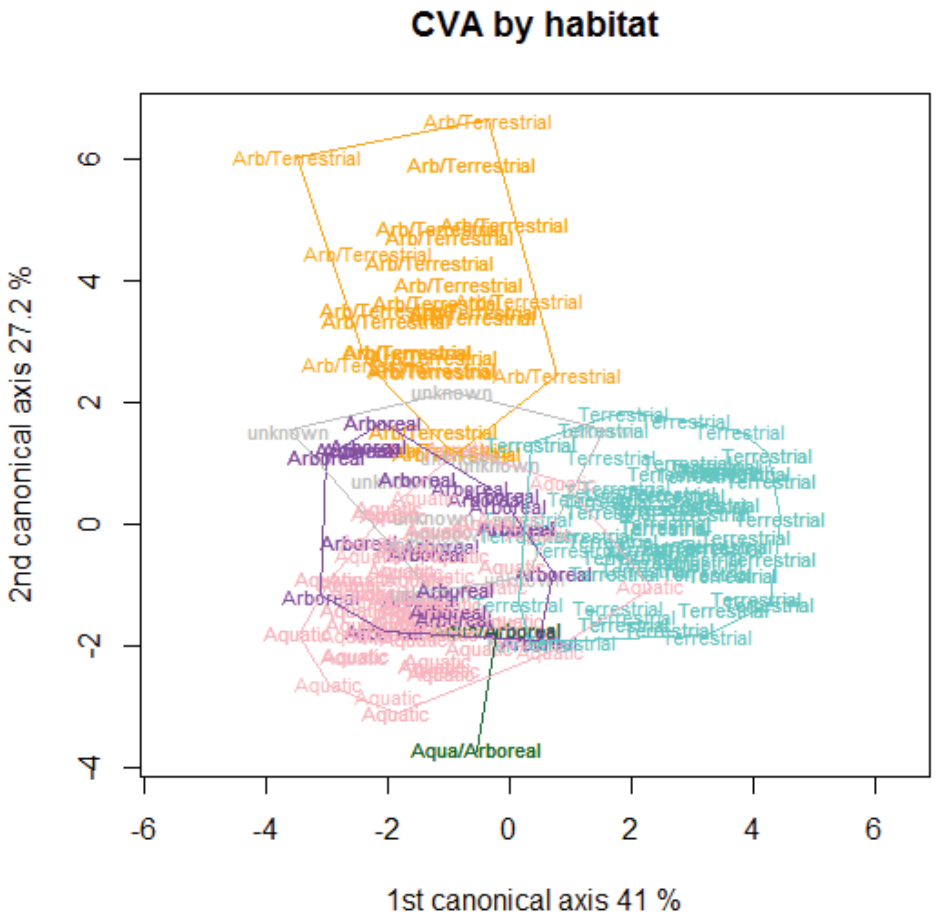


Figure 14. Dorsal snout canonical variates analysis by habitat. Terrestrial and arboreal/terrestrial are distinct from all other habitat groups.

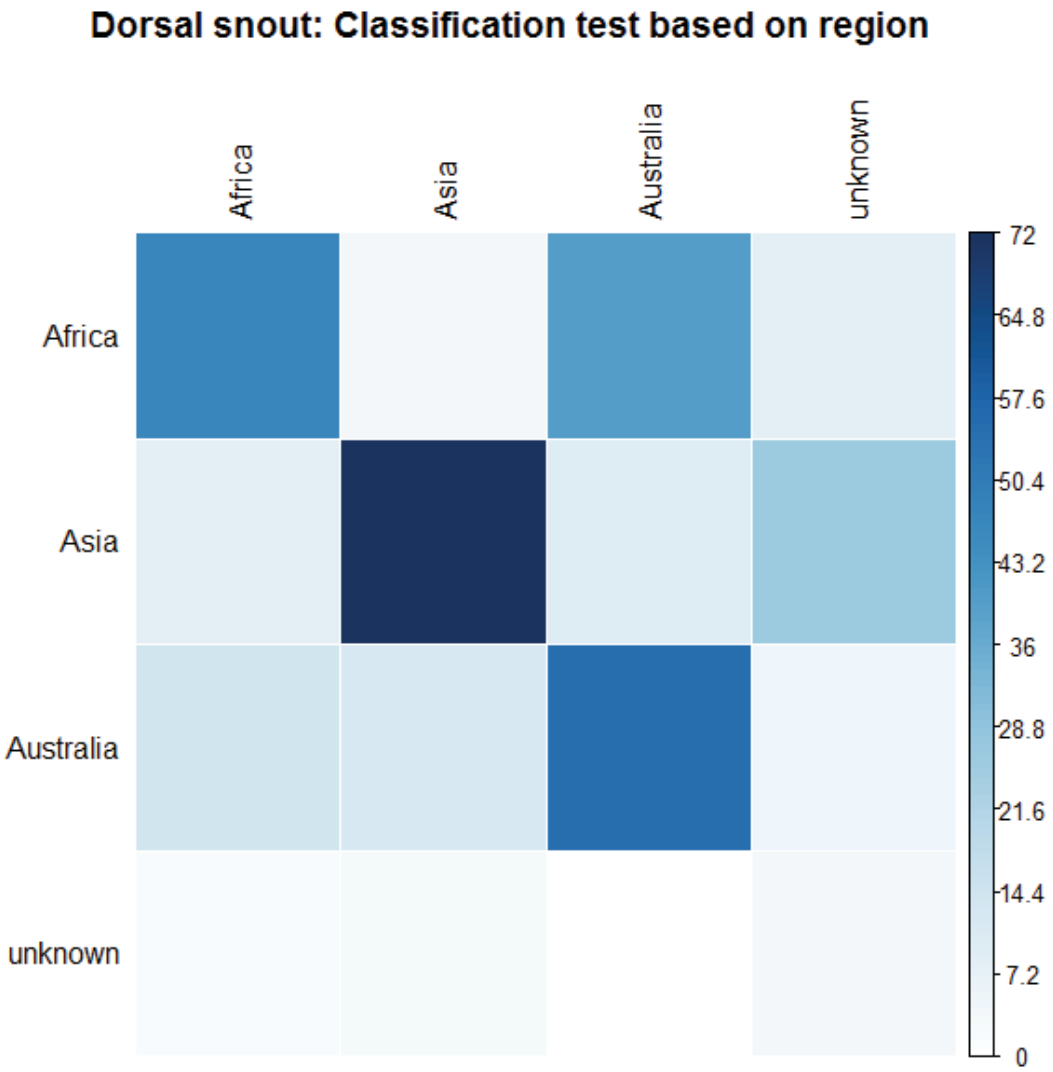


Figure 15. Dorsal snout classification/group affinity test based on the regional classification. See text for a thorough description of the type class analysis. Darker shades of blue indicate larger number of specimens falling in that category. Notice that Indo-Asian taxa tend to be correctly classified. When African specimens are randomly subsampled and placed in the analysis, they tend to fall in both African and Indo-Australian categories.

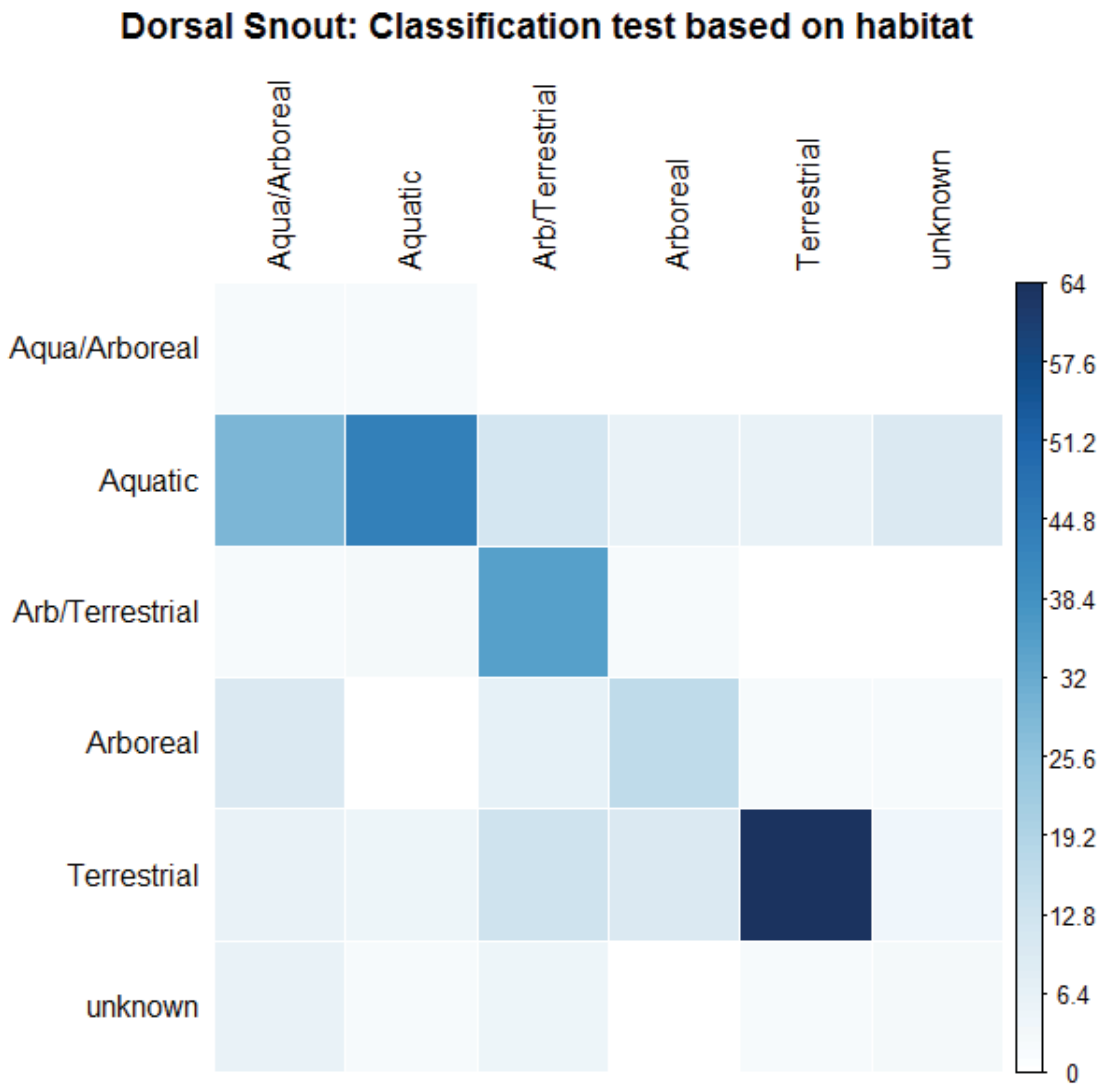


Figure 16. Dorsal snout classification/group affinity test based on the habitat classification. See text for a thorough description of the type class analysis. Darker shades of blue indicate larger number of specimens falling in that category. Notice that terrestrial taxa tend to be correctly classified, followed by aquatic, and finally arboreal/terrestrial. Interestingly, specimens defined as aquatic often fall within the aquatic/arboreal category.

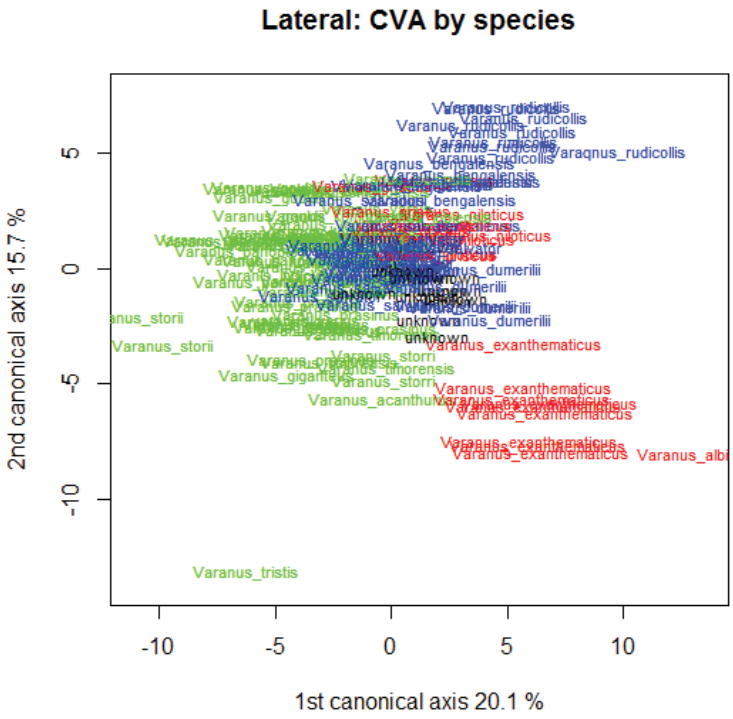


Figure 17. Lateral canonical variates analysis by species. There is generally a great deal of overlap among all taxa, but regionally, taxa tend to clump in space.

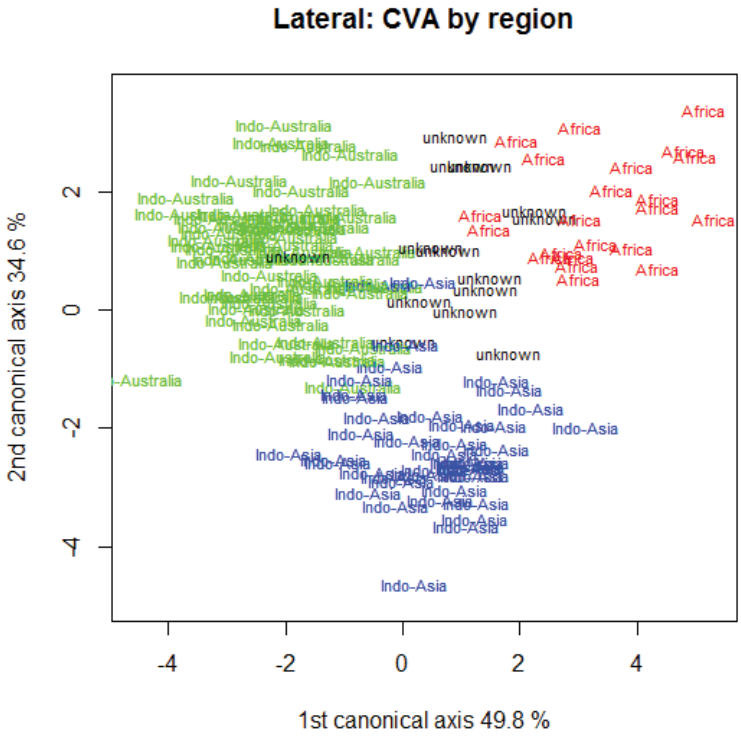


Figure 18. Lateral canonical variates analysis by region. Similar to dorsal analysis, regions do not tend to overlap in space.

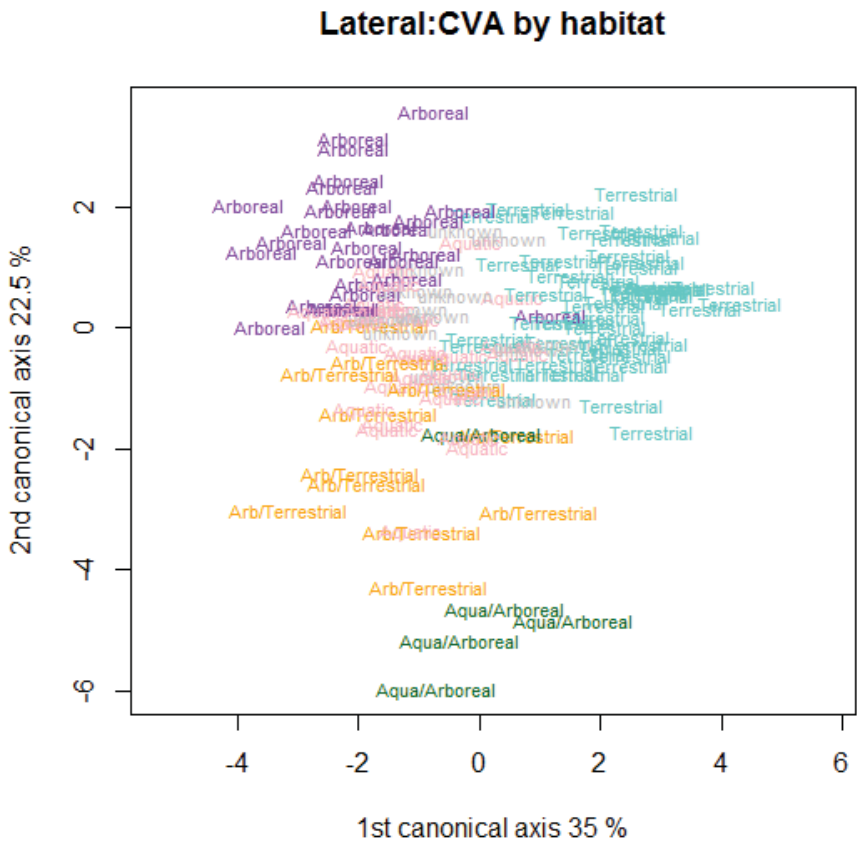


Figure 19. Lateral canonical variates analysis by habitat. Notice that, unlike dorsal CVA by habitat, there is separation among arboreal, arboreal/terrestrial, aquatic/arboreal, and terrestrial specimens.

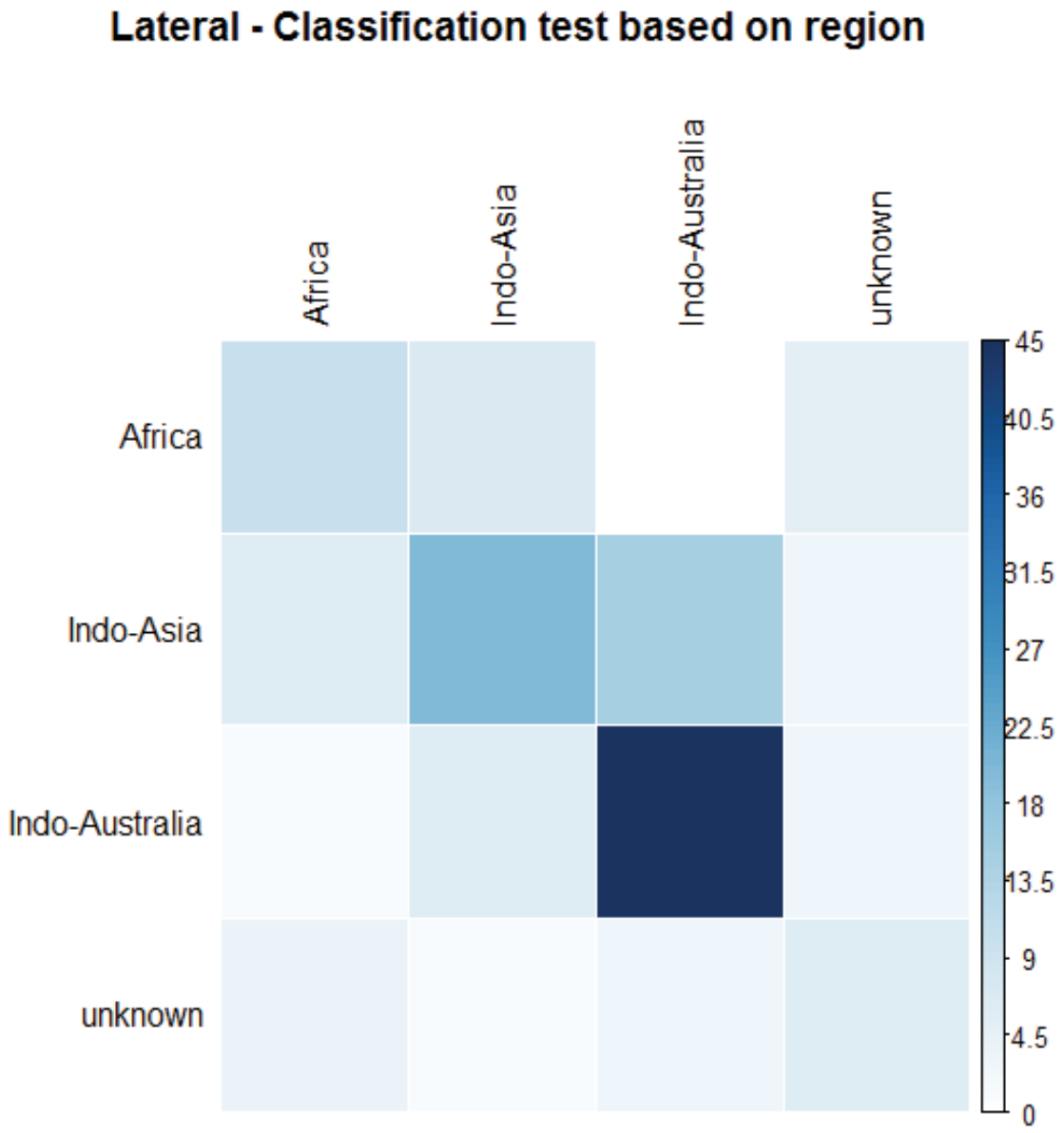


Figure 20. Lateral classification test based on resampling among regions. Notice that Indo-Australian specimens are the most likely to fall within their own group. See text for a thorough description of results.

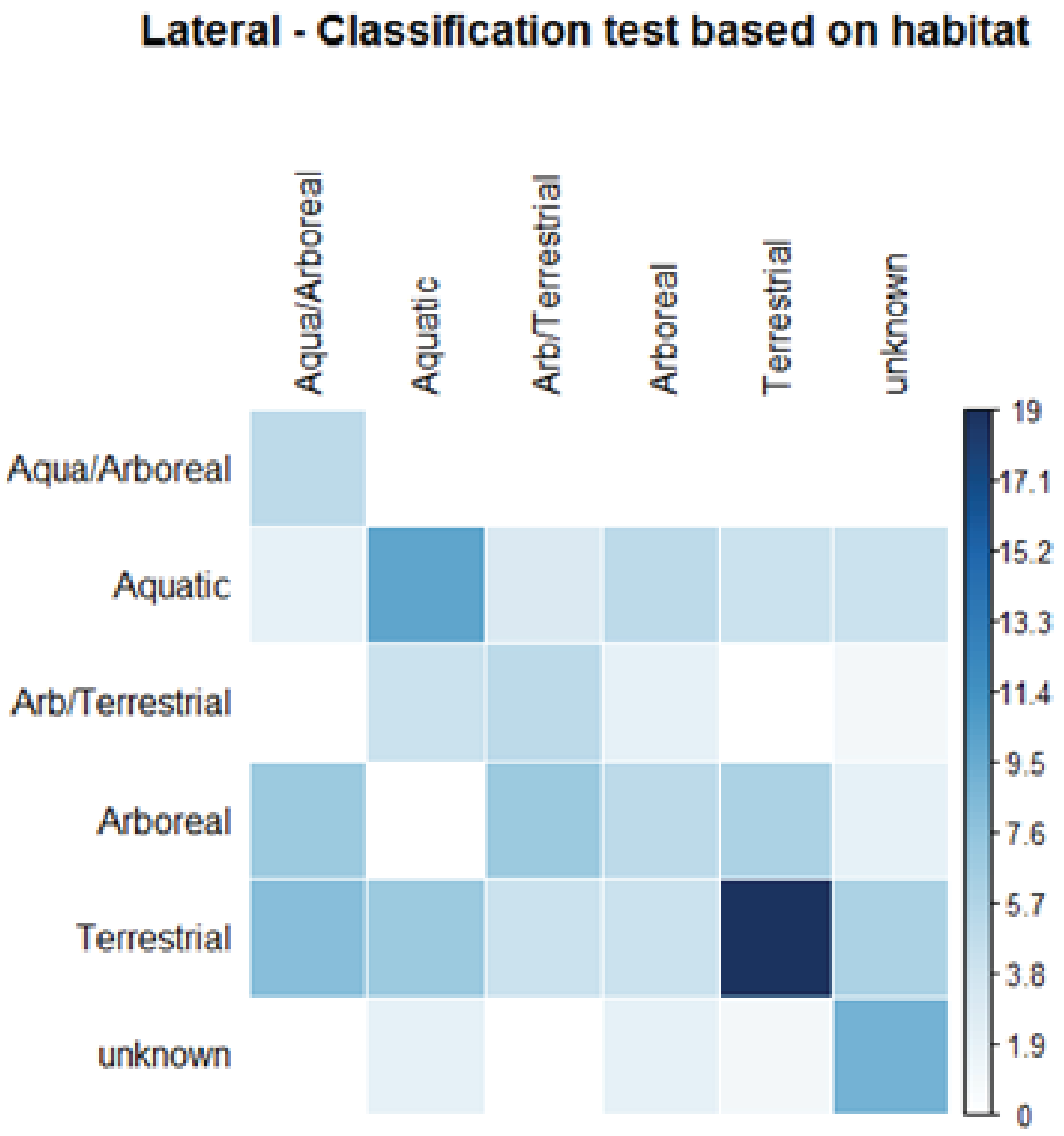


Figure 21. Lateral classification test based on habitat. Terrestrial specimens tend to fall within their own groups, and all other classifications fall within low to middle values. See text for a more thorough explanation of results.

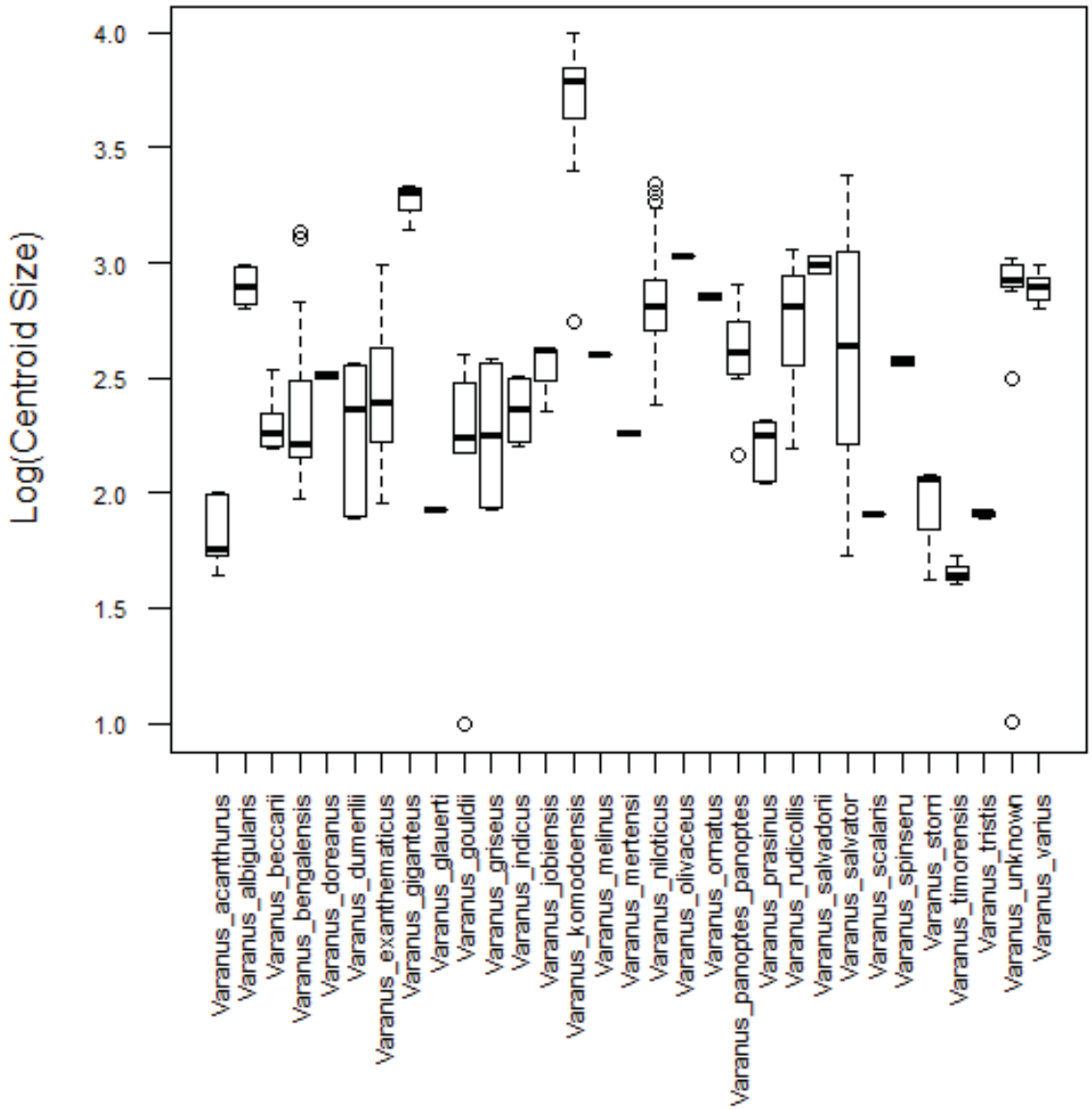


Figure 22. Dorsal log centroid size (CS) range among taxa. The range is determined by all specimens representing each species.

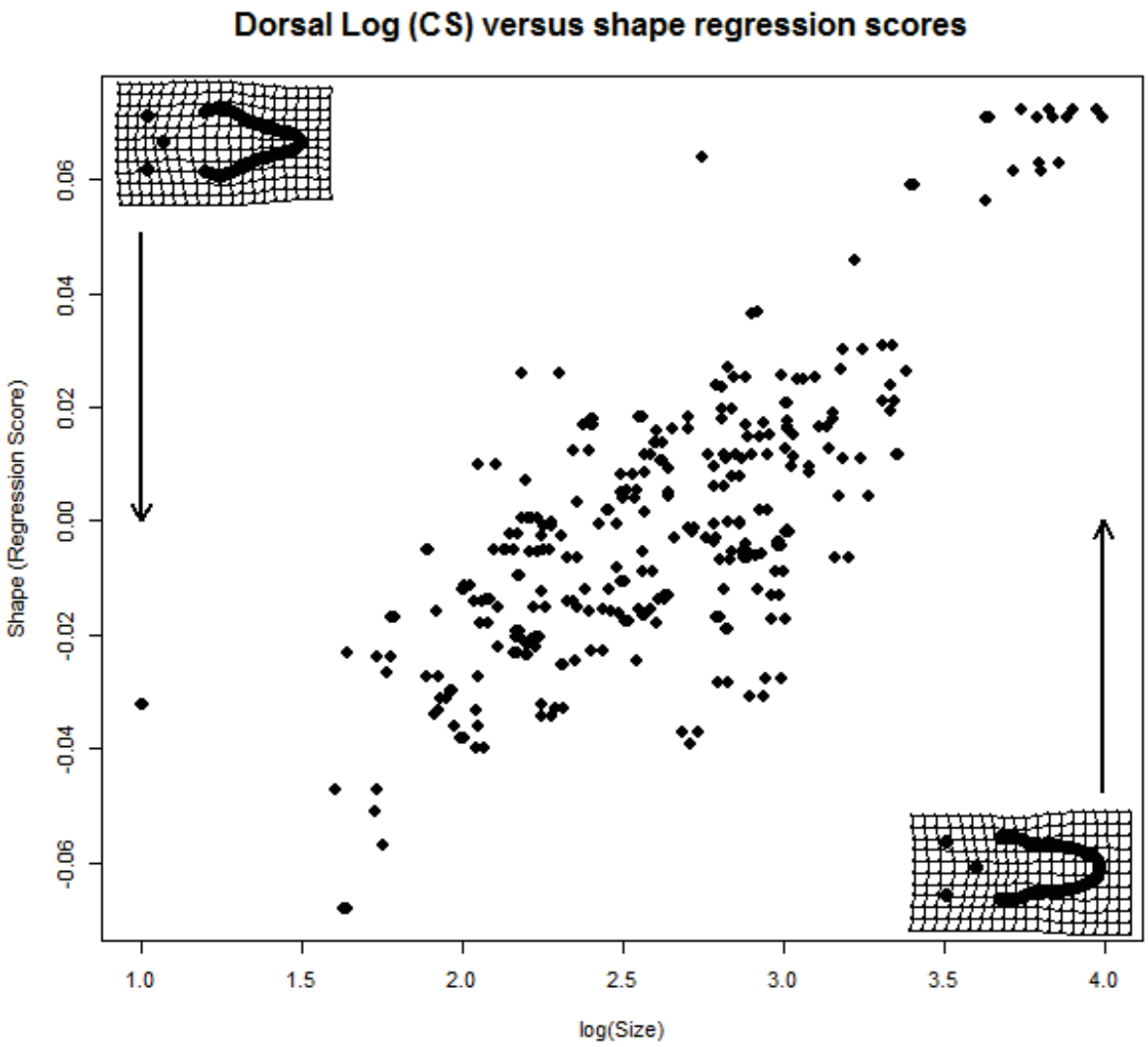


Figure 23. Dorsal log centroid size (CS) versus shape regression scores for specimens. F=20.08, p=0.004. Greater cranium size is associated with broader snouts and larger posterior portions of the skull, and smaller size is associated with thinner anterior portions of the snout and more reduced posterior portions of the skull. Highlighted specimens are *V. komodoensis.*

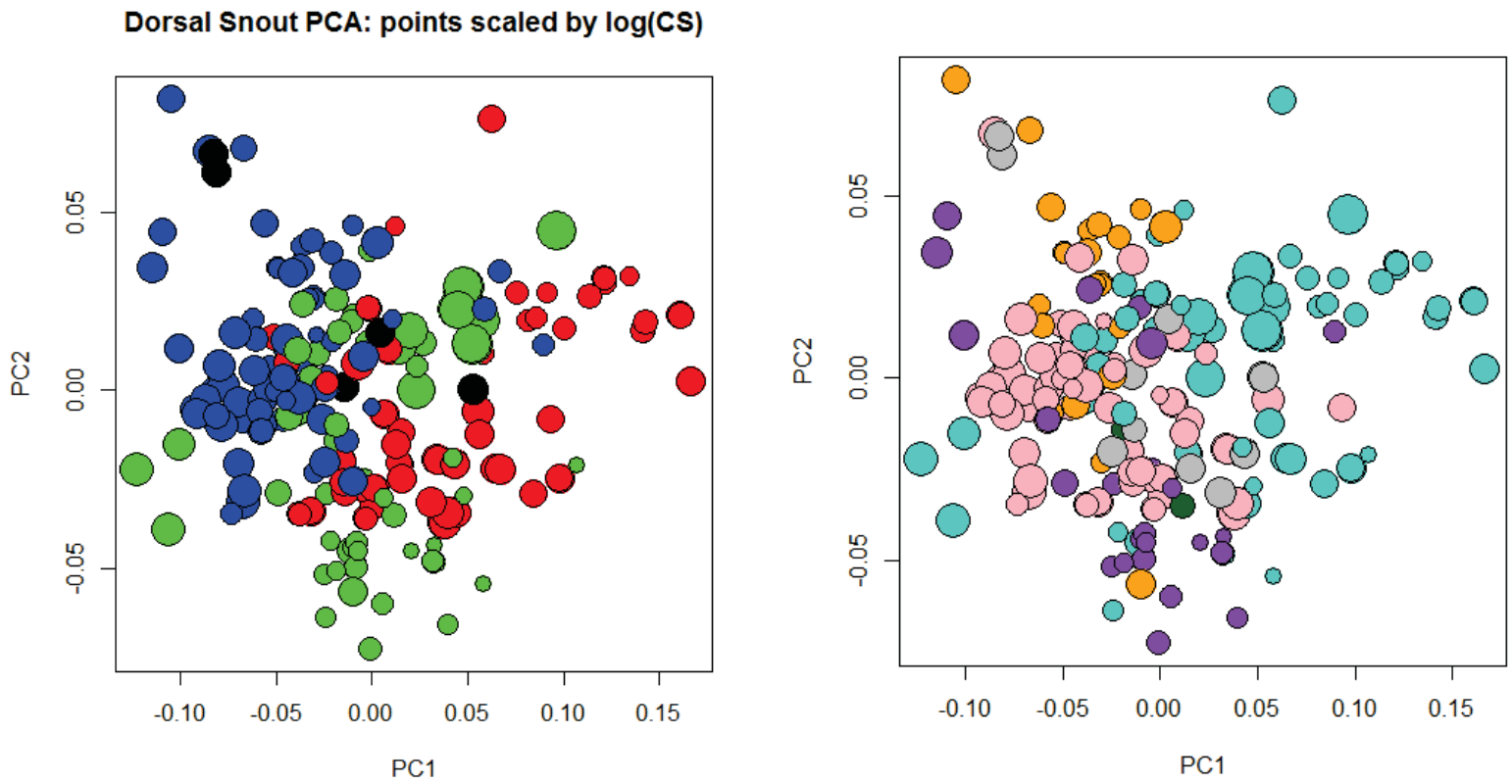


Figure 24. Dorsal snout PCA with specimens scaled to log (CS). Notice the lack of size trend.

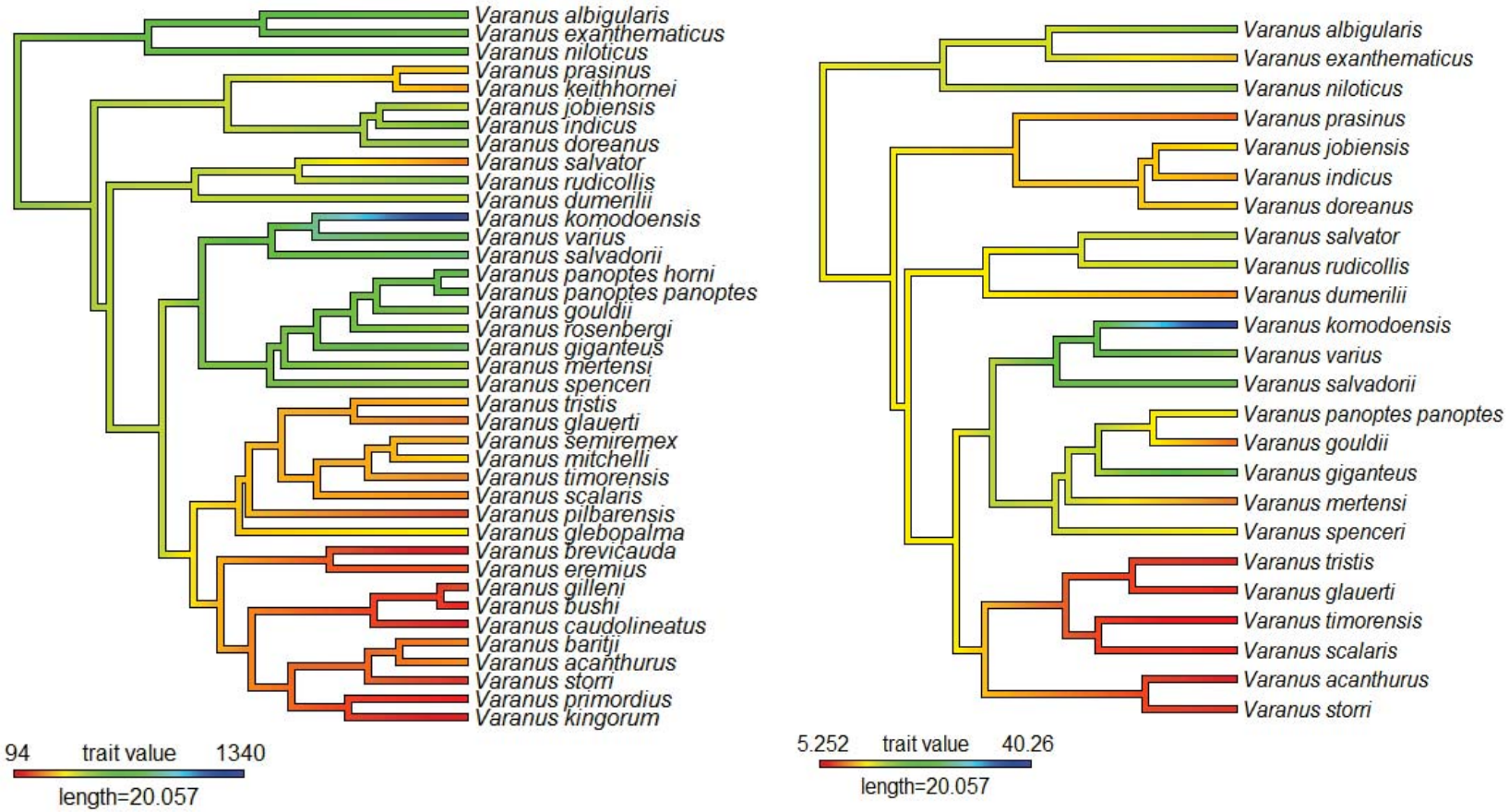


Figure 25. SVL and Dorsal CS across the Vidal et al. 2012 Varanus phylogeny. Ancestral nodes down the tree were estimated using maximum likelihood. Left: SVL across the whole tree. Right: CS on the modified Vidal et al. 2012 tree based on specimens used in this analysis. Red represents smaller values and blue larger values

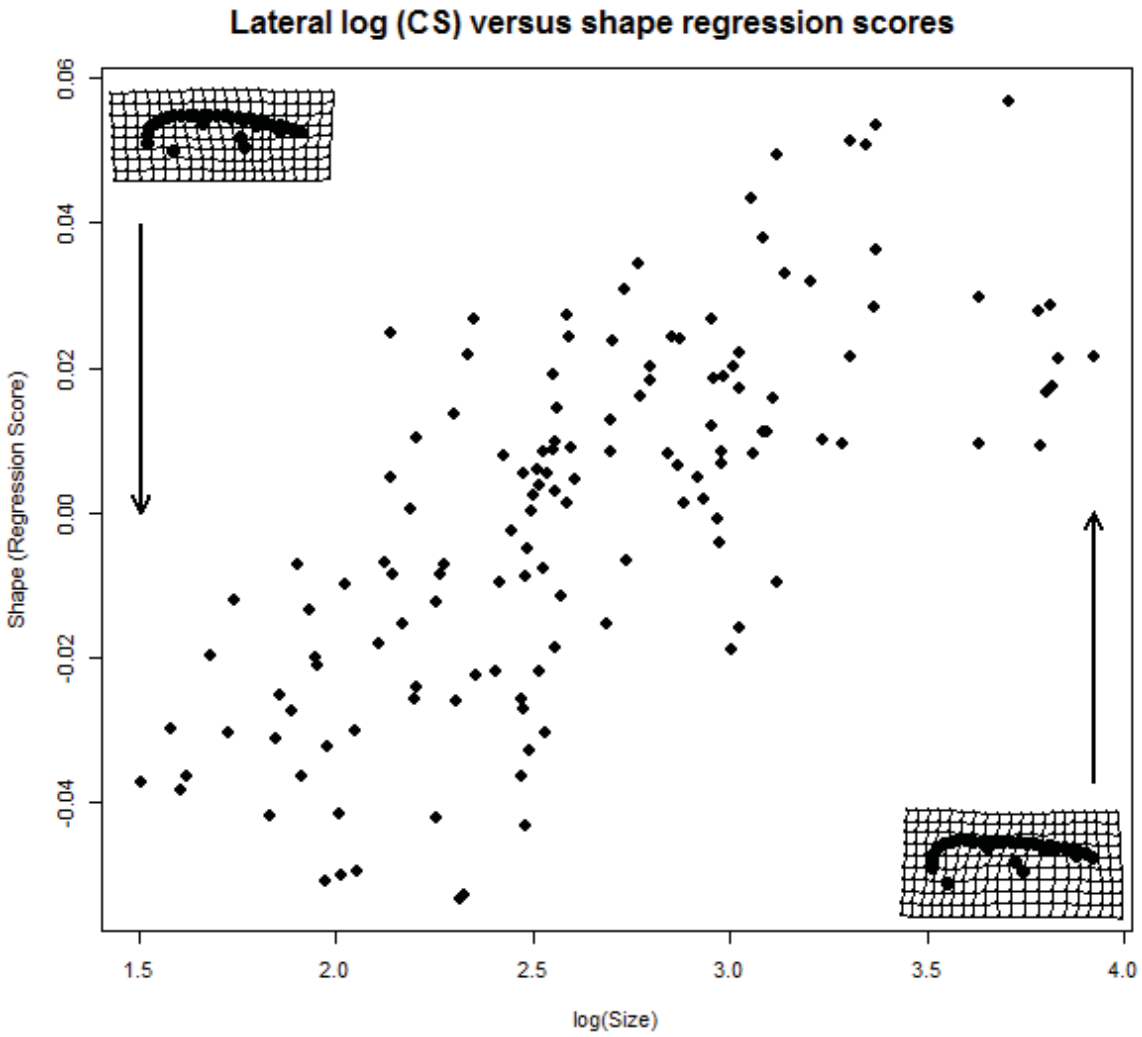


Figure 26. Lateral log centroid size versus shape regression scores. F= 15.488, p<0.001. Greater skull size is characterized by a slightly more curved posterior skull and elongate anterior snout region. The smaller specimens tend to have overall dorso-ventrally flatter skulls.

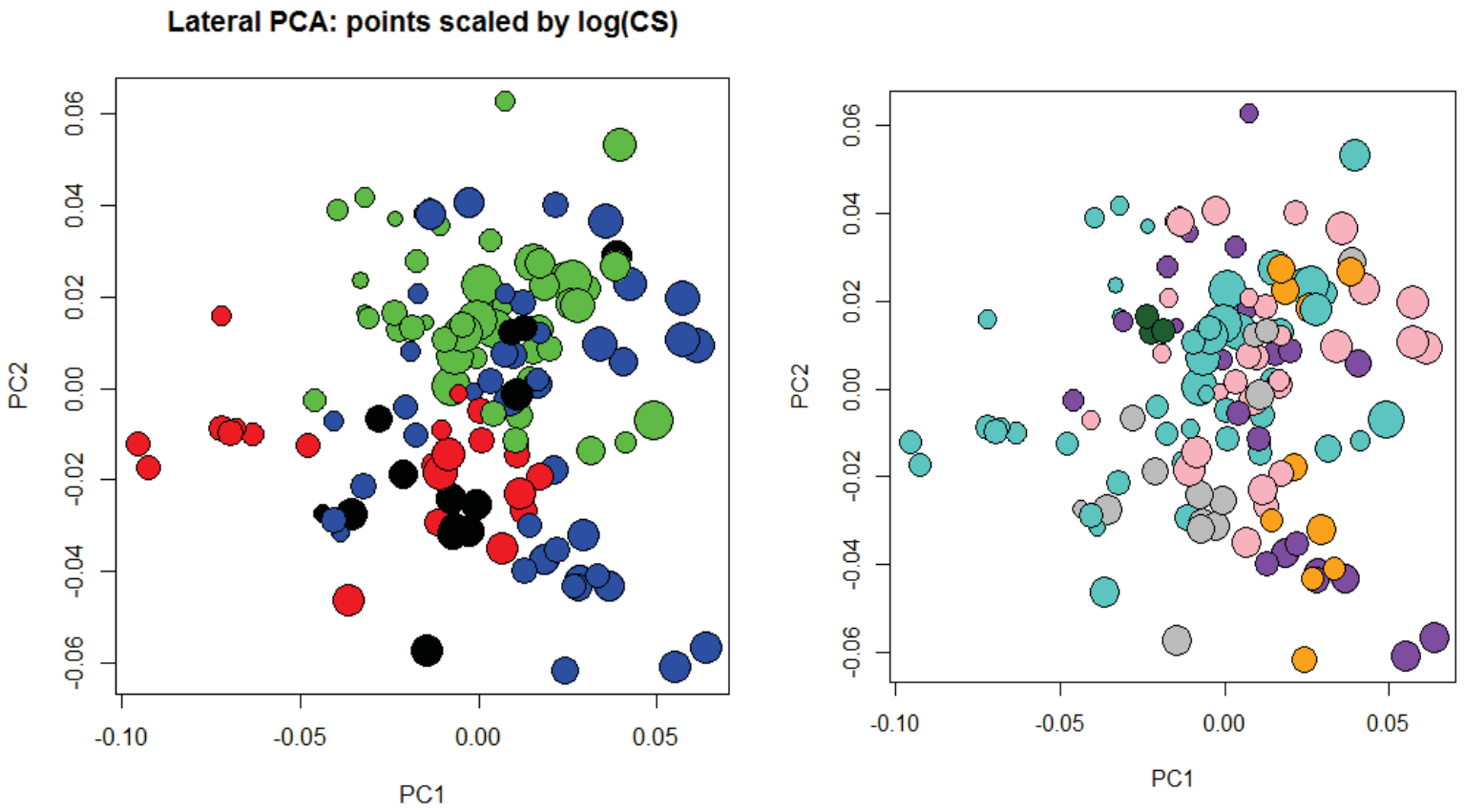


Figure 27. Lateral PCA plots with specimens scaled to log (CS). Left: Specimens are colored by region. Right: specimens are colored by habitat. Although there appears to be a mass of larger specimens in central morphospace, overall there is no size pattern.

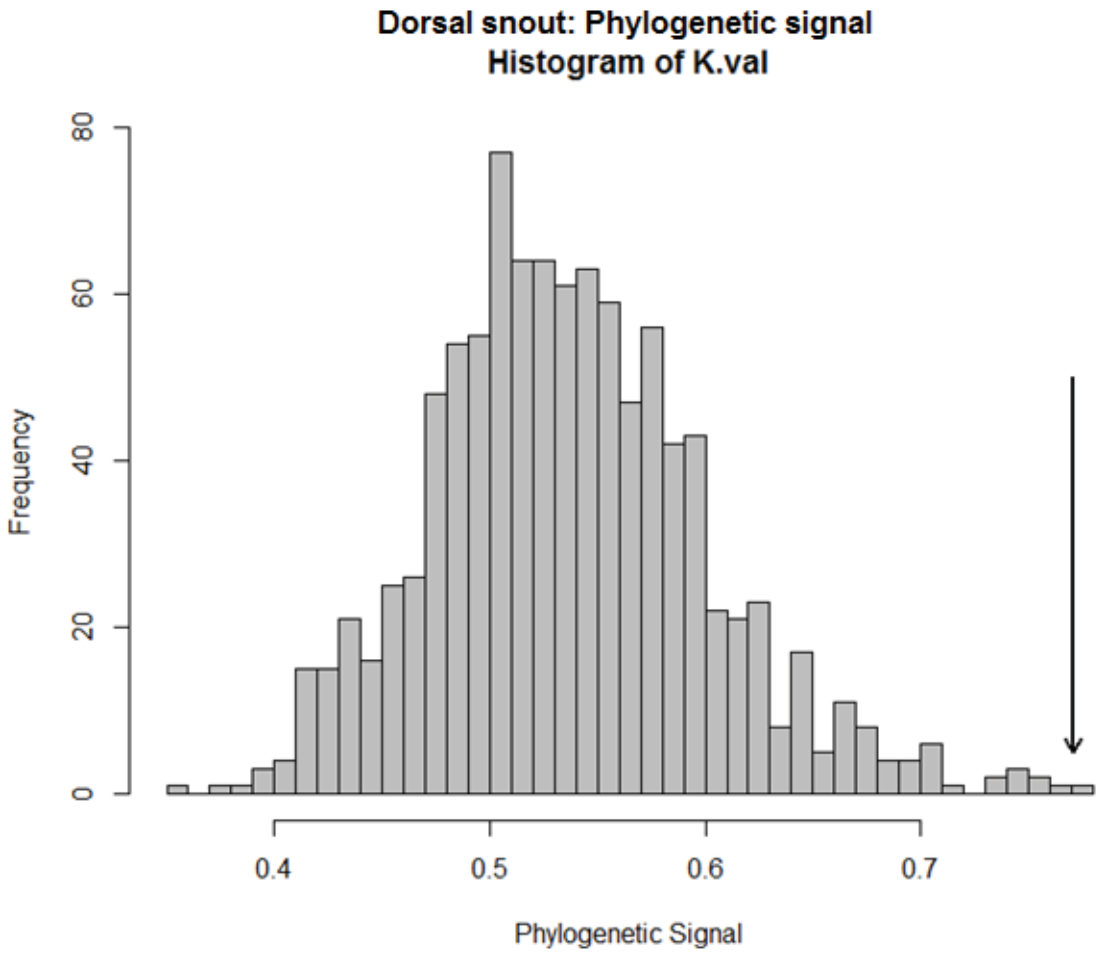


Figure 28. Dorsal snout phylogenetic signal analysis. Histogram of K values after 10000 iteration test of Kmult under a Brownian motion model. Arrow indicates observed K statistic. Kmult =0.771, p =0.004.

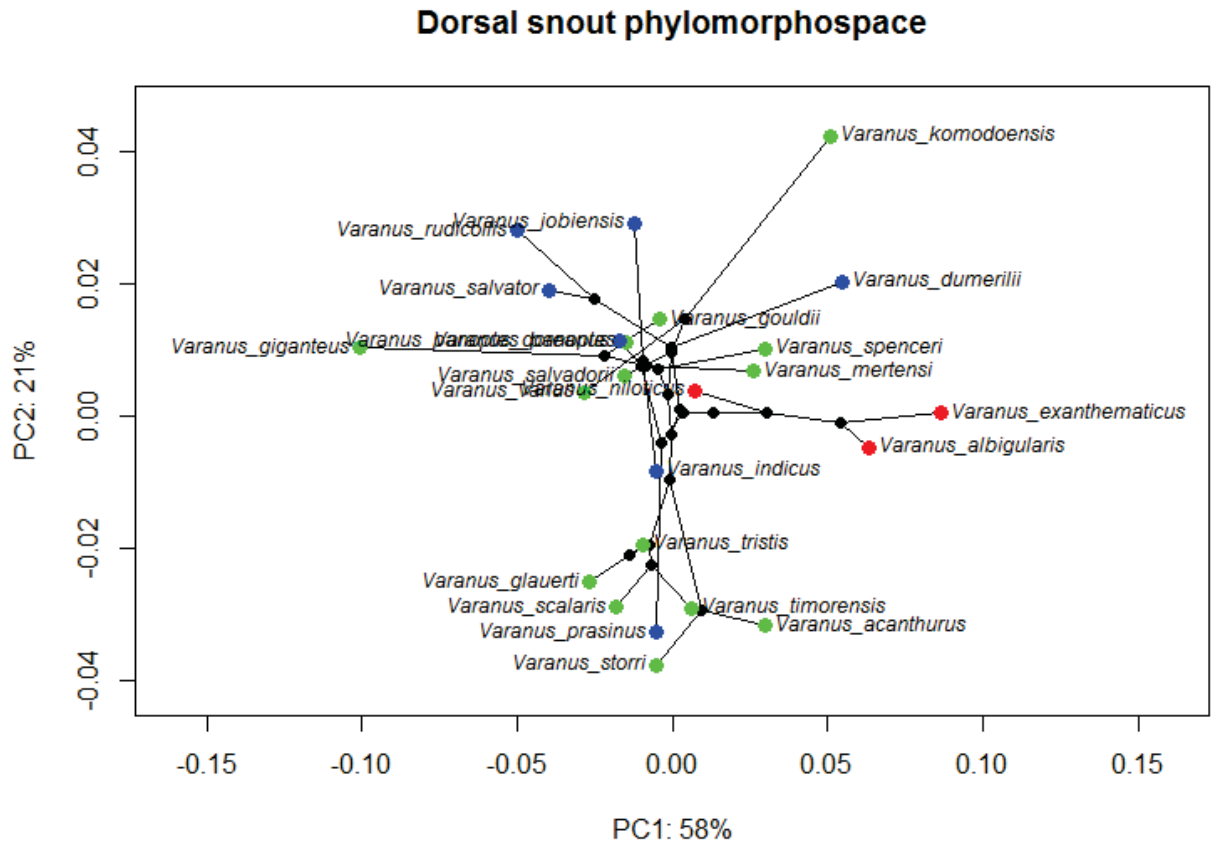


Figure 29. Principal components analysis of the mean dorsal shape of each species. The modified Vidal et al. 2012 phylogeny is plotted in shape space. Notice the central mass of ancestral nodes in shape space and overall lack of much overlap of branches.

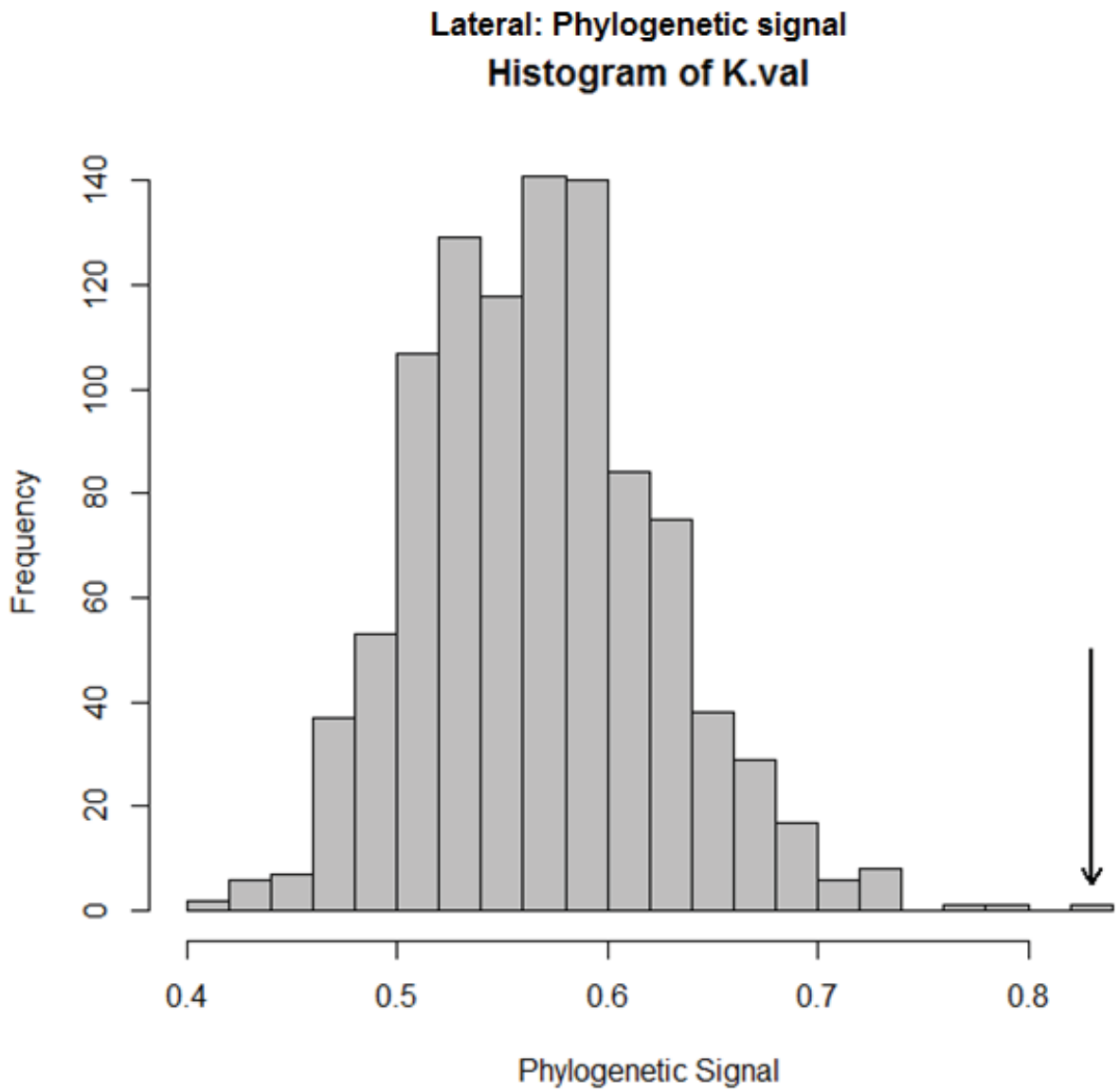


Figure 30. Lateral phylogenetic signal analysis. Histogram of K values after 10000 iteration test of Kmult under a Brownian motion model of evolution. Arrow indicates observed K statistic. Kmult = 0.83, p =0.001.

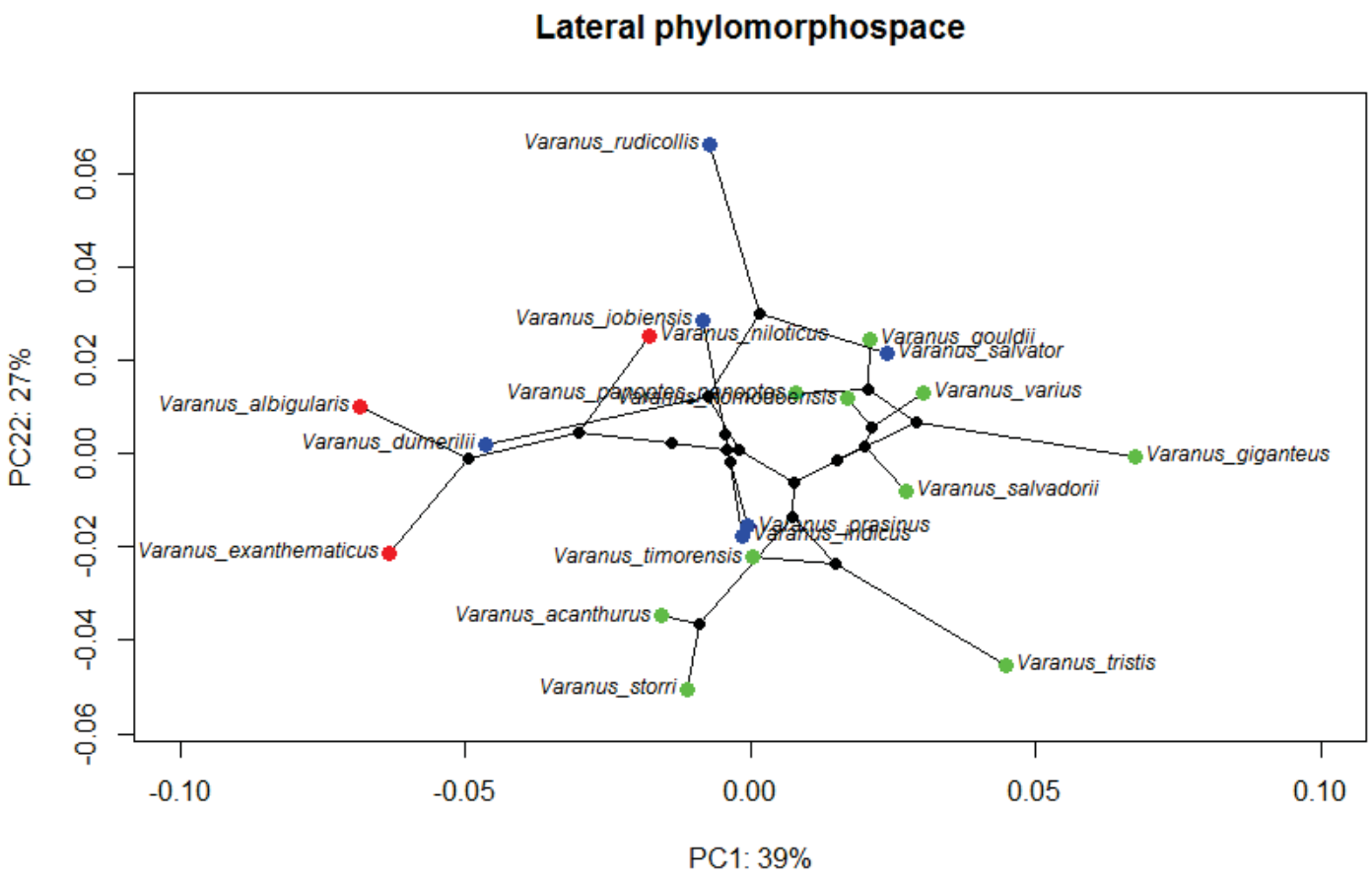


Figure 31. Lateral shape space (PCA) of species means. The modified Vidal et al. 2012 phylogeny is included in shape space. Tips are color coded by region. Notice that taxa are separated more in shape space than the dorsal phylomorphospace.

Appendix 1

Table A1. Dorsal snout Principal Components Analysis results. SD= Standard Deviation, POV= Proportion of Variance, and CP= Cumulative Proportion.

	PC1	PC2	PC3	PC4	PC5	PC6
SD	0.0614	0.03216	0.02351	0.01314	0.0116	0.00879
POV	0.6314	0.17318	0.09259	0.02891	0.02251	0.01293
CP	0.6314	0.80453	0.89712	0.92604	0.94855	0.96148
	PC7	PC8	PC9	PC10	PC11	PC12
SD	0.007445	0.006483	0.005872	0.005042	0.003975	0.003235
POV	0.00928	0.00704	0.00577	0.00426	0.00265	0.00175
CP	0.97077	0.97781	0.98358	0.98784	0.99048	0.99223
	PC13	PC14	PC15	PC16	PC17	PC18
SD	0.002577	0.002545	0.002341	0.002274	0.00191	0.001821
POV	0.00111	0.00108	0.00092	0.00087	0.00061	0.00056
CP	0.99334	0.99443	0.99535	0.99621	0.99682	0.99738
	PC19	PC20	PC21	PC22	PC23	PC24
SD	0.001583	0.001304	0.001268	0.00115	0.001042	0.0009869
POV	0.00042	0.00028	0.00027	0.00022	0.00018	0.00016
CP	0.9978	0.99808	0.99835	0.99857	0.99876	0.99892
	PC25	PC26	PC27	PC28	PC29	PC30
SD	0.000924	0.0008313	0.0007136	0.0006797	0.0006559	0.0005815
POV	0.00014	0.00012	0.00009	0.00008	0.00007	0.00006
CP	0.99906	0.99918	0.99926	0.99934	0.99941	0.99947
	PC31	PC32	PC33	PC34	PC35	PC36
SD	0.000563	0.0005432	0.0004976	0.0004759	0.00046	0.0004537
POV	0.00005	0.00005	0.00004	0.00004	0.00004	0.00003
CP	0.99952	0.99957	0.99961	0.99965	0.99969	0.99975
	PC37	PC38	PC39	PC40	PC41	PC42
SD	0.000433	0.0003969	0.0003835	0.0003615	0.0003387	0.00031
POV	0.00003	0.00003	0.00002	0.00002	0.00002	0.00002
CP	0.99978	0.9998	0.99982		0.99985	0.99986
	PC43	PC44	PC45	PC46	PC47	PC48
SD	0.000296	0.000281	0.0002783		0.0002618	0.0002421
POV	0.00002	0.00001	0.00001	0.00001	0.00001	0.00001
CP	0.99988	0.9999	0.99991	0.99992	0.99993	0.99994
	PC49	PC50	PC51	PC52	PC53	PC54
SD	0.000239	0.0002206	0.000202	0.0001917	0.0001642	0.0001547
POV	0.00001	0.00001	0.00001	0.00001	0	0
CP	0.99995	0.99996	0.99997	0.99997	0.99998	0.99998

Appendix 1. Cont.

	PC55	PC56	PC57	PC58	PC59	PC60
SD	0.00015	0.0001314	0.000116	9.50E-05	8.10E-05	7.55E-05
POV	0	0	0	0.00E+00	0.00E+00	0.00E+00
CP	0.99999	0.99999	0.99999	1.00E+00	1.00E+00	1.00E+00
	PC61	PC62	PC63	PC64	PC65	PC66
SD	6.79E-05	6.40E-05	5.47E-05	5.37E-05	5.06E-05	4.79E-05
POV	0.00E+00	0.00E+00	0.00E+00	0.00E+00	0.00E+00	0.00E+00
CP	1.00E+00	1.00E+00	1.00E+00	1.00E+00	1.00E+00	1.00E+00
	PC67	PC68	PC69	PC70	PC71	PC72
SD	4.48E-05	4.24E-05	3.82E-05	3.64E-05	3.34E-05	3.12E-05
POV	0.00E+00	0.00E+00	0.00E+00	0.00E+00	0.00E+00	0.00E+00
CP	1.00E+00	1.00E+00	1.00E+00	1.00E+00	1.00E+00	1.00E+00
	PC73	PC74	PC75	PC76	PC77	PC78
SD	2.77E-05	2.64E-05	2.57E-05	2.46E-05	2.19E-05	1.96E-05
POV	0.00E+00	0.00E+00	0.00E+00	0.00E+00	0.00E+00	0.00E+00
CP	1.00E+00	1.00E+00	1.00E+00	1.00E+00	1.00E+00	1.00E+00
	PC79	PC80	PC81	PC82	PC83	PC84
SD	1.84E-05	1.64E-05	1.46E-05	1.36E-05	4.66E-17	4.62E-17
POV	0.00E+00	0.00E+00	0.00E+00	0.00E+00	0.00E+00	0.00E+00
CP	1.00E+00	1.00E+00	1.00E+00	1.00E+00	1.00E+00	1.00E+00
	PC85	PC86				
SD	3.23E-17	2.63E-17				
POV	0.00E+00	0.00E+00				
CP	1.00E+00	1.00E+00				

Table A2. Lateral Principal Components Analysis results. SD= Standard Deviation, POV= Proportion of Variance, and CP= Cumulative Proportion.

	PC1	PC2	PC3	PC4	PC5	PC6
SD	0.04261	0.03426	0.02288	0.01998	0.01563	0.01367
POV	0.36269	0.2345	0.10457	0.07977	0.04881	0.03736
CP	0.36269	0.59719	0.70176	0.78153	0.83034	0.8677
	PC7	PC8	PC9	PC10	PC11	PC12
SD	0.01327	0.01153	0.009216	0.008503	0.006899	0.005347
POV	0.03519	0.02657	0.01697	0.01445	0.00951	0.00571
CP	0.90289	0.92946	0.94643	0.96087	0.97038	0.97609
	PC13	PC14	PC15	PC16	PC17	PC18
SD	0.005073	0.004421	0.003632	0.003458	0.003301	0.002781
POV	0.00514	0.0039	0.00264	0.00239	0.00218	0.00154
CP	0.98124	0.98514	0.98778	0.99017	0.99234	0.99389
	PC19	PC20	PC21	PC22	PC23	PC24
SD	0.002539	0.002264	0.001935	0.001906	0.001468	0.0013
POV	0.00129	0.00102	0.00075	0.00073	0.00043	0.00034
CP	0.99517	0.9962	0.99695	0.99767	0.9981	0.99844
	PC25	PC26	PC27	PC28	PC29	PC30
SD	0.001119	0.001067	0.001032	0.0008961	0.0007981	0.0007083
POV	0.00025	0.00023	0.00021	0.00016	0.00013	0.0001
CP	0.99869	0.99892	0.99913	0.99929	0.99942	0.99952
	PC31	PC32	PC33	PC34	PC35	PC36
SD	0.0006469	0.0006073	0.0005345	0.0004994	0.0004601	0.0004392
POV	0.00008	0.00007	0.00006	0.00005	0.00004	0.00004
CP	0.9996	0.99968	0.99973	0.99978	0.99983	0.99986
	PC37	PC38	PC39	PC40	PC41	PC42
SD	0.0003593	0.0003455	0.0003102	0.0002581	0.0002496	0.0002326
POV	0.00003	0.00002	0.00002	0.00001	0.00001	0.00001
CP	0.99989	0.99991	0.99993	0.99995	0.99996	0.99997
	PC43	PC44	PC45	PC46	PC47	PC48
SD	0.0002125	0.0001676	0.0001392	0.0001129	9.96E-05	9.22E-05
POV	0.00001	0.00001	0	0	0.00E+00	0.00E+00
CP	0.99998	0.99998	0.99999	0.99999	1.00E+00	1.00E+00
	PC49	PC50	PC51	PC52	PC53	PC54
SD	7.94E-05	7.00E-05	6.67E-05	4.98E-05	4.53E-05	3.87E-05
POV	0.00E+00	0.00E+00	0.00E+00	0.00E+00	0.00E+00	0.00E+00
CP	1.00E+00	1.00E+00	1.00E+00	1.00E+00	1.00E+00	1.00E+00
	PC55	PC56	PC57	PC58	PC59	PC60
SD	3.32E-05	2.85E-05	2.38E-05	2.03E-05	4.73E-17	3.34E-17
POV	0.00E+00	0.00E+00	0.00E+00	0.00E+00	0.00E+00	0.00E+00

CP	1.00E+00	1.00E+00	1.00E+00	1.00E+00	1.00E+00	1.00E+00

	PC61	PC62
SD	1.04E-17	9.97E-18
POV	0.00E+00	0.00E+00
CP	1.00E+00	1.00E+00

Appendix 2. Canonical variates analyses Mahalanobis distances

Table A2.1. Dorsal Species CVA results Mahalanobis distances

	acanthurus	*albigularis*	*beccarii*	*bengalensis*	*doreanus*	*dumerilii*	*exanthematicus*
albigularis	11.341431						
beccarii	12.190894	13.8349					
bengalensis	11.966868	10.9372	11.8083				
doreanus	19.14889	19.4369	17.9266	18.1292			
dumerilii	13.275277	10.0205	13.3524	10.2266	18.251092		
exanthematicus	10.932142	8.6957	11.5115	9.2964	16.781355	10.7795	
giganteus	15.708938	16.8995	15.0414	14.779453	17.460962	16.62658	15.46475
glauerti	18.912752	18.9804	17.6683	17.209856	24.464172	18.5424	18.02198
gouldii	11.188937	10.7257	10.8967	7.498076	17.380785	10.3368	9.333503
griseus	19.993306	19.1194	20.5532	16.533416	25.235277	19.5839	18.41723
indicus	12.271426	12.4507	11.2677	11.0146	18.021768	13.6404	10.49406
jobiensis	15.820715	14.7206	15.3405	12.030644	19.510158	13.2414	13.82035
komodoensis	22.356001	18.9521	19.7876	20.418056	18.671746	17.7307	18.09122
melinus	18.218646	16.8311	16.0984	12.446326	19.561131	14.9081	15.99375
mertensi	12.765765	12.77	11.9549	11.658281	19.386603	12.9193	10.89206
niloticus	11.517496	9.704	9.2316	8.097417	16.133711	10.1472	7.432297
olivaceus	19.66412	18.4919	17.4175	15.993034	20.344309	19.1125	16.56786
ornatus	14.376861	13.2228	13.2539	12.271388	18.731858	14.931	10.19268
panoptes	11.17517	9.8766	10.2231	6.59105	17.061711	9.7878	8.877659
prasinus	11.156341	11.8968	7.0878	10.109954	16.858036	12.0169	9.980581
rudicollis	13.333242	12.844	11.7331	7.308989	18.14407	11.7048	10.58305
salvadorii	46.42371	44.4343	45.1251	45.44084	41.110895	42.5186	44.09487
salvator	10.679892	9.7292	10.1019	6.408176	15.922494	9.2684	9.070416
scalaris	16.118794	17.4723	16.1799	15.537491	22.251828	18.2001	16.39416
spinseru	14.287304	15.428	17.9439	14.48255	22.810867	15.9306	14.56285
storri	19.775209	21.2958	22.0936	23.416921	30.373329	24.6276	22.82702
timorensis	13.024997	14.6853	11.8101	12.685167	18.189622	14.3115	11.71843
tristis	13.530152	13.7563	14.5237	14.74545	18.36359	13.9978	13.43905
unknown	11.760827	9.7649	10.9193	6.528981	16.883037	9.1034	8.809715
varius	13.837555	12.9216	12.6630	10.886157	16.504529	12.394	11.67696

Appendix 2 (cont.)

Table A2.1. Dorsal Species CVA results Mahalanobis distances

	giganteus	*glauerti*	*gouldii*	*griseus*	*indicus*	*jobiensis*
albigularis						
beccarii						
bengalensis						
doreanus						
dumerilii						
exanthematicus						
giganteus						
glauerti	19.00635					
gouldii	13.03662	16.49356				
griseus	19.53161	22.12077	15.64244			
indicus	12.86544	17.37828	9.888558	18.28014		
jobiensis	16.48578	18.12806	12.74822	19.3487	14.87067	
komodoensis	22.89892	26.49071	20.91975	26.91294	20.52306	20.63939
melinus	17.10435	19.34656	14.75984	21.33268	15.12916	15.45191
mertensi	15.55304	19.69421	11.52417	19.81526	8.127884	16.16025
niloticus	13.79094	16.92014	8.765899	17.99306	9.351237	11.49382
olivaceus	20.25244	23.40298	17.47915	24.70007	17.71746	18.01614
ornatus	15.60164	17.60686	12.669	19.03427	13.51975	15.07289
panoptes_panoptes	12.97699	14.81941	6.081201	16.00841	9.542844	11.59272
prasinus	12.30158	17.25652	9.666505	19.1791	9.214531	13.93864
rudicollis	15.03707	17.96381	9.062078	18.4393	10.9114	12.78498
salvadorii	43.04459	44.31588	44.69794	46.97164	45.73924	44.14725
salvator	12.18767	16.92128	6.96755	17.33095	8.634743	12.02674
scalaris	16.54826	21.11669	16.10414	23.18165	14.16228	18.42536
spinseru	20.17539	22.60056	15.48516	19.4962	16.36262	16.63836
storri	24.60475	27.73812	22.90057	27.54699	21.81495	26.94757
timorensis	15.59166	15.12271	12.04182	20.62607	13.41161	14.60991
tristis	14.90632	19.69994	13.62486	19.86223	14.98438	14.86846
unknown	14.0045	16.77179	7.654636	16.95272	9.735006	11.71663
varius	15.05968	18.08632	11.57268	18.17322	11.37379	12.93482

Appendix 2 (cont.)

Table A2.1. Dorsal Species CVA results Mahalanobis distances

	komodoensis	*melinus*	*mertensi*	*niloticus*	*olivaceus*	*ornatus*
albigularis						
beccarii						
bengalensis						
doreanus						
dumerilii						
exanthematicus						
giganteus						
glauerti						
gouldii						
griseus						
indicus						
jobiensis						
komodoensis						
melinus	*19.98799*					
mertensi	*20.7699*	*15.15918*				
niloticus	*17.12092*	*13.52919*	*10.5174*			
olivaceus	*20.62596*	*19.05464*	*18.98583*	*13.25772*		
ornatus	*20.89587*	*16.64868*	*14.11286*	*9.218152*	*17.6142*	
panoptes_panoptes	*19.06985*	*13.00752*	*11.67216*	*7.465459*	*16.41131*	*12.40874*
prasinus	*19.24571*	*14.32163*	*10.69302*	*7.889077*	*16.66652*	*11.73258*
rudicollis	*19.27004*	*14.06042*	*12.74726*	*8.768731*	*15.41368*	*13.28844*
salvadorii	*42.65796*	*45.08952*	*45.62697*	*43.51064*	*46.83077*	*42.47086*
salvator	*18.43478*	*12.29674*	*10.20129*	*6.029179*	*15.44571*	*11.42885*
scalaris	*25.51443*	*18.35789*	*16.12088*	*16.2383*	*21.24583*	*19.94922*
spinseru	*22.9501*	*19.81447*	*16.05587*	*13.77175*	*20.01356*	*17.42288*
storri	*30.83536*	*26.78377*	*21.52646*	*22.91544*	*27.90614*	*25.9431*
timorensis	*21.94714*	*16.04565*	*14.86707*	*11.31909*	*19.00535*	*12.82749*
tristis	*20.11753*	*18.5421*	*15.71854*	*11.95546*	*20.31103*	*14.5285*
unknown	*18.14706*	*12.69186*	*10.3507*	*5.875949*	*15.10164*	*11.26966*
varius	*16.57969*	*14.13584*	*12.7609*	*9.334457*	*17.84257*	*13.83729*

Appendix 2 (cont.)

Table A2.1. Dorsal Species CVA results Mahalanobis distances

	panoptes	*prasinus*	*rudicollis*	*salvadorii*	*salvator*	*scalaris*	*spinseru*
albigularis							
beccarii							
bengalensis							
doreanus							
dumerilii							
exanthematicus							
giganteus							
glauerti							
gouldii							
griseus							
indicus							
jobiensis							
komodoensis							
melinus							
mertensi							
niloticus							
olivaceus							
ornatus							
panoptes							
prasinus	*8.649*						
rudicollis	*8.067*	*10.708*					
salvadorii	*44.799*	*44.015*	*45.869*				
salvator	*5.831*	*7.769*	*7.299*	*44.606*			
scalaris	*14.650*	*13.736*	*16.358*	*50.353*	*14.876*		
spinseru	*14.679*	*15.764*	*15.133*	*47.363*	*14.147*	*20.000*	
storri	*21.969*	*21.520*	*25.217*	*56.737*	*22.346*	*22.082*	*21.750*
timorensis	*11.282*	*10.773*	*14.177*	*43.913*	*11.628*	*17.089*	*17.554*
tristis	*13.036*	*13.671*	*14.315*	*42.011*	*11.804*	*20.393*	*17.148*
unknown	*6.781*	*8.792*	*7.504*	*43.889*	*5.730*	*15.357*	*14.045*
varius	*10.110*	*11.119*	*10.225*	*43.334*	*9.456*	*17.378*	*15.178*

Appendix 2 (cont.)

Table A2.1. Dorsal Species CVA results Mahalanobis distances

	storri	*timorensis*	*tristis*	*unknown*
albigularis				
beccarii				
bengalensis				
doreanus				
dumerilii				
exanthematicus				
giganteus				
glauerti				
gouldii				
griseus				
indicus				
jobiensis				
komodoensis				
melinus				
mertensi				
niloticus				
olivaceus				
ornatus				
panoptes				
prasinus				
rudicollis				
salvadorii				
salvator				
scalaris				
spinseru				
storri				
timorensis	*24.190*			
tristis	*24.550*	*15.239*		
unknown	*23.447*	*12.616*	*13.213*	
varius	*24.112*	*14.216*	*12.952*	*8.974*

Appendix 2 (cont.)

Table A2.2. Lateral Species CVA results Mahalanobis distances

	unknown	*acanthurus*	*albigularis*	*bengalensis*	*dumerilii*	*exanthematicus*
acanthurus	12.336531					
albigularis	22.259889	26.477908				
bengalensis	7.465944	16.116484	23.825894			
dumerilii	8.240034	15.303326	23.293985	10.076965		
exanthematicus	9.96359	15.811174	20.690574	12.535435	9.889454	
giganteus	15.273588	19.467037	27.845219	17.635935	17.657852	17.806665
gouldii	10.777311	17.111949	27.542897	11.378721	13.705206	15.690996
griseus	9.615972	17.35663	24.984761	9.464672	9.622762	12.671787
indicus	11.016188	16.794613	26.021393	9.821154	12.198955	15.151633
jobiensis	11.301042	19.342114	24.293219	12.007427	12.269065	14.809974
komodoensis	8.326957	15.48189	25.740817	9.354342	11.82921	13.461022
melinus	7.860385	14.257832	26.021866	10.268374	11.065785	13.434791
niloticus	5.356689	13.50378	22.69071	8.099887	9.784438	11.834804
panoptes	8.665085	15.022349	26.168334	10.504926	11.444163	14.006349
prasinus	7.130717	13.125017	25.528974	10.240897	9.912158	11.945181
rudicollis	9.607665	16.354098	25.226099	8.129375	11.16687	14.79335
salvadorii	13.350018	19.854836	26.385739	13.639066	14.609514	16.823656
salvator	5.485248	14.057447	24.379727	6.713633	7.456219	10.734405
storii	17.163419	20.111011	30.826774	17.522737	18.048448	20.454659
timorensis	10.787865	10.250074	27.097522	12.929856	13.574717	14.19176
tristis	22.49379	20.021897	31.780334	25.559273	24.833157	24.826864
varius	11.399025	15.493227	25.36698	14.167257	14.065652	15.479085
	giganteus	*gouldii*	*griseus*	*indicus*	*jobiensis*	*komodoensis*
acanthurus						
albigularis						
bengalensis						
dumerilii						
exanthematicus						
giganteus						
gouldii	17.042484					
griseus	17.152176	10.427492				
indicus	17.62297	14.3853	12.754502			
jobiensis	18.470963	13.396038	12.937149	16.353134		
komodoensis	15.340522	10.348127	10.906553	11.919937	12.038849	
melinus	15.318361	8.379097	9.992594	12.014435	12.61565	9.599851
niloticus	16.521861	11.456099	9.230673	12.602653	11.586265	9.812364

	giganteus	gouldii	griseus	indicus	jobiensis	komodoensis
panoptes	14.678453	6.577083	9.553451	12.910828	12.107585	9.533553
prasinus	14.274908	10.305759	10.932876	10.373134	12.328443	8.720567
rudicollis	19.801586	13.690031	11.323531	13.944432	12.788575	12.280939
salvadorii	17.131994	15.367574	16.059572	14.982746	14.234939	14.151002
salvator	14.932662	9.732734	8.860922	9.390304	10.921933	7.247176
storii	20.037302	15.462065	16.574964	15.265834	19.655913	16.555643
timorensis	17.493178	14.837148	14.356409	13.165115	17.536717	12.355086
tristis	21.660377	25.791203	25.889725	23.863722	27.171575	23.699382
varius	16.133425	12.953355	14.662067	15.75934	14.186874	11.451791
	melinus	niloticus	panoptes	prasinus	rudicollis	salvadorii
acanthurus						
albigularis						
bengalensis						
dumerilii						
exanthematicus						
giganteus						
gouldii						
griseus						
indicus						
jobiensis						
komodoensis						
melinus						
niloticus	8.400184					
panoptes	7.480162	9.771084				
prasinus	6.714219	9.097058	7.351436			
rudicollis	12.228827	9.072211	13.051762	12.605077		
salvadorii	13.289388	13.836673	14.086101	11.981436	15.807819	
salvator	7.060128	7.410827	7.788458	5.841091	9.619443	12.788508
storii	14.381686	18.915882	14.085108	14.701033	21.061747	20.19089
timorensis	11.41539	12.733454	13.860016	10.98562	13.875466	17.90478
tristis	22.240374	24.191773	23.254155	21.798393	26.506361	26.987408
varius	10.764114	12.36275	11.410942	10.916538	15.820835	13.784275
	salvator	storii	timorensis	tristis	varius	
storii	15.872201					
timorensis	10.729311	18.080671				
tristis	22.954916	24.492264	19.202962			
varius	11.181288	18.115277	13.079015	21.621685		

Appendix 2 (cont.)

Table A2.3. Dorsal Region CVA results Mahalanobis distances

	Africa	Indo-Asia	Indo-Australia
Indo-Asia	4.554		
Indo-Australia	4.152	3.846	
Unknown	8.589	7.892	8.425

Table A2.4. Lateral Region CVA results Mahalanobis distances

	Africa	Indo-Asia	Indo-Australia
Indo-Asia	5.053		
Indo-Australia	5.541	4.017	
Unknown	4.784	4.572	4.501

Table A2.5 Dorsal Habitat CVA results Mahalanobis distances

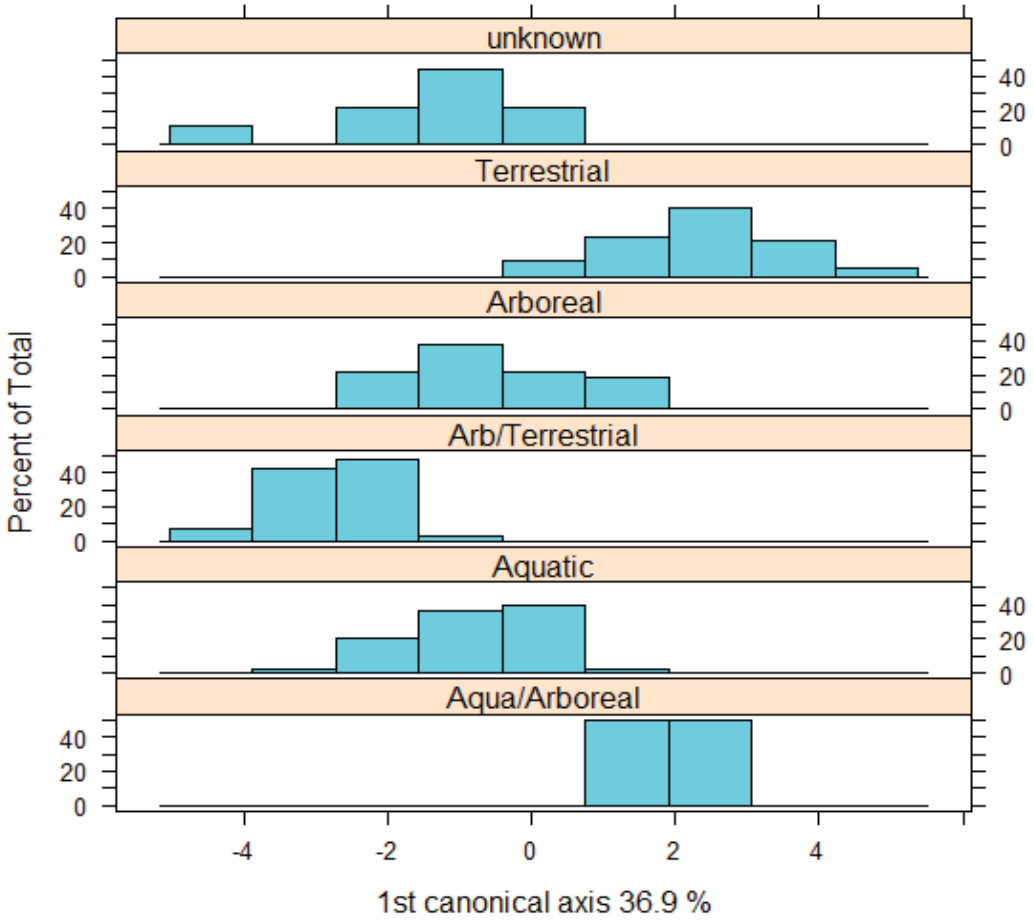
	Aqua/Arboreal	Aquatic	Arb/Terrestrial	Arboreal	Terrestrial
Aquatic	9.093				
Arb/Terrestrial	10.389	4.833			
Arboreal	9.047	3.972	5.719		
Terrestrial	8.886	3.975	5.652	4.824	
Unknown	9.867	4.882	5.828	5.672	5.640

Appendix 2 (cont.)

Table A2.5 Lateral Habitat CVA results Mahalanobis distances

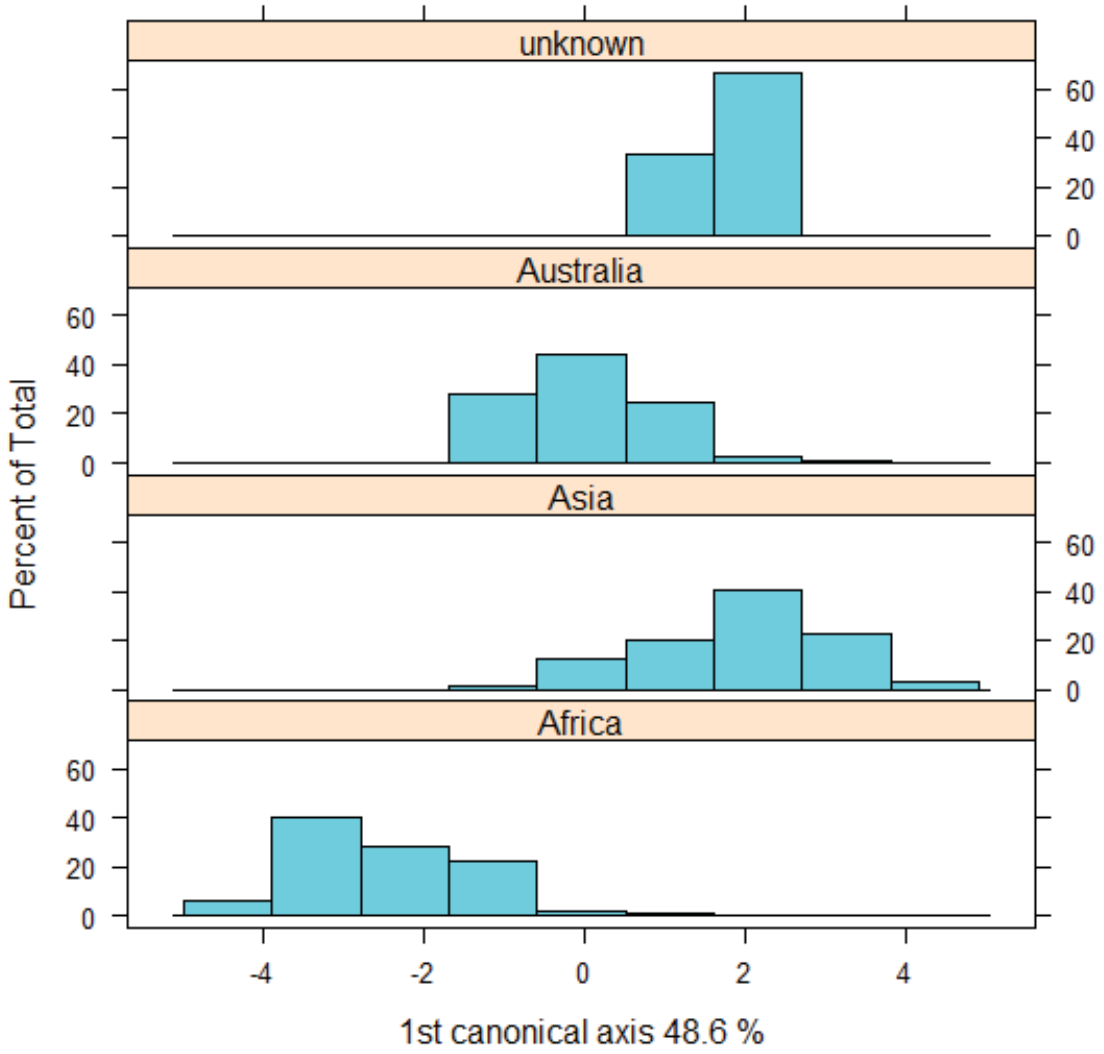
	Aqua/Arboreal	Aquatic	Arb/Terrestrial	Arboreal	Terrestrial
Aquatic	6.500				
Arb/Terrestrial	6.805	3.578			
Arboreal	7.094	3.313	4.671		
Terrestrial	6.632	3.542	4.703	4.219	
Unknown	7.145	3.925	5.102	4.492	4.259

Figure A2. 1. Histogram of the first canonical axis for dorsal habitat CVA



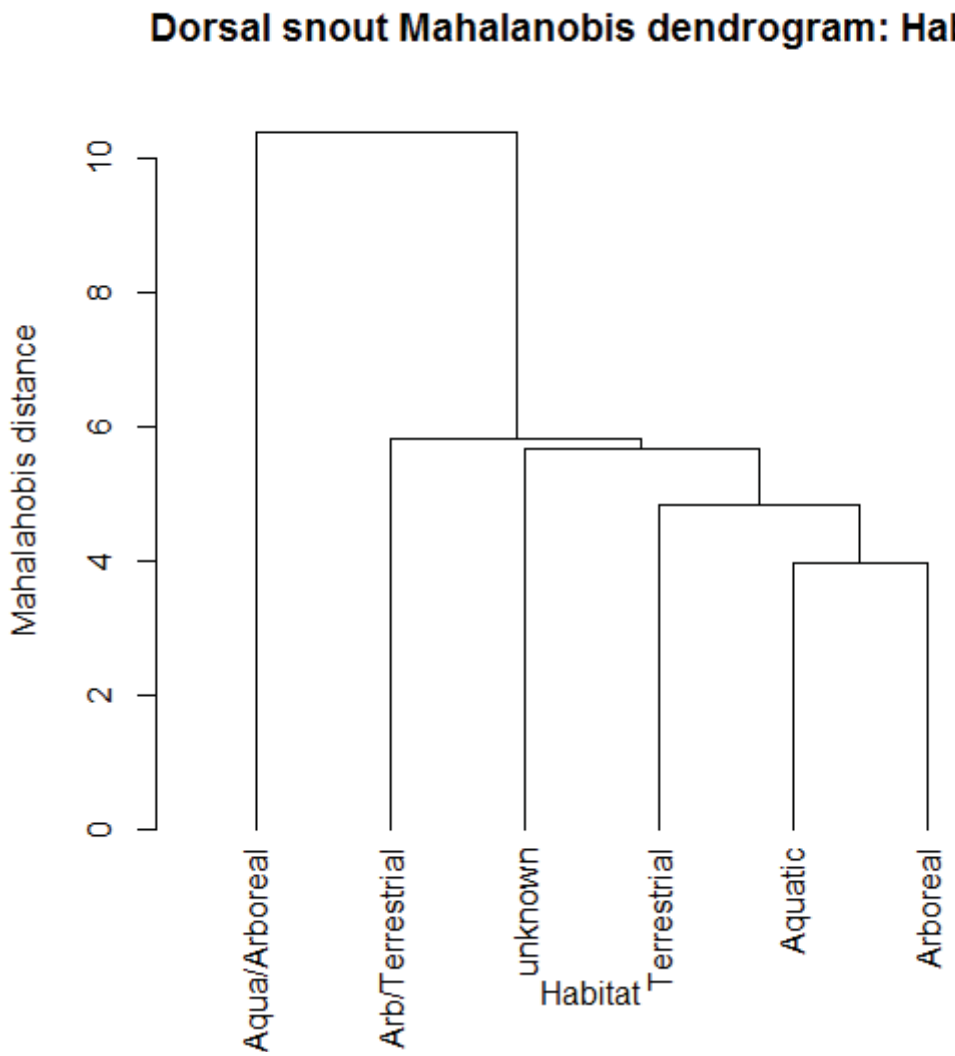
Appendix 2 (cont.)

Figure A2. 2. Histogram of the first canonical axis for dorsal region CVA

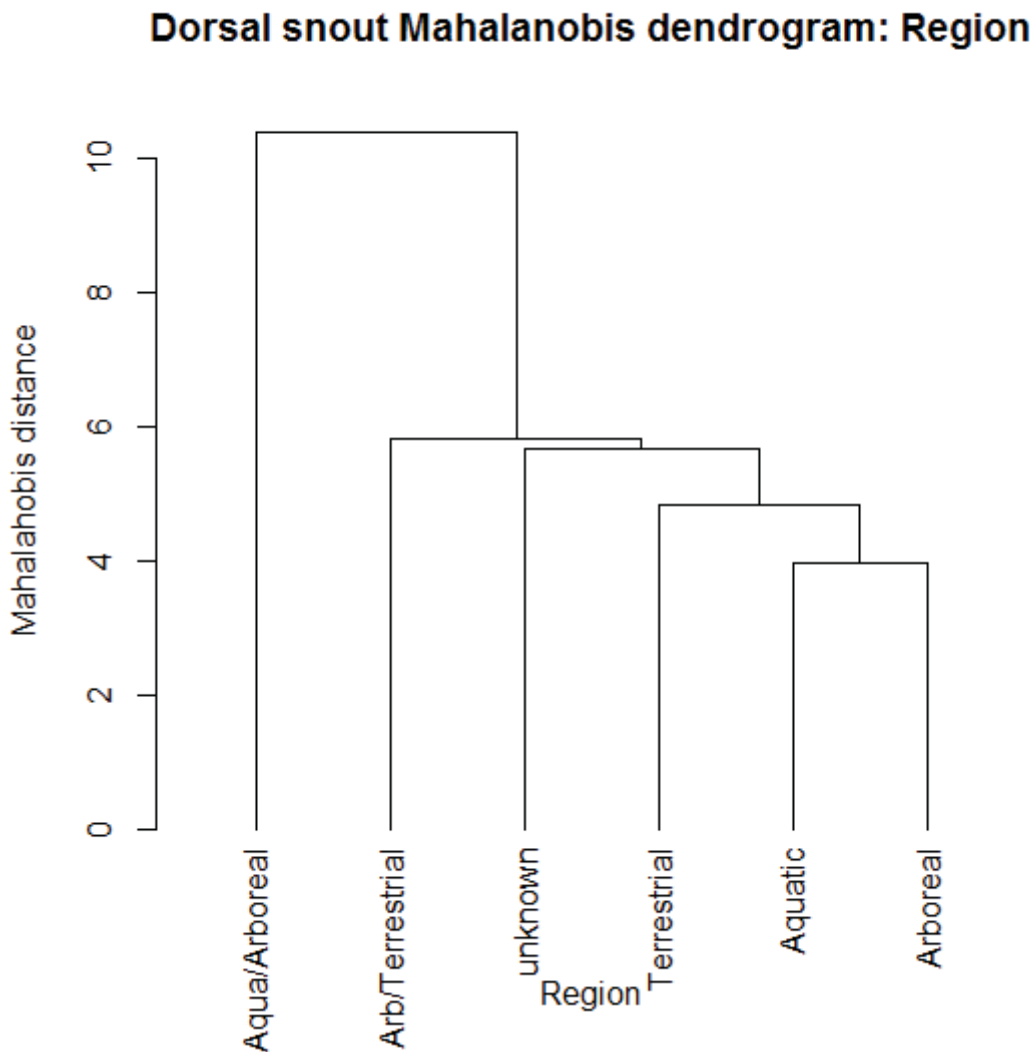


Appendix 2(cont.)

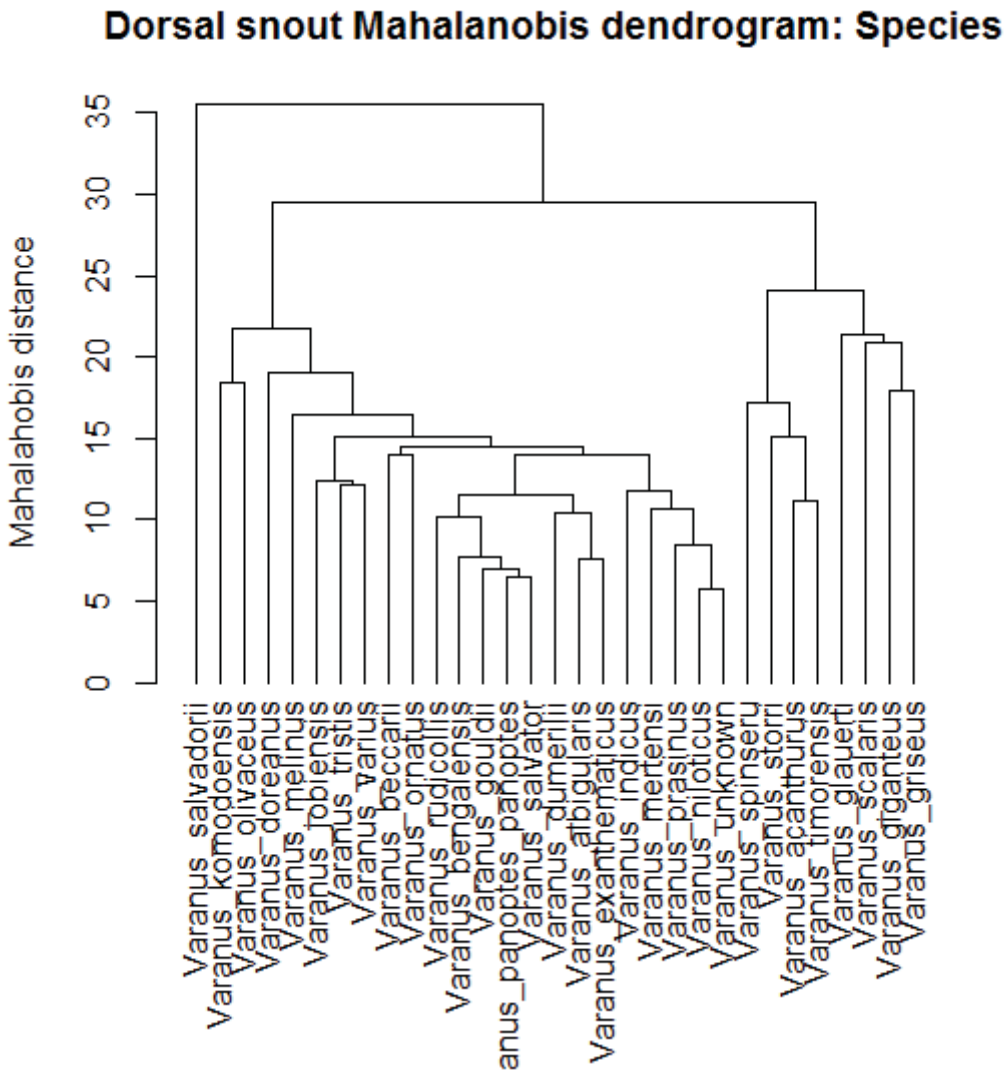
Figure A2. 3. Dorsal snout dendrograms based on Mahalanobis distances



Appendix 2 (cont.)

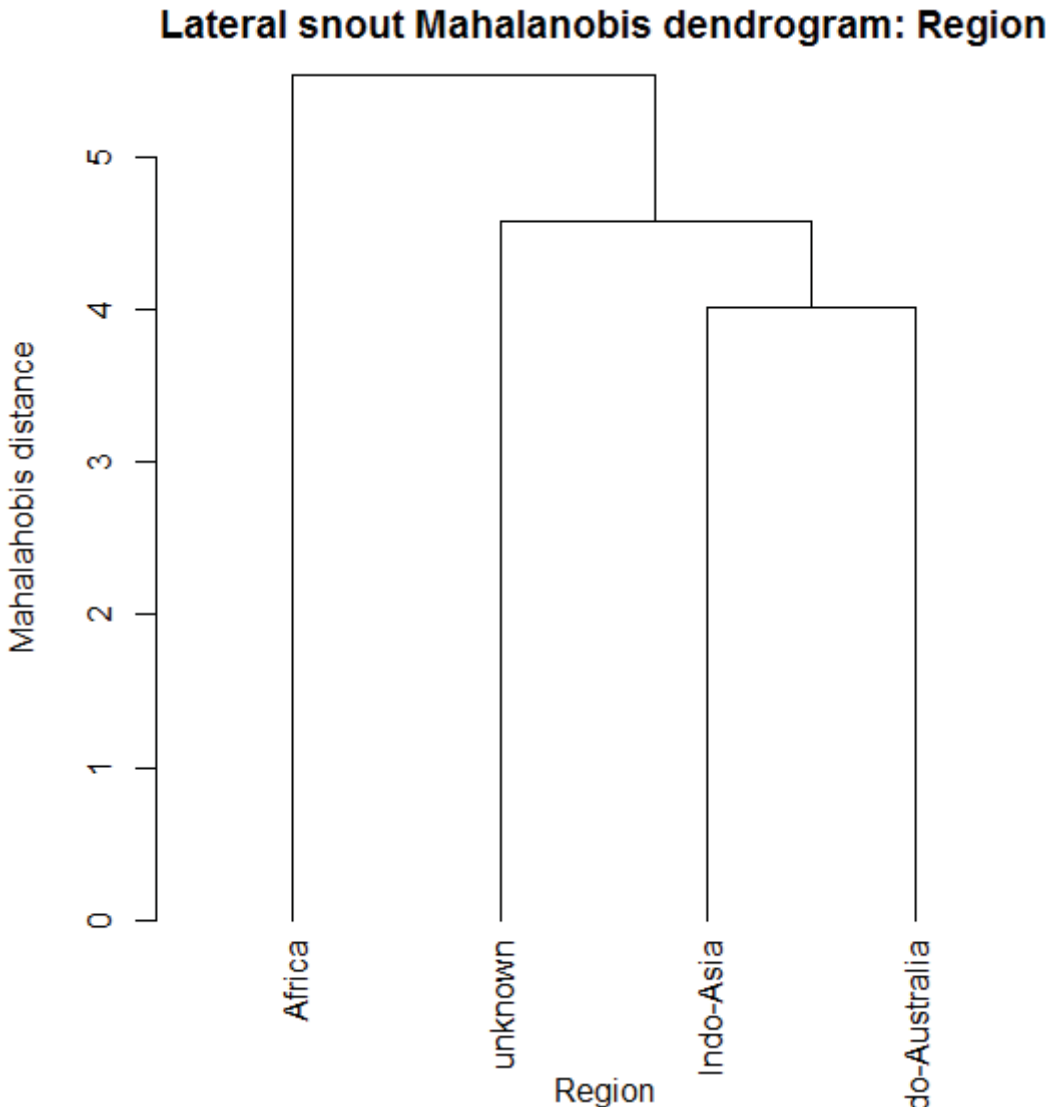


Appendix 2 (cont.)

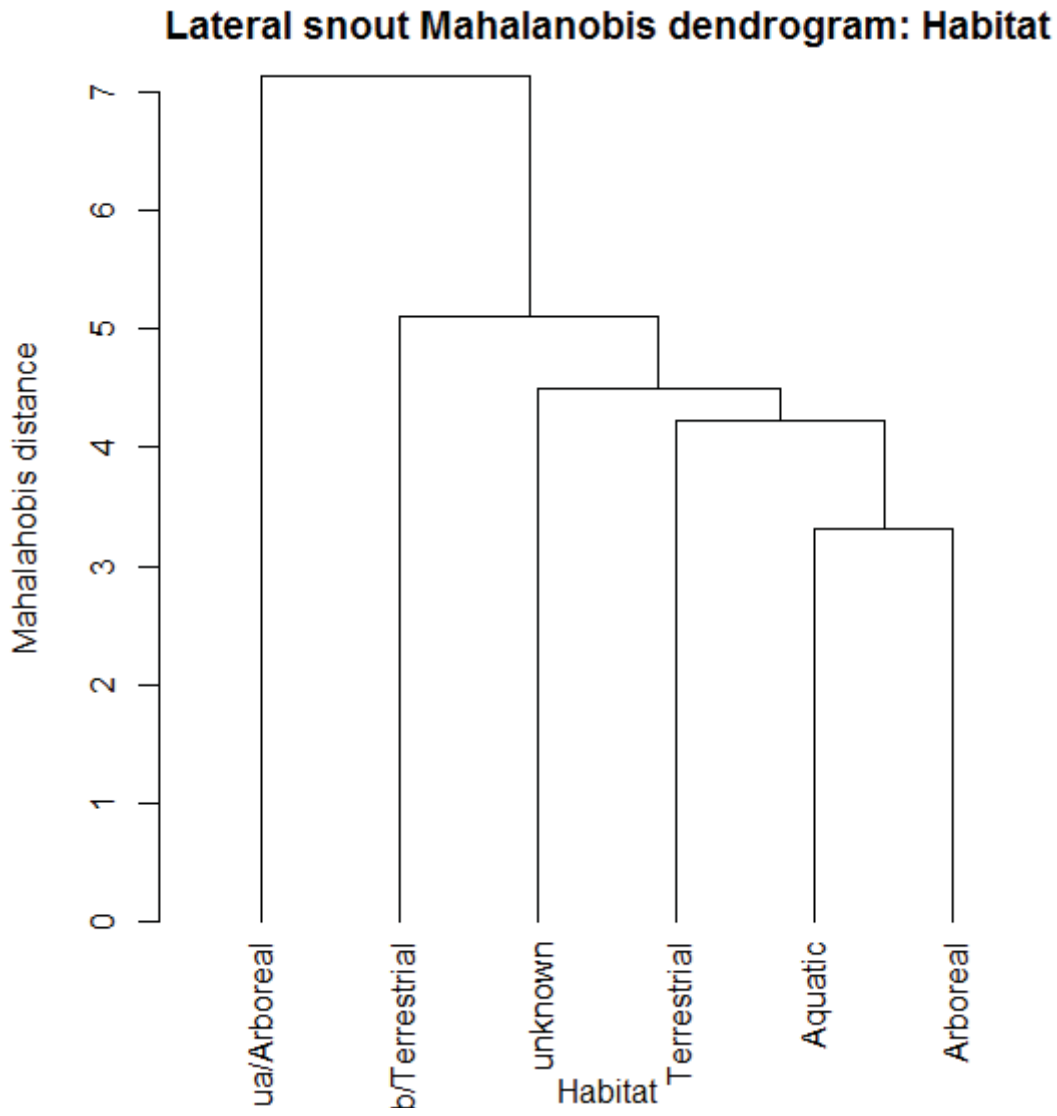


Appendix 2 (cont.)

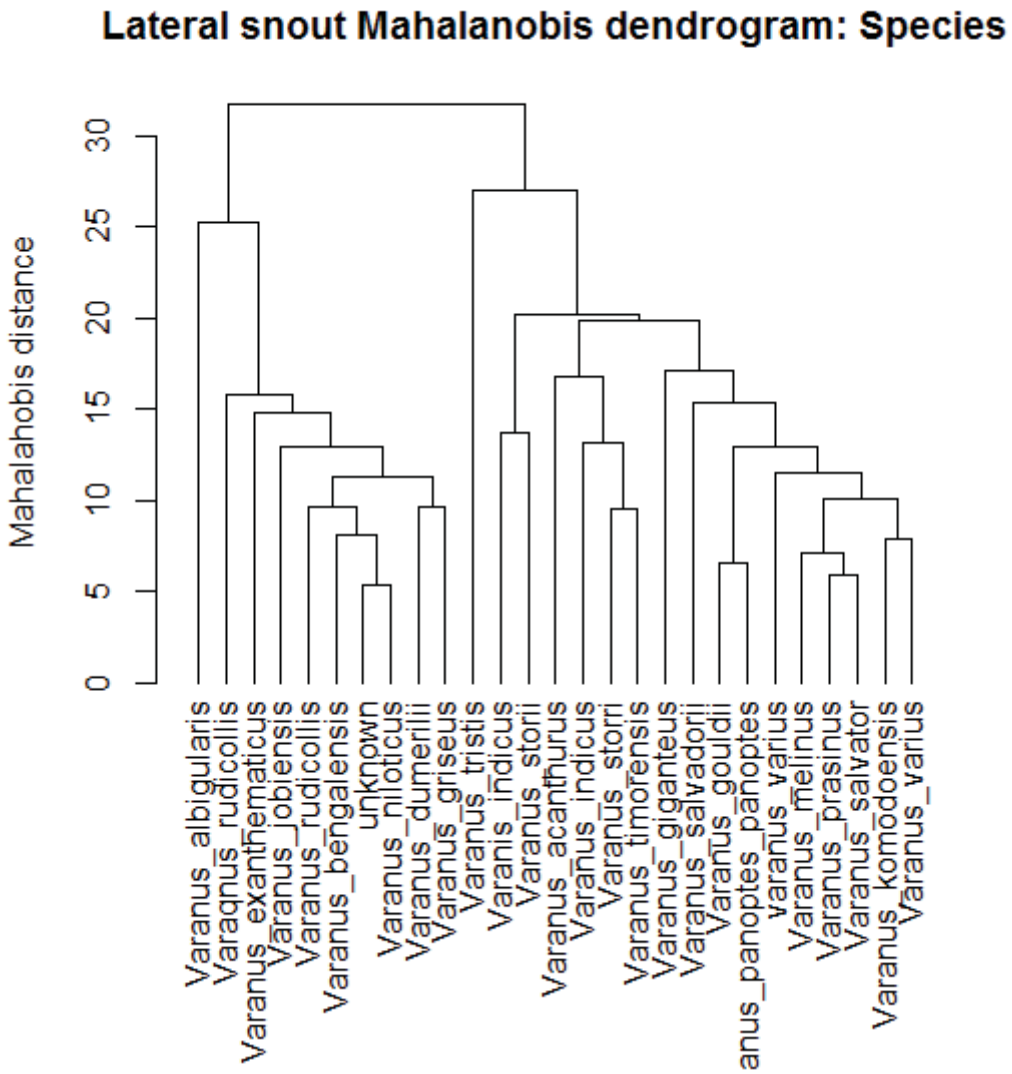
Figure A2. 4. Lateral analysis dendrograms based on Mahalanobis distances



Appendix 2 (cont.)



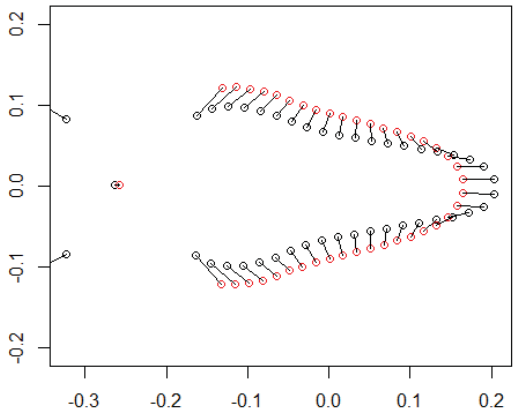
Appendix 2 (cont.)



Appendix 2 (cont.)

Figure A2. 5. Dorsal CVA visualization of shape change from score -5 to 5

Region



Habitat

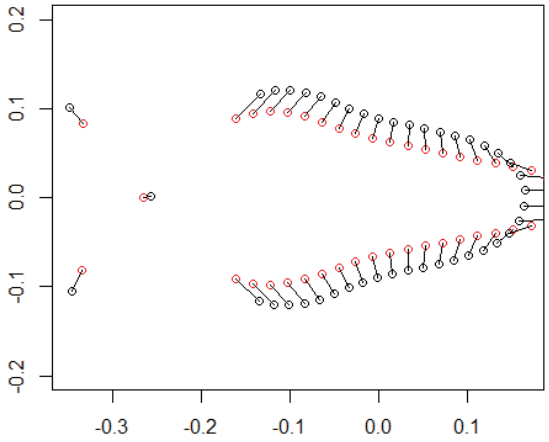
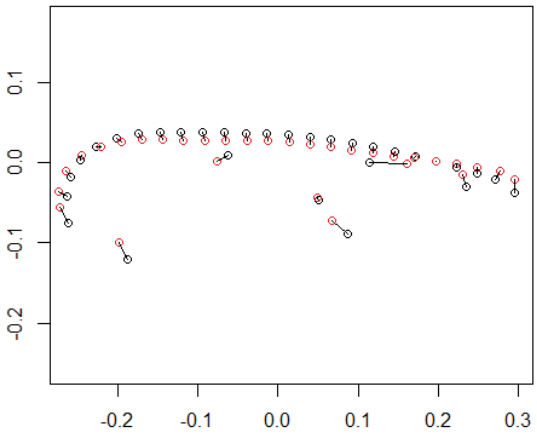
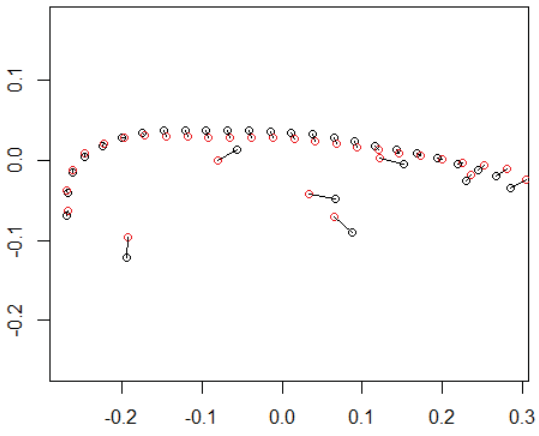


Figure A2. 6. Lateral CVA visualization of shape change from score -5 to 5

Region

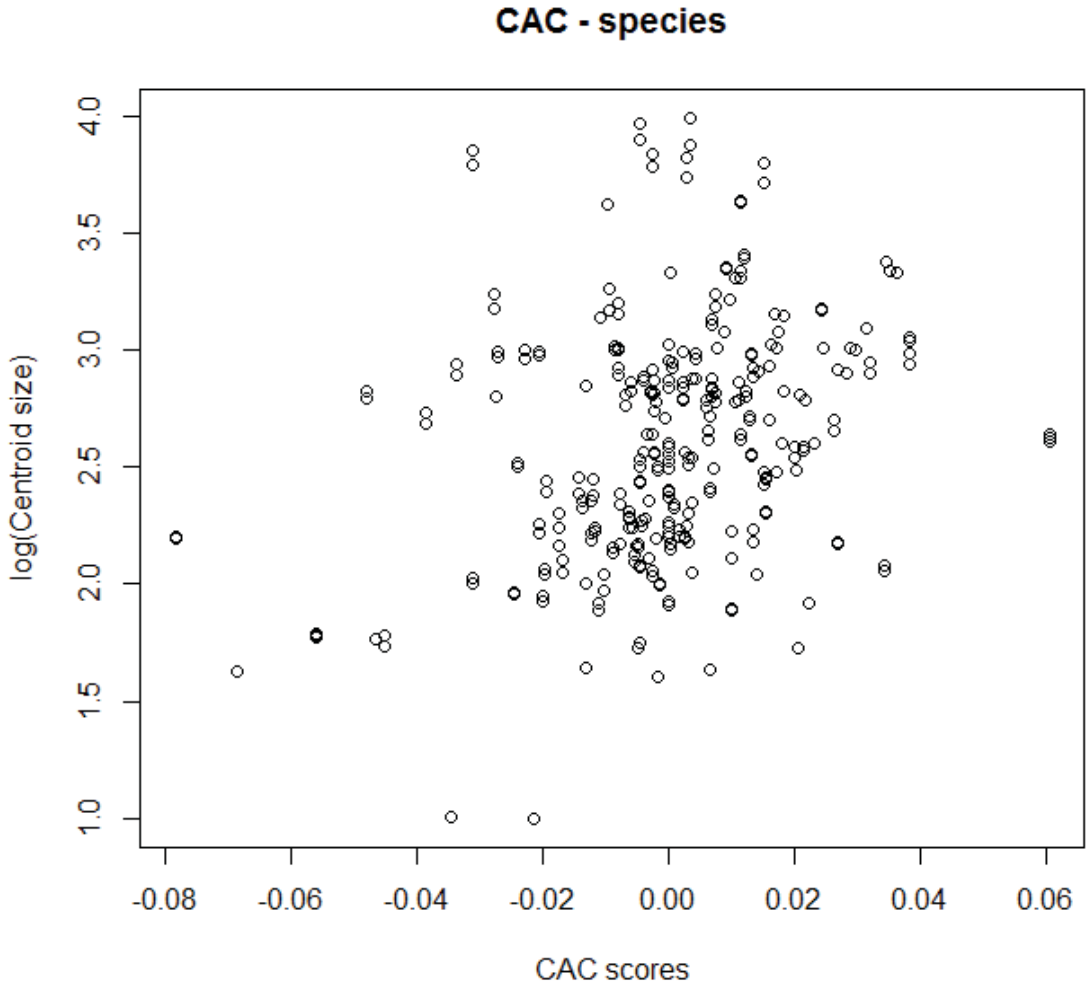


Habitat



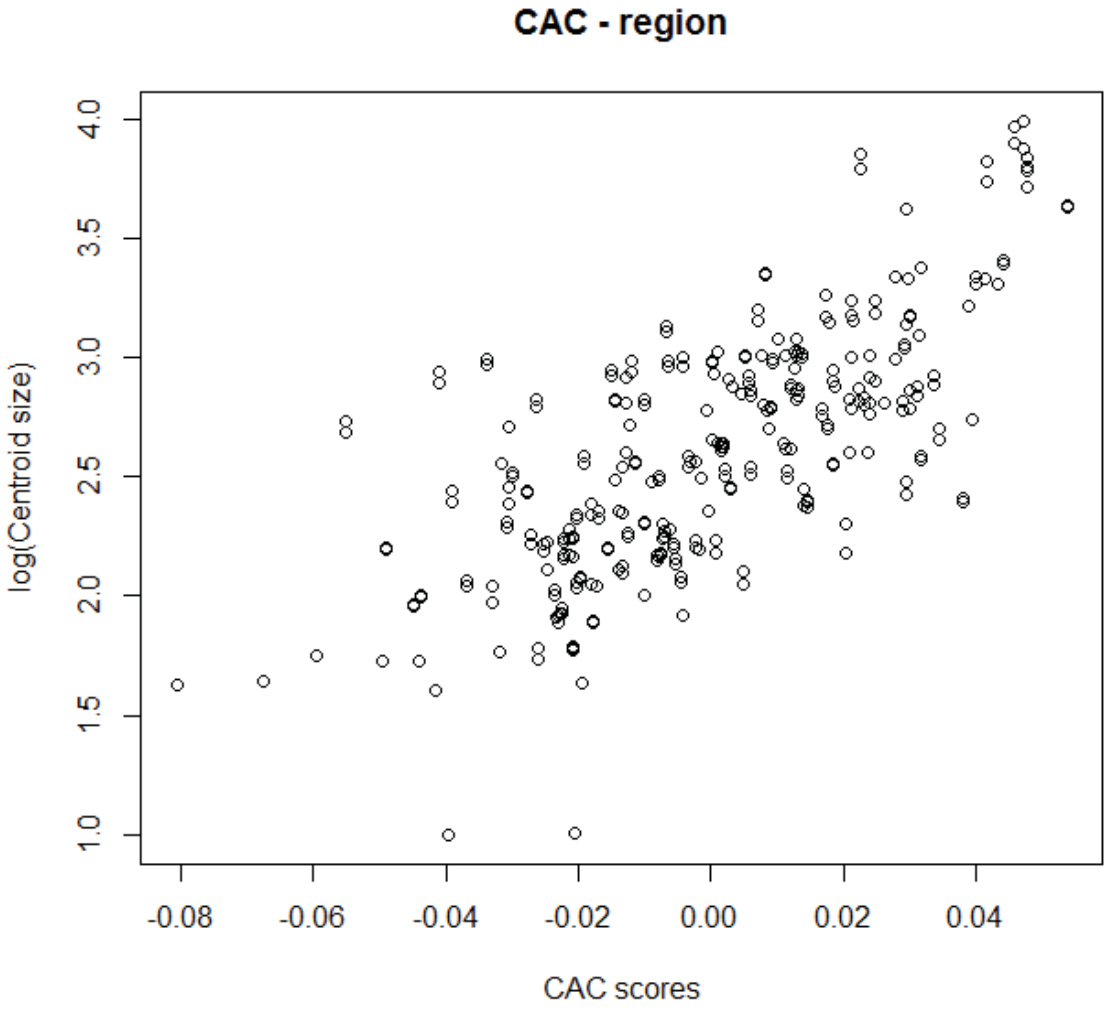
Appendix 3: Common allometric component analyses results

Figure A3. 1. Dorsal snout common allometric components accounting for species. T statistic: 5.4935, P-value = 8.263e-08, and Pearson product correlation : 0.299



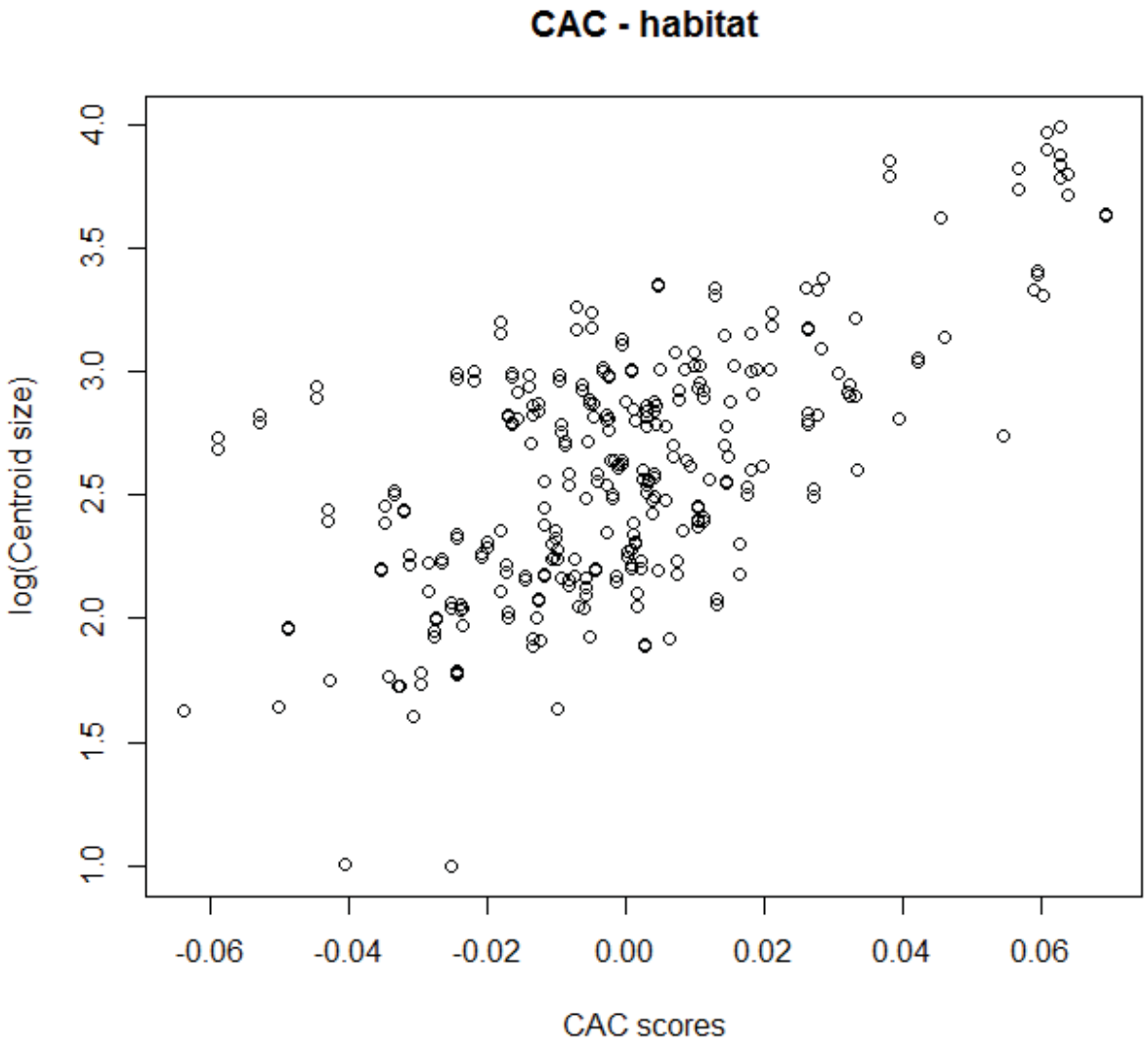
Appendix 3 (cont.)

Figure A3. 2. Dorsal snout common allometric components accounting for region. t: statistic: 17.855, p-value: < 2.2e-16, and a Pearson product correlation : **0.713.**



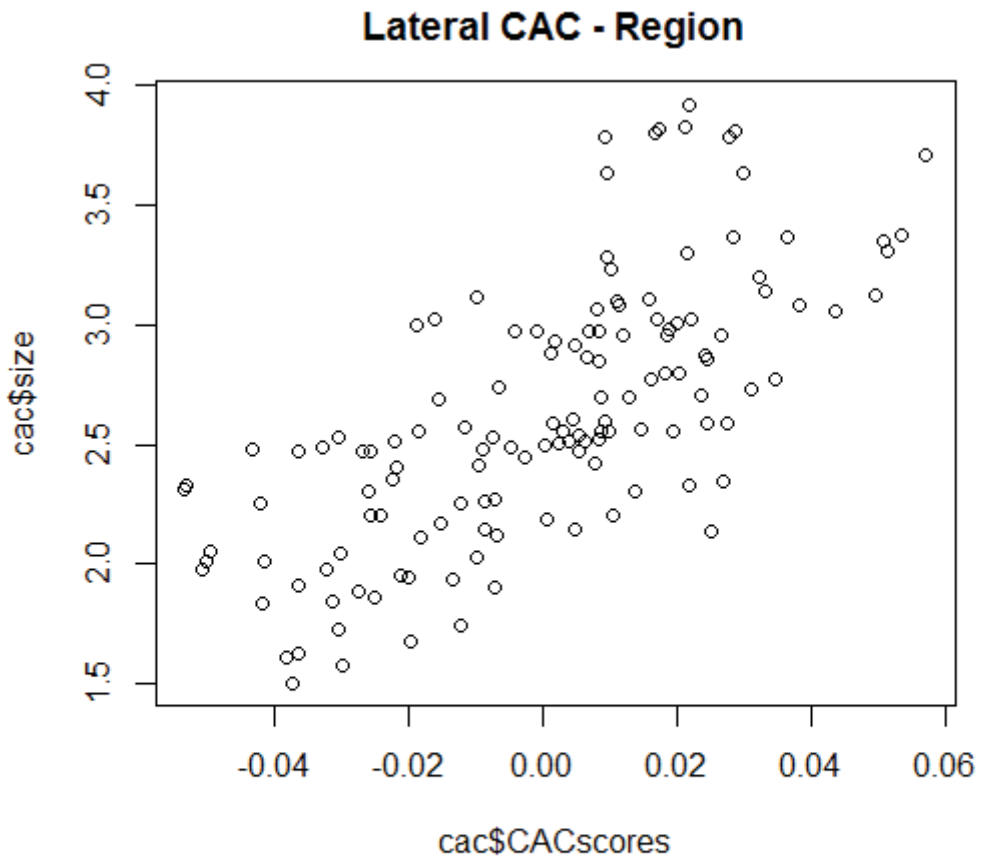
Appendix 3 (cont.)

Figure A3. 3. Dorsal snout common allometric components accounting for habitat. t: statistic:14.8933, p-value: < 2.2e-16, Pearson product correlation: **0.647.**



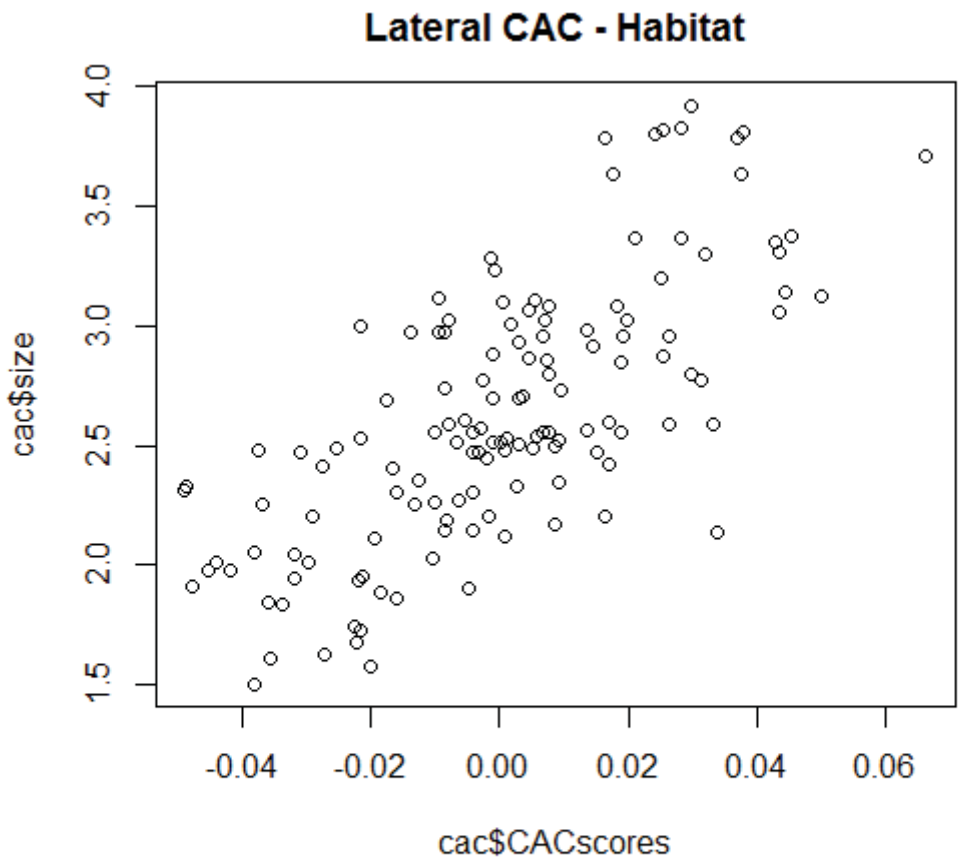
Appendix 3 (cont.)

Figure A3. 4. Lateral snout common allometric components accounting for region. t::11.47, p-value: < 2.2e-16, Pearson product correlation: **0.705.**



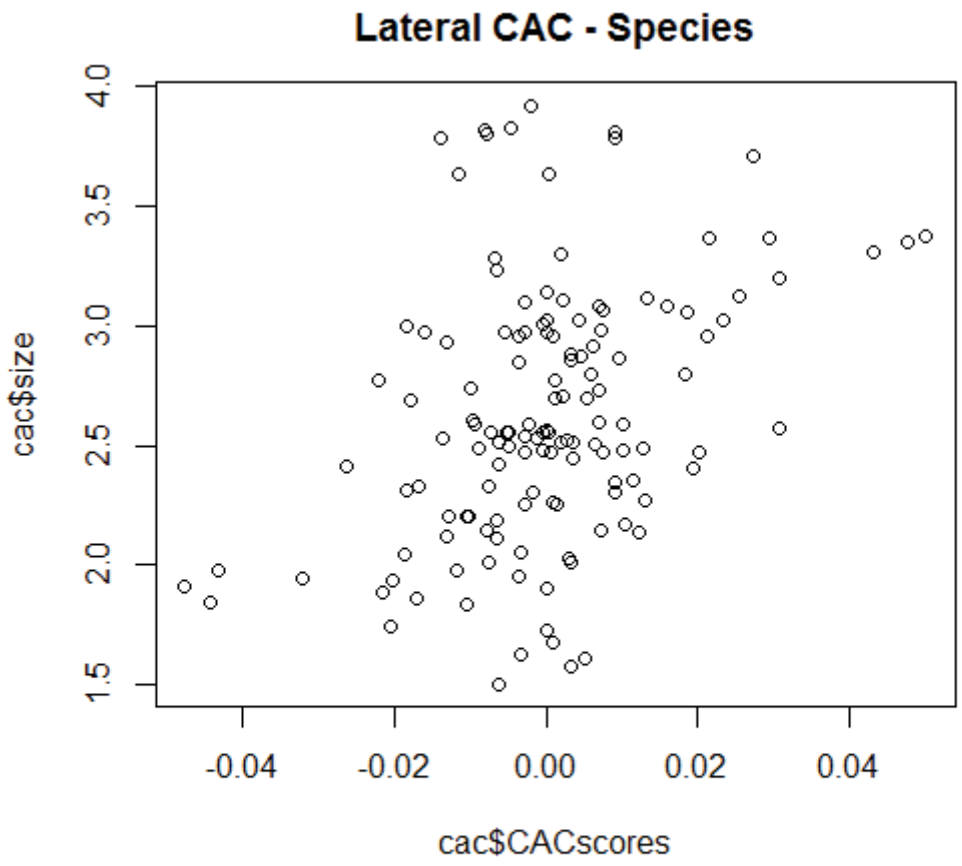
Appendix 3 (cont.)

Figure A3. 5. Lateral snout common allometric components accounting for habitat. t::11.81, p-value: < 2.2e-16, Pearson product correlation: **0.715.**



Appendix 3 (cont.)

Figure A3. 5. Lateral snout common allometric components accounting for habitat. t::4.72, p-value: 5.803e-06, Pearson product correlation: **0.379.**



Appendix 4

Table A4.1. Dorsal species average principal component analysis results. SD: standard deviation, POV: proportion of variance, and CP: cumulative proportion.

Importance of components:

	PC1	PC2	PC3	PC4	PC5	PC6	PC7
SD	0.03604	0.0223	0.01846	0.01016	0.00841	0.006719	0.006045
POV	0.5272	0.2019	0.13828	0.04187	0.02871	0.01833	0.01483
CP	0.5272	0.7291	0.86743	0.9093	0.93801	0.95633	0.97117
	PC8	PC9	PC10	PC11	PC12	PC13	PC14
SD	0.004491	0.003338	0.002982	0.002642	0.002368	0.002054	0.001778
POV	0.00819	0.00452	0.00361	0.00283	0.00228	0.00171	0.00128
CP	0.97935	0.98388	0.98749	0.99032	0.9926	0.99431	0.99559
	PC15	PC16	PC17	PC18	PC19	PC20	PC21
SD	0.001518	0.001396	0.001162	0.001099	0.0009681	0.000814	0.0007856
POV	0.00094	0.00079	0.00055	0.00049	0.00038	0.00027	0.00025
CP	0.99653	0.99732	0.99787	0.99836	0.99874	0.99901	0.99926
	PC22	PC23	PC24	PC25	PC26	PC27	PC28
SD	0.0007322	0.0006641	0.000535	0.0004255	0.000357	0.0003088	0.0002628
POV	0.00022	0.00018	0.00012	0.00007	0.00005	0.00004	0.00003
CP	0.99947	0.99965	0.99977	0.99984	0.9999	0.99993	0.99996
	PC29	PC30	PC31				
SD	0.0002472	0.000181	3.82E-17				
POV	0.00002	0.00001	0.00E+00				
CP	0.99999	1	1.00E+00				

Appendix 4 (cont.)

Table A4. 2. Lateral species average principal component analysis results. SD: standard deviation, POV: proportion of variance, and CP: cumulative proportion.

Importance of components:							
	PC1	PC2	PC3	PC4	PC5	PC6	PC7
SD	0.03438	0.02873	0.01721	0.01459	0.01326	0.01042	0.008655
POV	0.39505	0.27584	0.09897	0.07111	0.0588	0.03632	0.02504
CP	0.39505	0.67089	0.76987	0.84098	0.89978	0.93609	0.96113
	PC8	PC9	PC10	PC11	PC12	PC13	PC14
SD	0.005939	0.004803	0.004079	0.003893	0.003132	0.002673	0.002055
POV	0.01179	0.00771	0.00556	0.00506	0.00328	0.00239	0.00141
CP	0.97292	0.98063	0.98619	0.99125	0.99453	0.99692	0.99833
	PC15	PC16	PC17	PC18	PC19		
SD	0.001454	0.001314	0.000866	0.000641	4.51E-17		
POV	0.00071	0.00058	0.00025	0.00014	0.00E+00		
CP	0.99903	0.99961	0.99986	1	1.00E+00		

Chapter 4: Taxonomic Diversity, Morphospace occupation and Subclade Disparity Through Time in Monitor Lizards

INTRODUCTION

Among relatively recent studies of variation in morphological shape (e.g., Simpson, 1953; Van Valen, 1965; Caumul and Polly, 2005; Zelditch et al. 2012), a great deal of work has been done on testing factors that influence the divergence of shape within or across related groups (e.g., Caumul and Polly, 2005; Zelditch et al., 2012;), and the evolutionary or ecological implications of morphological variation (Van Valen, 1965; Foote, 1993(a); Fortey, Briggs, and Wills, 1996; Foote, 1997; Carroll, 2000; Nosil and Reimchen, 2005). Some hypotheses predict a relationship between taxonomic diversification and morphological divergence rates. It might be expected that these rates are positively correlated (Adams et al. 2009). For example, interest in patterns of evolutionary radiations, or splitting events followed by divergences in ecology or morphology, has stimulated research on whether divergences are distinctive to lineages or if groups follow more general rules (Schluter, 2000; Harmon et al. 2003). Punctuated equilibrium (Gould and Eldredge, 1977) theorizes that most morphological divergence occurs at splitting events. Others have suggested that, among lineages, phenotypic divergence at cladogenetic events may produce a correlation in rates of speciation and phenotypic diversification (Ricklefs, 2006a). Results may also be confounded by radiations that are non-adaptive or of cryptic species that are morphologically indistinguishable but different genetically (Kozak, Weisrock, and Larsen, 2006; Adams et al, 2009).

Though related, it should be understood that diversification rates differ from counts of taxonomic diversity. Studies of extant clades have shown that average morphological differences among taxa may not vary with taxonomic diversity (Ricklefs and Miles, 1994). Also, regions with low taxonomic diversity have shown both low and high levels of disparity (McClain, 2005; Hopkins, 2013), and measures of diversity might peak at different points in evolutionary history (Foote, 1993b, 1997; Wagner, 1997; Lupia, 1999). Some have stated that discrepancies between taxonomic and morphological diversity could arise simply from taxonomic practice (Foote, 1993b). It is important, though, to understand that these patterns might reflect true biological processes, and so could be evolutionarily informative (Gould, 1991; Foote, 1993b).

Although there has been interest in taxa that show a great deal of morphological diversity, or disparity, in these kinds of studies, interestingly, paleontological work has shown that the conservation of morphology or certain aspects of shape is fairly common in the fossil record (Eldredge et al., 2005). The degree to which organismal shape is maintained over a range of sizes, and the consequences of doing so, has long been of interest (Huxley, 1950), but only recently have the tools become available to directly test

alternative hypotheses (Klingenberg, 2010). Even more interesting is the degree to which shape can be maintained through time, or how any measure of morphological diversity (disparity) relates to taxonomic, or taxic, diversity. In extant organisms, studying the long-term conservation of morphology is difficult because many groups lack long-term (i.e., fossil) data. However, paleontological methods can be useful to neontological studies, and recent phylogenetic research can be useful for deep time questions, because they can both change the whole picture entirely. Also, the advent of new techniques has increased the ability to integrate phylogenetic relationships into measures of morphology (Harmon et al. 2003; Slater et al., 2010). I wanted to know how we might usefully quantify and analyze variation in shape through time, so in this study I quantified temporal shape variation in varanids, a morphologically conservative but taxonomically diverse group.

Monitor lizards

Varanids, also known as monitor lizards or monitors, are a charismatic group of lizards found in Africa, Arabia, southern Asia, and through the Southeast Asian islands to Australia (Bennett, 1995; Molnar, 2004). Their taxonomic diversity varies among 3 major biogeographic regions defined by Vidal et al. (2012): Africa (6 species), Indo-Asia (~40 species), and Indo-Australia (~30). These regions house monophyletic groups, although Vidal et al. (2012) did find two monophyletic groups in Indo-Asia (Fig. 1). They are a good model organism for this kind of study because they are ecologically diverse and show a great deal of variation in size (Losos and Greene, 1988; Pepin, 2001; Collar et al., 2011). In the single genus *Varanus* alone (approximately 70 species), extant members have a 4000-fold body mass range, and vary in total body length from 0.2 m to around 3 m long (Losos and Greene, 1988; Pianka, 1995; Pianka and King, 2004; Molnar, 2004; Collar et al. 2011). The largest variation in size range is seen in Indo-Australian members, which include *V. komodoensis* and the pygmy subgenus, *Odatria*. Varanids live in aquatic, arboreal, and terrestrial habitats or some combination thereof (Losos and Greene, 1988; Pianka, 1994; Pepin, 2001). Work has shown that ecology and size might be correlated (Losos and Greene, 1988; Collar et al., 2011). Even though they show a great deal of versatility in these factors, monitors are considered morphologically conservative because they all share a general and versatile body plan. I used varanids as a case study to test the relationship between morphological disparity and taxonomic diversity through time among regions and size ranges. The principal questions to be asked are whether larger groups show greater comparative disparity than smaller groups do, whether any clustering of morphological patterns occurs geographically, and whether these are broadly related to phylogenetic or ecological factors.

Varanus temporal diversity dynamics

Here I present analyses of morphospace and disparity through time in extant monitor lizards to investigate trends and tempos of morphological evolution, using size and quantified shape data. Geometric morphometrics (GM) quantifies shape by reducing data to principal components that describe the greatest amount of shape variation. It also removes the effects of size on shape (Zelditch et al., 2012). Both size and shape in previous studies have correlated with each other, along with other factors such as habitat (chapter 3 of this dissertation; Losos and Greene, 1988; Collar et al. 2011). I was interested in whether patterns of size and shape, then, would be correlated when analyzed as separate components through time. I then discuss the implications of these results for specific methods, and their bearing on the evolutionary history of monitor lizards.

MATERIALS AND METHODS

Tree choice

Because new extant and fossil taxa of *Varanus* are constantly being discovered, and molecular analyses are becoming more refined, hypothesized relationships are often ambiguous or even contentious. Cladistic analyses of *Varanus* have used both molecular and morphological data. Ast (2001) generated a molecular tree that was relatively inclusive of extant *Varanus.* The results of that analysis differed significantly from Conrad et al. (2008)'s morphology-based tree, which had included a number of non-varanid and fossil taxa, and several extant *Varanus*. Many studies tend to differ in taxonomic breadth and sampling. In my study, I decided to use the tree produced by Vidal et al. (2012) because it is one of the most recent, is time- calibrated, and contains a broad taxonomic sample of extant *Varanus*. The time-calibrated molecular phylogeny was digitized and used as a framework to determine how patterns of lineage diversification and disparity compare in historical patterns of this extant clade

(a) Lineages through time. Lineage-through-time (LTT) plots show the number of lineages in a clade that exist at any given time. When using a phylogeny that has time-calibrated branch lengths, it is assumed that a taxon exists in any given period that its branch crosses (Nee et al, 1995). If there is no extinction and origination is constant, then these plots are expected to show exponential growth, and any deviations from that may indicate changes in diversification rate through time. Changes in standing diversity are a function of speciation and extinction (Harmon et al. 2003).

A LTT plot was used to examine the tempo of increase in species richness in the Vidal et al. (2012) tree. I wanted to understand what the LTT trend would look like under a null expectation of pure-birth (also called a Yule diversification) process. Using the parameters from the Vidal et al. (2012) tree - number of taxa and branching times - one can create a Yule process null by obtaining maximum likelihood values. I created a range of LTT possibilities and used the p-values to produce confidence intervals (CI). I

plotted the observed LTT over the hypothesized null Yule distributions with colors representing different p-values. All analyses were done using the *ape* (Paradis et al. 2004) and *laser* (Rabosky and Schliep, 2013) packages as well as my own modified code from previous work done by Nicholas Matzke in R (R core team, 2014).

(b) Diversification tests. I also tested for changes in diversification rates within the tree to compare with patterns of morphological disparity. The gamma statistic (γ) measures where the center of mass is located on a phylogeny, or the distance of internal nodes of a phylogeny to the root of the tree, and tests whether they are closer than would be expected (Fordyce, 2010; Quental and Marshall, 2010). The build-up of nodes closer to the root of a tree has been interpreted as an early burst of diversification (Fordyce, 2010; Slater et al., 2010). Results are compared to a null model of constant diversification (γ=0). For example, negative γ and significant P-values are considered to indicate a slowdown in splitting events through time across a tree. The γ statistic assumes complete sampling of a phylogeny, so I also ran a Monte Carlo constant rates test, which conducts a γ statistic analysis (Pybus and Harvey, 2000) while accounting for incompletely sampled trees. This works by simulating trees (5000 simulations in this instance) to full clade size under a null model of pure-birth, or Yule diversification. I used one of the most recent estimates of the number of living *Varanus* species (73) for the clade size parameter (Vidal et al., 2012). The method then prunes the simulated trees to represent the incomplete taxon sampling of the tree being tested. A null distribution of γ is generated from these trees, with a new critical γ and adjusted p-value (Pybus and Harvey, 2000; Brock et al., 2011).

I also tested two constant and six varying diversification rates models on the tree. The constant rate models were a Yule (pure birth) model where diversification rate is constant throughout the entire history of the clade, and a birth-death (bd) model with constant extinction and origination rates. The six varying diversification rate models included logistic (DDL) and exponential diversity dependence (DDX), where diversity is considered to have a capacity, a model testing for two different rates of diversification across the tree (two-rate Yule), varying origination rates (SPVAR), varying extinction rates (EXVAR), and both varying origination and extinction rates (Kendall, 1948; Nee et al., 1992, 1994a, 1944b; Rabosky ,2006; Rabosky and Lovette, 2008). I used likelihood scores and the Akaike Information Criterion (AIC) to test these various models. AIC is defined as 2k-2log(likelihood), and the lower the AIC score, the more likely that model fits the tree. All analyses were done using the *laser* (Rabosky and Schliep, 2013) package in R.

(c) Morphospace through time. To create morphospace through time plots, the chainsaw function described in chapter 2 of this dissertation was used on the Vidal et al. (2012) tree. Results of a geometric morphometric (GM) analysis on snout shape from Chapter 3 were used to recreate shape space. Because geometric morphometric data

were not available for each species on the Vidal et al. (2012) tree, a smaller, modified version of the phylogeny was used, which included only taxa from the GM analysis. All morphometric analyses were done using the *geomorph* (Adams and Otarola-Castillo, 2013) package in R. The phylogeny was chainsawed at 5 my time bins, and a new tree was generated representative of each bin. The tip labels for those time bin trees were returned and used as a list of taxa living at those designated times (See Appendix 1 of Chapter 3 for a specimen list, and Appendix 1 of this chapter for a taxa list). Using those time bin communities, morphospaces were reconstructed based on the first two principal components (PCs) of the geometric morphometric results (see Appendix 2 for PC scores). These morphospaces were based on all specimens designated to specific taxa, so they also included the variances of each taxon within that space. This method assumed that no morphological change occurred through time in any lineage.

At each time bin, morphospace size was measured in two different ways, using the average Procrustes Variance (PV) (Zelditch et al., 2012) as well as Minimum Convex Polygon size of all the specimens. PV was measured using the Procrustes superimposed coordinates, or the shape, of the specimens. PV is computed as the difference between the mean shape of a defined group, in this case all of the specimens existing at a time period, and the grand mean of the morphospace (Zelditch et al., 2012). Measurement of PV was done using the *morphol.disparity()* function in the *geomorph* (Adams and Otarola-Castillo, 2013) package. The Minimum Convex Hull method is based on space generated by the first two principal components, so a 2-dimensional shape space. Somewhat differently than other morphometric studies, I used methods common in estimating taxonomic home range size that use latitude and longitude coordinates. The minimum convex hull is computed by estimating the smallest convex hull around a set of coordinates, in this case time bin specimens (each has a PC1 and PC2 score). This estimation is done after removal of 5% percent of the specimens farthest from the centroid of the morphospace hull, which is computed by obtaining the mean of the hull and comparing it to the coordinates of each specimen. In studies using point observations to determine home ranges of taxa, which is defined as the area traversed by a taxon during ordinary activities (Mohr, 1947), removing a small percentage of observations farthest from the centroid of the range before estimation represents the elimination of possibly large moves to unusual places outside its typical home range. These outliers are not considered normal activities, and so in my case I am estimating some specimens as outliers in shape. Because the GM analysis is based on the available specimens and landmarks placed by me, some outliers due to human or landmarking error are expected that can be removed from these estimations of “normal” shape space. I measured morphospace size or range of whole time bin communities as well as space represented by the three geographic regions defined in Vidal et al. (2012) – Africa, Indo-Asia, and Indo-Australia. Size and overlap of these regions were measured to compare changes in regional taxonomic diversity through

time to morphospace size. Overlap was measured as the proportion of regional convex hull overlap at any given time bin. All analyses were done using functions from the *adehabitat* (Calenge, 2006) package in R.

(d) Disparity through time. Disparity through time (DTT), sensu Harmon et al. (2003) and Slater et al. (2010), was also analyzed. Snout-vent length (SVL) is used as a size metric and a proxy for ecological and morphological traits that scale with size (Losos and Greene, 1988; Collar et al. 2011). For this analysis, I compiled data on adult SVL of taxa for each species in the Vidal et al. (2012) phylogeny from a literature search (Losos and Greene, 1988; Pepin, 2001; Collar et al. 2011). SVL of each taxon can be found in Appendix 1. Length estimates were favored over mass because mass can have more confounding factors that affect its variability. Total body length data were natural log (ln)-transformed before analyses. For shape, the data from the 2-dimensional geometric morphometric snout shape data was also used. After Procrustes superimposition and principal components analysis, principal components of axes of shape variation were generated. Coordinates representing 95% of shape variation were factored into the analysis (Appendix 2). Not all taxa from the Vidal et al. (2012) tree had geometric morphometric data collected for analyses, so the pruned tree (Fig. 2) generated for the morphospace size analysis was analyzed.

Following methods in Harmon et al (2003) and Slater et al. (2010), I calculated mean subclade disparity-through-time (DTT) for body size and the geometric morphometric data. The observed DTT for these data sets across the Vidal et al. (2012) tree were compared with patterns expected under a Brownian process, by running 10,000 iterations simulating size or shape evolution across the tree. Mean subclade disparity and 95% confidence intervals (generated by the simulations) were plotted with age. The morphological disparity index (MDI) was also calculated. MDI is a quantification of the difference in disparity of a clade to expected disparity under the null model of Brownian motion, and is the distance between the observed DTT of the data and the estimated result of the simulations. Negative MDI values indicate lower subclade disparity than expected, and positive, higher disparity (Harmon et al. 2003; Slater et al. 2010). All disparity analyses were conducted in R using the *ape* (Paradis et al. 2004) and *geiger* (Harmon et al. 2008) packages.

RESULTS

(a) Lineages through time. Because there is no extinction in an extant-only tree, the number of lineages steadily increases through time. The log lineage accumulation curve is relatively straight, indicating a fairly steady increase in the number of lineages through time (Fig. 3). Near the recent (approximately 30 time units from the basal divergence) the curve begins to flatten, signifying a slowing in diversification. When compared to the expected pure-birth model results (Fig. 4), at approximately 20 Mya, observed values

begin to increase above various CI limits, and at 6 Mya emerge above any CI expectations. This suggests that, at least near the recent, the number of taxa in the tree does not follow the patterns of an expected pure-birth model. However, counts quickly return within expected limits at the recent.

(b) Diversification tests. The gamma statistic and MCCR test results were negative (MCCR γ = -2.67), although not significant (p = 0.98), indicating no evidence for accelerated diversification early in the history of *Varanus* (Table 1). This is visually evident in the LTT plots (Fig. 3; Fig. 4), where there is no evidence of an early burst of diversity above expected range. But because the results were not significant, I cannot rule out the possibility. I found more support for declining diversification (DDL) or 2-rate-Yule model (Table 2). The slope of the log LTT plot changes toward the recent, which normally indicates a change in lineage accumulation, or diversification, rate. It is not surprising, then, that these two models would come out as most likely. DDL recognizes a slowing in diversification, and the flattening near the Recent of the log LTT plot is considered indicative of declining diversification. The 2-rate Yule model simply recognizes at least two different diversification rates in the tree. It has been shown that the molecular signature of clades in decline, meaning results from purely molecular trees, can be similar to those produced from diversity-dependent diversification (Quental and Marshall, 2011). The 2-rate Yule is also to be expected, because it would consider the change in diversification near the Recent to mean several diversification rates in the history of the group. I cannot rule out either declining diversification rates or the clade being in decline. Varying diversification also seems a possibility, although neither likelihood nor AIC indicates that it is more probable than declining diversity (Table 2).

(c) Morphospace through time. Morphospace variance increases through time in the phylogeny, which is expected in a phylogeny that contains no extinct taxa (Fig. 5, Fig. 6). A large extent of morphospace is occupied fairly early, by around 20 - 15 Mya, after which most originations of new taxa fall well within the already established breadth of morphospace occupied up to that point. This can be seen visually in the total morphospace plots through time (Fig. 5, upper figures). At approximately 15 Mya, new taxa appear both in already established areas of morphospace and in areas that are expanding previous morphospace size, using either PV or Morphospace Range/Hull size (Fig. 6) as a measure. Both measures increase from the base of the tree to 30 Mya, after which they decline steadily toward 20 Mya before rising again at 15 Mya and maintaining their high measure to the present (Fig. 6). With the addition of new taxa or specimens through time, the resampling measure used to remove outliers changes, including specimens that may not have been included in the hull estimations of previous time bins (Fig. 5; notice that more outliers begin to be included through time). New taxa, which bring new data points in morphospace, might change where the centroid of the measured time bin hull falls, showing that outlier resampling measures can also shift

and affect the size (and sometimes shape) of the morphospace through time. Measures of PV show slightly stronger responses to the appearance of new taxa in time bins, but the overall trend is similar to convex hull size.

Using the pruned tree of sampled taxa (Fig. 2) and using morphospace range size, I found extant *Varanus* taxonomic diversity to be lowest in Africa, and depending on how regions are defined, highest in Indo-Australia, followed by Indo-Asia (Pepin, 2001; Vidal et al., 2012). Early on, origination of new taxa is slow and steady, but even so there is a fairly large jump in the morphospace size in the Indo-Australian portion of the tree (Fig. 7, 30 My time bin). The number of Indo-Australian taxa increases steadily to the present, correlating with a slow and steady increase in Indo-Australian morphospace size as well. Interestingly, even though there is a slow increase in the number of Indo-Asian taxa through time, they share a similar early increase in morphospace size alongside the Indo-Australian group (Fig. 7). By contrast, the lineages comprising the African taxa show a distinctly different pattern. Once African taxa appear in time bins, even if they are only represented by one group, they quickly fill large portions of the morphospace (Fig. 7 a). African diversity is always very low, because in this analysis only 3 taxa were included, but they show a great deal of morphological variation. At 15 Mya, all African taxa included in the analysis are present and they take up the largest amount of morphospace (Fig. 5; Fig. 7a).

Morphospace size itself does not offer any information on how taxa are distributed in morphospace, but measures of overlap provided some insight into this question. Africa takes up a great deal of morphospace, so it is not surprising that other regions, specifically Indo-Australia, have a large overlap with African space (Fig. 8). This can also be seen visually in the time bin plots (Fig. 5). The temporal increase of Indo-Australian morphospace size tends to occur within already occupied African morphospace, so there is an overall rise in measures of overlap between those regions toward the present. Indo-Asian taxa are found in a more confined region of morphospace, so it takes time before their shape space increases enough to show strong overlap with other regions, and even then it is always lower than the overlap between Africa and Indo-Australia (Fig. 8).

(d) Disparity through time. Size (SVL) disparity among subclades was measured across the full Vidal et al. (2012) tree. Size DTT is lower than expected under a Brownian motion model of size evolution, which can be seen as observed values that fall below the median line (Fig. 9). This is supported by a negative Mean Disparity Index value, although it is not significant (MDI = -0.163, P-value= 0.38). Overall, there is a decreasing trend in DTT through time. Observed DTT values fall well below expected range and stay low throughout most of the history of the clade: however, there is one jump between approximately 18-16 Mya (Fig. 9; peak slightly after 18 Mya). This is

coincident with concurrent radiations of several groups in the Indo-Australian portion of the tree (Fig. 1).

The pattern for skull shape disparity is very different. Subclade DTT is slightly higher than expected under Brownian motion (Fig. 10), which is also reflected in the positive MDI (MDI = 0.093, P-value= 0.059). Similarly to size DTT, there is an overall trend of decreasing disparity throughout the history of the lineage. Interestingly, several jumps in DTT are coincident with diversification across the *Varanus* tree. Just before 24 Mya, there is a dip in DTT below the expected mean. Although there is a slight increase in the number of lineages at this time (Fig. 10, red dotted line), it is mostly confined to the Indo-Australian portion of the tree. Two jumps above the 95% CI, approximately 18-15 Mya, coincide with an overall increase in diversification across the tree (Fig. 2; Fig. 10).

DISCUSSION

Previous work on *Varanus* cranial morphological variation has shown that a variety of factors – phylogeny, habitat, allometry, region – can influence trends in shape and size variation (Chapter 2 in this dissertation; Collar et al., 2011; Openshaw and Keogh, 2014), although they are a morphologically conservative group. Different measures of morphology, be it multivariate shape or body size, can produce different interpretable temporal patterns. This study showed that lineages in taxonomically depauperate regions can still occupy a substantial portion of morphospace through time. Both size and shape subclade DTT seemed to be well established early in *Varanus* (at least with the members included in the phylogeny used), and DTT generally tended to decrease (Fig. 9, Fig. 10). Although the number of observed lineages increased slightly above expected levels under a Yule model approximately 8-6 Mya (Fig. 4), the rate of diversification may have been slowing at that time (Fig. 3). Certain likelihood model tests support this (Table 2). Even accounting for missing taxa, I found no evidence for an early burst of diversification in extant *Varanus* based on the γ statistic (Pybus and Harvey, 2000), but I cannot discount the possibility of a multi-rate, DDL, or declining diversification process (Table 2). Based on these results, there also seems to be no correlation between taxonomic and morphological diversification.

Diversification

The Vidal et al. tree has only origination, and does not contain all living *Varanus* taxa. Even so, both γ and the MCCR test are conservative with respect to extinction, so there might be a higher possibility of failing to reject a false null of γ=0 (Pybus and Harvey 2000; Rabosky and Lovette 2008; Slater et al. 2010). With these studies, it should also be stated that measures of γ, and other diversification models, can be affected by the evolutionary stage of a lineage and whether changes in diversification patterns have removed any information on previous patterns within the lineage (Pybus and Harvey,

2000; Quental and Marshall, 2009; Slater et al. 2010). For example, a new lineage might still be maintaining a high level of diversification. Using the model-fitting analyses (Rabosky and Lovette, 2008), I found that the logistic density-dependent (DDL) and 2-rate Yule models both receive about the same weight (Table 2). Based on the Vidal et al. (2012) tree, then, it appears that *Varanus* diversification is not constant through time. Because these methods do not discriminate between models such as diversity dependent diversification or declining diversity (which have been shown to have similar signatures when measuring molecular phylogenies), it may not be possible to distinguish which of these processes are in play with other data, such as the fossil record (Quental and Marshall, 2011). Even so, decreasing or changing diversification could be explained if varanids saturated a great deal of ecological roles early in the history of the lineage, not leaving much ecospace to be taken up by succeeding originations. To test the effects of ecospace filling, though, more work would need to be done on what these patterns look like regionally and within habitats.

Taxonomic vs Morphological Diversity

I was able to look at trends of taxonomic diversity (considered here as trends in the lineage through time analyses) temporally across the *Varanus* tree and compare them to different measures of morphology through time. My results show that temporally, morphology and taxonomic diversity do not appear to be correlated. Although there is a fairly steady increase in the number of taxa through time, certain times bins show discrepancies in measures of disparity. For example, the steady increase in the number of taxa between 30 My and 15 My time bins is not correlated with an equal increase in morphospace size or Procrustes variance, both of which actually decrease between these times (Figs. 3; 4; and 6). These metrics rely on measuring variance from a mean, and if the shape space taken up by the new taxa falls close to the group mean (in this case, time bin community means), then resulting measures will decrease. It appears, then, that at these times origination of new taxa fall well within the previously defined shape space. This might suggest that monitors explored a great deal of their morphological variabilty early in the history of the lineage.

Morphospace occupation vs subclade disparity through time

Different patterns of disparity are produced when looking at total morphospace size as opposed to subclade average squared DTT. Through time, as new taxa originated and were included in the morphospace of time bins, there were instances (Fig. 5, 30-15 My time bins) when they fell well within already occupied regions of morphospace. Because morphospace size was measured as the distance of specimens to the grand mean of the space, when more specimens begin to fall near the grand mean, it decreases the size of the time bin’s morphospace convex hull. Similar patterns are seen in the PV

measures, which use the actual superimposed shape variables. Although there is a general increase in morphospace size through time, there is a peak around 15 Mya, where morphospace size seems to be maintained (Fig. 6). Different regions tend to form monophyletic groups (Fig. 1), so regional measures of morphospace size actually provide insight into what sections of the *Varanus* tree are influencing changes in morphospace size. Diversity and disparity do not appear linked in *Varanus*, because the low-diversity African region takes up a great deal of morphospace early on, and the succeeding increases in diversity and disparity in other regions never seem to quite reach the levels of shape variation attained in Africa (Fig. 7). In general, these measures of morphospace size are greatly influenced by where new taxa, or specimens in morphospace, fall compared to the grand mean of the shape space.

Patterns of DTT differed from those of morphospace measures in subclades because they used a phylogeny, and thus relationships of taxa, as a framework for disparity measures. There was a general decrease in DDT through time. These results are typical when there is increased nestedness of origination across the tree. Representatives of clades across the tree appear early on the phylogeny, so successive originations would be expected to be fairly nested. Interestingly, size and snout shape differed in their comparisons from expected patterns: the MDI for size was -0.16 and that for snout shape was 0.09 (Fig. 9; Fig. 10). These differences may be explained by several possible reasons. There is a great deal of size variation in extant varanids, so it could be that when modeled under Brownian motion, the DDT model expected a higher level of SVL subclade disparity through time. The jump slightly after 18 Mya might not be surprising because it coincides with diversification in the Indo-Australian portion of the tree, which contains both *V. komodoensis*, the largest living monitor lizard, and members of the dwarf *Odatria* subgenus, some of the smallest members (Fig .1). The positive MDI for snout shape could result because analysis was run on the smaller, modified Vidal et al. (2012) tree, which might have affected the overall measure of expected DDT. The only positive excursion outside the 95% interval is also correlated with diversification in the Indo-Australian portion of the tree (Fig.2; Fig. 10). It would seem that although African varanids are diverse when measured in morphospace, Indo-Australian taxa do help explain a significant amount of shape variation in the monitor lizards included in this analysis. Indo-Australia does take up a significant amount of morphospace, and its varanids do have the largest variation in body size. This result supports previous analyses that showed a strong relationship between skull shape and size (Chapter 3 in this dissertation; Openshaw and Keogh, 2014).

The evolution of disparity in Varanus *and its evolutionary implications*

Varanids were chosen as a model in this study because they are morphologically conservate, but variable in ecology and size. Previous work (Chapter 3 in this dissertation; Collar et al., 2011; Openshaw and Keogh, 2014) has found a link between

skull shape, and to an extent size, with habitat, phylogeny, region, and other factors. Size and shape, then, have strong evolutionary implications in varanids. Because varanids tend to be morphologically conservative, finding any significant pattern relating to shape was surprising and extremely interesting. Previous studies on squamate DDT have found a negative relationship between patterns of morphological radiation (MDI) and certain measures of tempo of lineage diversification (Harmon et al. 2003). Although many caveats surround the diversification results in this study, if one accepts the findings, then a decrease in diversification follows with a decrease in DTT.

My disparity-through-time analysis shows that size and snout shape variation, and therefore possibly aspects of ecology, were most likely shown by subclades relatively early. Although these analyses only included extant taxa, this is in broad agreement with the varanid fossil record. The fossil record of varanoids spans over 90 million years (Pianka and King, 2004; Molnar, 2004; Conrad et al. 2012). Fossil taxa attributed to the genus *Varanus*, or close relatives within the family Varanidae, are normally based on fragmentary material and many specimens may only be recognized to the family level. Because so much material is fragmentary, many fossil taxa or hypothesized relationships among fossil varanoids are ambiguous or indeterminate (Molnar, 2004; Conrad et al., 2012). Even so, the more complete material seems to indicate a great deal of morphological conservatism within this group. For example, phylogenetic analyses of the Eocene fossil taxon *Saniwa* repeatedly place the genus as sister to *Varanus* (and sometimes within) because there is so much morphological similarity (Conrad et al. 2008). The extinct Australian taxon, *Megalania prisca* (1.8 Mya – 40 kya) was renamed *Varanus priscus* because of such strong morphological similarities to extant goannas (Molnar, 2004), and continued recent cladistic work places it within extant *Varanus* (Conrad et al., 2008).

Although material is typically fragmentary, the morphology of specimens is comparable to that of extant members, and size estimates can be made*. V. priscus*, also known as *Megalania*, was a top predator in Australia between approximately 4 million and 30,000 years ago. The estimated body length of *V. priscus* has ranged between 26 ft to 11 ft in total body length, depending on the method used and how one decides to reconstruct the anatomy of the tail (Wroe, 2002; Molnar, 2004; Conrad et al. 2012). Recently, the earliest example of a large *Varanus* comes from the Miocene of Greece, and is estimated to be >600 mm pre-caudal length (Conrad et al. 2012). The estimated decrease in size DTT and negative MDI, then, might be expected because fossil members greatly surpass the size variation seen today. This opens questions about the cause of evolution of large size in this group. Studies had proposed that a lack of mammalian competitors might have allowed evolution of large size, but, for example, the newly discovered large *Varanus* from Greece achieved gigantism in a region populated by a fairly diverse community of mammalian competitors (Conrad et al. 2012). Cladistic analysis also nests the fossil within an East Asian clade, expanding the

evolution of large size outside the Indo-Australian portion of the tree (Conrad et al. 2012).

Morphospace analyses indicate that monitor lizards may have explored large amounts of shape space early in their evolution. Although fossils were not included in this analysis, previous geometric morphometric work including extinct and extant varanid specimens repeatedly places extinct members within extant *Varanus* shape space (Chapter 3 of this dissertation). Sister taxa, such as *Saniwa*, fall well within *Varanus* morphospace (depending on landmarks used) and share a number of characteristics that fall within extant *Varanus* trait variation (Chapter 3 of this dissertation; Conrad et al., 2012). This exploration of shape variation, and how it differs among regions (Fig. 7), raises the question whether exploration of size and shape occurred similarly in different regions through time. The oldest known fossil taxon recognized as part of extant *Varanus* is probably *Varanus rusingensis*. If recognized as *Varanus*, this taxon shows that *Varanus* diversified and reached Africa by the Early Miocene (Clos, 1995; Conrad et al., 2008), and the analysis and discovery of more material can provide insight into the exploration of morphology both early in *Varanus* history and in Africa. A major question regarding *Varanus* has been where the lineage originated, and more analyses of sister groups, diversification rates, shape variation, and interrelationships will shed more light on this question.

CONCLUSION

My work specifies the importance of examining several forms of diversity when interpreting temporal clade dynamics. Morphology be measured in different ways, and analysis on the resulting shape data can also be flexible. Just analyzing extant taxa in a temporal context with a time-calibrated phylogeny, for example, it is possible to find patterns of morphological evolution. Although they use similar datasets, analyses of morphospace size and subclade disparity can give very different patterns because they might be telling very different stories. Morphospace size measures relate to total shape space encompassed by specimens deemed to be representative of time bins, whereas DTT seems to relate more to how morphological variation is partitioned across a tree and among taxa. It may be that the influence of the origination of some groups is not retained in certain measures, such as lineage-though-time, diversification rate models, or even morphospace occupation. For example, the appearance of some Indo-Australian taxa, which encompass a large size range, did not greatly influence measures of morphospace size, but did affect patterns of DTT, and might factor in possible changes of diversification rates. Previous work on other groups has suggested that the general trend of decreasing DTT could be expected if early lineage diversification also resulted in the filling of many ecological roles, which would reduce the amount of opportunities for lineages that originated later (Harmon et al., 2003; Slater

et al., 2010). For monitors, it is hard to tell whether there is a link between diversification and morphological or ecomorphological diversity, although some results seem to show that diversity and disparity are not necessarily correlated. The dataset used in this study must be expanded in order to help answer these questions. This is when fossils become important, because they provide a chance to test these questions more fully as more phylogenetic work provides more information on relationships among taxa.

ACKNOWLEDGMENTS

I thank Drs. Kevin Padian, Patricia Holroyd, and Charles Marshall for their feedback. Dr. Nicholas Matzke was helpful in developing the code that was used to partition a larger time calibrated tree into smaller phylogenies representative of time bins. I also thank Dr. Graham Slater for discussion about his team's disparity-through-time analysis technique, and its versatility in these types of studies. I thank the curators and staff of the UC Museum of Paleontology, UC Museum of Vertebrate Zoology, National Museum of Natural History, American Museum of Natural History, Yale Peabody Museum, Australian Museum, and the Western Australian Museum for access to *Varanus* skeletal material, and use of photographs for morphometric analysis. This research forms part of a dissertation in partial fulfillment of the Ph.D. degree in Integrative Biology at the University of California, Berkeley.

REFERENCES

Adams, D. C., C. M. Berns, K. H. Kozak, and J. J. Wiens. 2009. Are rates of species diversification correlated with rates of morphological evolution? Proceedings of the Royal Society of London B: Biological Sciences, rspb-2009.

Adams, D. C., and E. Otarola-Castillo. 2013. geomorph: an R package for the collection and analysis of geometric morphometric shape data. Methods in Ecology and Evolution, 4:393-399.

Ast, J. C. 2001. Mitochondrial DNA evidence and evolution in Varanoidea (Squamata). Cladistics,17:211–226.

Bennett, D. 1995. A Little Book of Monitor Lizards. Viper Press, Aberdeen, U.K.

Brock, C. D., L. J. Harmon, and M. E. Alfaro. 2011. Testing for temporal variation in diversification rates when sampling is incomplete and nonrandom. Systematic Biology, syr007.

Calenge, C. 2006. The package adehabitat for the R software: a tool for the analysis of space and habitat use by animals. Ecological Modelling, 197:516-519.

Carroll, S. B. 2000. Endless forms: the evolution of gene regulation and morphological diversity. Cell, 101(6): 577-580.

Caumul, R., and P. D. Polly. 2005. Phylogenetic and environmental components of morphological variation: skull, mandible, and molar shape in marmots (Marmota, Rodentia). Evolution, 59(11): 2460-2472.

Clos, L. M. 1995. A new species of Varanus (Reptilia, Sauria) from the Miocene of Kenya. Journal of Vertebrate Paleontology, 15:254–267

Collar, D. C., J. A. Schulte and J. B. Losos. 2011. Evolution of extreme body size disparity in monitor lizards (Varanus). Evolution, 65: 2664–2680

Conrad, J., A. Balcarcel, and C. Mehling. 2012. Earliest example of a giant monitor lizard (Varanus, Varanidae, Squamata). PLoS ONE,. *7*(8): e41767-e41767.

Eldredge, N, J. N. Thompson, P. M. Brakefield, S. Gavrilets, D. Jablonski, J. BC. Jackson, R. E. Lenski, B. S. Lieberman, M. A. McPeek, and W. Miller III. 2005. The dynamics of evolutionary stasis. Paleobiology, 31(5): 133-145.

Foote, M. 1993(a). Contributions of individual taxa to overall morphological disparity. Paleobiology: 403-419.

Foote, M. 1993(b). Discordance and concordance between morphological and taxonomic diversity. Paleobiology, 19: 185–204.

Foote, M. 1997. The evolution of morphological diversity. Annual Review of Ecology and Systematics: 129-152.

Fordyce, J.A. 2010. Interpreting the gamma statistic in phylogenetic diversification rate studies: a rate decrease does not necessarily indicate an early burst. PLoS One. 23, 5(7):e11781. doi: 10.1371/journal.pone.0011781.

Fortey, R. A., D. E.G Briggs, and M. A. Wills. 1996. The Cambrian evolutionary 'explosion': decoupling cladogenesis from morphological disparity. Biological Journal of the Linnean Society, 57(1): 13-33.

Gould, S. J. 1991. The disparity of the Burgess Shale arthropod fauna and the limits of cladistic analysis: why we must strive to quantify morphospace. Paleobiology, 17:411-423.

Gould S.J., N. Eldredge. 1977. Punctuated equilibria: the tempo and mode of evolution reconsidered. Paleobiology, 3: 115–151.

Harmon, L., J. Schulte J., A. Larson, and J. Losos. 2003. Tempo and mode of evolutionary radiation in iguanian lizards. Science, 301: 961–964.

Harmon, L., J. Weir, C. Brock, R. Glor, and W. Challenger. 2008. Geiger: investigating evolutionary radiations. Bioinformatics, 24:129–131.

Hopkins, M. J. 2013. Decoupling of taxonomic diversity and morphological disparity during decline of the Cambrian trilobite family Pterocephaliidae. Journal of evolutionary biology, 26(8): 1665-1676.

Huxley, J. S. 1950, Relative growth and form transformation. Proc. R. Soc. London, 137: 465-469.

Kendall, D. G. 1948. On the generalized "birth-and-death" process. Ann. Math. Stat., 19:1-15

Klingenberg, C. P. 2010. Evolution and development of shape: integrating quantitative approaches. Nature Reviews Genetics, 11:623–635

Kozak K.H., D. W. Weisrock, and A. Larson. 2006. Rapid lineage accumulation in a non-adaptive radiation: phylogenetic analysis of diversification rates in eastern North American woodland salamanders (Plethodontidae: Plethodon). Proc. R. Soc. B., 273: 539–546.

Losos, J., and H. Greene. 1988. Ecological and evolutionary implications of diet in monitor lizards. Biological Journal of the Linnean Society, 35: 379-407.

Lupia, R. 1999. Discordant morphological disparity and taxonomic diversity during the Cretaceous. Paleobiology, 25: 1–29.

McClain, C. R. 2005. Bathymetric patterns of morphological disparity in deep-sea gastropods from the western North Atlantic Basin. Evolution, 59: 1492–1499.

Mohr, C. O. 1947. Table of equivalent populations of north american small mammals. The American Midland Naturalist, 37: 223-249.

Molnar, R. 2004. Dragons in the Dust. Bloomington: Indiana University Press.

Nee, S., A. Mooers, and P. H. Harvey. 1992. Tempo and mode of evolution revealed from molecular phylogenies. Proc. Natl. Acad. Sci. USA 89:8322-8326.

Nee, S., E. C. Holmes, R. M. May, and P. H. Harvey. 1994a. Extinction rates can be estimated from molecular phylogenies. Philos. Trans. R. Soc. Lond. B, 344:77-82.

Nee, S., R. M. May, and P. H. Harvey. 1994b. The reconstructed evolutionary process. Philos. Trans. R. Soc. Lond. B, 344:305-311.

Nee, S., E. C. Holmes, A. Rambaut, and P. H. Harvey. 1995. Inferring population history from molecular phylogenies. Philosophical Transactions of the Royal Society of London. Series B., Biological Sciences, 349: 25–31.

Nosil, P., and T. E. Reimchen. 2005. Ecological opportunity and levels of morphological variance within freshwater stickleback populations. Biological Journal of the Linnean Society 86(3): 297-308.

Openshaw, G. H., and J. S. Keogh. 2014. Head shape evolution in monitor lizards (Varanus): interactions between extreme size disparity, phylogeny and ecology. Journal of evolutionary biology, 27(2): 363-373.

Paradis E., J. Claude and K. Strimmer. 2004. APE: analyses of phylogenetics and evolution in R language. Bioinformatics, 20: 289-290.

Pepin, D. J. 2001. Evolution and life history of varanid lizards. Ph.D. thesis. Washington Univ., St. Louis, MO.

Pianka, E. R. 1994. Comparative ecology of Varanus in the Great Victoria Desert. West. Aust. Nat., 15:37–44.

Pianka, E. R. 1995. Evolution of body size: varanid lizards as a model system. Am. Nat., 146:398–414.

Pianka, E. R., and D. King, and R. A. King. 2004. Varanoid lizards of the world. Indiana Univ. Press, Bloomington, IN.

Pybus, O. G., and P. H. Harvey. 2000. Testing macro-evolutionary models using incomplete molecular phylogenies. Proceedings of the Royal Society of London Series B-Biological Sciences, 267:2267–2272.

Quental, T .B. and C. R. Marshall. 2010. Diversity dynamics: molecular phylogenies need the fossil record.Trends in Ecology and Evolution, 25: 434–441.

Quental, T. B., and C. R. Marshall. 2011. The Molecular Phylogenetic Signature of Clades in Decline. PLoS ONE 6(10): e25780. doi:10.1371/journal.pone.0025780

R Core Team (2014). R: A language and environment for statistical computing. R Foundation for Statistical Computing, Vienna, Austria. URL http://www.R-project.org/.

Rabosky, D. L. 2006. Likelihood methods for inferring temporal shifts in diversification rates. Evolution, 60:1152-1164.

Rabosky, D. L. and I. J. Lovette. 2008. Explosive evolutionary radiations: decreasing speciation or increasing extinction through time? Evolution, doi:10.1111/j.1558-5646.2008.00409.x

Rabosky, D. and K. Schliep. 2013. Laser: Likelihood Analysis of Speciation/Extinction Rates from Phylogenies. R package version 2.4-1. http://CRAN.R-project.org/package=laser

Ricklefs R. E. 2006(a).Time, species, and the generation of trait variance in clades.Syst. Biol., 55:151–159

Ricklefs, R. E. and D. B. Miles. 1994. Ecological and evolutionary inferences from morphology: an ecological perspective. In: Ecological Morphology (P.C. Wainwright, S.M. Reilly, eds), pp. 13–41. University of Chicago Press, Chicago.

Roy, K., Jablonski, D. and J. W. Valentine. 2004. Beyond species richness: biogeographic patterns and biodiversity dynamics using other metrics of diversity. In: Frontiers of Biogeography: New Directions in the Geography of Nature (M.V. Lomolino, L.R. Heaney, eds), pp. 151–170. Sinauer, Sunderland, MA

Schluter, D. 2000. The Ecology of Adaptive Radiation. Oxford Univ. Press, New York.

Simpson, G. G. 1953. The Major Features of Evolution. Columbia Univ. Press, New York.

Slater, G. J., S. A. Price, F. Santini, and M. E. Alfaro. 2010. Diversity versus disparity and the radiation of modern cetaceans. Proceedings of the Royal Society of London B: Biological Sciences, 277(1697): 3097-3104.

Van Valen, L. 1965. Morphological variation and width of ecological niche. American Naturalist: 377-390.

Vidal, N., J. Marin, J. Sassi, F. U. Battistuzzi, S. Donnellan, A. Fitch, et al. 2012. Molecular evidence for an Asian origin of monitor lizards followed by Tertiary dispersals to Africa and Australasia. Biol. Lett., 8: 853–855.

Wagner, P.J. 1997. Patterns of morphological diversification among the Rostroconchia. Paleobiology, 23: 115–150.

Wroe, S. 2002. A review of terrestrial mammalian and reptilian carnivore ecology in Australian fossil faunas, and factors influencing their diversity: the myth of reptilian domination and its broader ramifications. Australian Journal of Zoology, 50: 1-24

Zelditch, M. L., D. L. Swiderski, and H. D. Sheets. 2012. Geometric morphometrics for biologists: a primer. Academic Press.

Table 1. Gamma statistics of varanid tree. As the tree used does not contain all living taxa, MCCR corrected values were obtained.

No. of species included in phylogeny	Total no. of species in clade	γ statistic	*P* value	MCCR corrected γ statistic (critical value)	MCCR corrected *P* value
39	~73	-3.52	0.0002	-2.672391	0.988

Table 2. Fits of rate-constant and rate-variable model to branching times of the Vidal et al. 2012 tree. First 2 rows are constant rate models.

Model	LH	AIC	lam0	k	mu0	z	r1	r2	st1
Pure Birth	-39.7	81.5	NA	NA	NA	NA	0.057	NA	NA
Birth-Death	-39.7	83.5	NA	NA	NA	NA	0.0557	NA	NA
DDL	-32.2	68.4	NA	NA	NA	NA	0.115	NA	NA
DDX	-36.1	76.3	NA	NA	NA	NA	0.276	NA	NA
2 rate-Yule	-30.9	67.8	NA	42.3		NA	0.082	0.009	5.78
SPVAR	-35.7	77.4	0.215	0.048	0.001	NA	NA	NA	NA
EXVAR	-39.8	85.7	0.057	NA	0.001	1.006	NA	NA	NA
SP/EX VAR	-35.7	79.4	0.215	0.048	0.001	0.5	NA	NA	NA

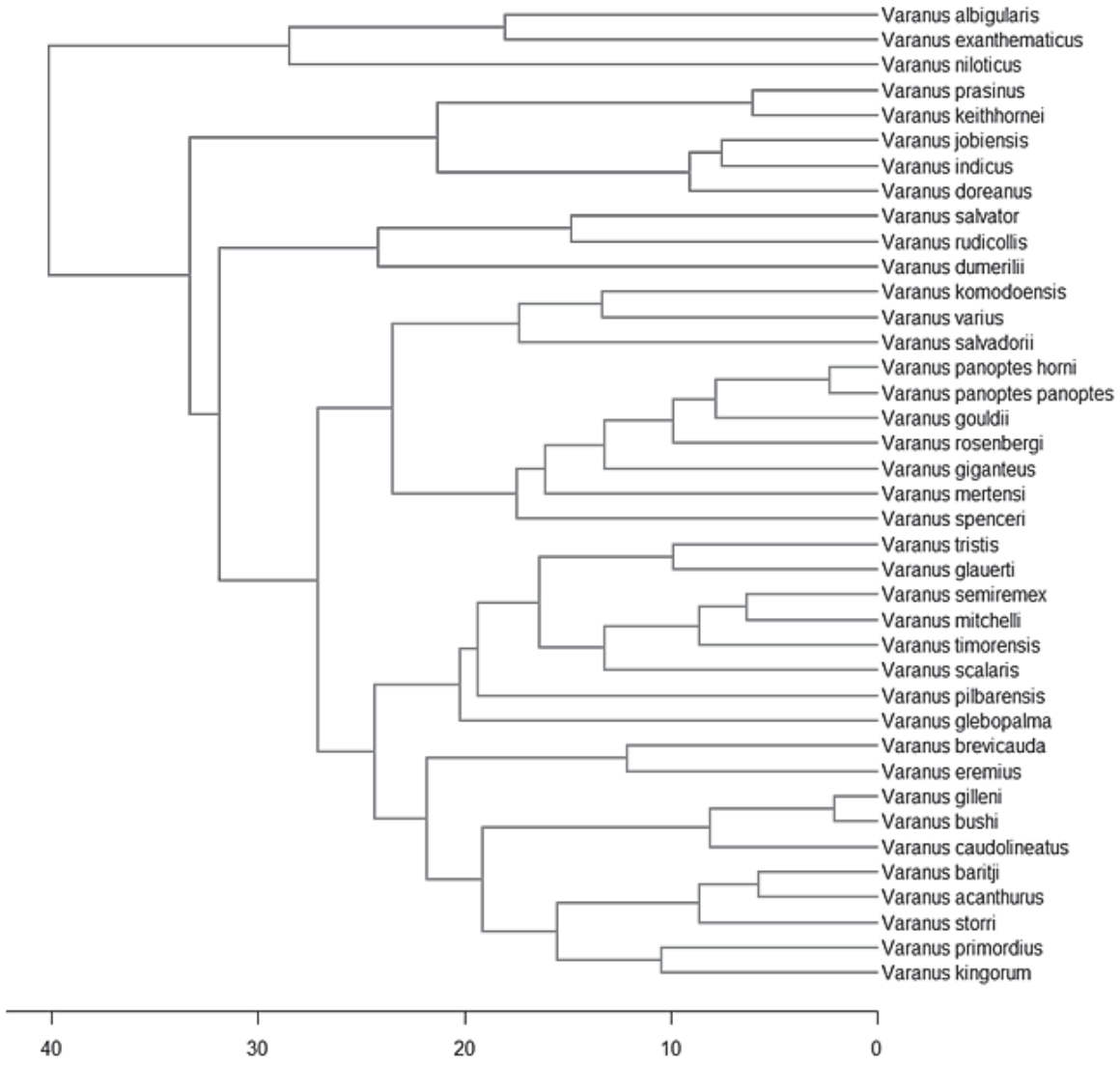


Figure 1. Varanus time calibrated tree modifed from Vidal et al. 2012. Scale is in million years.

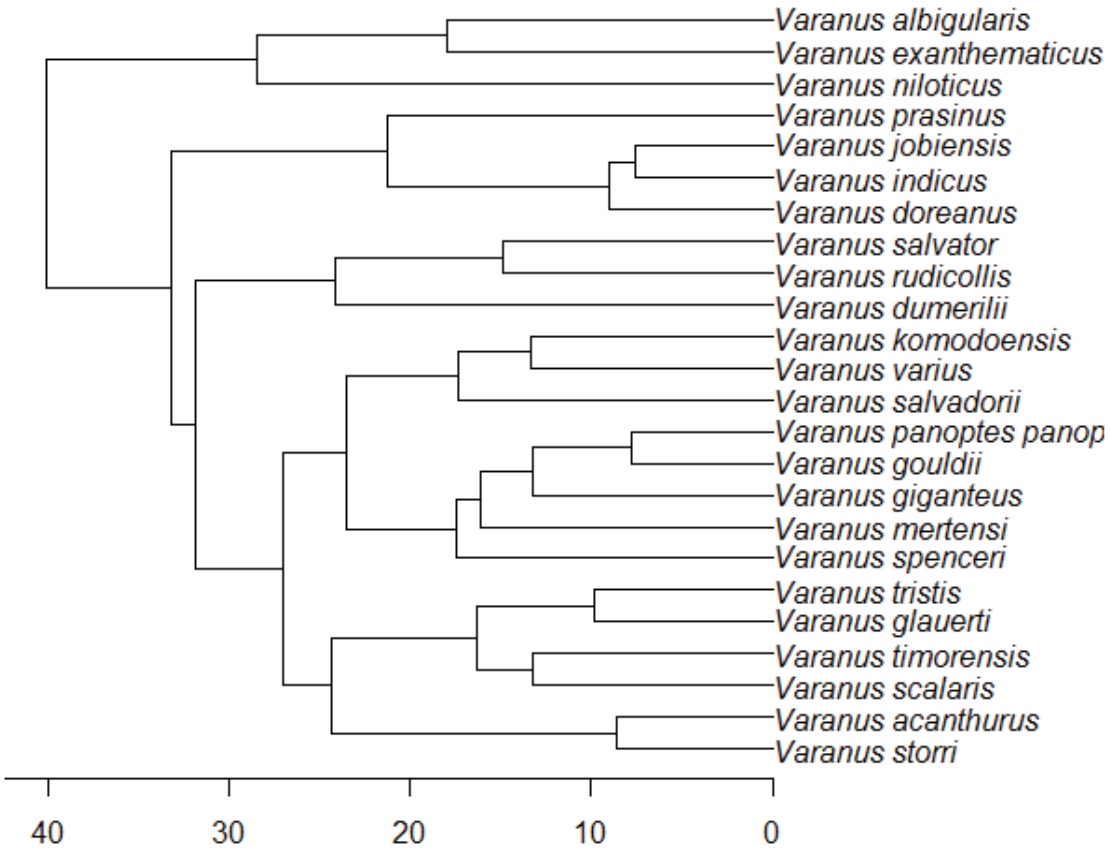


Figure 2. Modified version of the Vidal et al. tree containing only taxa for which geometric morphometric is available.

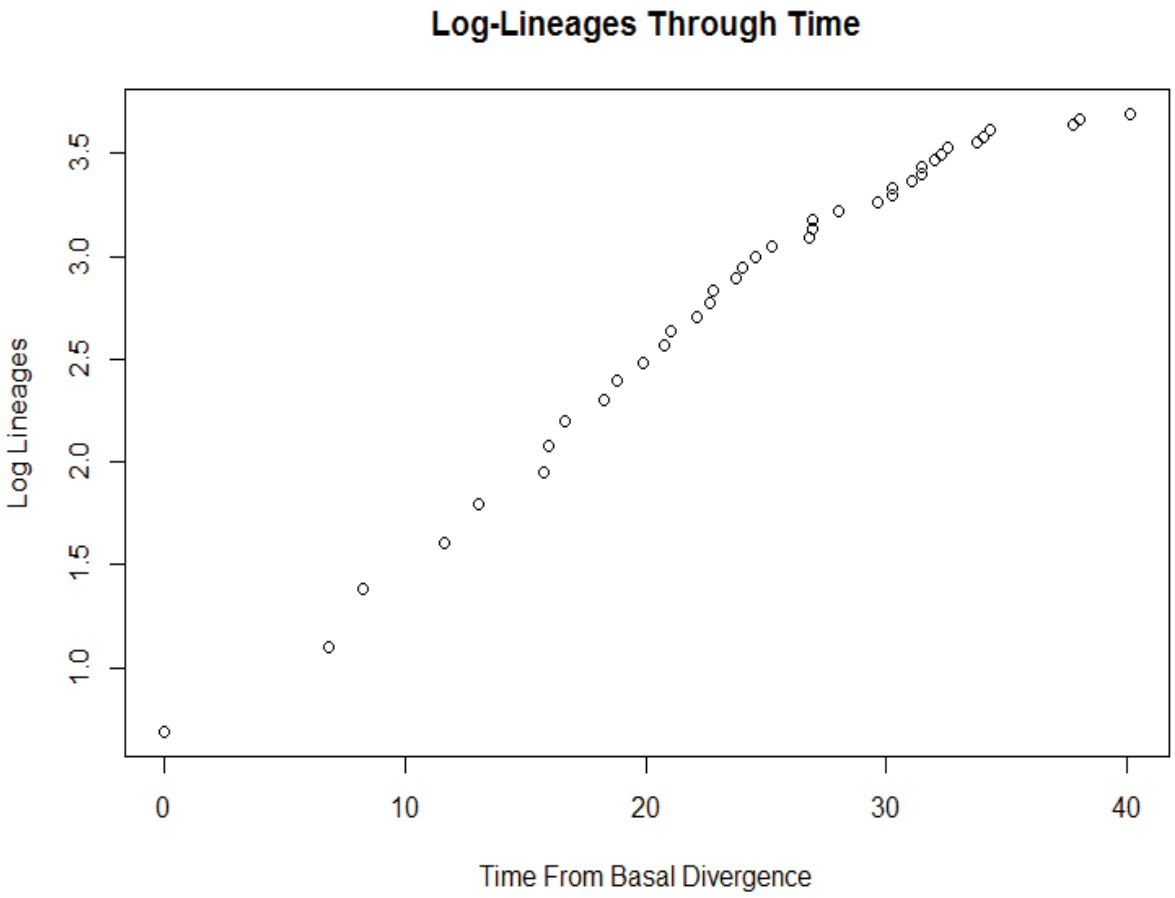


Figure 3. Log-lineage-through-time plot of the varanid tree (Fig. 1). X axis is numbered and scaled to time from basal divergence (left). There seems to be a steady diversification rate (slope) and increase in the number of taxa from the base of the tree until about 30 time points from basal divergence where lineage accumulation rate decreases.

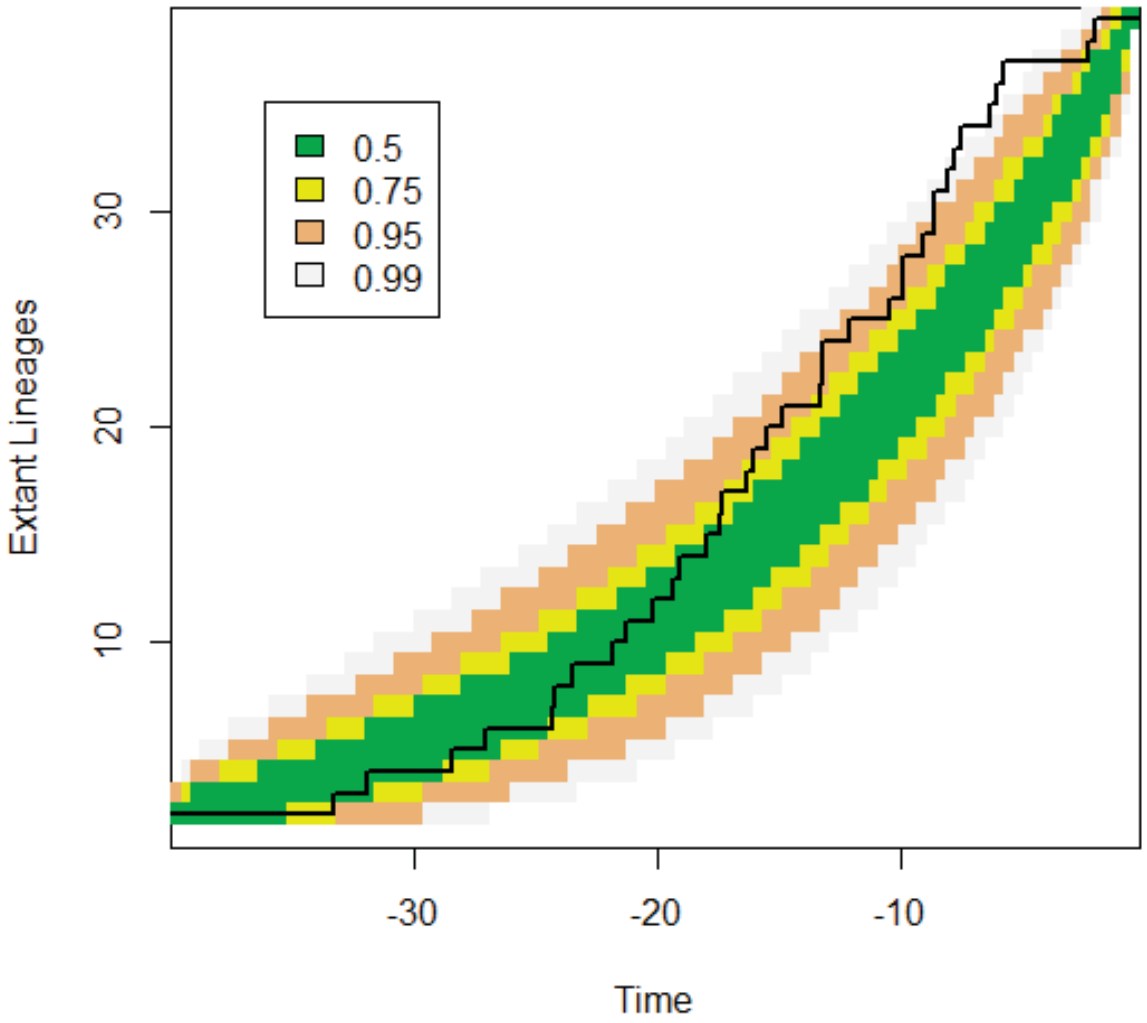


Figure 4. Observed varanid LTT (black line) with expectations under the null Yule, or pure-birth model generated from 1000 iterations of simulated trees with the same parameters to the Vidal et al. tree. Time is expressed as time from the present (right). Colors represent different confidence intervals (CI; see legend in figure). Notice that for most of the history of the clade, observed LTT falls within various CI ranges until about 15-16 mya where it quickly jumps quickly above the 99% CI, and then quickly returns to expected in the present.

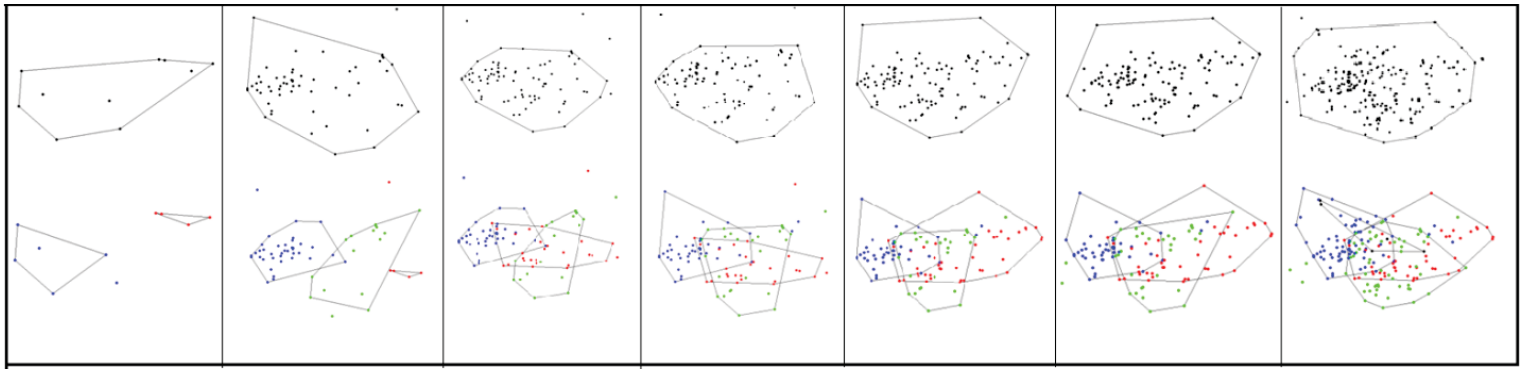


Figure 5. Time bin morphospaces. Images on the top are of total morphospace space with convex hulls surrounded all of the specimens (black points). On the bottom half hulls are defined by regions, and specimens are color coded by region. Red=Africa, Green=Indo-Australia, and Blue-Indo-Asia. Each time bin morphospace was resampled 1000 times with bootstrap analyses to determine possible outliers (which are found outside of the hulls). All subsequent morphospace size and overlap analyses were conducted on illustrated convex hulls.

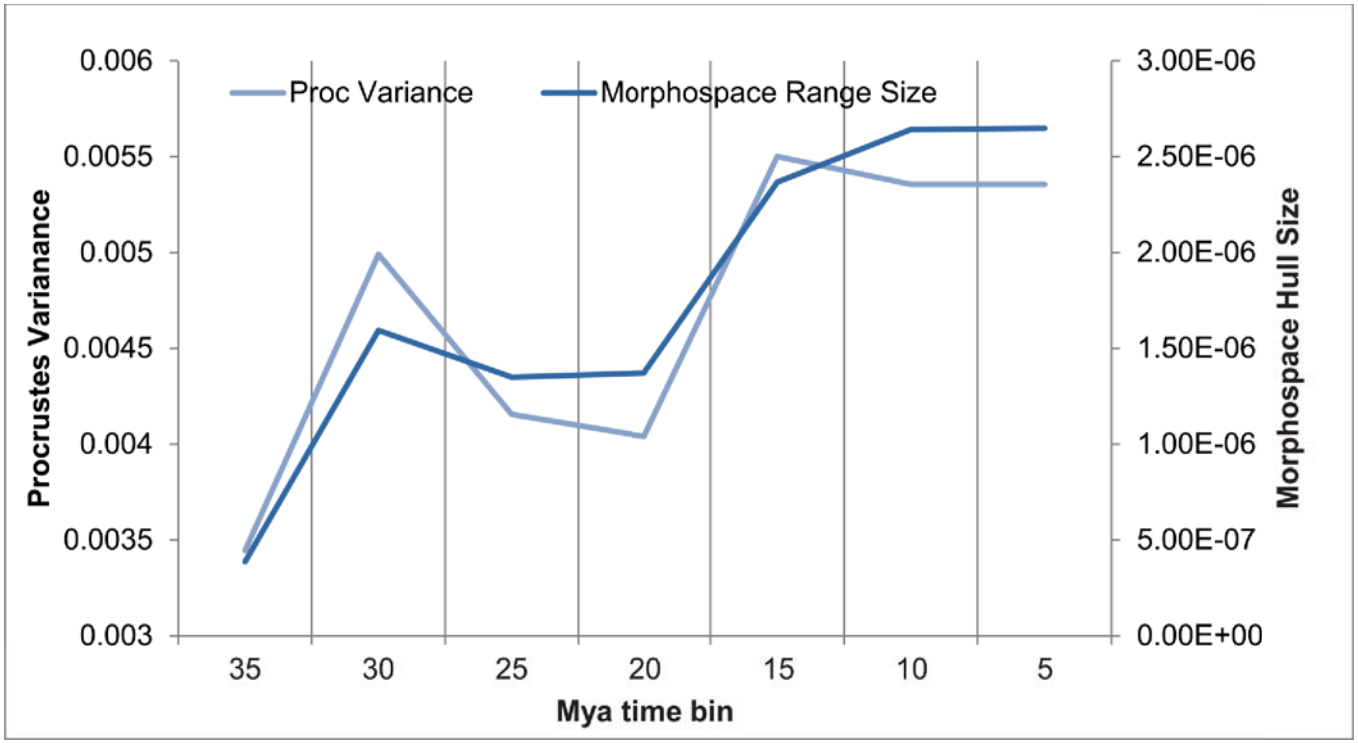


Figure 6. Varanid Procrustes Variance and Morphospace Range Size at designated time bins. Although based on different measures of morphospace, both follow similar patterns. Notice a strong drop in size from 30-20 Mya before increases to today's largest morphospace size.

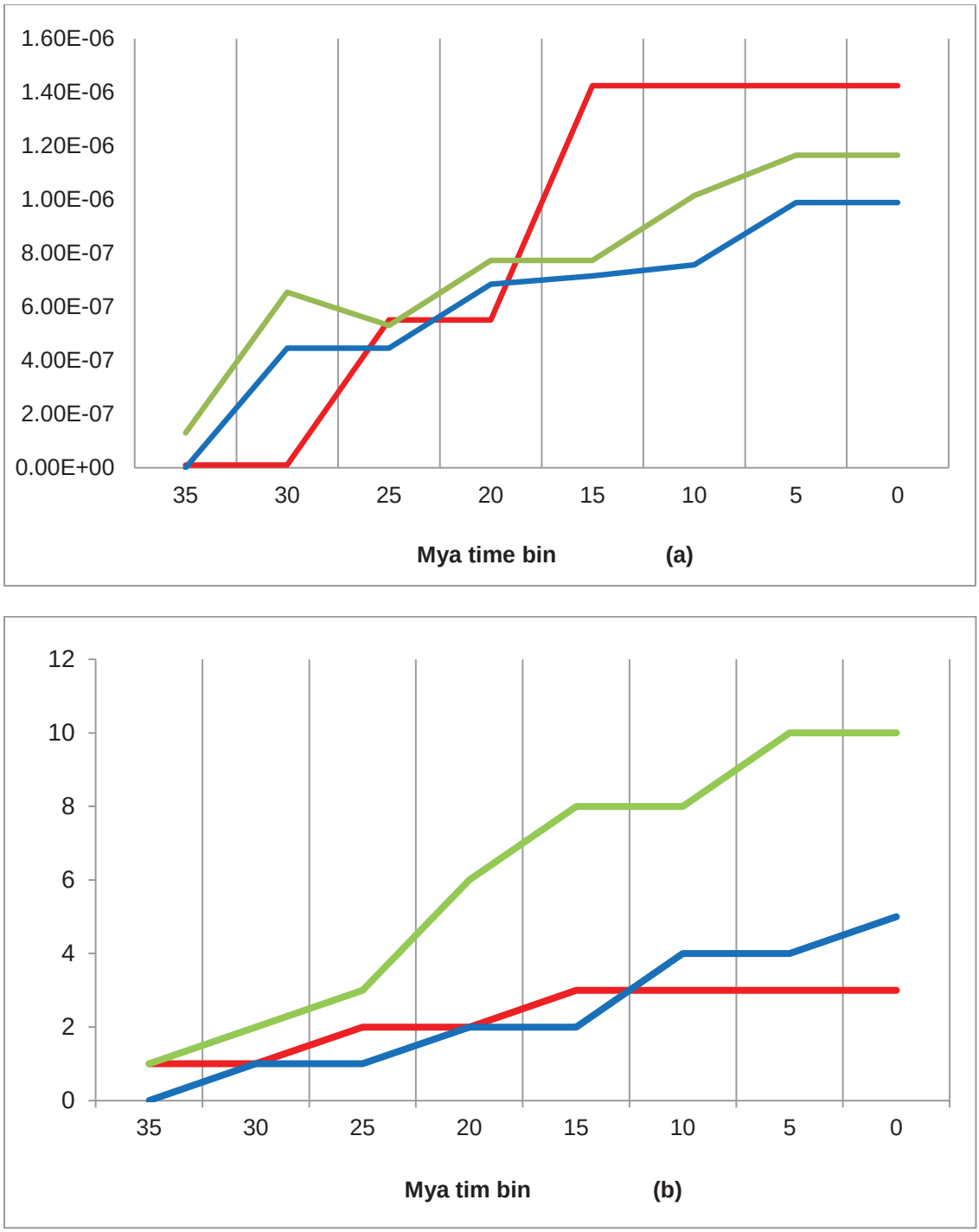


Figure 7. Regional morphospace size (a) and taxonomic diversity (b) through time in varanids within 5 My time bins.

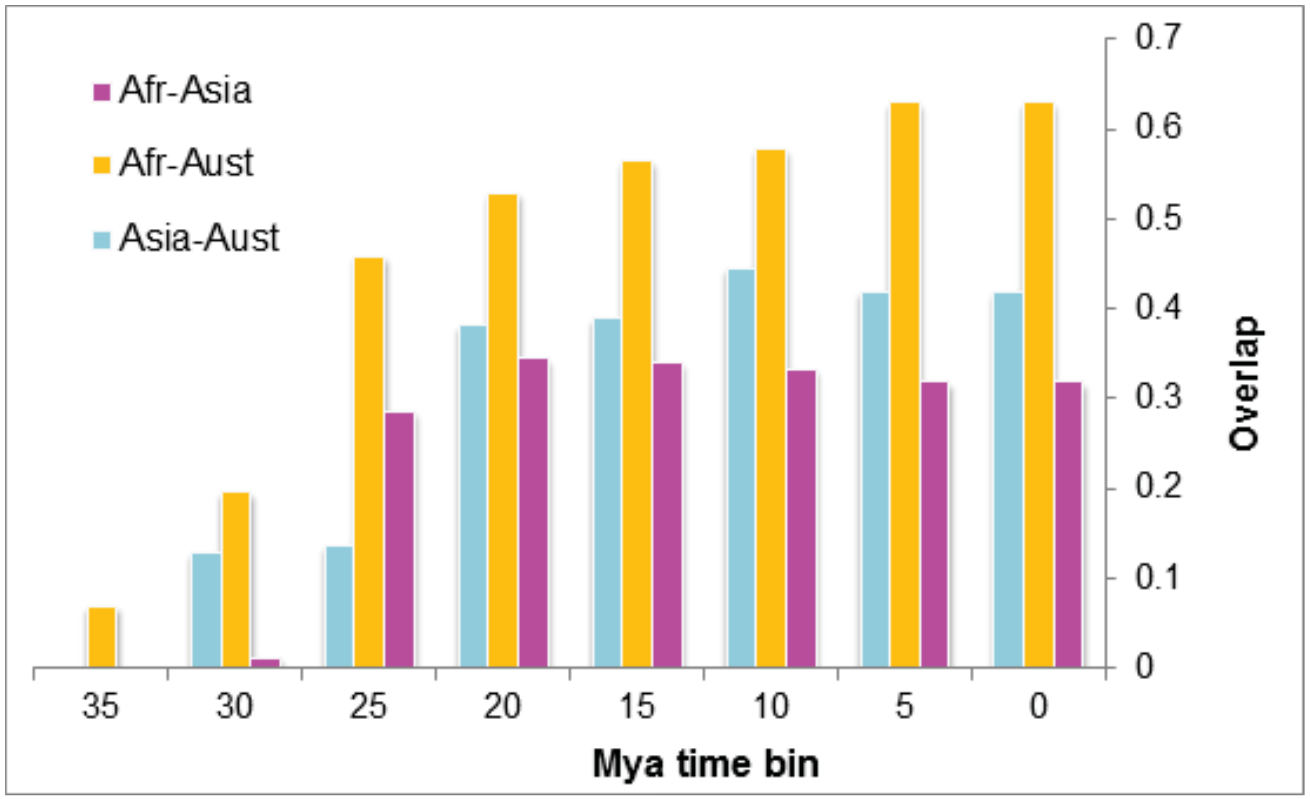


Figure 8. Overlap of varanid regional morphospace within 5 My time bins. Colors are based on overlap of previously defined regional colors. Afr=Africa, Asia=Indo-Asia, and Aust=Indo-Australia. Because Africa and Indo-Australia encompass a great deal of total morphospace, they tend to overlap greatly with each other, and have so for a great deal of time. Indo-Asian taxa tend to fall in one are of morphospace, so they have less overlap with other groups.

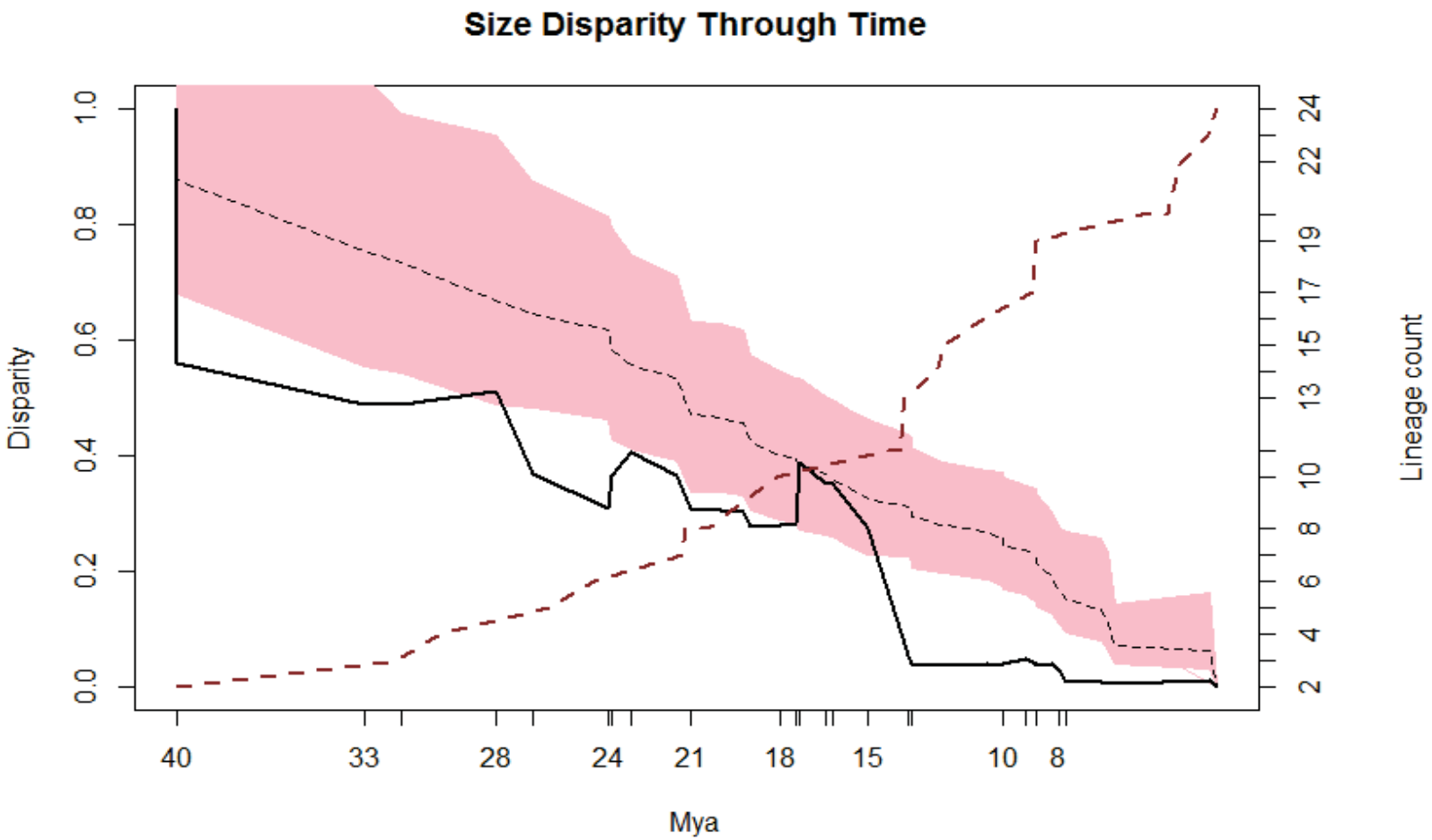


Figure 9. Mean subclade disparity through time (DTT) for *Varanus* body size (lower solid line). The black dashed line represents the median subclade DTT based on 10,000 Brownian motion simulations of character evolution on the Vidal et al. 2012 phylogeny. The red dashed line is the number of lineages through time. The pink shaded area represents the 95% confidence interval DTT range determined by the simulated data.

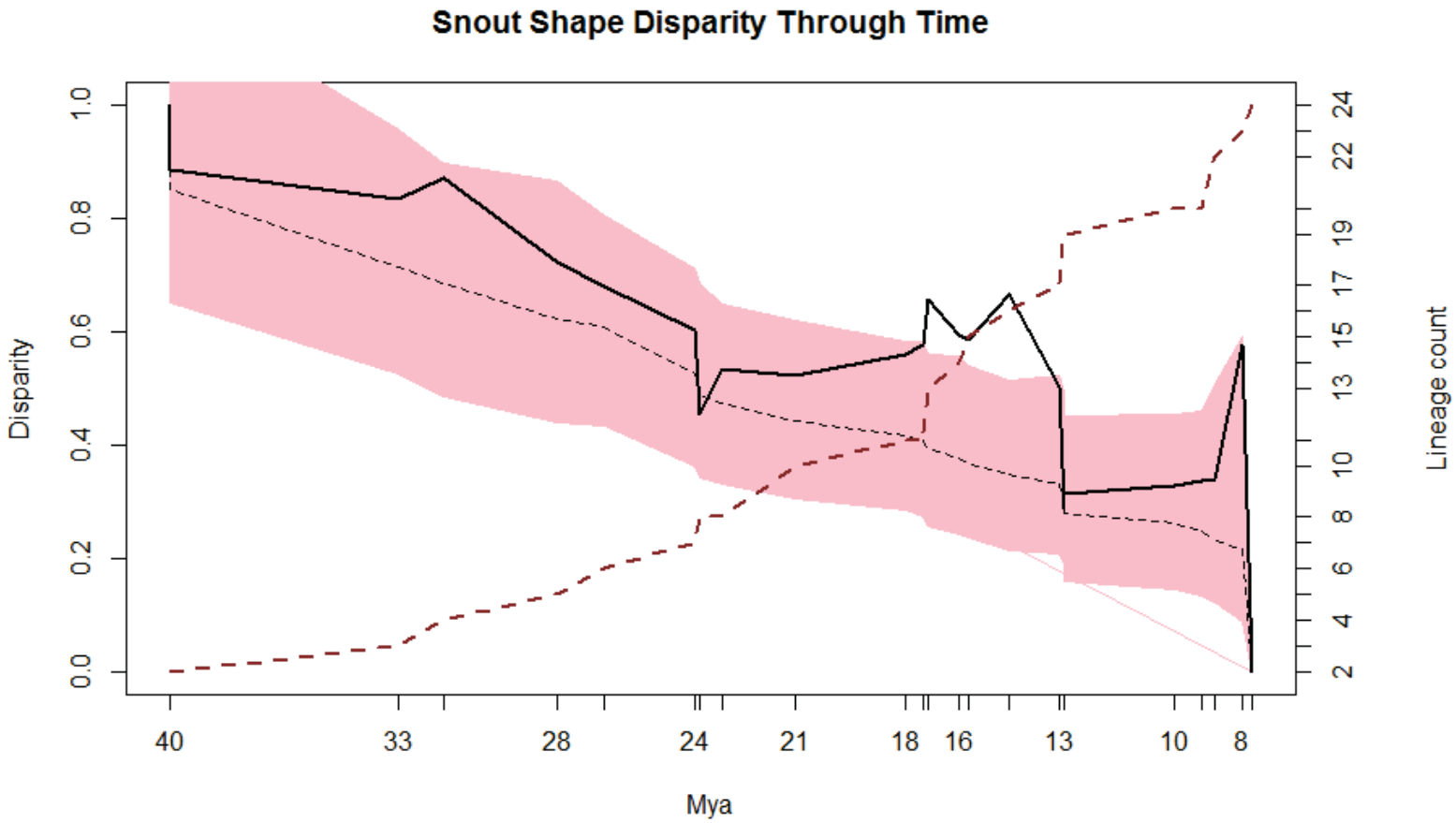


Figure 10. Mean subclade disparity through time (DTT) for *Varanus* snout shape space based on principal components representing 95% shape variation from geometric morphometric analysis (lower solid line). The black dashed line represents the median subclade DTT based on 10,000 Brownian motion simulations of shape evolution on the Vidal et al. 2012 phylogeny. The red dashed line represented the number of lineages through time. The pink shaded area represents the 95% confidence interval DTT range determined by the simulated data.

Appendix 1.

Taxon list and time bin occupation based on the Vidal et al. 2012 phylogeny. 1 indicates that the taxon or lineage leading to that taxon exists in the designated MY time bin.

	Mya Time bins							
Species on Vidal et al. tree	**40-35**	**35-30**	**30-25**	**25-20**	**20-15**	**15-10**	**10-5'**	**5-0'**
Varanus_kingorum	0	0	0	0	0	0	1	1
Varanus_primordius	0	0	0	0	0	1	1	1
Varanus_storri	0	0	0	0	0	0	1	1
Varanus_acanthurus	0	0	0	1	1	1	1	1
Varanus_baritji	0	0	0	0	0	0	1	1
Varanus_caudolineatus	0	0	0	0	0	0	1	1
Varanus_bushi	0	0	0	0	0	0	0	1
Varanus_gilleni	0	0	0	0	0	0	0	1
Varanus_eremius	0	0	0	0	1	1	1	1
Varanus_brevicauda	0	0	0	0	0	1	1	1
Varanus_glebopalma	0	0	0	0	1	1	1	1
Varanus_pilbarensis	0	0	0	0	1	1	1	1
Varanus_scalaris	0	0	0	0	1	1	1	1
Varanus_timorensis	0	0	0	0	0	1	1	1
Varanus_mitchelli	0	0	0	0	0	0	1	1
Varanus_semiremex	0	0	0	0	0	0	1	1
Varanus_glauerti	0	0	0	0	0	0	1	1
Varanus_tristis	0	0	0	1	1	1	1	1
Varanus_spenceri	0	0	0	0	1	1	1	1
Varanus_mertensi	0	0	0	0	0	1	1	1
Varanus_giganteus	0	0	0	0	0	1	1	1
Varanus_rosenbergi	1	1	1	1	1	0	1	1
Varanus_gouldii	0	0	0	0	0	0	1	1
Varanus_panoptes	0	0	0	0	1	1	1	1
Varanus_panoptes_horni	0	0	0	0	0	0	0	1
Varanus_salvadorii	0	0	0	0	1	1	1	1
Varanus_varius	0	0	0	0	0	1	1	1
Varanus_komodoensis	0	1	1	1	1	1	1	1
Varanus_dumerilii	0	0	0	1	1	1	1	1
Varanus_rudicollis	0	0	0	0	0	1	1	1
Varanus_salvator	0	1	1	1	1	1	1	1
Varanus_doreanus	0	0	0	0	0	0	1	1
Varanus_indicus	0	0	0	0	0	0	1	1
Varanus_jobiensis	0	0	0	1	1	1	1	1

Varanus_keithhornei	0	0	0	0	0	0	1	1
Varanus_prasinus	1	1	1	1	1	1	1	1
Varanus_niloticus	0	0	1	1	1	1	1	1
Varanus_exanthematicus	0	0	0	0	1	1	1	1
Varanus_albigularis	1	1	1	1	1	1	1	1

Appendix 2.

The first 5 principal component scores of the dorsal snout Principal components analysis (95% of shape variation). The geometric morphometric analysis in chapter 3 used 249 specimens, whereas this version includes duplicates (310 samples) to test for measurement error (which was negligible), and the analysis produced the same results as the analysis in Chapter 3. The specimen list is still the same as that of Chapter 3.

PC1	PC2	PC3	PC4	PC5
-0.03027	2.62E-02	7.94E-03	1.64E-02	0.000514
-0.03034	2.57E-02	8.39E-03	1.68E-02	-0.00024
-0.05313	6.59E-03	-9.81E-03	-5.23E-03	-0.00684
-0.05313	6.59E-03	-9.81E-03	-5.23E-03	-0.00684
-0.02311	3.74E-03	5.87E-03	-1.02E-03	-0.00114
-0.04534	1.16E-02	-1.56E-02	-1.87E-03	0.002371
-0.03593	7.70E-03	-9.43E-03	6.83E-03	-0.01335
0.013642	-1.21E-02	-5.05E-03	-3.09E-02	-0.05
0.013642	-1.21E-02	-5.05E-03	-3.09E-02	-0.05
0.141909	1.67E-02	1.82E-02	-1.56E-03	0.006479
-0.03034	-2.31E-02	2.93E-02	6.89E-03	-0.01247
0.026925	1.33E-02	4.35E-03	1.65E-02	-0.00347
-0.04478	7.84E-03	2.77E-03	-6.48E-03	0.009122
0.122433	2.99E-02	5.07E-03	7.20E-03	-0.00961
0.08157	1.94E-02	2.51E-02	-1.23E-02	0.004455
-0.03833	3.50E-02	1.46E-02	-6.82E-04	-0.00259
-0.03297	2.58E-02	1.53E-02	3.24E-02	0.006397
-0.03722	2.52E-02	2.82E-02	1.80E-03	-0.00182
-0.03601	4.06E-02	8.66E-03	4.84E-04	-0.00432
-0.02098	3.88E-02	2.09E-02	3.93E-04	-0.00478
-0.04915	3.45E-02	1.84E-02	5.91E-03	-0.00545
-0.06153	1.99E-02	1.14E-02	5.39E-03	-0.00204
-0.04195	-2.30E-04	2.50E-02	3.04E-03	-0.0116
-0.00984	4.65E-02	1.90E-02	1.06E-02	-0.01635
-0.0514	1.51E-02	3.63E-03	3.00E-03	0.016516
0.058447	1.01E-02	1.11E-02	-1.58E-02	0.001834
0.048807	2.63E-02	-6.28E-02	-6.40E-03	-0.00153
-0.00261	3.76E-02	4.45E-02	-1.51E-02	-0.01997
-0.03034	2.57E-02	8.39E-03	1.68E-02	-0.00024
-0.05313	6.59E-03	-9.81E-03	-5.23E-03	-0.00684
-0.02311	3.74E-03	5.87E-03	-1.02E-03	-0.00114
-0.04534	1.16E-02	-1.56E-02	-1.87E-03	0.002371
-0.03593	7.70E-03	-9.43E-03	6.83E-03	-0.01335

PC1	PC2	PC3	PC4	PC5
0.013642	-1.21E-02	-5.05E-03	-3.09E-02	-0.05
0.141909	1.67E-02	1.82E-02	-1.56E-03	0.006479
-0.03034	-2.31E-02	2.93E-02	6.89E-03	-0.01247
0.026925	1.33E-02	4.35E-03	1.65E-02	-0.00347
-0.04478	7.84E-03	2.77E-03	-6.48E-03	0.009122
0.122433	2.99E-02	5.07E-03	7.20E-03	-0.00961
0.08157	1.94E-02	2.51E-02	-1.23E-02	0.004455
-0.03833	3.50E-02	1.46E-02	-6.82E-04	-0.00259
-0.03297	2.58E-02	1.53E-02	3.24E-02	0.006397
-0.03722	2.52E-02	2.82E-02	1.80E-03	-0.00182
-0.03601	4.06E-02	8.66E-03	4.84E-04	-0.00432
-0.02098	3.88E-02	2.09E-02	3.93E-04	-0.00478
-0.04915	3.45E-02	1.84E-02	5.91E-03	-0.00545
-0.06153	1.99E-02	1.14E-02	5.39E-03	-0.00204
-0.04195	-2.30E-04	2.50E-02	3.04E-03	-0.0116
-0.00984	4.65E-02	1.90E-02	1.06E-02	-0.01635
-0.0514	1.51E-02	3.63E-03	3.00E-03	0.016516
0.058447	1.01E-02	1.11E-02	-1.58E-02	0.001834
0.048807	2.63E-02	-6.28E-02	-6.40E-03	-0.00153
-0.00261	3.76E-02	4.45E-02	-1.51E-02	-0.01997
0.161158	2.11E-02	2.80E-02	4.32E-03	0.000228
0.032388	-4.81E-02	1.28E-02	-8.88E-04	0.000737
0.015517	-1.21E-02	-1.59E-02	-8.43E-03	-0.00025
0.038375	-3.73E-02	-1.97E-02	1.88E-02	0.015922
-0.03207	-3.39E-02	-1.63E-02	1.14E-02	-0.00696
0.00148	-3.21E-02	-2.06E-02	-9.95E-03	0.01082
0.006826	-6.50E-03	-8.55E-03	-1.18E-02	0.00329
-0.00487	-2.75E-02	-6.54E-04	4.02E-03	0.012322
0.001367	-2.78E-02	1.07E-03	-2.63E-03	0.007949
-0.0377	-3.48E-02	-1.48E-02	3.14E-02	0.004447
0.034433	-1.94E-02	-8.85E-03	1.57E-03	0.000273
0.047628	2.81E-02	-6.19E-02	-9.35E-03	0.004809
-0.02454	4.97E-04	1.89E-02	-9.59E-03	0.017434
-0.06058	1.43E-02	7.91E-03	5.89E-03	-0.00136
-0.02015	1.37E-02	2.61E-02	9.24E-03	-0.00058
0.055174	-5.74E-03	-2.82E-02	-7.43E-03	-0.00583
0.052772	2.41E-04	1.06E-02	-9.44E-03	0.009743
-0.00662	7.50E-03	-1.96E-02	-7.11E-03	0.011086
0.113793	2.62E-02	1.74E-02	-5.55E-03	0.007553
0.100005	1.74E-02	9.42E-03	-8.99E-03	-0.0016

PC1	PC2	PC3	PC4	PC5
-0.00737	-4.30E-02	4.96E-03	2.12E-02	0.000792
-0.01354	3.24E-02	1.49E-03	2.00E-03	0.024032
0.090953	2.74E-02	8.06E-03	1.73E-02	-0.00106
0.075217	2.75E-02	1.52E-04	1.49E-02	-0.01792
0.086033	2.03E-02	4.71E-03	-2.71E-04	-0.0275
-0.02333	2.15E-03	-2.35E-02	2.88E-02	0.004756
0.090138	1.27E-02	1.24E-02	1.24E-02	-0.00217
-0.00869	-4.96E-02	3.93E-03	-1.35E-02	-0.01476
-0.04585	-8.15E-03	-2.84E-04	-1.35E-03	0.006013
-0.08203	3.83E-05	-7.69E-03	1.52E-02	-0.00155
-0.01881	-1.42E-02	-1.34E-03	-5.47E-03	-0.01286
-0.02879	1.53E-02	1.67E-02	1.89E-02	-0.0292
0.013749	-2.04E-02	1.76E-02	-2.40E-02	0.010103
0.014918	-2.07E-02	1.66E-02	-2.17E-02	0.011416
-0.04262	-7.29E-03	-1.45E-02	-7.72E-03	0.003003
0.043745	-3.46E-02	1.49E-02	-2.44E-02	-0.00372
0.01415	1.25E-02	-6.06E-02	-9.12E-03	-0.00892
0.052501	1.29E-02	-7.49E-02	-4.75E-03	0.000982
0.020313	1.66E-02	-7.47E-02	-1.39E-03	-0.00891
0.047641	2.93E-02	-7.38E-02	-4.61E-04	-0.0081
0.045021	2.27E-02	-7.64E-02	-2.14E-03	-0.01037
0.063988	-2.18E-02	3.16E-03	-8.36E-03	0.026699
0.067569	-2.24E-02	6.08E-03	-4.48E-03	0.020421
0.084758	-2.91E-02	1.09E-02	-1.77E-02	0.018422
-0.07761	1.42E-03	-1.31E-02	-2.04E-02	-0.00051
0.008424	1.15E-02	-9.88E-03	-5.66E-03	0.021772
0.098384	-2.46E-02	8.11E-03	-1.26E-02	0.030009
0.002847	4.17E-02	2.00E-02	-1.19E-02	0.037354
-0.01529	-2.00E-02	7.60E-03	-1.49E-02	0.012199
-0.00319	-3.60E-02	-1.12E-02	-6.64E-03	-0.02313
-0.01359	-2.87E-02	-1.54E-02	-1.52E-02	-0.00749
0.012286	-1.52E-02	-5.98E-04	-1.43E-03	0.008209
0.093209	-8.34E-03	2.29E-02	-1.10E-02	0.015891
-0.04458	1.43E-02	-1.71E-02	-8.68E-03	0.005047
-0.08273	6.66E-02	-6.03E-03	9.55E-03	-0.00245
-0.0816	6.15E-02	-8.26E-03	9.55E-03	-0.00177
0.039224	-6.60E-02	3.59E-03	2.83E-02	-0.00966
0.012397	4.62E-02	3.92E-02	5.25E-03	-0.01503
0.012003	-3.52E-02	-4.75E-03	-4.94E-03	-0.00142
-0.00206	2.32E-02	3.56E-02	-1.18E-02	0.017741

PC1	PC2	PC3	PC4	PC5
-0.01686	1.65E-02	-3.49E-04	1.26E-03	-0.00537
0.004507	1.65E-02	1.05E-02	-1.53E-03	0.020441
-0.03786	-2.42E-03	2.85E-03	-1.66E-02	0.016361
0.039831	-3.45E-02	-1.97E-03	4.29E-03	0.023294
-0.01456	-2.60E-02	8.81E-03	7.05E-03	0.005728
0.0316	-3.17E-02	-1.19E-02	4.05E-03	0.008188
0.015643	-2.50E-02	-3.29E-03	3.94E-03	0.008771
0.043029	-2.09E-02	8.13E-03	-1.48E-02	0.000199
0.023002	2.52E-04	-7.07E-02	2.14E-02	0.007214
-0.00031	-4.63E-03	1.62E-02	1.58E-02	-0.01549
-0.02401	-6.37E-02	-1.16E-02	4.44E-02	0.001389
-0.01817	-1.00E-02	-1.18E-02	-3.72E-02	-0.02073
0.166315	2.44E-03	4.30E-03	8.52E-03	-0.00314
-0.05065	-3.38E-04	8.51E-03	2.49E-02	0.001883
-0.11409	3.45E-02	8.51E-03	-3.19E-02	-0.00472
-0.04585	3.38E-03	3.95E-03	-1.18E-02	0.003577
0.006841	-3.03E-02	9.09E-03	-4.02E-03	-0.01776
0.066429	3.37E-02	-7.40E-03	2.08E-03	0.004816
-0.0442	-2.94E-03	1.28E-02	3.54E-03	-0.00727
0.121629	3.15E-02	1.45E-02	7.65E-03	0.004124
0.134857	3.19E-02	2.93E-02	-1.06E-02	-0.00232
-0.0493	-2.86E-02	-2.29E-02	1.49E-02	0.001117
0.059057	2.28E-02	1.44E-02	-3.99E-03	0.013293
0.023456	6.46E-03	-7.30E-03	1.60E-02	-0.01433
-0.00101	-7.28E-02	-5.72E-03	-5.27E-03	-0.00915
-0.05857	-5.97E-03	-1.20E-03	-1.07E-03	0.007445
-0.05816	-1.17E-02	-1.80E-03	2.69E-03	0.00813
0.005764	-6.03E-02	4.79E-03	-1.24E-02	-0.01999
-0.0099	-2.55E-02	-1.90E-02	-1.57E-02	0.006772
0.011251	2.01E-02	5.42E-03	9.26E-03	-0.00502
-0.05711	-1.14E-02	1.87E-02	-1.79E-03	-0.01048
-0.101	1.19E-02	1.02E-02	-6.22E-03	0.003581
-0.03616	2.43E-02	4.85E-04	1.35E-02	0.011135
0.142754	1.90E-02	1.83E-03	6.48E-03	-0.00464
0.042705	-1.93E-02	1.77E-02	3.14E-02	-0.00656
-0.0098	-5.64E-02	-1.63E-02	4.62E-04	-0.0023
0.096591	4.50E-02	-5.68E-02	-9.14E-03	-0.00338
-0.01103	-4.52E-02	3.28E-02	-1.88E-02	0.000221
0.032471	-4.38E-02	1.98E-02	2.40E-02	-0.0084
0.020762	-4.52E-02	1.94E-02	1.64E-02	-0.01525

PC1	PC2	PC3	PC4	PC5
-0.00923	2.11E-02	2.22E-02	-8.17E-03	-0.01588
-0.0276	1.03E-02	1.83E-02	6.52E-03	0.007844
-0.00279	1.34E-02	2.38E-02	-1.99E-02	-0.01055
-0.01796	2.54E-02	8.65E-03	-4.23E-03	-0.00095
-0.04355	1.33E-02	1.08E-02	1.24E-03	-0.00431
0.058557	-5.48E-02	3.43E-02	7.50E-03	-0.02104
0.107129	-2.10E-02	3.08E-02	3.00E-02	-0.02654
-0.03575	-1.35E-03	-2.44E-02	2.28E-04	0.000427
0.034353	-4.88E-02	3.62E-02	3.06E-03	0.009511
-0.0104	1.97E-02	-2.73E-04	2.62E-02	0.007925
-0.10863	4.46E-02	-1.42E-04	3.79E-03	-0.01318
-0.02345	-2.91E-02	1.62E-02	-7.96E-03	-0.02627
-0.02525	-5.16E-02	1.15E-02	1.13E-03	-0.0149
-0.00992	-4.40E-02	4.23E-03	2.48E-02	-0.01044
-0.03903	-5.80E-03	7.53E-03	-3.74E-03	0.001983
-0.0148	8.09E-04	1.81E-03	-5.26E-02	-0.00185
0.057572	1.95E-02	-5.62E-02	-2.29E-03	-0.00326
-0.00085	3.92E-02	2.90E-02	-2.23E-02	-0.00676
-0.0318	3.36E-03	2.45E-02	-6.39E-03	0.000854
-0.10094	-1.53E-02	-6.05E-03	2.70E-02	0.01426
-0.00312	-2.44E-02	2.09E-03	1.00E-02	-0.02804
0.032388	-4.81E-02	1.28E-02	-8.88E-04	0.000737
0.015517	-1.21E-02	-1.59E-02	-8.43E-03	-0.00025
0.038375	-3.73E-02	-1.97E-02	1.88E-02	0.015922
-0.03207	-3.39E-02	-1.63E-02	1.14E-02	-0.00696
0.00148	-3.21E-02	-2.06E-02	-9.95E-03	0.01082
0.006826	-6.50E-03	-8.55E-03	-1.18E-02	0.00329
-0.00487	-2.75E-02	-6.54E-04	4.02E-03	0.012322
0.001367	-2.78E-02	1.07E-03	-2.63E-03	0.007949
-0.0377	-3.48E-02	-1.48E-02	3.14E-02	0.004447
0.034433	-1.94E-02	-8.85E-03	1.57E-03	0.000273
0.047628	2.81E-02	-6.19E-02	-9.35E-03	0.004809
-0.02454	4.97E-04	1.89E-02	-9.59E-03	0.017434
-0.06058	1.43E-02	7.91E-03	5.89E-03	-0.00136
-0.02015	1.37E-02	2.61E-02	9.24E-03	-0.00058
0.055174	-5.74E-03	-2.82E-02	-7.43E-03	-0.00583
0.052772	2.41E-04	1.06E-02	-9.44E-03	0.009743
-0.00662	7.50E-03	-1.96E-02	-7.11E-03	0.011086
0.113793	2.62E-02	1.74E-02	-5.55E-03	0.007553
0.100005	1.74E-02	9.42E-03	-8.99E-03	-0.0016

PC1	PC2	PC3	PC4	PC5
-0.00737	-4.30E-02	4.96E-03	2.12E-02	0.000792
-0.01354	3.24E-02	1.49E-03	2.00E-03	0.024032
0.090953	2.74E-02	8.06E-03	1.73E-02	-0.00106
0.075217	2.75E-02	1.52E-04	1.49E-02	-0.01792
0.086033	2.03E-02	4.71E-03	-2.71E-04	-0.0275
-0.02333	2.15E-03	-2.35E-02	2.88E-02	0.004756
0.090138	1.27E-02	1.24E-02	1.24E-02	-0.00217
-0.00869	-4.96E-02	3.93E-03	-1.35E-02	-0.01476
-0.04585	-8.15E-03	-2.84E-04	-1.35E-03	0.006013
-0.08203	3.83E-05	-7.69E-03	1.52E-02	-0.00155
-0.01881	-1.42E-02	-1.34E-03	-5.47E-03	-0.01286
-0.02879	1.53E-02	1.67E-02	1.89E-02	-0.0292
0.014918	-2.07E-02	1.66E-02	-2.17E-02	0.011416
0.013749	-2.04E-02	1.76E-02	-2.40E-02	0.010103
-0.04262	-7.29E-03	-1.45E-02	-7.72E-03	0.003003
0.043745	-3.46E-02	1.49E-02	-2.44E-02	-0.00372
0.01415	1.25E-02	-6.06E-02	-9.12E-03	-0.00892
0.052501	1.29E-02	-7.49E-02	-4.75E-03	0.000982
0.020313	1.66E-02	-7.47E-02	-1.39E-03	-0.00891
0.047641	2.93E-02	-7.38E-02	-4.61E-04	-0.0081
0.045021	2.27E-02	-7.64E-02	-2.14E-03	-0.01037
0.063988	-2.18E-02	3.16E-03	-8.36E-03	0.026699
0.067569	-2.24E-02	6.08E-03	-4.48E-03	0.020421
0.084758	-2.91E-02	1.09E-02	-1.77E-02	0.018422
-0.07761	1.42E-03	-1.31E-02	-2.04E-02	-0.00051
0.008424	1.15E-02	-9.88E-03	-5.66E-03	0.021772
0.098384	-2.46E-02	8.11E-03	-1.26E-02	0.030009
0.002847	4.17E-02	2.00E-02	-1.19E-02	0.037354
-0.01529	-2.00E-02	7.60E-03	-1.49E-02	0.012199
-0.00319	-3.60E-02	-1.12E-02	-6.64E-03	-0.02313
-0.01359	-2.87E-02	-1.54E-02	-1.52E-02	-0.00749
0.012286	-1.52E-02	-5.98E-04	-1.43E-03	0.008209
0.093209	-8.34E-03	2.29E-02	-1.10E-02	0.015891
-0.04458	1.43E-02	-1.71E-02	-8.68E-03	0.005047
0.161158	2.11E-02	2.80E-02	4.32E-03	0.000228
-0.03062	4.22E-02	1.24E-02	8.98E-03	0.01229
-0.05576	4.69E-02	-4.51E-03	-1.91E-02	-0.00571
-0.08476	6.76E-02	-1.99E-02	8.64E-03	-0.00553
0.062562	7.62E-02	-1.19E-02	3.30E-02	-0.00193
-0.06689	6.81E-02	1.40E-02	2.09E-02	0.013991

PC1	PC2	PC3	PC4	PC5
-0.10447	8.21E-02	9.06E-03	3.77E-03	-0.01375
-0.06721	-7.90E-03	1.45E-03	-1.13E-03	0.01065
-0.06907	-3.49E-03	2.99E-03	-1.46E-02	0.003674
-0.02567	-8.32E-03	-6.34E-03	-3.03E-03	0.022745
-0.09145	-5.29E-03	2.79E-03	-1.74E-02	0.004036
-0.06948	-2.09E-02	1.01E-02	-4.30E-02	-0.00842
-0.06662	-3.17E-02	-1.53E-02	4.71E-03	0.025032
-0.06637	-2.85E-02	-1.64E-02	7.75E-03	0.028314
-0.03677	3.43E-02	2.85E-02	-2.49E-03	0.013947
-0.08668	-2.64E-03	-1.24E-02	-5.89E-04	0.01012
-0.00378	9.53E-03	-1.47E-02	-1.47E-03	-0.01838
-0.05543	-9.89E-03	3.03E-02	-4.20E-03	0.010977
-0.07797	-9.75E-03	-1.16E-02	-2.09E-02	0.011299
-0.09125	-6.82E-03	-2.20E-03	-1.60E-02	0.001139
-0.05727	-2.67E-03	-1.32E-02	-2.28E-02	-0.01586
-0.08147	-7.02E-03	-3.40E-03	-8.40E-03	0.002537
-0.04479	3.20E-03	6.69E-03	-1.07E-02	-0.00027
-0.04498	2.01E-03	6.45E-03	-9.08E-03	-0.00153
-0.0715	1.63E-02	3.03E-03	-6.03E-03	0.011684
-0.05407	3.19E-04	-5.75E-03	1.56E-02	-0.00191
-0.07313	-3.48E-02	6.86E-03	1.85E-02	-0.0205
-0.02397	-2.05E-02	-1.74E-02	2.18E-02	0.021824
-0.01304	-1.41E-02	-6.39E-03	7.69E-03	0.005547
-0.07947	7.00E-03	-4.97E-03	-7.03E-03	-0.00247
-0.06111	5.53E-03	3.10E-03	-3.59E-05	0.006527
0.055921	-1.24E-02	-4.70E-03	-3.95E-03	0.007591
-0.0816	6.15E-02	-8.26E-03	9.55E-03	-0.00177
-0.08273	6.66E-02	-6.03E-03	9.55E-03	-0.00245
-0.02122	-4.25E-02	2.16E-02	1.83E-02	0.007405
-0.018	-5.11E-02	-1.31E-03	1.40E-02	0.008415
-0.12219	-2.23E-02	-8.53E-03	-1.88E-03	0.012847
-0.00697	-4.53E-02	8.94E-03	7.10E-03	-0.02105
-0.10566	-3.93E-02	-1.79E-02	-6.18E-03	0.00171
-0.04145	3.31E-02	-1.90E-05	2.06E-02	0.002126
-0.03831	1.12E-02	1.31E-02	1.02E-02	0.009293
0.047939	-2.96E-02	3.73E-02	9.59E-03	-0.00917
0.039224	-6.60E-02	3.59E-03	2.83E-02	-0.00966
0.012397	4.62E-02	3.92E-02	5.25E-03	-0.01503
0.012003	-3.52E-02	-4.75E-03	-4.94E-03	-0.00142
-0.00206	2.32E-02	3.56E-02	-1.18E-02	0.017741

PC1	PC2	PC3	PC4	PC5
-0.01686	1.65E-02	-3.49E-04	1.26E-03	-0.00537
0.004507	1.65E-02	1.05E-02	-1.53E-03	0.020441
-0.03786	-2.42E-03	2.85E-03	-1.66E-02	0.016361
0.039831	-3.45E-02	-1.97E-03	4.29E-03	0.023294
-0.01456	-2.60E-02	8.81E-03	7.05E-03	0.005728
0.0316	-3.17E-02	-1.19E-02	4.05E-03	0.008188
0.015643	-2.50E-02	-3.29E-03	3.94E-03	0.008771
0.043029	-2.09E-02	8.13E-03	-1.48E-02	0.000199
0.023002	2.52E-04	-7.07E-02	2.14E-02	0.007214
-0.00031	-4.63E-03	1.62E-02	1.58E-02	-0.01549
-0.02401	-6.37E-02	-1.16E-02	4.44E-02	0.001389
-0.01817	-1.00E-02	-1.18E-02	-3.72E-02	-0.02073
0.166315	2.44E-03	4.30E-03	8.52E-03	-0.00314
-0.05065	-3.38E-04	8.51E-03	2.49E-02	0.001883
-0.11409	3.45E-02	8.51E-03	-3.19E-02	-0.00472
-0.04585	3.38E-03	3.95E-03	-1.18E-02	0.003577
0.006841	-3.03E-02	9.09E-03	-4.02E-03	-0.01776
0.066429	3.37E-02	-7.40E-03	2.08E-03	0.004816
-0.0442	-2.94E-03	1.28E-02	3.54E-03	-0.00727
0.121629	3.15E-02	1.45E-02	7.65E-03	0.004124
0.134857	3.19E-02	2.93E-02	-1.06E-02	-0.00232
-0.0493	-2.86E-02	-2.29E-02	1.49E-02	0.001117
0.059057	2.28E-02	1.44E-02	-3.99E-03	0.013293
0.023456	6.46E-03	-7.30E-03	1.60E-02	-0.01433
-0.00101	-7.28E-02	-5.72E-03	-5.27E-03	-0.00915
-0.05857	-5.97E-03	-1.20E-03	-1.07E-03	0.007445
-0.05816	-1.17E-02	-1.80E-03	2.69E-03	0.00813
0.005764	-6.03E-02	4.79E-03	-1.24E-02	-0.01999
-0.0099	-2.55E-02	-1.90E-02	-1.57E-02	0.006772
0.011251	2.01E-02	5.42E-03	9.26E-03	-0.00502
-0.05711	-1.14E-02	1.87E-02	-1.79E-03	-0.01048
-0.101	1.19E-02	1.02E-02	-6.22E-03	0.003581
-0.03616	2.43E-02	4.85E-04	1.35E-02	0.011135
0.142754	1.90E-02	1.83E-03	6.48E-03	-0.00464
0.042705	-1.93E-02	1.77E-02	3.14E-02	-0.00656
-0.0098	-5.64E-02	-1.63E-02	4.62E-04	-0.0023
0.096591	4.50E-02	-5.68E-02	-9.14E-03	-0.00338

Appendix 3.

Snout vent length measures of each species of Varanus included on the Vidal et al. 2012 phylogeny. SVL is in millimeters. Habitat was included to aid in discussion.

Taxon	Max SVL (mm)	Habitat
Varanus_kingorum	120	Rock/Terrestrial
Varanus_primordius	137	Terrestrial
Varanus_storri	155	Terrestrial
Varanus_acanthurus	261	Terrestrial
Varanus_baritji	250	Terrestrial
Varanus_caudolineatus	133	Arboreal
Varanus_bushi	145	Arboreal
Varanus_gilleni	186	Arboreal
Varanus_eremius	192	Terrestrial
Varanus_brevicauda	94	Fossorial
Varanus_glebopalma	383	Arboreal
Varanus_pilbarensis	178	Rock/Terrestrial
Varanus_scalaris	260	Arboreal
Varanus_timorensis	253	Arboreal
Varanus_mitchelli	346	Aqua/Arboreal
Varanus_semiremex	299	Aqua/Arboreal
Varanus_glauerti	240	Arboreal
Varanus_tristis	302	Arboreal
Varanus_spenceri	530	Terrestrial
Varanus_mertensi	496	Aquatic
Varanus_giganteus	837	Terrestrial
Varanus_rosenbergi	517	Terrestrial
Varanus_gouldii	550	Terrestrial
Varanus_panoptes_panoptes	670	Terrestrial
Varanus_panoptes_horni	670	Terrestrial
Varanus_salvadorii	850	Arboreal
Varanus_varius	765	Arb/Terrestrial
Varanus_komodoensis	1340	Terrestrial
Varanus_dumerilii	478	Terrestrial
Varanus_rudicollis	580	Arboreal
Varanus_salvator	250	Aquatic
Varanus_doreanus	540	Terrestrial
Varanus_indicus	580	Aqua/Arboreal
Varanus_jobiensis	450	Arboreal
Varanus_keithhornei	288	Arboreal
Varanus_prasinus	335	Arboreal

Varanus_niloticus	780	Aquatic
Varanus_exanthematicus	606	Terrestrial
Varanus_albigularis	795	Terrestrial